Process Control in the Pulp and Paper Industry I

Notes From a Course given in Spring 1972

Åström, Karl Johan

1975

Document Version:
Publisher's PDF, also known as Version of record

TFRT-3124

PROCESS CONTROL IN THE PULP AND PAPER INDUSTRY I

- NOTES FROM A COURSE GIVEN IN SPRING 1972

K. J. ÅSTRÖM

Report 7524(C) September 1975
Department of Automatic Control
Lund Institute of Technology

CONTENTS

1. COURSE OUTLINE
2. PAPPERSMASKINREGLERING DEL 1
3. HEAD BOX FLOW DYNAMICS AND CONTROL
4. DYNAMICS OF THE WET END OF A PAPER MACHINE
5. SAMMANFATTNING AV MATEMATISK MODELL FÖR PAPPERSMASKIN
6. APPLICATIONS TO PAPER MAKING

PROCESSREGLERING I PAPPERS- OCH CELLULOSAINDUSTRIN

DOKTORANDKURS I REGLERTEKNIK VT 1972

1. INLEDNING
2. PROCESSBESKRIVNING
3. PAPPERSMASKINREGLERING
4. PRODUKTIONSSTYRNING
5. KOKARSTYRNING EV.
6. EXEMPEL PÅ DATORPROJEKT

1. INLEDNING

Kursens roll i doktorsutbildningen

Studierna hittils metodinriktade. Vi har svagheter i tillämpning. Vi vet litet om givare praktiska tillämpningar. Industriell processreglering mångfasetterat problem Ingen blir expert på en enda kurs.

Organisation

Föreläsningar
KJA följer ett givet program
Gästföreläsare
Lidby, Iggesund Häggman
Bohlin SCA
Wahren STFI
(ev ytterligare)
Studiebesök (Billerud)
Tentamen ? (lista) + uppgifter
Kursmaterial

Målsättning

Få viss känsla för verkliga problem. Tillämpa vad vi kan på problem och modeller. Vi kommer således att utnyttja pappersprocesser som ett verktyg för att illustrera modellbyggnads och identifiering, dimensionering av regulatorer, industriella reglerproblem, mättekniska problem, industriella automatiseringsprojekt.

2. PROCESSBESKRIVNING

Industrins storlek och betydelse. (Se skrift från pappersindustriföreningen).

Genomgång av processchema. (Se utdrag ur FOCUS tekniken).

Något om den industriella miljön och reglerteknikens betydelse för processautomatisering.

- Processdesign (gjorda för manuell drift)
- Ständiga processförbättringar
- Kontinuerlig drift
- Konjunkturkänslighet

State of the art.

- Förståelse av ingående processer på makroskopisk och mikroskopisk nivå.
- Kunskap om processdynamik och störningar.
- Mättekniska problem.

DOKTORANDUTBILDNING I REGLERTEKNIK

Kursen Processreglering i pappersindustrin

Nedan ges ett förslag på enskilda uppgifter i samband med kursen. Uppgifterna är tänkta att ta cirka två veckors heltid. Samarbete är tänkbart.

Uppgifternas karaktär är ganska varierande. Det omfattar således litteraturstudier, modellbygge, analys, simulering och syntes. Samtliga uppgifter skall presenteras i ett kort seminarium. Skriftlig dokumentation bör lämnas.

MODELLBYGGE OCH IDENTIFIERING

Dessa uppgifter går i korthet ut på att studera litteraturen och uppställa eller förfina någon av de modeller som behandlats i föreläsningen. Dessa uppgifter kan kompletteras med analys eller simulering av modellen.

1. Ventiler och pumpar

Ventiler och pumpar har behandlats mycket summariskt i föreläsningar. De är dock viktiga systemkomponenter. Uppgiften består i att gå igenom litteraturen vad beträffar ventilkarakteristika och pumpkarakteristika. Ställ upp de modeller som finns och undersök hur den förenklade modell som givits på föreläsningarna bör kompletteras för att få en mera realistisk representation av verkligheten. Resultaten bör lämpligen simuleras för att visa skillnaderna. Ett lämpligt studieobjekt är t ex blandningspumpen med omgivande cirkulationssystem.

2. Viramodeller

Läs igenom litteraturen om viramodeller. Programmera en modell med vars hjälp den våta linjen kan bestämmas. Komplettera den förenklade modell som givits på föreläsningarna med den mer komplicerade modell och diskutera vilka skillnader som erhålles.

3. Drivsystem

Gå igenom litteraturen på drivsystem. (Förmodligen är det en bra idé att ta kontakt med ASEA!) Ställ upp en matematisk modell för drivsystemet och ge typiska storleksordningar på tidskonstanter och relevanta parametrar. Komplettera den förenklade modell som givits i föreläsningarna med den mera detaljerade modellen av drivsystemet och undersök vilka konsekvenser det kan ha för hela systemets dynamik.

4. Presspartiet

Läs in litteraturen om presspartiet och undersök huruvida den i föreläsningarna givna hypotesen om att fukthalten efter press-partiet är konstant är relevant. Om så icke är fallet, gör en modifiering av den förenklade modellen och diskutera konsekvensen.

5. Torkpartiet

Läs in litteraturen om torkpartiet och gör en mer detaljerad modell, gärna baserad på fysikaliska grunddata. Komplettera den i föreläsningarna givna modellen och diskutera skillnader med den förenklade modellen.

6. Flerfraktionsmodeller

I föreläsningarna behandlades genomgående modeller där man endast studerade tvåkomponentflöde, fibrer och vatten. I själva verket är fibrerna ganska olika och i många mälder finns dessutom tillsatsmedel såsom lera. För att beskriva sådana mälder räcker det ej med att behandla två komponenter. Läs in litteraturen på området och komplettera den förenklade modellen som givits på föreläsningarna till en flerfraktionsmodell. Arbetet bör åtminstone omfatta tre komponenter vatten, fibrer och lera, men det skulle vara trevligt om det kunde göras generellt.

7. Massaegenskaper

I den modell som givits i föreläsningarna har massan behandlats mycket summariskt. Massans egenskaper, malgrad, porositet, dränage-egenskaper påverkar dock de flesta processer över hela pappersmaskinen. Läs igenom litteraturen på detta område och undersök i vilken utsträckning man borde komplettera den förenklade modellen.

8. Identifiering

Utnyttja de experimentella data som vi har tillgängliga till att bestämma koefficienterna i den förenklade modell som givits på föreläsningarna.

9. Ytvikts- och fukthaltsvariationer

Sammanställ och analysera de data som finns tillgängliga på störningens egenskaper, helst i både längs och tvärsled.

10. Tryckvariationer

Sammanställ och analysera de data som finns tillgängliga på koncentrations- och tryckvariationer hos tjockmassaflödet. Ställ upp lämpliga matematiska modeller som kan användas i simulering.

ANALYS OCH SIMULERING

Dessa uppgifter omfattar analys och simulering av givna modeller på analogimaskin eller på PDP:n. Det vore önskvärt att arbetet genomfördes på båda apparaterna för att få en viss känsla av när den ena metoden av simuleringar är att föredra jämfört med den andra. Jag tror att PDP:n ofta användes för simulering även i fall då analogimaskinen är lämpligare.

1. Simulering av den enkla modellen

Simulera den enkla modellen som givits på föreläsningarna på analogimaskin och PDP. Komplettera modellen med den tidsför-

dröjning som finns genom att papperet måste löpa genom torkpartiet. Använd simuleringsmodellen för att studera de konventionella reglersystem som finns för pappersmaskireglering.

2. Inloppslådereglering

Simulera reglering av en inloppslåda. Trimma in konventionella regulatorer så att de fungerar bra i ett driftstillstånd. Undersök i vilken utsträckning regleringens prestanda påverkas då den totala produktionen ändras (systemet kommer då att få andra parametrar, det är inte längre säkert att regulatorn fungerar bra!).

3. Koncentrationsreglering

Undersök en enkel koncentrationsreglerkrets. Då produktionen ändras, ändras löptiden från koncentrationsmätning till reglerventil. Analysera i vilken utsträckning det är nödvändigt att justera regulatorinställning för att ta hänsyn till den förändrade tidsfördröjning. Processen kan approximeras med en tidskonstant och en tidsfördröjning som är två à fem gånger större än tidskonstanten.

SYNTES

Använd den förenklade modellen för att undersöka i vilken utsträckning inloppslådereglering och ytviktsreglering kan interferera med varandra. Dimensionera en vettig regulator för den förenklade modellen baserad på linjärkvadratsteori och jämför med den förenklade modellen.

MÄTGIVARE OCH PRAKTISKA PROBLEM

Nedanstående uppgifter avser att något mera detaljerat studera de givare och praktiska system som används i samband med pappersmaskinreglering.

1. Koncentrationsmätning och koncentrationsreglering

Studiet bör omfatta åtminstone skärkraftgivare och optiska givare. Undersök kalibreringsproblem, reglerproblem etc.

2. Fukthaltsmätare

Undersökningen bör omfatta kapacitiva mikrovågsmätare och infrarödmätare.

3. Ytviktsmätare

Undersökningen bör åtminstone omfatta betamätare, infrarödmätare och akustiska mätare. I undersökningen bör även ingå uppskattningar av de priser på komponenterna som finns.

4. Flödesmätning

Undersökningen bör omfatta magnetiska flödesmätare, tryckdifferensmätare och venturierör.

5. Kommersiella system för pappersmaskinreglering

Studiet bör omfatta de datorstyrda system som för närvarande finns på marknaden t ex Measurex, Brun, ASEA, Accuray, Egenskaperna hos de olika systemen bör sammanställas.

PROCESSREGLERING i PAPPERSINDUSTRIN
Föredrag nr 3 1972-03-09
K.J. Åström

Pappersmaskinreglering del 1.

3. PAPPERSMASKINREGLERING

3.1. Inledning

En pappersmaskin kan grovt indelas i följande delar:

1. Inloppslåda
2. Viraparti
3. Pressparti
4. Torkparti
5. Efterbehandlings- och upprullningsanordningar
6. Motordrift

Det finns huvudsakligen tre typer av reglerproblem vid en pappersmaskin:

1. Reglering vid stationär drift
2. Omställningar (från en papperssort till en annan, men även mellan start och stopp)
3. Reglering vid katastroftillstånd

Hur man skall reglera vid stationär drift känner man till ganska bra, medan reglering vid omställningar är mindre undersökt.

Det bör noteras att de variabler som beskriver papperet är tvådimensionella: en längs-koordinat och en tvärs-koordinat. Det är då naturligt att tala om en variabels längsprofil respektive tvärsprofil.

Det finns en tro (som kan vara riktig) hos pappersmakare, som säger att alla variationer tvärs papperet är långsamma, medan alla variationer längs papperet är snabba.

De primära reglervariablerna hos en pappersmaskin är det totala mäldflödet (fiberflödet) och koncentrationen av fibrer i mälden.

Inloppslådans dynamik är väl utredd och de reglervariabler som är

av intresse är dels spaltbredden (läpp-öppningen) och dels luft-trycket (om man har en sluten inloppslåda).

Kunskapen om vad som händer på viran är mycket liten, men genom identifieringsexperiment hoppas man så småningom få större inblick i förloppet. Hastigheten hos viran är en variabel som går att reglera i denna del av pappersmaskinen.

Presspartiet är inte så mycket att orda om, ty här försöker man helt enkelt att pressa ut så mycket vatten som möjligt.

Torkpartiet är en komplicerad del, och exempel på reglervariabler är här ångtillflödet (man blåser ånga genom torkpartiet) och värme-tillförseln (man värmer upp valsarna). Hastigheten hos valsarna kan också regleras.

Motordriften slutligen kan beskrivas med välkända fysikaliska lagar.

De störningar som kommer in är huvudsakligen variationer av mäld-flödet och koncentrationen i mälden.

3.2 Inloppslådan

Syftet med inloppslådan är att se till att den mäld, som flyter in i inloppslådan genom ett rör, sprutar ut på viran med konstant hastighet och fiberkoncentrationen (konstant både i tiden och tvärs viran).

Det huvudsakliga reglerproblemet är att hålla utloppshastigheten (utsprutningshastigheten) konstant i tiden.

Man brukar definiera den s k utloppskvoten = $\frac{\text{utloppshastigheten}}{\text{virahastigheten}}$, som skall vara ungefär ett.

Om utloppskvoten inte är konstant, så kommer naturligtvis pappers-tjockleken att variera.

I fig. 3.2.1 visas en öppen inloppslåda. Utloppshastigheten bestäms huvudsakligen av vätskepelarens höjd, och med de hastigheter man idag kör pappersmaskiner (ca 400 m/min, tidningspappersmaskiner ända upp till 800 m/min), skulle denna höjd behöva vara flera tio-tal meter hög.

Det är därför naturligt att man gör inloppslådan sluten och höjer lufttrycket ovanför vätskepelaren istället (se fig. 3.2.2).

I fig. 3.2.3 finns en variant, nämligen sluten inloppslåda med Beloyt-hål. Man får en automatisk reglering av vätskenivån, vilken bör hållas relativt konstant av tekniska skäl. Hålet medför naturligtvis att det blir ett tryckfall i lådan jämfört med lådan i fig. 3.2.2.

En annan variant av sluten inloppslåda med överflödsskydd, där man slipper tryckfallet som blir i den föregående lådan, finns i fig. 3.2.4.

De störningar som kommer in är temperaturvariationer hos mälden och luften som pumpas in, samt variationer av mäldflödet och koncentrationen av fibrer i mälden. Även ojämn gång hos luftkompressorn kan ge störningar.

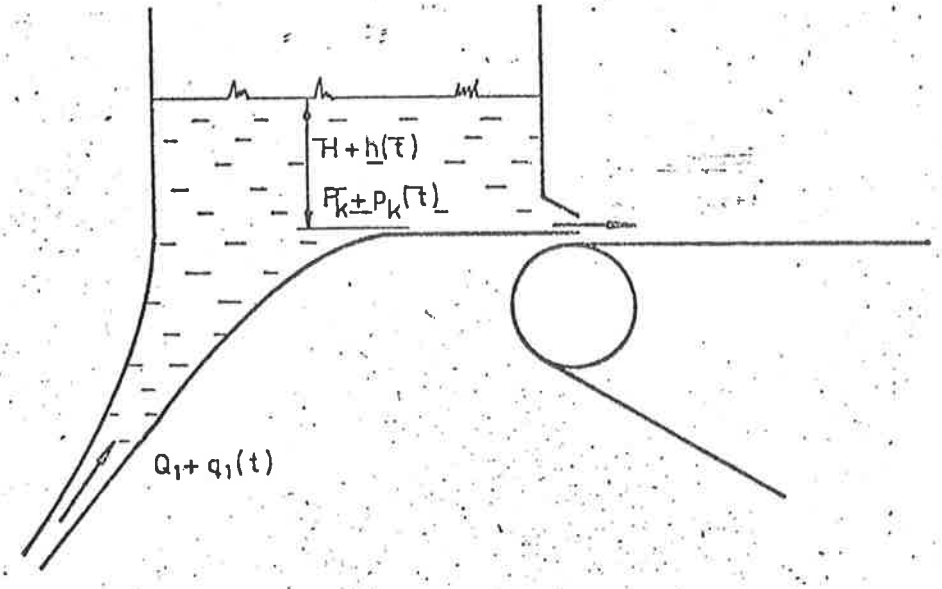

Fig. 3.2.1 SCHEMATIC DIAGRAM OF THE OPEN HEAD BOX.

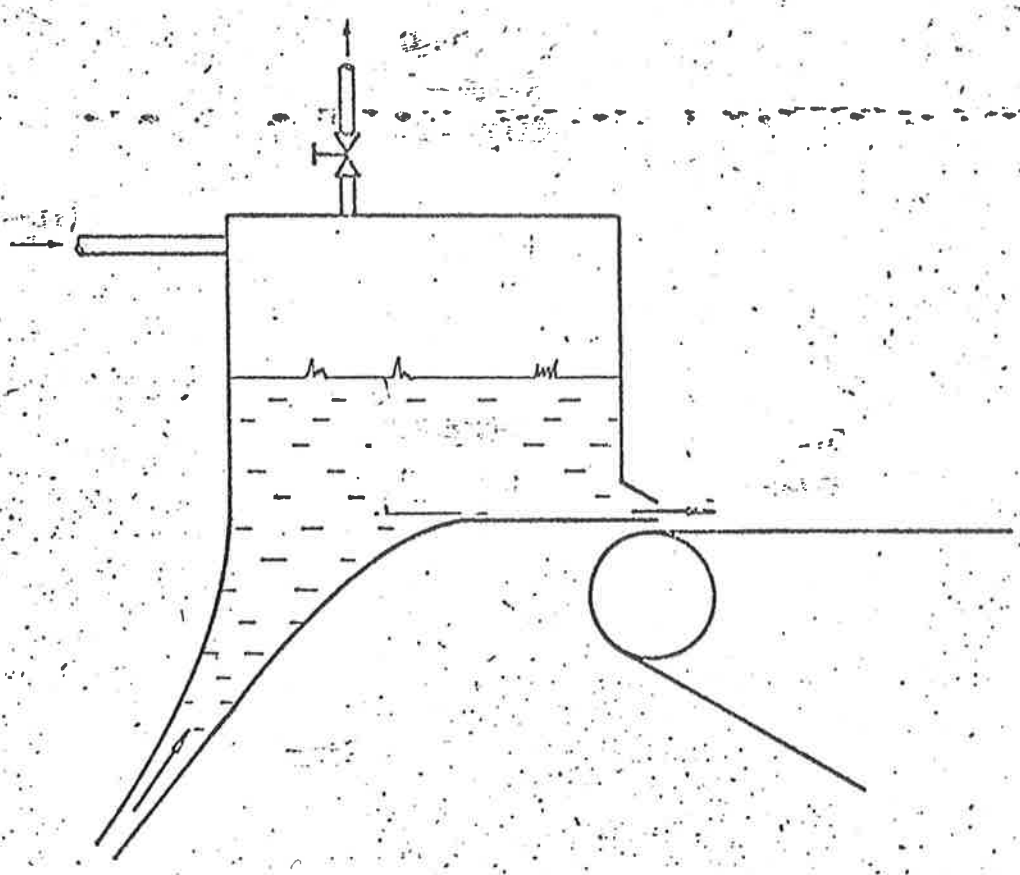

Fig. 3.2.2. SCHEMATIC DIAGRAM OF THE CLOSED HEAD BOX.

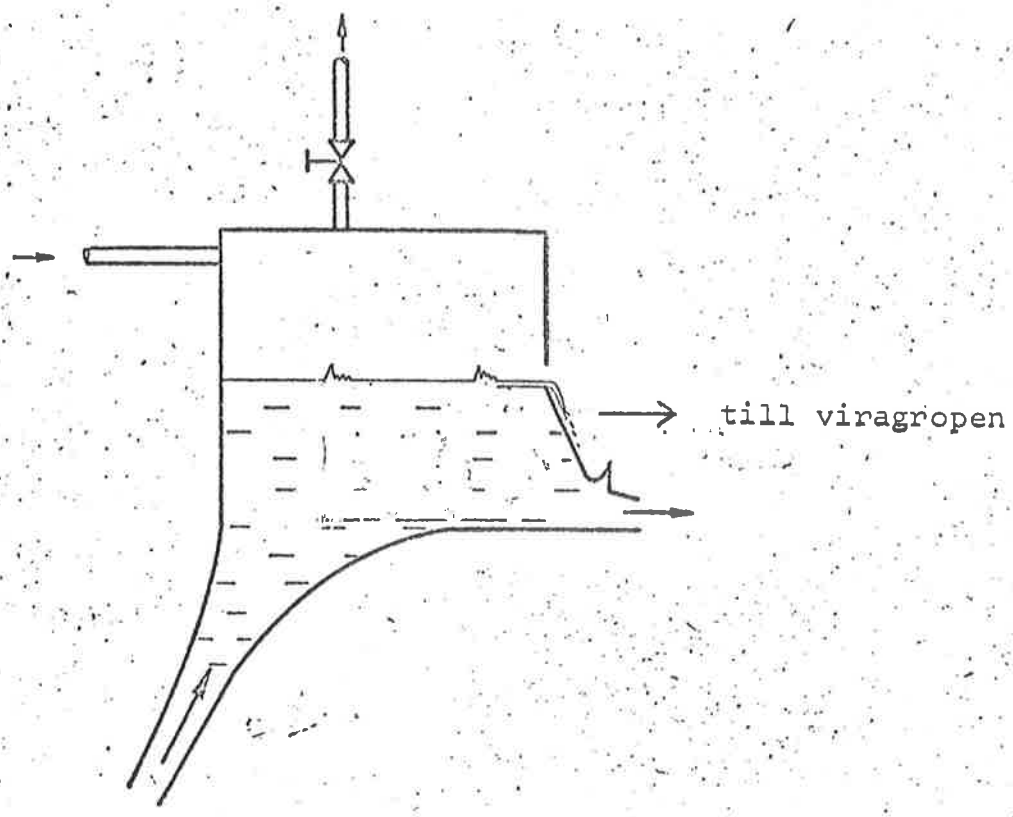

Fig. 3.2.3 SCHEMATIC DIAGRAM OF THE CLOSED HEAD BOX WITH Beloyt Hole

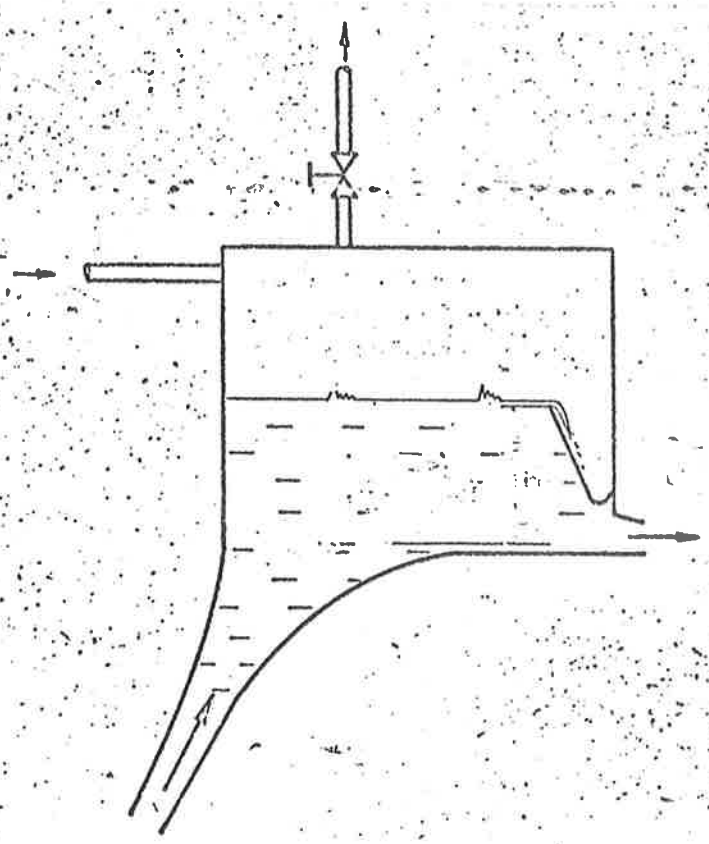

Fig 3.2.4. SCHEMATIC DIAGRAM OF THE CLOSED HEAD BOX WITH OVERFLOW.

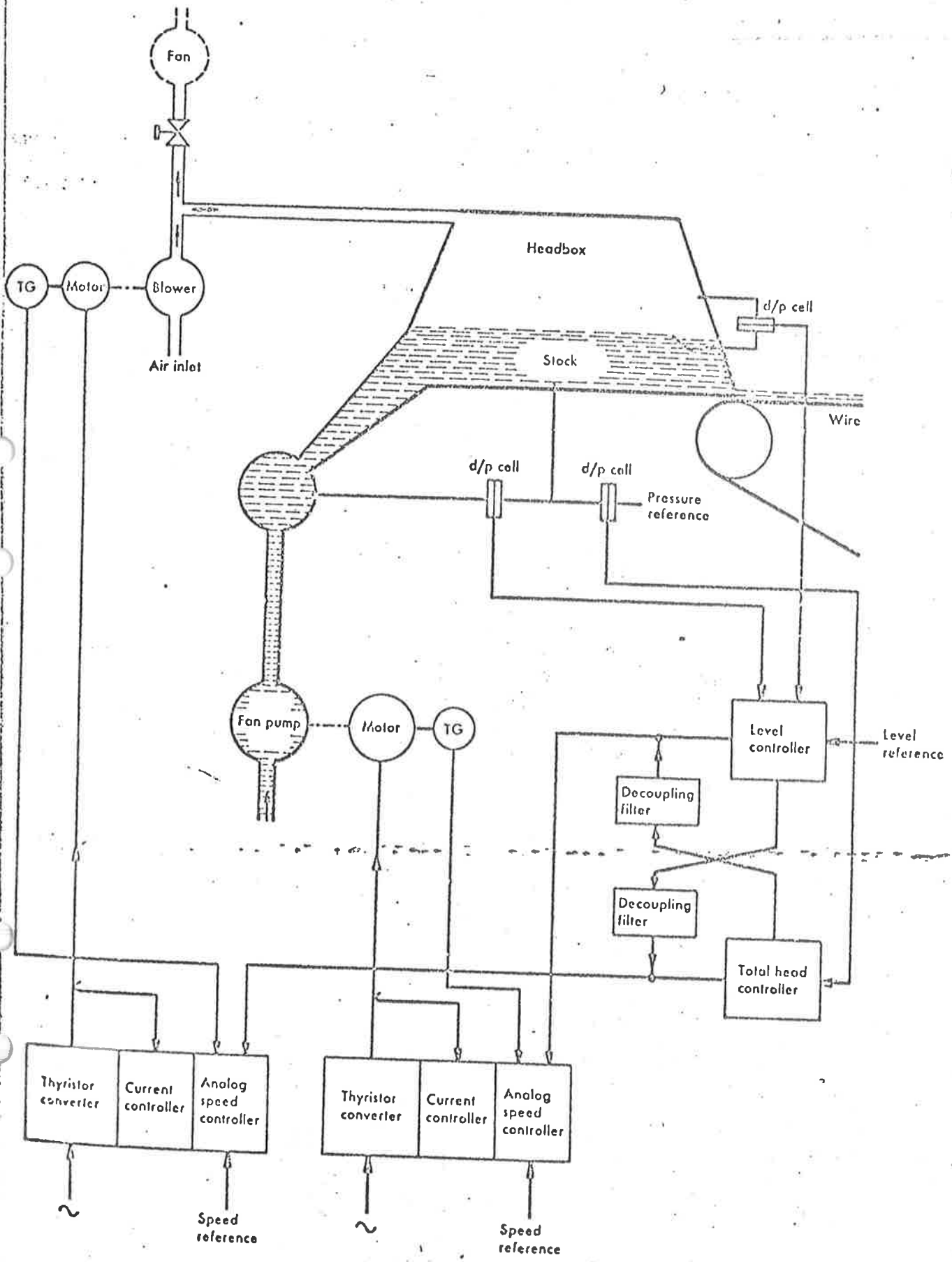

Fig.3.2.5. Schematic diagram of the ASEA headbox control system.
- Integrated total head and level control in the overflow channel.

De krav man brukar ställa på systemet är att utloppshastigheten får variera ca 1% av pappersmaskinhastigheten, medan vätskepelaren, som brukar ha en höjd av omkring 1 m, får variera ca 1 cm.

I fig. 3.2.5 finns ett schematiskt diagram över ett styrsystem för en inloppslåda. Det finns två ingångar, nämligen mälden och luften, och det finns två utgångar som man vill reglera, nämligen utloppshastigheten och vätskenivån. Det går även att justera läppöppningen men då påverkas i första hand mängden mäld som kommer ut på viran och i andra hand utloppshastigheten. Se fig. 3.2.6. Eftersom tidskonstantet är så lång (10-tal sekunder) används inte möjligheten att ändra på läppbalkens utseende för att reglera utloppshastigheten, medan den däremot används för att få en lämplig tvärsprofil av papperet.

Fig. 3.2.6. Exempel på hur man med skruvarna kan ändra på läppbalkens utseende (utböjningen något överdriven).

I fig. 3.2.5 finns element med beteckningen "d/p cell", d v s "differential pressure cell". I fig. 3.2.7-3.2.13 finns några olika tryckdetektorer. För funktionsbeskrivningar hänvisas till O.A. Solheim:"Instrumenteringsteknikk",Tapirs forlag, Trondheim 1966, sid 119-123.

Tidskonstanten för d/p-cellerna i reglersystemet i fig. 3.2.5 är liten (<0,1 sek). För att mäta en tryckdifferens med en d/p-cell måste man leda en del vätska genom ett rör till d/p-cellen och den totala tiden för att detektera en tryckändring i inloppslådan blir 0,5-1 sek. Genom att använda flänsmonterade tryckmätare kan tids-

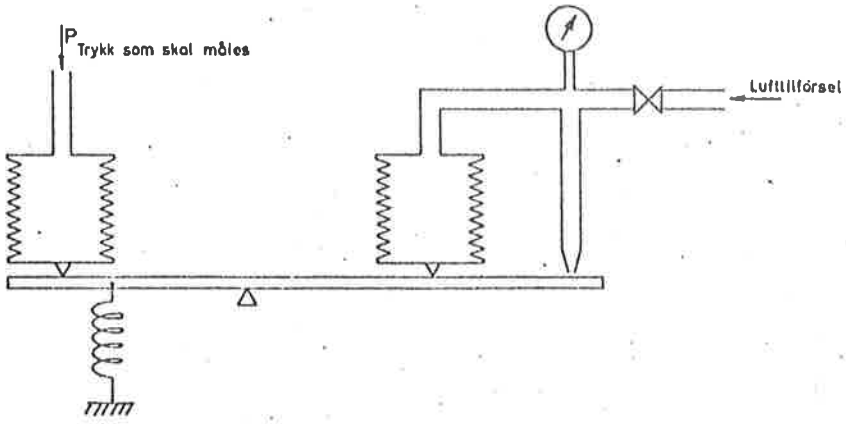

Fig. 3.2.7 Pneumatisk trykkdetektor, prinsipp.

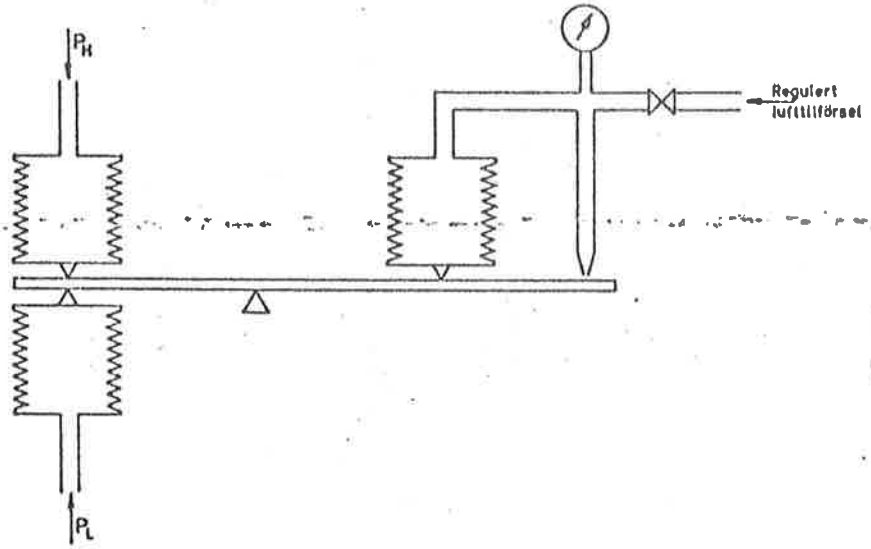

Fig. 3.2.8. Pneumatisk differensialtrykkdetektor, prinsipp.

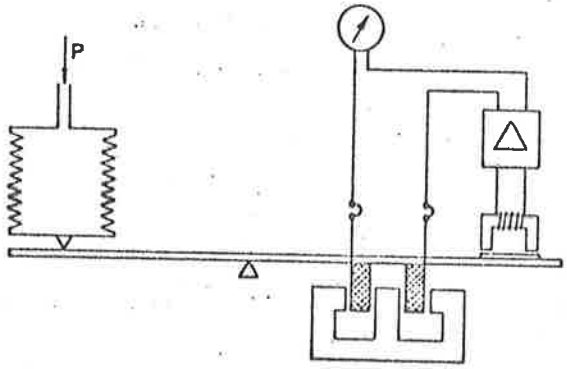

Fig. 3.2.9 Elektrisk trykkdetektor, prinsipp.

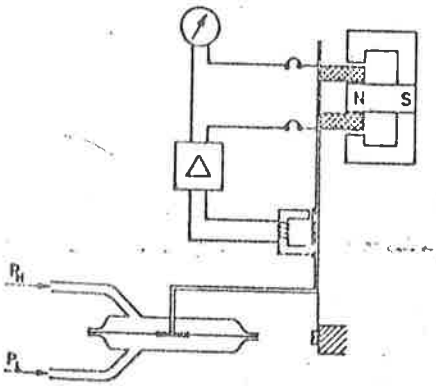

Fig.3.2.10 Elektrisk differensialtrykkdetektor, lineær karakt.

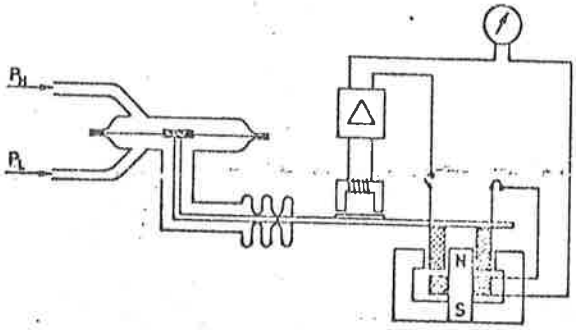

Fig.3.2.11 Elektrisk differensialtrykkdetektor, kvadratisk karakt.

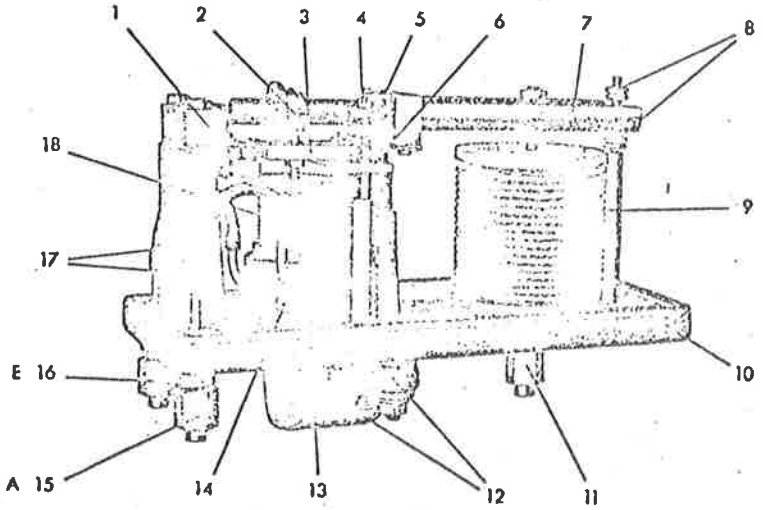

Fig. 3.2.12 Pneumatisk trykkdetektor (Samson).

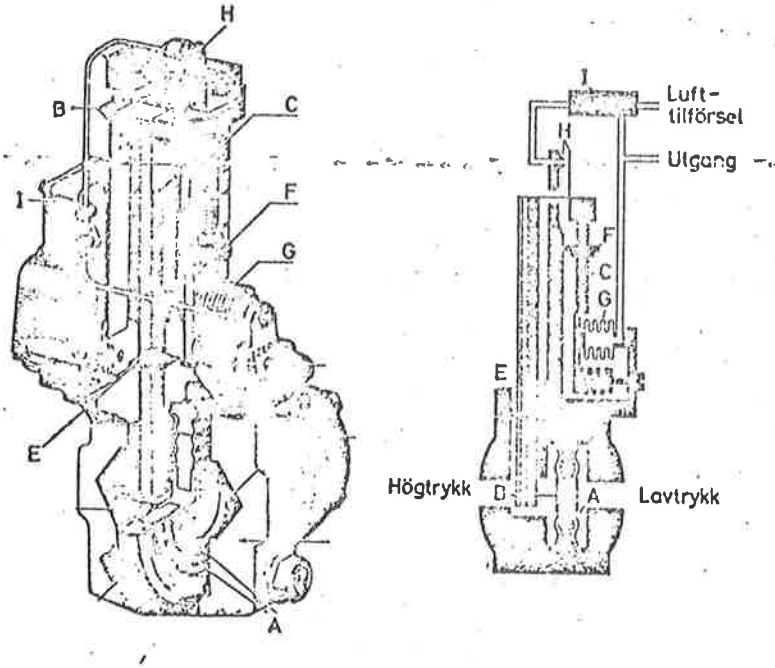

Fig. 3.2.13 Pneumatisk differensialtrykkdetektor (Foxboro).

konstanten minskas något. Detta har dock den nackdelen, att om tryckmätaren går sönder går det inte bara att stänga av flödet till mätaren och byta ut denna som man kan göra i det första fallet.

En tyristorstyrd blandningspump har en tidskonstant på 80-100 msek.

Istället för att styra flödet med blandningspumpen kan man använda en shuntventil enligt fig. 3.2.14.

Detta sätt används då man har tjocka rör. Man gör först en grovinställning med den stora ventilen och reglerar sedan med reglerventilen. Tidskonstanten är ca 1 sek, vilken är liten jämfört med om man bara hade reglerat med den stora ventilen.

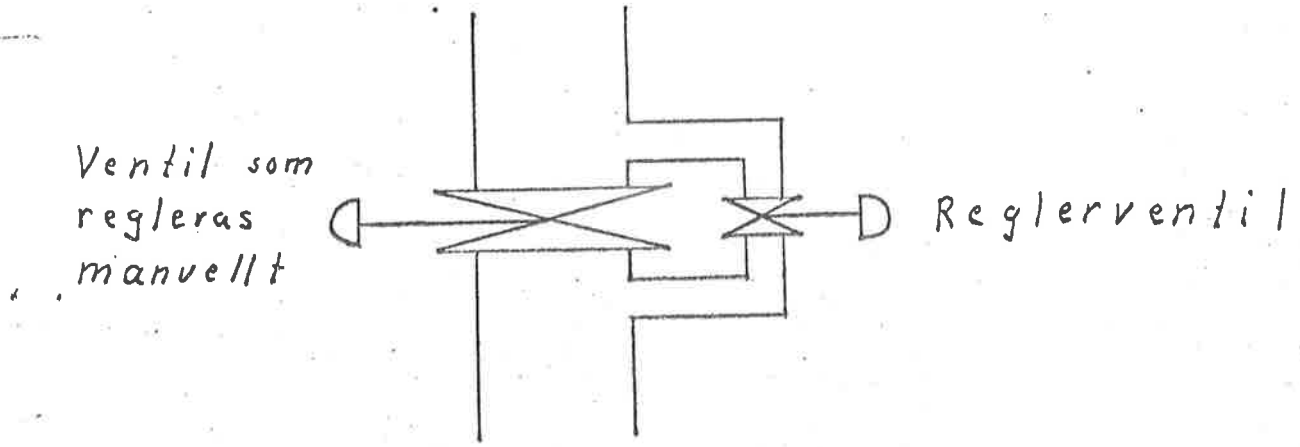

Fig. 3.2.14 Shuntventil

I fig. 3.2.5 styr man mäldflödet med blandningspumpen genom att mäta olika tryckdifferenser i inloppslådan. Ett annat sätt vore att mäta mäldflödet med en flödesmätare och sedan återkoppla till blandningspumpen.

I fig. 3.2.15-3.2.17 finns två typer av flödesmätare. Närmare beskrivning finns i Solheims bok sid. 127-144.

Det finns flera olika matematiska modeller som beskriver inloppslådans dynamik i litteraturen. I fig. 3.2.18-3.2.19 finns ett exempel som visar att man måste vara något försiktig när man använder

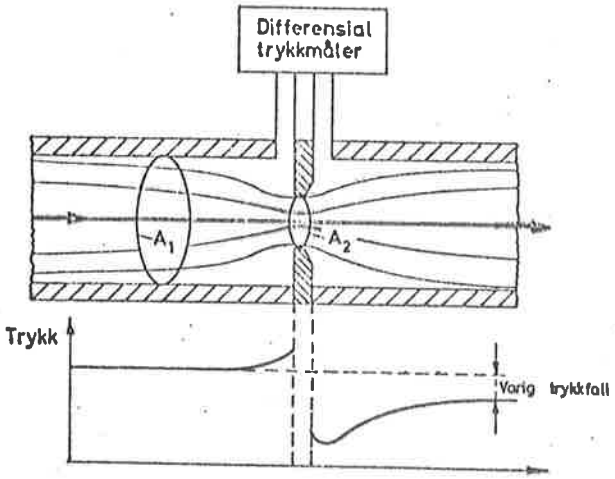

Fig. 3.2.15 Måleblende.

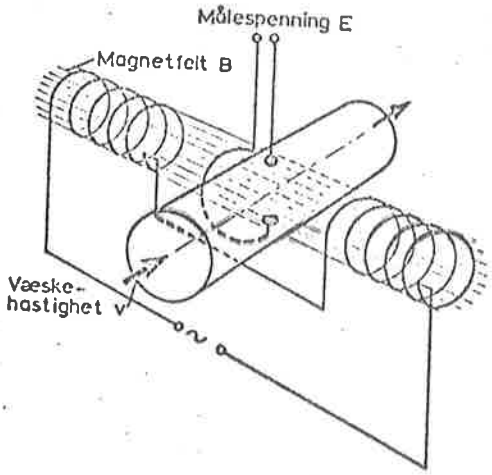

Fig. 3.2.16 Magnetisk strømningsmåler, prinsipp.

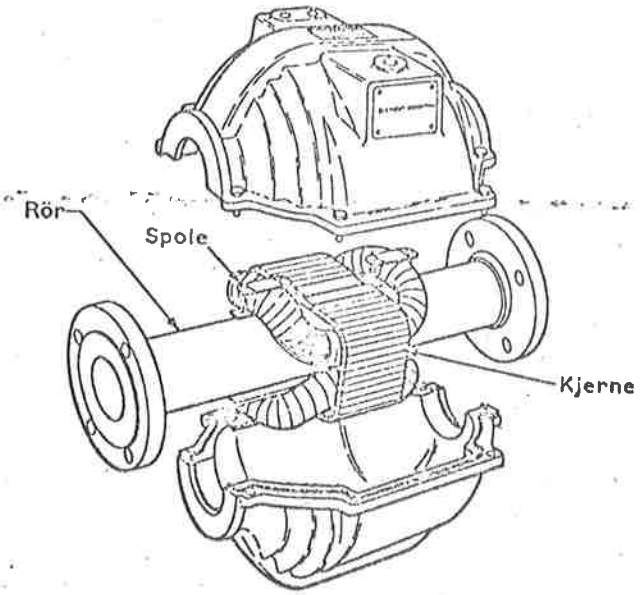

Fig. 3.2.17 Magnetisk strømningsmåler, konstruktiv utforming.

dem. Modellen ser ut att vara av 3:e ordningen men är egentligen av 2:a ordningen, ty två av blocken har samma nämnare. I fig. 3.2.20-3.2.22 finns några stegsvar uppritade.

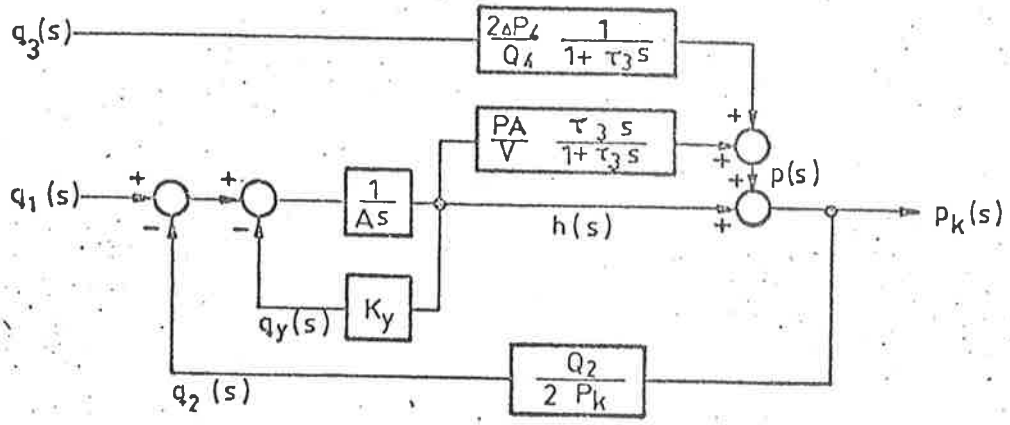

Fig.3.2.18 BLOCK SCHEME OF THE CLOSED HEAD BOX WITH OVERFLOW.

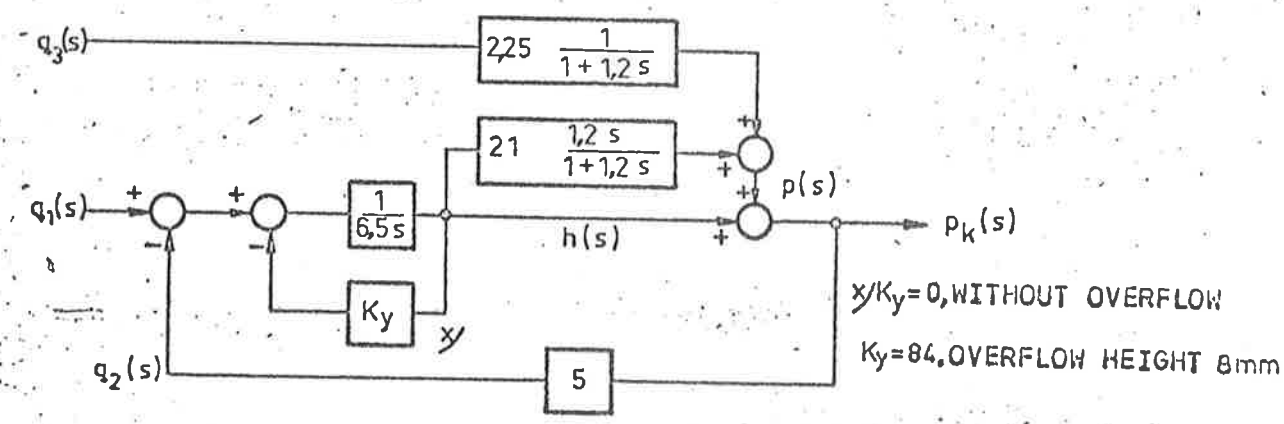

Fig.3.2.19 BLOCK SCHEME OF THE STUDIED HEAD BOX.

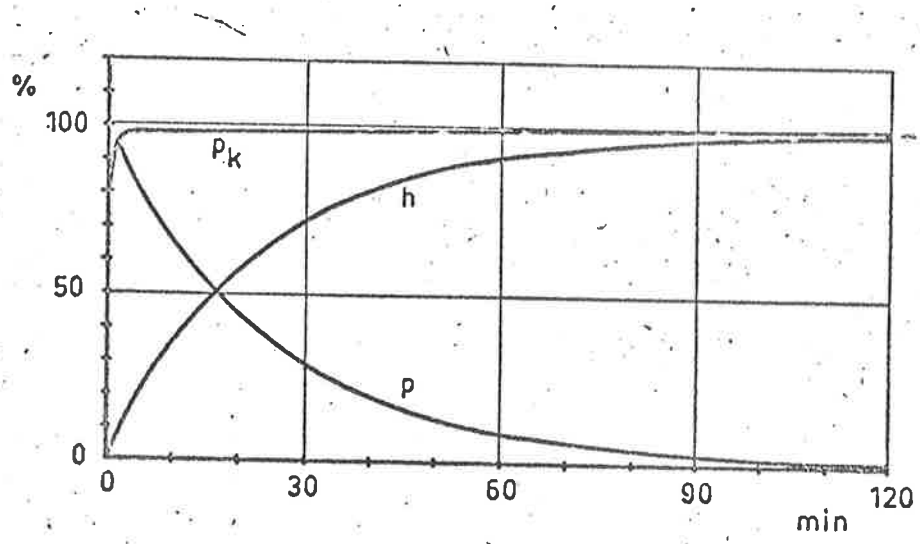

Fig.3.2.20 STEP RESPONSE FOR LIQUID INFLOW. NO CONTROLS APPLIED.

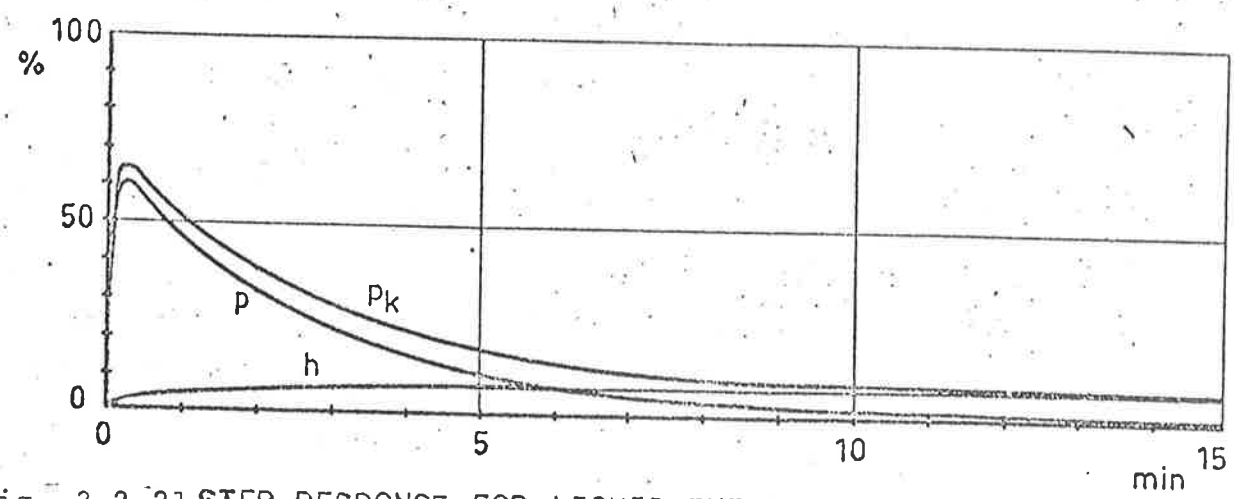

Fig. 3.2.21 STEP RESPONSE FOR LIQUID INFLOW. HEAD BOX WITH OVERFLOW. NO CONTROLS APPLIED.

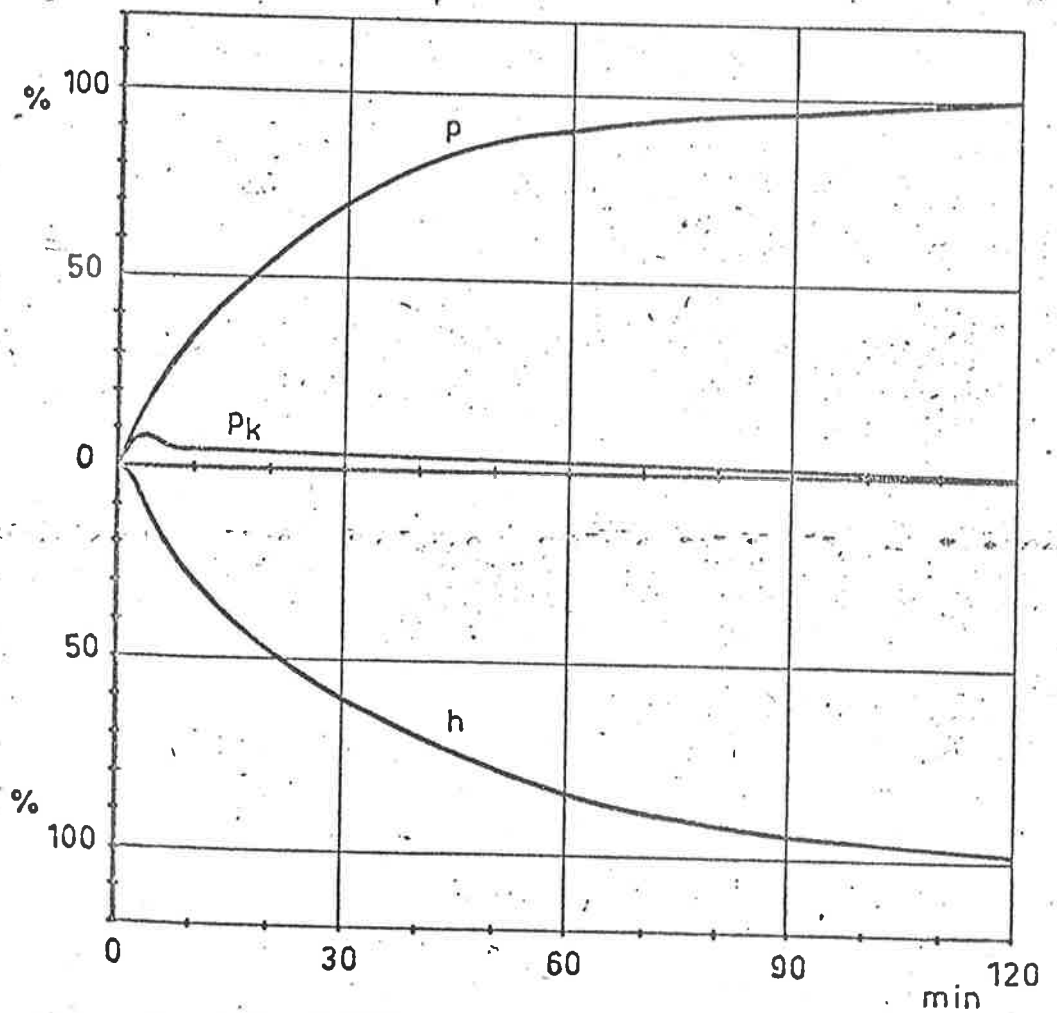

Fig.3.2.22 STEP RESPONSE FOR AIR INFLOW. NO CONTROLS APPLIED.

LECTURE NOTES ON PAPER MACHINE CONTROL

HEAD BOX FLOW DYNAMICS AND CONTROL

K J Åström

1. INTRODUCTION
2. WATER TANK DYNAMICS
3. AIR TANK DYNAMICS
   Discussion of Equation (3.4)
   Linearization
   Exercises
4. A NONLINEAR HEAD BOX MODEL
   The Stock Flow System
   The Air Flow System
   Summary
   Exercises
5. LINEARIZATION
   Block Diagram
   Observability and Controllability
   Invertibility
   Transfer Functions
   A Numerical Example
   Exercises
6. DESIGN OF CONTROL STRATEGIES
   Review of Disturbances
   Conventional Control
      The Total Pressure/Stock Flow System
      The Total Pressure/Air Flow System
   Pole Placement
   Design Using Linear Quadratic Control Theory
      Example 6.1
      Example 6.2
   Sensor and Actuator Dynamics
   Exercises
7. NOTES AND REFERENCES

1. INTRODUCTION

The purpose of the headbox is to change the turbulent flow in the tube going into the headbox to a sheet flow out of the head box. The properties of the headbox has a significant effect on the characteristics of the produced paper. In particular the ratio of the jet speed to the wire speed has been found to correlate nicely with many important quality variables. To control this ratio it is crucial to control the jet velocity accurately. A change in the jet speed will also influence the basis weight directly.

The headbox and its associated flow system is a complicated hydrodynamical device. In its design great care has been taken to ensure that no clustering of fibres can occur and that the flow is uniform. There are many different designs of headboxes. At low machine speed the headbox is frequently open. See fig. 1.1. Since the jet velocity is given by $\sqrt{2gh}$ we find that h = 1 m gives v = 4.42 m/sec (= 265 m/min). At higher machine speeds the headbox is closed and pressurized in order to make it possible to have higher jet velocities with reasonable values of h. The head box is then provided with an air pump and a control system to maintain air pressure. Fig. 1.2. A closed head box is sometimes also used at lower speeds. In such a case the pressure in the air cushion can be lower than the atmospheric pressure.

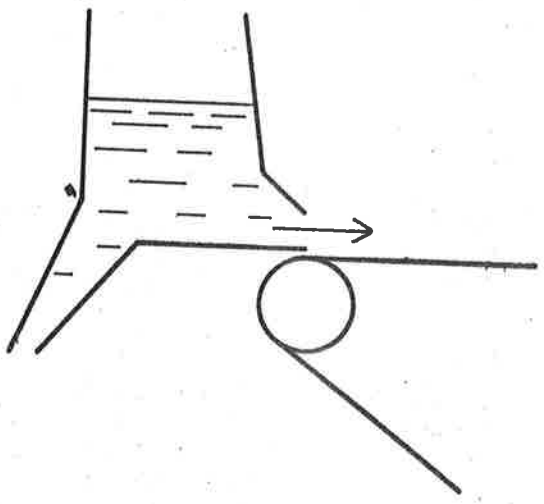

Fig. 1.1. Schematic diagram of an open headbox.

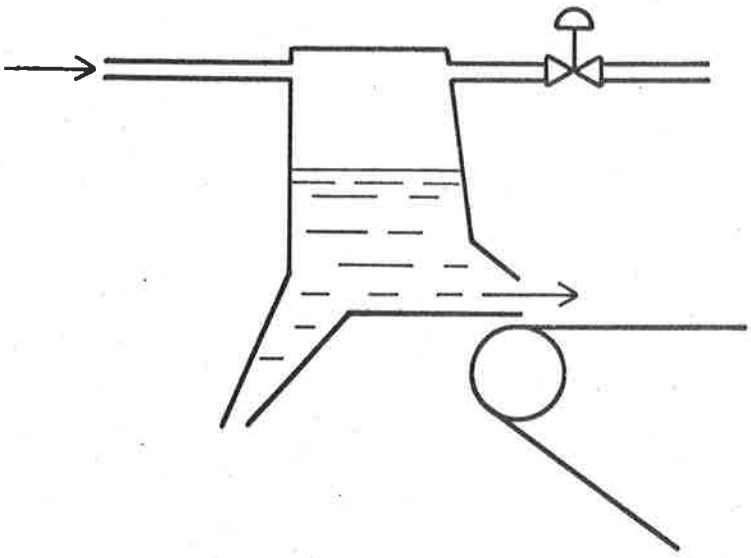

Fig. 1.2. Schematic diagram of a closed headbox.

The most important control problem for a headbox is thus to maintain constant jet velocity and to have a good dynamic behaviour when changing the headbox level. The variations are changes in stockflow and airflow into the headbox. These variables are in turn influenced by changes in stock temperature, stock consistency, air temperature, compressor flow etc. According to Lindström [1969] it is reasonable to require a peak-to-peak variation of jet speed of about 1 % at machine speeds below 8 m/sec and less at higher machine speeds. It is also of interest to keep the level variations within reasonable bounds. According to Lindström [1969] peak-to-peak variations of 2 - 20 mm are reasonable. Measurements by Lindström on many headbox systems in Sweden has shown that difficulties have been observed with pressure variations in the frequency range of 0.05 - 1 Hz and corresponding variations in jet speed of a few per cent.

The primary sensors are pressure ganges for total pressure (directly related to jet speed $v = \sqrt{2(p-p_o)/\rho}$) and air pressure. The major control variables are airflow and total stock flow. The airflow can be manipulated by a valve or by the compressor speed. The stock flow is manipulated through speed control of the mixing pump through a valve in a bypass line or through a level control of a levelbox (Källe). Many different systems are available for headbox control. Some systems have internal overflows and the level is regulated automatically. See Fig. 1.3. Other systems have the so-called Hornbostel hole which is simply a direct outlet as indicated in Fig. 1.4.

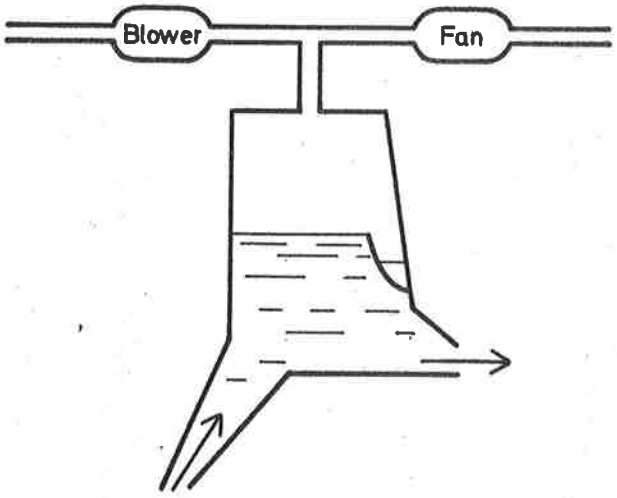

Fig. 1.3. An example of a control system for a headbox. The level is controlled using an internal overflow. The jet velocity is controlled by regulating the pressure in the air cushion.

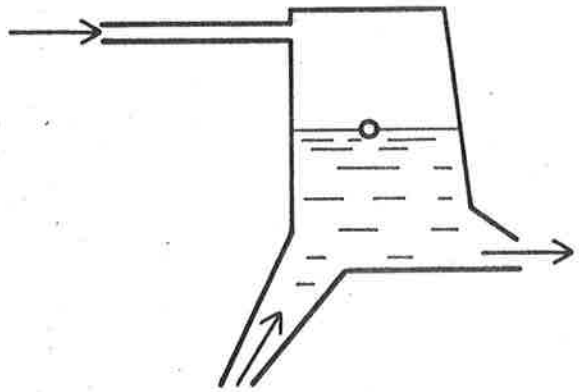

Fig. 1.4. Head box with Hornbostel hole. The level is controlled using an external overflow. The jet velocity is controlled by a feedback from the total pressure to the stock flow.

The dynamics of a closed headbox is simply the dynamics of interconnected fluid and gas-flow systems. The system is a good example of one which can be modeled fairly accurately from physical principles. The system has two inputs and two outputs and the coupling between the airflow system and the stockflow system is significant, it is therefore a true multivariable system.

The report is organized as follows.
Water tank dynamics and air tank dynamics are briefly reviewed in section 2 and section 3. In section 4 a nonlinear model of a headbox is then presented. This model is simply a combination of the water tank and gas tank dynamics discussed in the previous section. The nonlinear model is linearized in section 5. It turns out that the linearized model can be characterized by three coefficients only, the time constants associated with the water tank and gas tank dynamics and a coefficient which describes the interaction between the systems. The linearized dynamics are illustrated using

data for typical systems. The problems of headbox control are discussed in section 6. The discussion is based on the simple model of section 5 which does not include sensor and actuator dynamics. The effect of these are discussed in section 7 which also contains a discussion of other practical aspects of the headbox control problem as well as a few examples of commercial headbox control systems.

2. WATER TANK DYNAMICS

Consider a tank illustrated in fig. 2.1. Let h be the water level measured from the centre of the outlet, let A be the free surface and a the effective surface at the water outlet. The area A will in general depend on h. The outlet surface is assumed so small that there are no significant velocity variations across the surface.

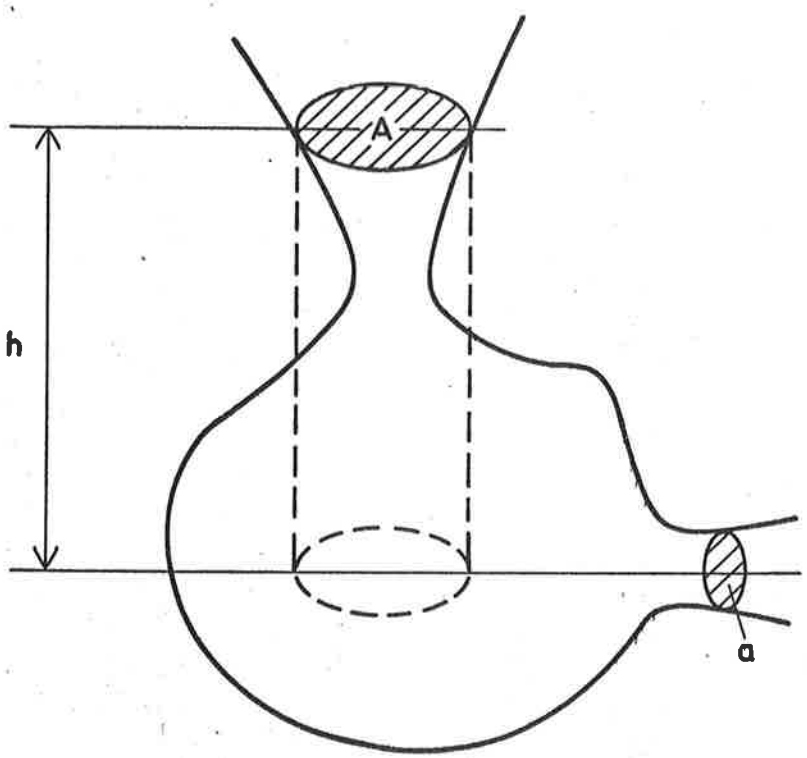

Fig. 2.1. Schematic diagram of a water tank.

Assuming constant density of the fluid a massbalance for the tank gives

$$\frac{d}{dt} V = q_1 - q_2 \qquad (2.1)$$

where q_1 is the input flow and q_2 the output flow. To determine q_2 an energy balance is used.

Applying Bernoullis theorem to a streamline starting at the free surface and ending in the outlet we get

$$\int_A^B \frac{\delta v}{\delta t} \cdot dr + \frac{1}{2}(v_B^2 - v_A^2) + \Omega + \int_A^B \frac{dp}{\rho} = 0 \qquad (2.2)$$

Neglecting the momentum term $\int \frac{\delta v}{\delta t}\, dr$, assuming that the density is constant and that the pressure at the outlet equals atmospheric pressure the energy equation (2.2) reduces to

$$\left[1 - \left(\frac{a}{A}\right)^2\right] v_B^2 = 2gh \qquad (2.3)$$

Assume that $a/A << 1$.

Since $V(h) = \int^h A(h)dh$ we get

$$\frac{dV}{dt} = A \frac{dh}{dt} \qquad (2.4)$$

the mass balance for the water tank can thus be represented by the differential equation

$$\frac{dh}{dt} = \frac{q_1}{A} - \frac{a}{A} \cdot \sqrt{2gh} \qquad (2.5)$$

It is thus first order dynamics with the level h as a state variable. The input flow q_1 and the area a can be regarded as input signals.

Linearization

It is often of interest to know the linearized dynamics. Assuming constant inflow $q_1 = q_o$ and constant outlet area a_o the steady state level is given by

$$h_o = \frac{1}{2g}\left(\frac{q_o}{a_o}\right)^2 \qquad (2.6)$$

Linearizing around this steady state value we find

$$\frac{d}{dt}(h-h_o) = -a(h-h_o) + b_1(q-q_o) + b_2(a-a_o) \qquad (2.7)$$

where

$$a = \frac{a\sqrt{2gh_o}}{2\,Ah_o} = \frac{q_o}{2V_o} \tag{2.8}$$

$$b_1 = 1/A$$

$$b_2 = \frac{q_o}{Aa_o}$$

The time constant of the system is thus

$$T = \frac{2V_o}{q_o} = \frac{2A_o h_o}{q_o} = \frac{A_o}{a_o}\sqrt{\frac{2h_o}{g}} = \frac{A_o q_o}{a_o^2 g} \tag{2.9}$$

where V_o is the volume of a cylinder of height h_o with base area A_o. The time constant is thus twice the time it takes to empty the volume V_o with the steady state flow q_o. The time constant is thus proportional to the steady state throughput flow q_o or proportional to the square root of the steady state level.

Exercises

1. Determine the equation corresponding to (2.5) when the crossection of the outlet is not small in comparison with the liquid area A. Also determine the corresponding linearized dynamics.

2. Determine the water tank dynamics when the diameter of the outlet is not small in comparison with h. Assume in particular that the outlet has a rectangualr crossection.

3. Analyse the effect of neglecting the momentum term in the water tank dynamics, Assume in particluar that the outlet is a cylinder with length ℓ and a crossection a_o. Introduce reasonable numerical values to illustrate the order of magnitude.

3. AIR TANK DYNAMICS

The dynamics of a tank containing a compressible gas will now be discussed. See fig. 3.1. The flow into the tank and the outlet area will be considered as input. Let the volume of the tank be V, the density of the gas in the tank be ρ and the pressure p. The dynamics are obtained using mass and energy balances and a state equation for the gas.

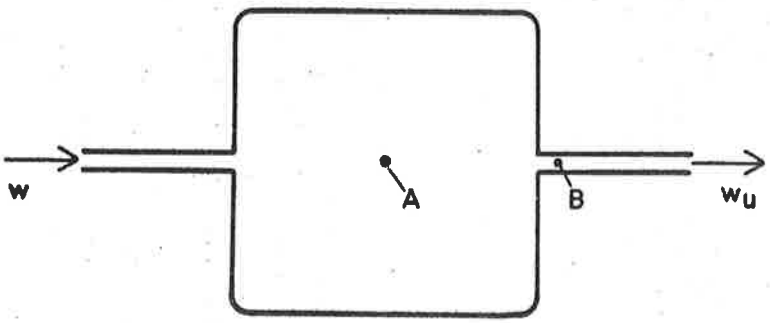

Fig. 3.1. Schematic diagram of an air tank.

A mass balance gives

$$\frac{d}{dt}(\rho V) = w_1 - w_2 \qquad (3.1)$$

where w_1 is the input massflow and w_2 the output massflow. The output massflow can be determined from an energy balance. (Bernoullis law eq.(2.2)). Neglecting the momentum term and the potential of the external forces and assuming that the velocity at the point A in fig. 3.1 can be neglected, Bernoullis law gives the velocity at B as

$$\frac{V_B^2}{2} + \int_A^B \frac{dp}{\rho} = 0 \qquad (3.2)$$

To evaluate the integral it is necessary to have a relation between p and ρ. This is obtained from the state equation of the gas. Assuming adiabatic state changes we find

$$p = p_A \left(\frac{\rho}{\rho_A}\right)^{\kappa} \qquad (3.3)$$

Differentiation of (3.3) gives

$$dp = \kappa p_A \left(\frac{\rho}{\rho_A}\right)^{\kappa-1} \frac{1}{\rho_A} d\rho$$

Hence

$$\int_A^B \frac{dp}{\rho} = \frac{\kappa}{\kappa-1} \cdot \frac{p_A}{\rho_A^{\kappa}} \cdot \left[\rho_B^{\kappa-1} - \rho_A^{\kappa-1}\right]$$

and the velocity of B is given by

$$v_B^2 = \frac{2\kappa}{\kappa-1} \cdot \frac{p_A}{\rho_A} \cdot \left[1 - \left(\frac{\rho_B}{\rho_A}\right)^{\kappa-1}\right] = \frac{2\kappa}{\kappa-1} \cdot \frac{p_B}{\rho_B} \cdot \left[\left(\frac{\rho_A}{\rho_B}\right)^{\kappa-1} - 1\right]$$

The massflow at B is thus given by

$$w_2 = \rho a V_B = a\sqrt{\frac{2\kappa}{\kappa-1} p_B \rho_B \left[\left(\frac{\rho_A}{\rho_B}\right)^{\kappa-1} - 1\right]}$$

$$= a\sqrt{\frac{2\kappa}{\kappa-1} \cdot p_A \rho_A \left[\left(\frac{p_B}{p_A}\right)^{2/\kappa} - \left(\frac{p_B}{p_A}\right)^{\frac{\kappa+1}{\kappa}}\right]} \qquad (3.4)$$

where the last equality is obtained using the state equation (3.3).

Discussion of Equation(3.4)

The expression (3.4) for the massflow will now be discussed. For this purpose it is assumed that the pressure p_A inside the tank is kept constant and that the external pressure p_o is changed. According to (3.4) the massflow is uniquely given by the pressure ratio p_B/p_A. See fig. (3.2).

When p_A is close to p_B the pressure p_B equals the external pressure. When p_B/p_A equals one, the massflow is zero.

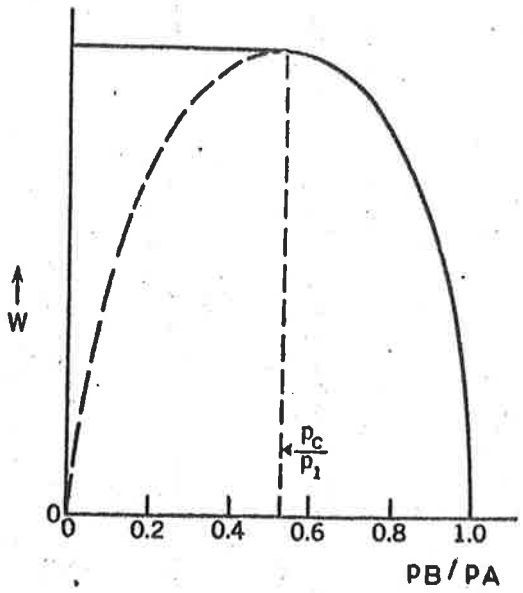

Fig. 3.2. The massflow w is given by (3.4) as a function of the pressure ratio (p_B/p_A).

As the external pressure is decreased the flow will increas until it reaches a maximum at the critical pressure.

$$P_B = P_c = P_A\left(\frac{2}{\kappa+1}\right)^{\frac{\kappa}{\kappa-1}} \qquad (3.4)$$

when the massflow is given by

$$w_c = a\cdot\left(\frac{2}{\kappa+1}\right)^{\frac{1}{\kappa-1}}\cdot\sqrt{\frac{2\kappa}{\kappa+1}\;P_A\rho_A} = a\left(\frac{2}{\kappa+1}\right)^{\frac{1}{\kappa-1}}\cdot\sqrt{\frac{2\kappa}{\kappa+1}\cdot\;P_o\rho_o\left(\frac{\rho_A}{\rho_o}\right)^{\kappa+1}}$$

If the external pressure p_o is reduced further the equation (3.4) indicates that the massflow will decrease. See dashed line in Fig. 3.2. This will not happen because the gas velocity will equal the speed of sound at the critical pressure p_c. The outside pressure then does not propagate into

the vessel he pressure difference $p_B - p_o$ will no longer be zero and the massflow will remain constant at w_c for further reductions of the outside pressure p_o.

Summing up we thus find that the massflow is given by

$$w_2 = \begin{cases} a\sqrt{\frac{2\kappa}{\kappa-1} p_o\rho_o \left[\left(\frac{\rho}{\rho_o}\right)^{\kappa-1} - 1\right]} & \frac{\rho}{\rho_o} < \left(\frac{\kappa+1}{2}\right)^{\frac{1}{\kappa-1}} \\ a\left(\frac{2}{\kappa+1}\right)^{\frac{1}{\kappa-1}} \sqrt{\frac{2\kappa}{\kappa+1} \cdot p_o\rho_o \left(\frac{\rho}{\rho_o}\right)^{\kappa+1}} & \frac{\rho}{\rho_o} > \left(\frac{\kappa+1}{2}\right)^{\frac{1}{\kappa-1}} \end{cases} \qquad (3.5)$$

For air we have $\kappa = 1.4$ and the critical pressure ration becomes $(p_B/p_A)_c = 1.89 ((\rho_B/\rho_A)_c = 1.58)$. The fact that the massflow is uniquely given by p_A and independent of p_B can be exploited to obatain an accurate massflow.

Having obtained an expression for the massflow out of the tank the dynamical properties can now be obtained by eliminating w between (3.1) and (3.5). Hence

$$\frac{d}{dt}(\rho V) = \begin{cases} w - a\sqrt{\frac{2\kappa}{\kappa-1} p_o\rho_o \left[\left(\frac{\rho}{\rho_0}\right)^{\kappa-1} - 1\right]}, & \frac{\rho}{\rho_0} < \left(\frac{\kappa+1}{2}\right)^{\frac{1}{\kappa-1}} \\ w - a\left(\frac{2}{\kappa+1}\right)^{\frac{1}{\kappa-1}} \sqrt{\frac{2}{\kappa+1} p_0\rho_0 \left(\frac{\rho}{\rho_0}\right)^{\kappa+1}}, & \frac{\rho}{\rho_0} > \left(\frac{\kappa+1}{2}\right)^{\frac{1}{\kappa-1}} \end{cases} \qquad (3.6)$$

Linearization

It is frequently of interest to consider small perturbations. The equations describing the tank can then be linearized. To linearize it is also assumed that the volume V is constant. Assuming that the massflow into the tank is constant w_s and that the outlet area is constant a_s. The gas density in the tank will then assume a stationary value ρ_s, Linearizing the equation (3.6) we get

$$\frac{d}{dt}(\rho-\rho_s) = -a_1(\rho-\rho_s) + b_1(w-w_s) + b_2(a-a_s) \qquad (3.7)$$

where

$$a_1 = \begin{cases} \dfrac{w_s}{\rho_s V} \quad \dfrac{\kappa-1}{2} \quad \dfrac{(\rho_s/\rho_0)^{\kappa-1}}{(\rho_s/\rho_0)^{\kappa-1}-1} & \rho_s/\rho_0 < \left(\dfrac{\kappa+1}{2}\right)^{\frac{1}{\kappa-1}} \\ \dfrac{w_s}{\rho_s V} \quad \dfrac{\kappa+1}{2} & \rho_s/\rho_0 > \left(\dfrac{\kappa+1}{2}\right)^{\frac{1}{\kappa-1}} \end{cases}$$

$$b_1 = 1/V \qquad (3.8)$$

$$b_2 = \frac{w_s}{aV}$$

The linearized tank dynamics can thus be described as a first order system with the time constant

$$T = \begin{cases} \dfrac{M}{w_s} \quad \dfrac{2}{\kappa-1} \quad \dfrac{(\rho_s/\rho_0)^{\kappa-1}-1}{(\rho_s/\rho_0)^{\kappa-1}} & \rho_s/\rho_0 < \left(\dfrac{\kappa+1}{2}\right)^{\frac{1}{\kappa-1}} \\ \dfrac{M}{w_s} \quad \dfrac{2}{\kappa+1} & \rho_s/\rho_0 > \left(\dfrac{\kappa+1}{2}\right)^{\frac{1}{\kappa-1}} \end{cases} \qquad (3.9)$$

Notice that M is the total mass of the gas inside the tank.

Exercises

1. Determine a dynamical model for an air tank when the momentum term is included. Assume in particular that the outlet is a tube of length ℓ with cross section a. Introduce reasonable numbers and give a (subjective) criterion which tells when the momentum term has a negligible effect on the dynamics.

2. Determine the air tank dynamics when it is assumed that the state changes of the gas are isotermic instead of adiabatic.

4. A NONLINEAR HEAD BOX MODEL

Having discussed the dynamics of a simple water tank and a simple air tank we will now consider the headbox dynamics. In the introduction it was stated that there are many variations in the design of a headbox. Since we are striving for insight rather than detailed analysis of a particular system only a simple version will be considered. Once the principles are understood it is then a straightforward matter to extend the analysis to other types of systems. It is thus assumed that the air cushion of the headbox is pressurized using a pump and that the airflow is manipulated either through the massflow into the headbox or through a valve at the outlet. A schematic diagram of the headbox is shown in fig. 4.1.

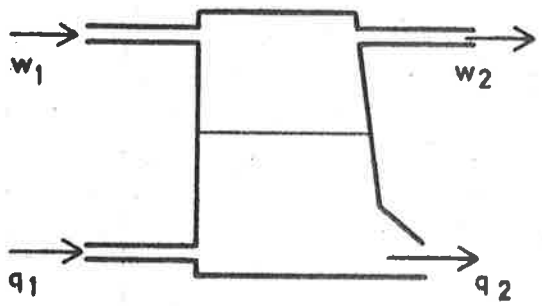

Fig. 4.1. Schematic diagram of a closed head box.

The model will be derived in a straight forward manner using mass-balances energy balances and state equations for the air and the stack in the head box.
Experience has shown that the models obtained in this way agree well with the dynamical behaviour observed in practice. See e.g. Lindström [1969] and Talvio [1969].

The major assumption done in the analysis are as follows.

- The momentum terms in the energy balances for the air and stock are neglected.

- The outlet areas are considered small in comparison with the cross section of the tank.

- The density of the stock is assumed constant.

- The state changes of the air are assumed adiabatic.

To describe the process the following notation is introduced

w_1 airflow into head box $[kg/sec]$
w_2 airflow out of head box $[kg/sec]$
q_1 stockflow into head box $[m^3/sec]$
q_2 stockflow out of head box $[m^3/sec]$
h water level $[m]$
A liquid area $[m^2]$
A_1 effective opening of air outlet $[m^2]$
A_2 effective slice area $[m^2]$
ρ air density in head box $[kg/m^3]$
ρ_o air density at atmospheric pressure $[N/m^2]$
p head box pressure $[N/m^2]$
p_o atmospheric pressure $[N/m^2]$
ρ_2 stock density $[kg/m^3]$
V air volume $[m^3]$

The dynamics of the system is the dynamics of the gas flow and the dynamics of the airflow. Since the air pressure has a significant effect of the stock flow and the level has a significant influence on the airflow the systems are strongly coupled.

The Stock Flow System

A massbalance for the stock in the head box gives

$$\frac{d}{dt}(\rho V) = \rho_2 q_1 - \rho_2 q_2 \qquad (4.1)$$

Since ρ_2 is assumed constant and

$$\frac{d}{dt} V_2 = A \frac{dh}{dt}$$

the massbalance (4.1) can be written as

$$A \frac{dh}{dt} = q_1 - q_2 \qquad (4.2)$$

The flow out of the head box can be determined from an energy balance (Bernoullis theorem). We get

$$\int_A^B \frac{\partial v}{\partial t} dr + \frac{1}{2}\left[v_B^2 - v_A^2\right] + \Omega_B - \Omega_A + \int_A^B \frac{\partial p}{\partial \rho} = 0 \qquad (4.3)$$

where v is the velocity dr the lineelement along a streamline, Ω the gravity potential, p the pressure and ρ the fluid density. To apply the Bernoulli therorem we neglect the momentum term. This is perfectly legitimate since this term gives rise to dynamics of the order of magnitude of the effective flow time through the system. To integrated (2.3) we must also have a relation between p and ρ. Assuming that the stock is incompressible i.e. $\rho = \rho_2$ we get

$$\frac{v^2}{2} = gh + \frac{p-p_0}{\rho_2}$$

or

$$q_2 = A_2 \sqrt{2gh + 2\frac{p-p_0}{\rho_2}}$$

The massbalance (4.2) for the stock can thus be written as

$$\frac{dh}{dt} = \frac{q_1}{A} - \frac{A_2}{A}\sqrt{2gh + 2\frac{p-p_0}{\rho_2}} \qquad (4.4)$$

Compare with the corresponding equation for a simple water tank system, eq. (2.5).

The Air Flow System

A massbalance for the air in the head box gives

$$\frac{d}{dt}(\rho V) = w_1 - w_2 \qquad (4.5)$$

To determine the air flow out of the head box an energy balance is used. The momentum term in (4.3) is again neglected. To integrate the term $\int dp/\rho$ a relation between the pressure and the density of the gas is needed. Under the assumption of adiabatic state changes we find

$$\frac{p}{p_0} = \left(\frac{\rho}{\rho_o}\right)^{\kappa} \qquad (4.6)$$

Neglecting the momentum term $\int \frac{\partial v}{\partial t}\, dr$ in the energy balance (2.2) the air velocity in the outlet becomes

$$v = \begin{cases} \sqrt{\frac{2\kappa}{\kappa-1}\,\frac{p_o}{\rho_o}\left[\left(\frac{\rho}{\rho_o}\right)^{\kappa-1} - 1\right]} & \frac{\rho}{\rho_o} < \left(\frac{\kappa+1}{\kappa}\right)^{\frac{1}{\kappa-1}} \\ \left(\frac{2}{\kappa+1}\right)^{\frac{1}{\kappa-1}} \sqrt{\frac{2\kappa}{\kappa-1} \cdot \frac{p_o}{\rho_o} \cdot \left(\frac{\rho}{\rho_o}\right)^{\kappa+1}} & \frac{\rho}{\rho_o} > \left(\frac{\kappa+1}{\kappa}\right)^{\frac{1}{\kappa-1}} \end{cases}$$

The massflow w_2 is then given by

$$w_2 = \rho_o A_1 v = \begin{cases} A_1 \sqrt{\frac{2\kappa}{\kappa-1} p_o \rho_o \left[\left(\frac{\rho}{\rho_o}\right)^{\kappa-1} - 1\right]} & \frac{\rho}{\rho_o} < \left(\frac{\kappa+1}{\kappa}\right)^{\frac{1}{\kappa-1}} \\ A_1 \left(\frac{2}{\kappa+1}\right)^{\frac{1}{\kappa-1}} \sqrt{\frac{2\kappa}{\kappa-1} p_o \rho_o \left(\frac{\rho}{\rho_o}\right)^{\kappa+1}} & \frac{\rho}{\rho_o} > \left(\frac{\kappa+1}{\kappa}\right)^{\frac{1}{\kappa-1}} \end{cases} \qquad (4.7)$$

Furthermore

$$\frac{d}{dt}(\rho V) = V \frac{d\rho}{dt} + \rho \frac{dV}{dt}$$

and

$$\frac{dV}{dt} = - A \frac{dh}{dt}$$

where A in general is a function of h.

Hence

$$\frac{d}{dt}(\rho V) = V \frac{d\rho}{dt} - \rho A \frac{dh}{dt} \qquad (4.8)$$

Combining the equations (4.5), (4.1) and (4.8) we now find that the massbalance for the air in the head box can be written as

$$\frac{d\rho}{dt} = - \frac{A_1}{V} \sqrt{\frac{2\kappa}{\kappa-1} p_o \rho_o \left[\left(\frac{\rho}{\rho_o}\right)^{\frac{\kappa+1}{\kappa}} - 1 \right]} + \frac{w_1}{V}$$

$$- \frac{\rho A_2}{V} \sqrt{2gh + 2 \frac{p_o}{\rho_2} \left[\left(\frac{\rho}{\rho_o}\right)^{\kappa} - 1 \right]} + \frac{q_1}{V} \qquad (4.9a)$$

when the airflow in the outlet is subsonic i.e. when

$$\frac{\rho}{\rho_o} < \left(\frac{\kappa+1}{\kappa}\right)^{\frac{1}{\kappa+1}}$$

and

$$\frac{d\rho}{dt} = - \frac{A_1}{V} \left(\frac{2}{\kappa+1}\right)^{\frac{1}{\kappa-1}} \sqrt{\frac{2\kappa}{\kappa-1} p_o \rho_o \left(\frac{\rho}{\rho_o}\right)^{\kappa+1}} + \frac{w_1}{V}$$

$$- \frac{\rho A_2}{V} \sqrt{2gh + 2 \frac{p_o}{\rho_2} \left[\left(\frac{\rho}{\rho_o}\right)^{\kappa} - 1 \right]} + \frac{\rho q_1}{V} \qquad (4.9b)$$

when the airflow in the outlet is supersonic i.e.

$$\frac{\rho}{\rho_o} \quad \left(\frac{\kappa+1}{\kappa}\right)^{\frac{1}{\kappa+1}}$$

The state equation (4.6) has been used to express p as a function of ρ in the third terms of the right members of (4.9a) and (4.9b).

Compare (4.9) with the corresponding equations for a simple air tank.eq. (3.6).

Summary

Summing up we find that the head box dynamics can be described by the equations

$$\frac{dh}{dt} = -\frac{A_2}{A}\sqrt{2gh + 2\frac{p_o}{\rho_2}\left[\left(\frac{\rho}{\rho_o}\right)^{\kappa} - 1\right]} + \frac{q_1}{A}$$

$$\frac{d\rho}{dt} = -\frac{A_1}{V}\sqrt{\frac{2\kappa}{\kappa-1}\,p_o\rho_o\left[\left(\frac{\rho}{\rho_o}\right)^{\kappa-1} - 1\right]} - \frac{\rho A_2}{V}\sqrt{2gh + 2\frac{p_o}{\rho_2}\left[\left(\frac{\rho}{\rho_o}\right)^{\kappa} - 1\right]}$$

$$+ \frac{w_1}{V} + \frac{q_1}{V}, \qquad \frac{\rho}{\rho_o} < \left(\frac{\kappa+1}{\kappa}\right)^{\frac{1}{\kappa+1}}$$

$$\frac{d\rho}{dt} = -\frac{A_1}{V}\left(\frac{2}{\kappa+1}\right)^{\frac{1}{\kappa-1}}\sqrt{\frac{2\kappa}{\kappa-1}\,p_o\rho_o\left(\frac{\rho}{\rho_o}\right)^{\kappa+1}} - \frac{\rho A_2}{V}\sqrt{2gh + 2\frac{p_o}{\rho_2}\left[\left(\frac{\rho}{\rho_o}\right)^{\kappa} - 1\right]}$$

$$+ \frac{w_1}{V} + \frac{q_1}{V}, \qquad \frac{\rho}{\rho_o} > \left(\frac{\kappa+1}{\kappa}\right)^{\frac{1}{\kappa+1}} \qquad (4.10)$$

where the air density ρ and the water-level in the head box are chosen as the state variables. Notice that A and V in general will be functions of h. It is frequently of interest to know the air pressure in the nead box and the velocity of the stock flow out of the head box. These variables are considered as outputs.

$$v = \sqrt{2gh + 2\frac{p-p_o}{\rho_2}} = \sqrt{2gh + 2\frac{p_o}{\rho_2}\left[\left(\frac{\rho}{\rho_o}\right)^{\kappa} - 1\right]}$$

$$p = p_o\left(\frac{\rho}{\rho_o}\right)^{\kappa} \qquad (4.11)$$

Notice the physical interpretations of the different terms of the model. The interaction of the air pressure on the level is only indirectly through the influence of the air pressure on outflow velocity. The stockflow influences the rate of change of ρ directly through the compression of the air cushion. Also notice that if there

was no interaction between the air and fourth ters of the right member of the equation for $\frac{dp}{dt}$ would vanish.

The head box dynamics can thus be represented by a second order nonlinear dynamical system. The model is characterized by 9 parameters. The parameters A, A_1, A_2 and V depend on the construction data. Five parameters are fundamental physical parameters ρ_o, ρ_2, p_o, κ and g. The values of q_1 and w_1 depend on the operating conditions. The unknown parameters are easy to determine for a given system.

Exercises

1. The choice of state variables is to a certain extent arbitrary. Propose other sets of state variables and discuss their relative merits.

2. Determine a nonlinear model for an head box according to Fig. 1.3 with an internal overflow.

3. Determine a nonlinear model for a head box with Hornbostel hole according to Fig. 1.4.

4. Determine the dynamics of a simple closed head box when the state changes of the air are assumed isotermic.

5. LINEARIZATION

It was found in section 4 that the head box dynamics can be described as a second order nonlinear dynamical system. To design control strategies for steady state control it is convenient to have linearized models which approximate the nonlinear dynamics for small perturbations around a steady state. Assume that the following control variables are constant.

$q_1 = q_s$	stock flow
$w_1 = w_s$	air flow
$A_1 = A_{1s}$	area of air outlet
$A_2 = A_{2s}$	area of slice opening

It then follows from the equations (4.10) that the stock level h and the air density ρ assume constant steady state values as given by

$$\rho_s = \rho_o \left(1 + \frac{\kappa-1}{\kappa} \cdot \frac{w_1^2}{p_o \rho_o A_1^2}\right)^{\frac{1}{\kappa-1}}$$

$$h_s = \frac{1}{g}\left[\frac{q_1^2}{2A_2^2 g} - \frac{p_o}{\rho_2 g}\left[\left(\frac{\rho_s}{\rho_o}\right)^{\kappa} - 1\right]\right] \tag{5.1}$$

Linearizing the equations (4.1) and (4.11) around the stationary solution h_s, q_s given by (5.1) we get

$$\frac{d}{dt}\begin{bmatrix} h-h_s \\ \rho-\rho_s \end{bmatrix} = \begin{bmatrix} a_{11} & a_{12} \\ a_{21} & a_{22} \end{bmatrix}\begin{bmatrix} h-h_s \\ \rho-\rho_s \end{bmatrix} + \begin{bmatrix} b_{11} & b_{12} & 0 & 0 \\ b_{21} & b_{22} & b_{23} & b_{24} \end{bmatrix}\begin{bmatrix} q_1 - q_s \\ A_2 - A_{1s} \\ w_1 - w_s \\ A_1 - A_{1s} \end{bmatrix} \tag{5.2}$$

$$p - p_s = \frac{\kappa p_s}{\rho_s}(\rho - \rho_s)$$

$$v - v_s = \frac{v_s}{2}\left[\frac{h-h_s}{h_{eff}} + \frac{\kappa \ell}{h_{eff}} \cdot \frac{\rho-\rho_s}{\rho_s}\right] \tag{5.3}$$

where

$$a_{11} = -\alpha_1 = -\frac{q_s}{2Ah_{eff}}$$

$$a_{12} = -\alpha_1 \frac{\kappa \ell}{\rho_s}$$

$$a_{21} = -\frac{\rho A}{V} \cdot \alpha_1$$

$$a_{22} = -\alpha_2 - \beta\alpha_1$$

$$\alpha_1 = \frac{q_s}{2Ah_{eff}}$$

$$\alpha_2 = \begin{cases} \dfrac{w_s}{2\rho_s V} \dfrac{(\kappa-1)(\rho_s/\rho_o)^{\kappa-1}}{(\rho_s/\rho_o)^{\kappa-1}-1} & \dfrac{\rho_s}{\rho_o} \leq \left(\dfrac{\kappa+1}{2}\right)^{\frac{1}{\kappa-1}} \\ \dfrac{w_s}{2\rho_s V}(\kappa+1) & \dfrac{\rho_s}{\rho_o} \geq \left(\dfrac{\kappa+1}{2}\right)^{\frac{1}{\kappa-1}} \end{cases}$$

$$\beta = \kappa A \ell / V$$

$$\ell = p_s/(\rho_2 g)$$

$$h_{eff} = h_s + (p_s - p_o)/(\rho_2 g)$$

$$b_{12} = -q_s/(A_{2s}A)$$

$$b_{21} = \rho_s/V$$

$$b_{22} = -\rho_s q_s/(VA_{2s})$$

$$b_{23} = 1/V$$

$$b_{24} = -w_s/(A_{1s}V) \qquad (5.4)$$

The effect of the input q_1 (stock) flow in the linearized model is thus the same as the effect of the input A_2 (slice area) and the effect of w_1 (air flow) is the same as the effect of A_1 (area of air outlet).

The parameters of the linearized model appear in a slightly more

convenient form if the state variables

$$x_1 = h - h_s$$
$$x_2 = (\kappa \ell/\rho_s)(\rho - \rho_s) \tag{5.5}$$

the inputs

$$u_1 = (q_1 - q_{1s})/A - \frac{q_s}{AA_{2s}}(A_2 - A_{2s})$$
$$u_2 = \frac{\kappa \ell}{\rho_s V}(w_1 - w_s) - (w_s/A_{1s})(A_1 - A_{1s}) \tag{5.6}$$

and the outputs

$$y_1 = x_1$$
$$y_2 = \frac{2h_{eff}(v - v_s)}{V_s} = x_1 + x_2 \tag{5.7}$$

are introduced. The state variable x_2 in (5.5) is the deviation in head box pressure measured in m H_2O, the input u_1 is the nomalized input due to stock flow or slice opening and the input u_2 is the normalized input due to air flow or opening of air outlet and that the output y_2 equals the total pressure measured in m H_2O. The linearized head box model now becomes

$$\frac{d}{dt}\begin{bmatrix} x_1 \\ x_2 \end{bmatrix} = \begin{bmatrix} -\alpha_1 & -\alpha_1 \\ -\beta\alpha_1 & -(\alpha_2 + \beta\alpha_1) \end{bmatrix} \begin{bmatrix} x_1 \\ x_2 \end{bmatrix} + \begin{bmatrix} 1 & 0 \\ \beta & 1 \end{bmatrix} \begin{bmatrix} u_1 \\ u_2 \end{bmatrix}$$

$$y = \begin{bmatrix} 1 & 0 \\ 1 & 1 \end{bmatrix} \begin{bmatrix} x_1 \\ x_2 \end{bmatrix} \tag{5.8}$$

With the chosen normalization the linearized head box model is thus characterized by three parameters α_1, α_2 and β where

$$\alpha_1 = \frac{q_s}{2Ah_{eff}}$$

$$\alpha_2 = \begin{cases} \dfrac{w_s}{2\rho_s V} \dfrac{(\kappa-1)(\rho_s/\rho_o)^{\kappa-1}}{(\rho_s/\rho_o)^{\kappa-1} - 1} & \dfrac{\rho_s}{\rho_o} < \left(\dfrac{\kappa+1}{2}\right)^{\frac{1}{\kappa-1}} \\ \dfrac{w_s}{2\rho_s V}(\kappa+1) & \dfrac{\rho_s}{\rho_o} > \left(\dfrac{\kappa+1}{2}\right)^{\frac{1}{\kappa-1}} \end{cases}$$

A comparison with the equations (2.7), (2.8) and (3.7), (3.7) shows that:

- o the parameter α_1 is the inverse time constant of a water tank with flow q_s, liquid area A and height $h_{eff} = h + p_s/(\rho_2 g)$
- o the parameter α_2 is the inverse time constant of an air tank with flow w_s, volume V and density ρ_s

The model (5.8) can be interpreted as a the dynamics of a coupled water tank air tank system. The parameter $\beta = \kappa \ell A/V$ expresses the coupling. If $\beta = 0$ the only coupling is through a_{12} i.e. the effect of the air pressure on the outlet velocity of the stock.

Block diagran

A block diagram of the linearized model is shown is Fig. 5.1

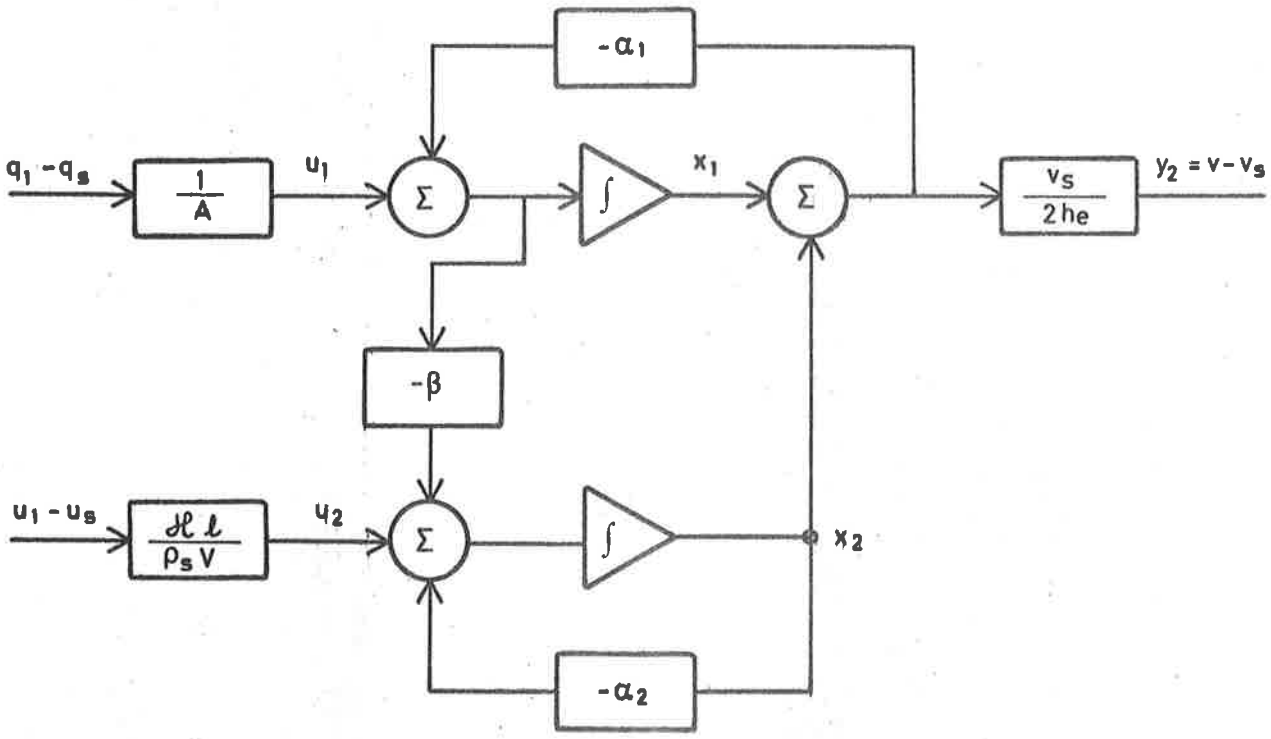

Fig. 5.1. Block diagram of linearized model for a simple closed head box.

Observability and Controllability

The controllability matrices for the inputs u_1 and u_2 becomes

$$W_1 = \begin{bmatrix} 1 & -\alpha_1(1+\beta) \\ \beta & -\alpha_1'\beta(1+\beta)-\beta\alpha_2 \end{bmatrix}$$

$$W_2 = \begin{bmatrix} 0 & -\alpha_1 \\ 1 & -(\alpha_2+\beta\alpha_1) \end{bmatrix}$$

The system is thus controllable from either input. The angle between the vectors of the controllability matrices are

$$|\sin \theta_1| = \frac{\beta\alpha_2}{\sqrt{(1+\beta^2) + \alpha_1^2(1+\beta)^2(1+\beta^2) + \alpha_2^2\beta^2 + 2\alpha_1\alpha_2\beta^2(1+\beta)}}$$

$$\sin \theta_2 = \frac{\alpha_1}{\sqrt{\alpha_1^2 + (\alpha_2+\beta\alpha_1)^2}}$$

Notice that for large β both angles are of the magnitude $1/\beta$.

The observability matrices becomes

$$Q_1 = \begin{bmatrix} 1 & \beta \\ -\alpha_1 & -\alpha_2 \end{bmatrix} =$$

$$Q_2 = \begin{bmatrix} 1 & 1 \\ -(1+p)\alpha_1 & -(1+p)\alpha_1 - \alpha_2 \end{bmatrix}$$

The system is thus observable from either output. The angle between the vectors of the observability matrices are given by

$$|\sin \theta_1| = \frac{\alpha_2}{\sqrt{\alpha_1^2 + \alpha_2^2}}$$

$$|\sin \theta_2| = \frac{\alpha_2}{\sqrt{2(\alpha_1^2(1+\beta)^2+\alpha_2^2+2\alpha_1\alpha_2(1+p))}}$$

Notice that for large β the angle θ_2 is of the order $1/\beta$ while θ_1 is significantly larger.

Invertibility

The inverse of the dynamical system (5.8) is obtained in a straight forward way. Since the output at (5.8) does not contain the control variable explicitely the output equation is differentiated. Hence

$$\frac{dy}{dt} = \begin{bmatrix} 1 & 0 \\ 1 & 1 \end{bmatrix} \begin{bmatrix} -\alpha_1 & -\alpha_1 \\ \beta\alpha_1 & -(\alpha_2+\beta\alpha_1) \end{bmatrix} \begin{bmatrix} x_1 \\ x_2 \end{bmatrix} + \begin{bmatrix} 1 & 0 \\ 1 & 1 \end{bmatrix} \begin{bmatrix} 1 & 0 \\ \beta & 1 \end{bmatrix} \begin{bmatrix} u_1 \\ u_2 \end{bmatrix}$$

$$= \begin{bmatrix} -\alpha_1 & -\alpha_2 \\ -(1+\beta)\alpha_1 & -(\alpha_2+\beta\alpha_1+\alpha_1) \end{bmatrix} \begin{bmatrix} x_1 \\ x_2 \end{bmatrix} + \begin{bmatrix} 1 & 0 \\ 1+\beta & 1 \end{bmatrix} \begin{bmatrix} u_1 \\ u_2 \end{bmatrix}$$

Hence

$$\begin{bmatrix} u_1 \\ u_2 \end{bmatrix} = \begin{bmatrix} 1 & 0 \\ -(1+\beta) & 1 \end{bmatrix} y - \begin{bmatrix} -\alpha_1 & -\alpha_1 \\ 0 & -\alpha_2 \end{bmatrix} \begin{bmatrix} x_1 \\ x_2 \end{bmatrix}$$

Introducing this in (5.8) we get the inverse system.

$$\frac{dx}{dt} = \begin{bmatrix} 0 & 0 \\ -\alpha_1 & -\alpha_1 \end{bmatrix} \begin{bmatrix} x_1 \\ x_2 \end{bmatrix} + \dot{y}$$

$$u = \begin{bmatrix} +\alpha_1 & +\alpha_1 \\ 0 & +\alpha_2 \end{bmatrix} \begin{bmatrix} x_1 \\ x_2 \end{bmatrix} x + \begin{bmatrix} 1 & 0 \\ -(1+p) & 1 \end{bmatrix} \dot{y}$$

which is stable but not asymptotically stable.

Transfer Functions

Transfer functions relating the state variables and the outputs to the inputs will now be derived. The characteristic equation of the linear model (5.8) is given by

$$A(s) = s^2 + s(\alpha_1 + \alpha_2 + \beta\alpha_1) + \alpha_1\alpha_2 = 0 \qquad (5.10)$$

The rool-locus of this equation is shown in Fig. 5.2

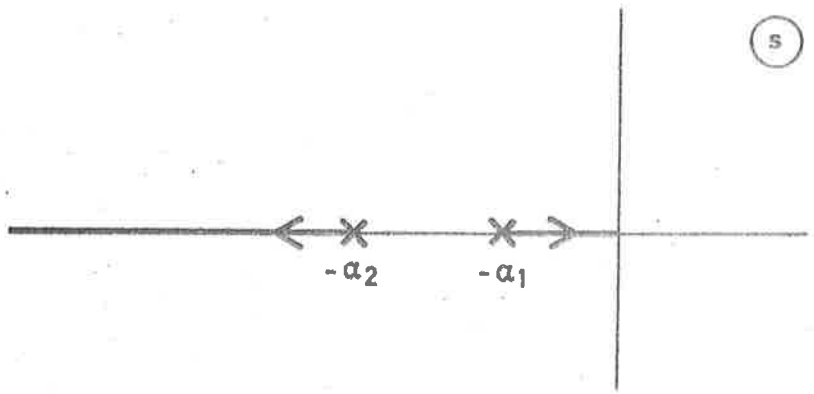

Fig. 5.2. Root locus of the equation (5.10) with respect to the cross coupling parameter β

The characteristic equation has negative real roots for all positive values of β. For $\beta = 0$ the roots are α_1 and α_2. As β increases the root closest to the origin will approach the origin and the other root will be further removed. For large values of β the roots are given by

$$s_1 \sim -\alpha_2 - \beta(1+\alpha_1)$$

$$s_2 \sim -\frac{\alpha_1\alpha_2}{\alpha_1+\alpha_2+\beta\alpha_1}$$

The transfer function relating the state variables to the input is given by

$$G_1(s) = \frac{1}{A(s)} \begin{bmatrix} s + \alpha_2 & -\alpha_1 \\ \beta s & s + \alpha_1 \end{bmatrix} \qquad (5.11)$$

The transfer function relating the outputs to the inputs is given by

$$G_2(s) = \frac{1}{A(s)} \begin{bmatrix} s + \alpha_2 & -\alpha_1 \\ (1+\beta)s+\alpha_2 & s \end{bmatrix} \qquad (5.12)$$

The character of the Bode diagrams of this transfer function is shown in Fig. 5.3 and Fig. 5.4. Fig. 5.3 shows that stock flow variations in the frequency range $(0, s_2)$ are transmitted to the jet velocity with practically no damping. Similarly Fig. 5.4 shows that fluctuations in the air flow in the frequency range (α_1, s_2) are transmitted to the jet velocity with very little damping. The graphs in Fig. 5.3 and 5.4 also indicate that variations in both inputs are transmitted to the stock level with significant damping for frequencies above $s_1 \sim \alpha_2/\beta$.

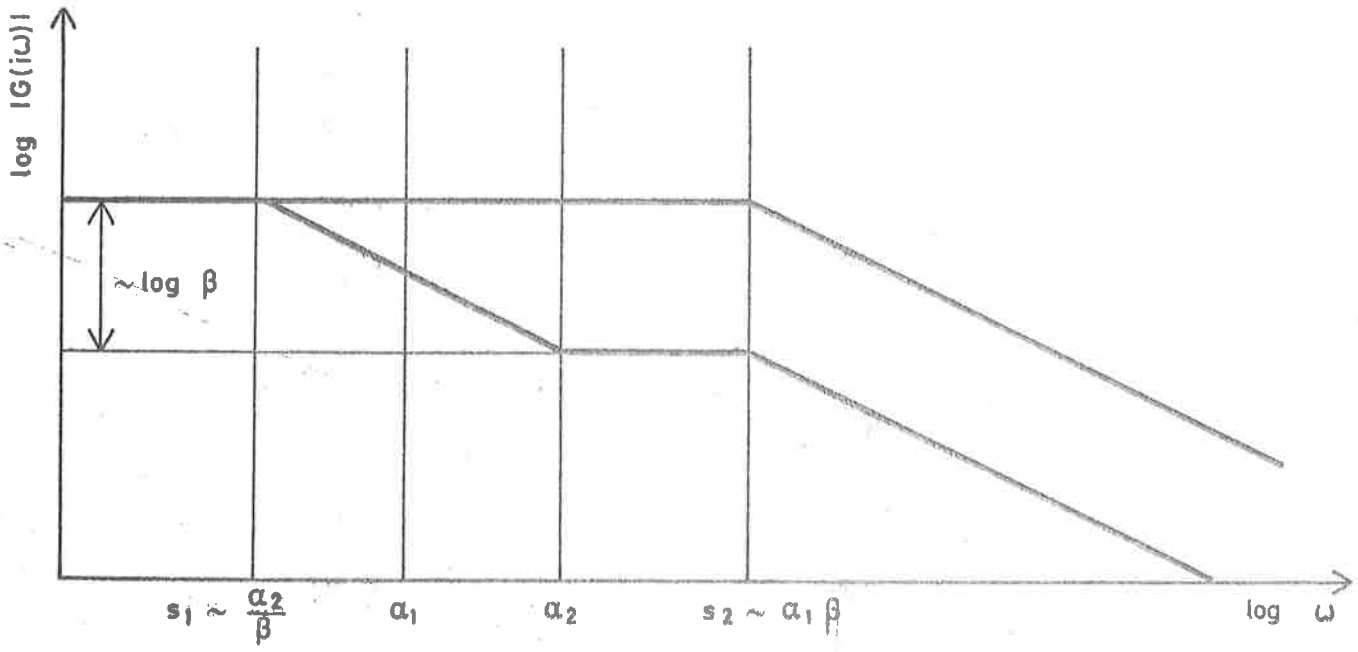

Fig. 5.3. Amplitude curves for the transfer functions relating jet velocity and stock level to stock flow.

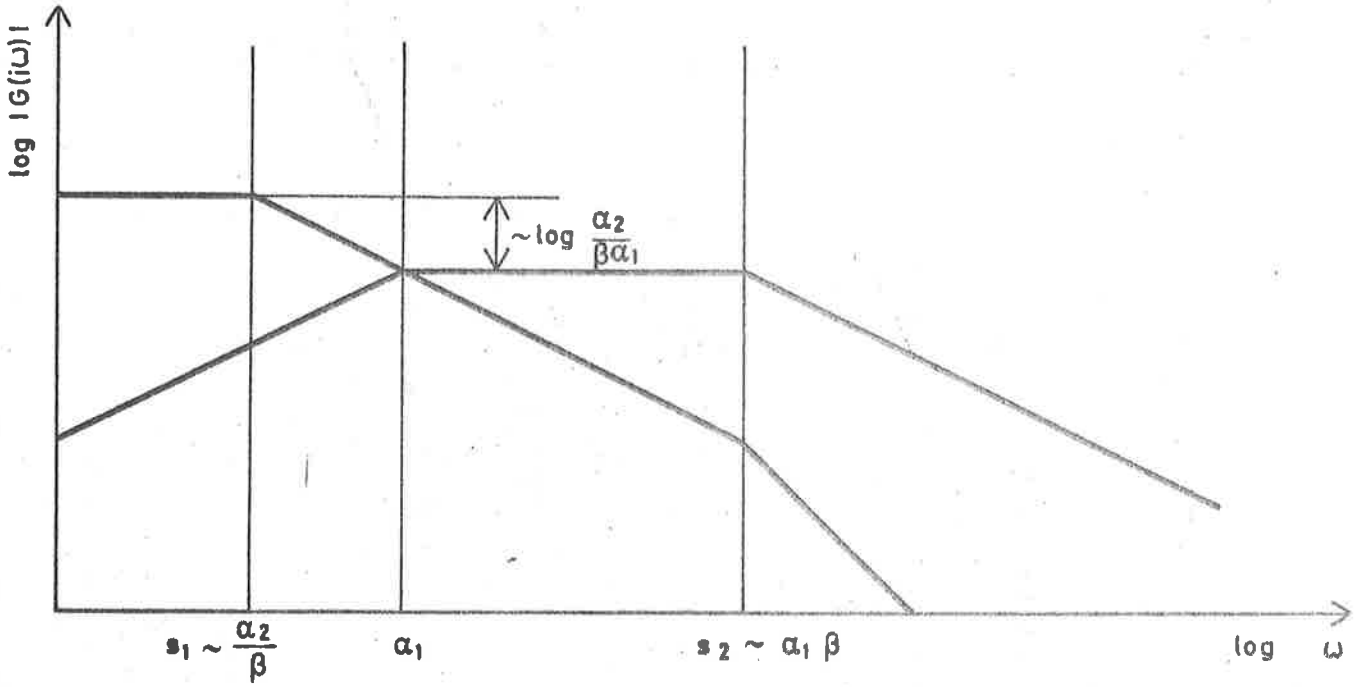

Fig. 5.4. Amplitude curves for the transfer function relating jet velocity and stock level to air flow.

A Numerical Example

Numerical values of the coefficients for a typical head box are given below.

Material constants

$\rho_2 = 1000$ kg/m^3
$\rho_o = 1.293$ kg/m^3
$p_o = 10.5\ \rho_2 g$
$\kappa = 1.4$
$g = 9.81$ m/s^2

Construction data

$V = 10$ m^3

$A = 10$ m^3

A_1 = given indirectly through q_s
A_2 = given indirectly through w_s

Operating data

$q_s = 1\ m^3/s$
$w_s = 0.245\ kg/s$
$h_s = 0.5\ m$
$\rho_s = 1.62\ kg/m^3$

Hence

$$P_s - P_o = 4.5\ \rho_2 g$$
$$h_{eff} = 0.5 + 4.5 = 5\ m$$
$$\ell = 10.5 + 4.5 = 15\ m$$
$$\alpha_1 = \frac{q_s}{2Ah_{eff}} = 0.01\ m$$
$$\alpha_2 = \frac{w_s}{2\rho_s V} \frac{(\kappa-1)\ (\rho_s/\rho_o)^{\kappa-1}}{(\rho_s/\rho_o)^{\kappa-1} - 1} = 0.03507$$
$$\beta = \frac{\kappa A \ell}{V} = 20.98$$

The stock flow q_s and the air flow w_s correspond to the following values of the control variables

$$u_{10} = \frac{q_s}{A} = 0.1 \quad m/s$$
$$u_{20} = \frac{\kappa w_s}{\rho_s V} = \frac{\beta w_s}{\rho_s A} = 0.317 \quad m/s$$

Compare with the equation (5.6).
The linearized model is then given by

$$\frac{d}{dt}\begin{bmatrix} x_1 \\ x_2 \end{bmatrix} = \begin{bmatrix} -0.01 & -0.01 \\ -0.21 & -0.25 \end{bmatrix} \begin{bmatrix} x_1 \\ x_2 \end{bmatrix} + \begin{bmatrix} 1 & 0 \\ 21 & 1 \end{bmatrix} \begin{bmatrix} u_1 \\ u_2 \end{bmatrix}$$

The outputs are

$y_1 = x_1$ liquid level [m]

$y_2 = x_2$ air pressure [m]

$y_3 = x_1 + x_2$ total pressure [m]

$y_4 = 0.99(x_1+x_2)$ slice velocity [m/s]

The characteristic equation of the system matrix is

$$s^2 + 0.26s + 0.0021 = 0$$

which has the solutions

$s_1 = -0.2585$

$s_2 = -0.0015$

The system thus has one fast mode with a time constant of about 4 s and one slow mode with a time constant of 670 s.

The responses of the system to step changes in the inputs are shown in Fig. 5.5, Fig. 5.6, Fig. 5.7 and Fig. 5.8.

Due to the large differences in time constants it is necessary to show two sets of curves with different time scales.

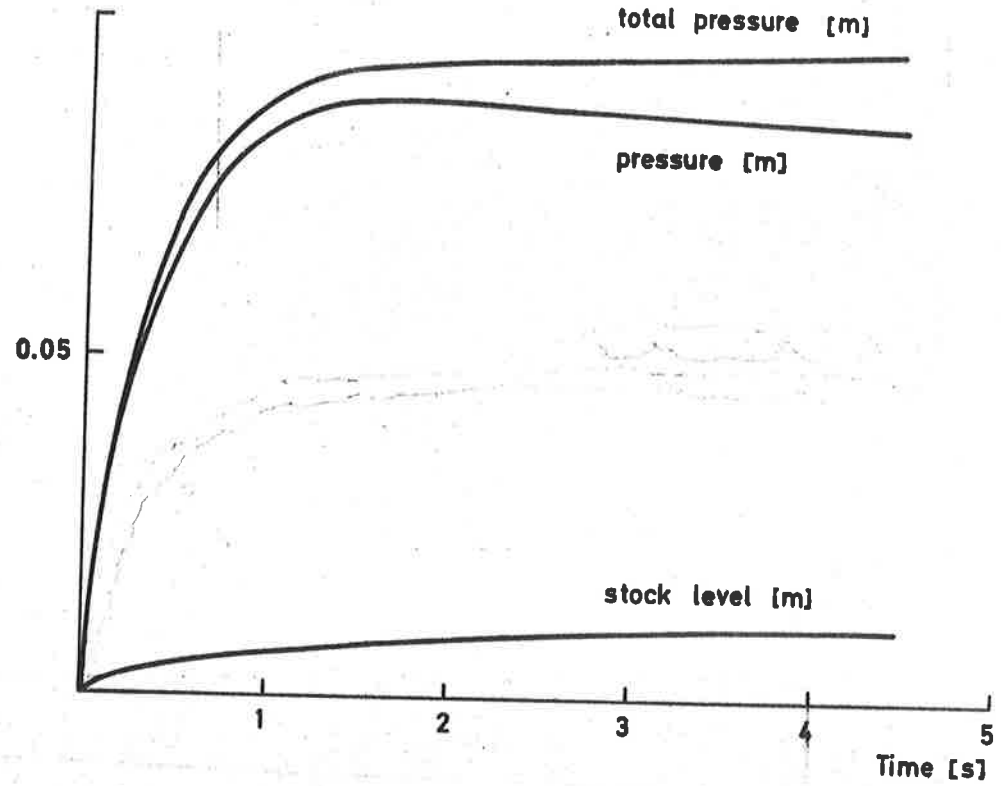

Fig. 5.5. Response of the head box model (5.13) to a step disturbance in stock flow with amplitude 0.01 m^3/s corresponding to 1 % of steady state flow.

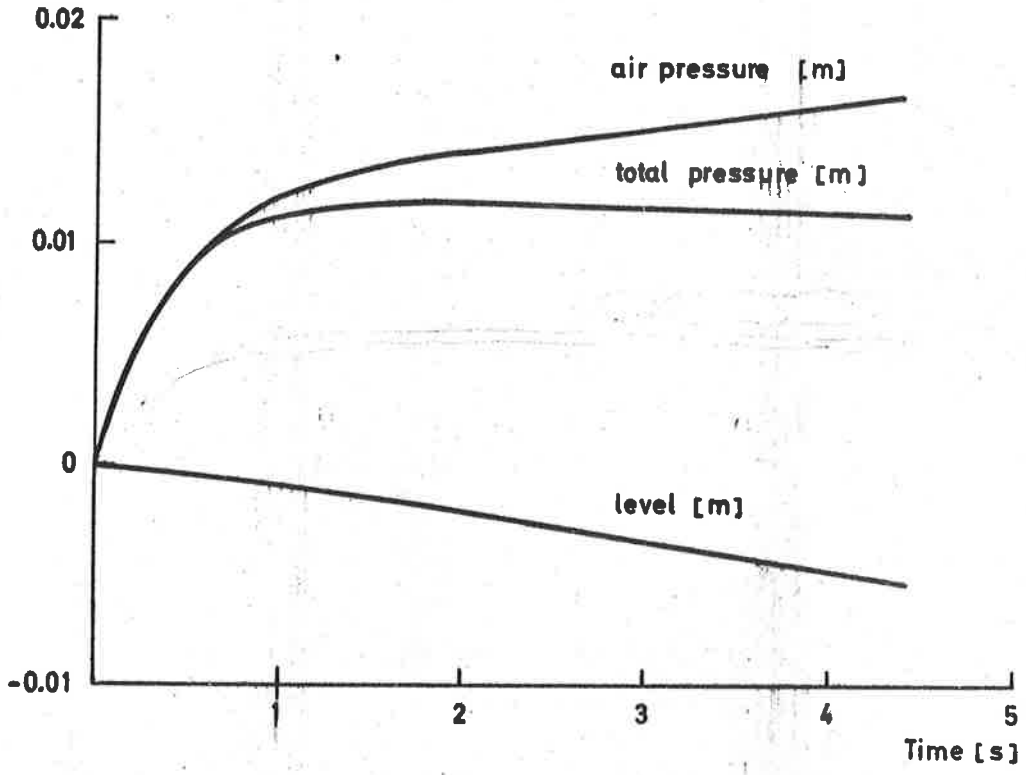

Fig. 5.6. Response of the head box model (5.13) to a step disturbance in air flow of 0.00245 kg/s corresponding to 1 % of steady state flow.

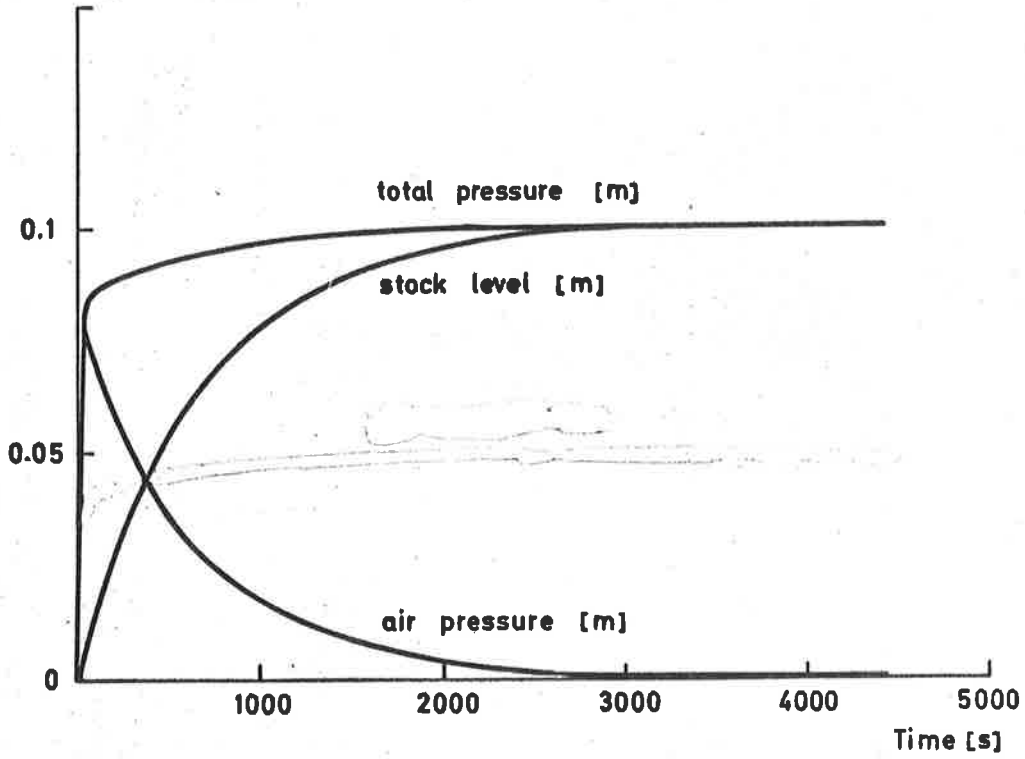

Fig. 5.7. Response of the head box model (5.13) to a step disturbance in stock flow with amplitude 0.01 m^3/s corresponding to 1 % of steady state flow.

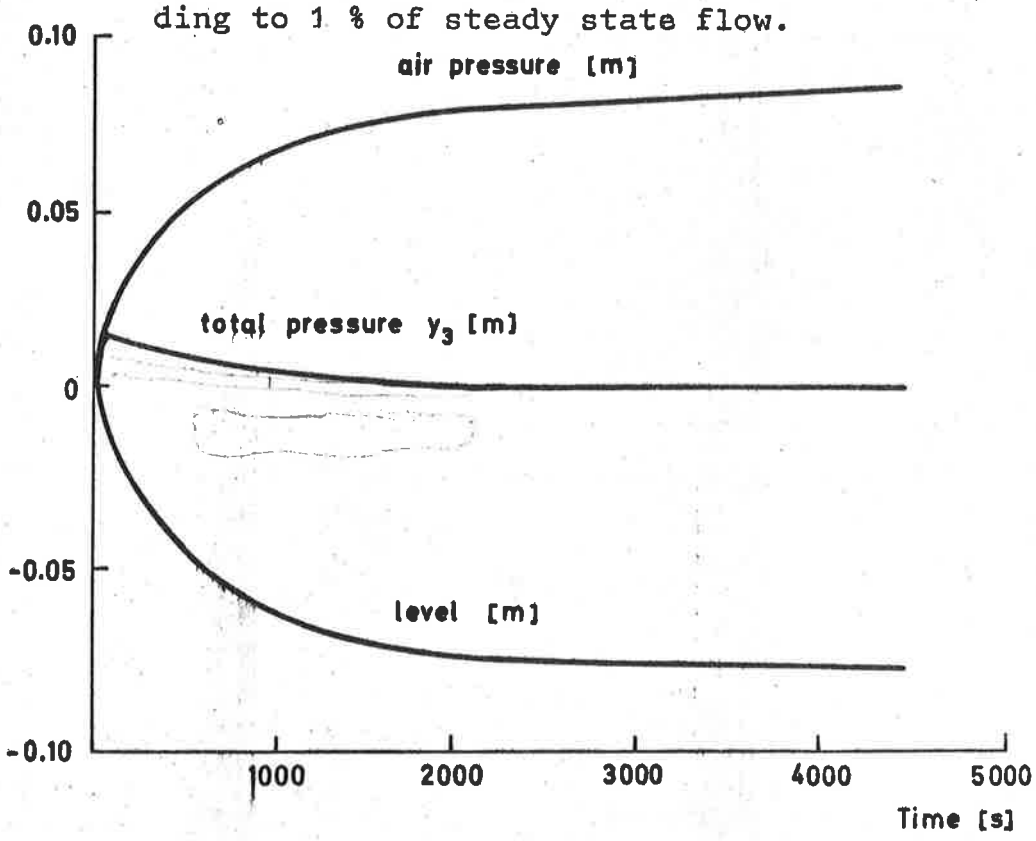

Fig. 5.8. Response of the head box model (5.13) to a step disturbance in air flow of 0.00245 kg/s corresponding to 1 % of steady state flow.

In response to a step change in the stock flow the air pressure will rise very quickly to reach a maximum two seconds after the application of the step (Fig. 5.5). The air pressure will then decay slowly to the steady state value (Fig.5.7). The liquid level x_1 will increase slowly in response to a step in stock flow and settle at a new steady state level after several thousand seconds. The total pressure and the slice velocity will respond very quickly to a step change in stock flow and settle on a new level after a few seconds.

Fig. 5.6 and Fig. 5.8 show that a step change in air flow will make the air pressure increase rapidly during the first seconds after the application of the step. The air pressure will then continue to increase slowly until a new steady state level is reached after several thousand seconds. The liquid level will decrease slowly until a new steady state level is reached after several thousand seconds.

The response of a zero input system with given initial conditions is shown in Fig. 5.9. This figure shows that the total pressure and the jet velocity decay with the fast time constant to levels that are close to zero which the stock level in essence decays with the long time constant.

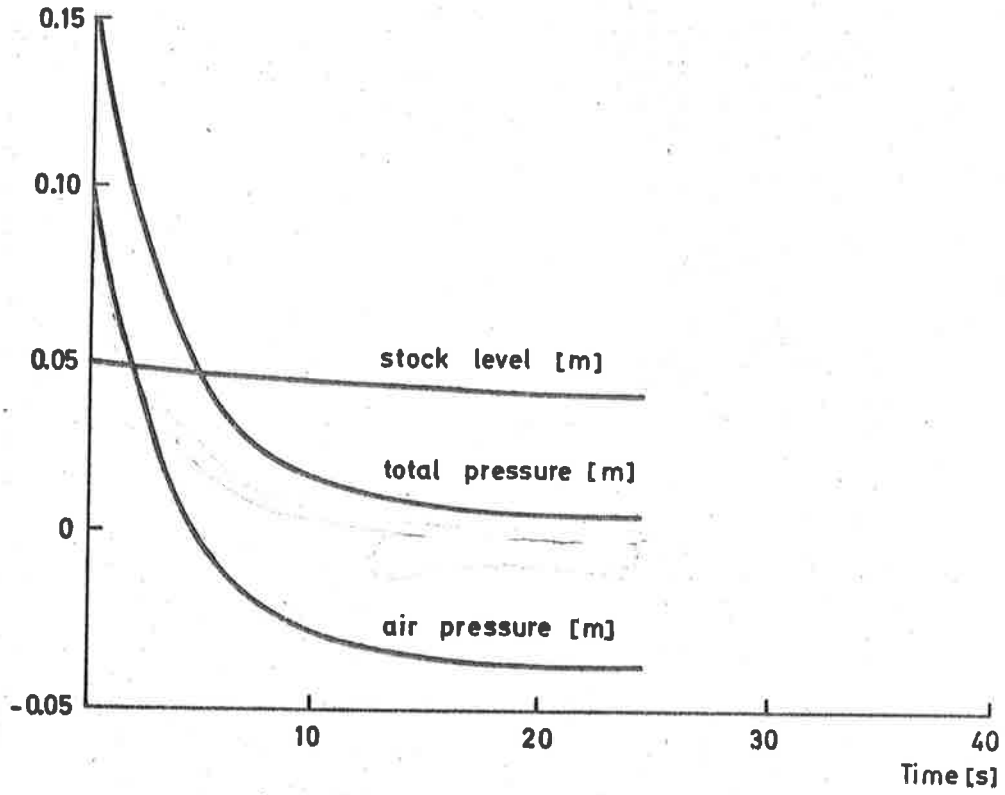

Fig. 5.9. Illustrates the solution of the system equations with zero inputs and given initial conditions.

Exercises

1.- Determine a linearized model for a closed head box according to Fig. 1.3 with an internal overflow.

2.- Determine a linearized model for a head box with Hornbostel hole according to Fig. 1.4.

3.- Compare the dynamics of the simple closed head box with the head boxes in exercises 1 and 2.

4.- Consider the linearized head box model according to equation (5.8). Assume that $\beta >> 1$. Show that the step responses of the state variables have the characteristic shown below.

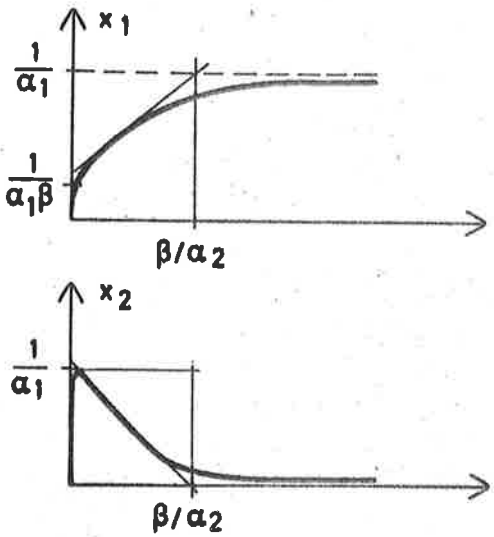

Responses to step in u_1

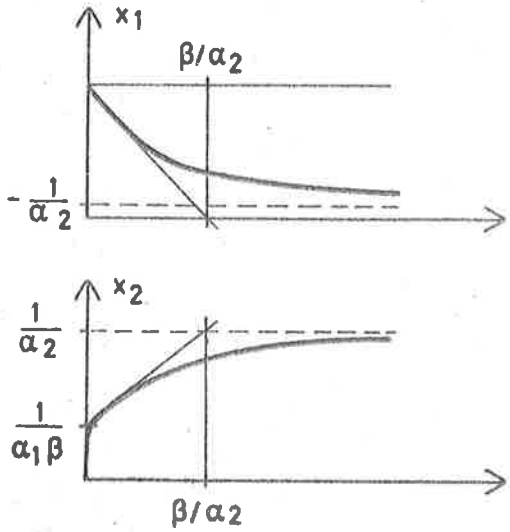

Responses to step in u_2

6. DESIGN OF CONTROL STRATEGIES

The linearized model of the head box obtained in section 5 will now be used to discuss the control problem and to design control strategies. The head box model is a second order dynamical system with two inputs and two outputs. The first input is the stock flow and the second input is either the air flow or the area of the air outlet. The outputs are the stock level and the jet velocity and the state variables were arbitrarily chosen as stock level and air pressure. The system is completely controllable and completely observable from any input and any output. The system also has a stable inverse. A characteristic feature of the system is that there is one fast mode and one slow mode. In the numerical example these modes correspond to time constants of 4 s and 670 s. The couplings of the system are, such that the fast mode dominates the response of the jet velocity to both inputs. It is thus possible to get a quick response in jet velocity through both inputs. We can thus conclude that the dynamic properties of the system indicate that the control problem is straight forward. It should be observed, however, that the closed head box can not be used without control. It was thus not possible to use the closed head box invented by Malkin until a suitable control system was invented.

The simple Hornbostel hole provided a solution. It was found that the Hornbostel hole has major disadvantages. It controls the level fairly accurately but it introduces fluctuations in jet velocity. The response of a head box with a Hornbostel hole is also oscillatory with low damping which implies that it actually amplifies some of the distrubances.

Review of Disturbances

As was stated in the introduction the major disturbances are fluctuations in stock flow and air flow. With a good flow control system there can easily be fluctuations in stock flow of about one per cent. Using the numerical example of section 5 we find for example that a variation in flow of 1 % corresponds to $u_1 = 0.001$. In the steady state this will correspond to a level variation of 0.1 m (20 %) and a variation in jet velocity of 0.05 m/s. (0.5 %). Considering relative variations the low frequency gain is thus 0.5. It follows from the Bode diagram

that this holds for frequencies up to 0.25 rad/s.

A variation in air flow of 1 % corresponds to u_2 = 0.003 kg/s. For low frequency variations this corresponds to a level variation of 0.1 m (20 %) and variations in the jet velocity of 0.05 m/s.

A reasonable criterion is that the level variations should be reduced to about 0.02 m and jet velocity variations to 0.01 m/sec.

Conventional Control

Since the head box is a multivariable system with strong interactions there is no straight forward way to design the control system using single loop concepts. In the literature and among the practitioners of head box control it is also possible to find several opinions concerning the most suitable control system. It is possible to distinguish between two different single loop systems. In one configuration the measurement of total head is used to control the stock flow and the level signal is used to control the air flow. In the other configuration the regulators are reversed in such a way that total head controls air flow and that stock flow is controlled by the stock level. See Fig. 6.1. Since the systems are completely characterized by giving one loop they are referred to as total head/stock flow and total head/air flow respectively.

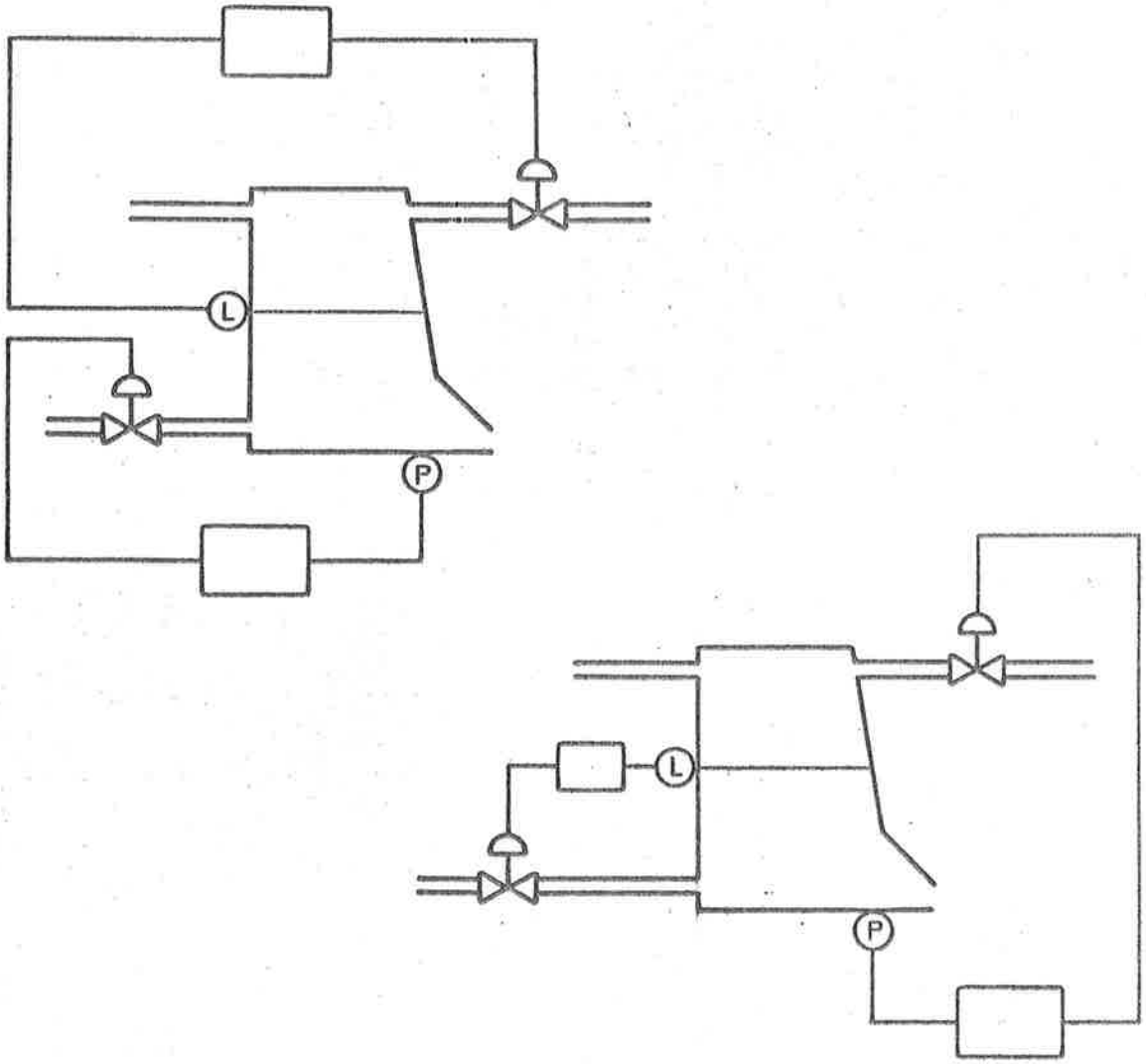

Fig. 6.1.

Schematic diagram of two schemes used for conventional control of head boxes. The system on the left is called the total head/stock flow system (scheme 1) and the other is called the total head/air flow system (scheme 2).

The systems have different characteristics as will now be discussed heuristically.

The Total Pressure/Stock Flow System

To see how this system behaves it will be assumed that the stock level and the air pressure are both too high initially. The response of the system without control in such a situation is shown in Fig. 5.9. The characteristic features of the system without control is thus that the total pressure drops fairly quickly to a low level which will decrease to zero slowly as the stock level goes to zero. If proportional

regulators are installed the action can be described as follows. The total pressure signal will decrease the stock flow which in turn will cause a decrease in both stock level and jet velocity. The other regulator will close the air valve which in turn will increase jet velocity and decrease the stock level. Both control actions will thus tend to decrease level while they have the opposite effect on the jet velocity.

The Total Pressure/Air Flow System

Assume again that both level and air pressure are too high initially. With proportional regulators the total pressure signal will open the air valve which in turn will decrease the jet velocity and increase the level. The level signal will decrease the stock flow which will cause a decrease in both level and in jet velocity. Both control actions will thus tend to decrease jet velocity while they have opposite effects on the level.

Pole Placement

Since the system is controllable the control system design can be achieved through pole placement. Introduce the linear feedback

$$u = -\begin{bmatrix} \ell_1 & \ell_2 \\ \ell_3 & \ell_4 \end{bmatrix}(x - x_{ref})$$

The closed loop system then becomes

$$\frac{dx}{dt} = \begin{bmatrix} -(\alpha_1+\ell_1) & -(\alpha_1+\ell_2) \\ -\beta(\alpha_1+\ell_1) - \ell_3 & -\alpha_2 - \beta\alpha_1 - \beta\ell_2 - \ell_4 \end{bmatrix} x$$

$$+ \begin{bmatrix} \ell_1 & \ell_2 \\ \ell_3+\beta\ell_4 & \ell_4 \end{bmatrix} x_{ref} + \begin{bmatrix} 1 & 0 \\ \beta & 1 \end{bmatrix} v$$

where the disturbance v is composed of variations in stock flow (v_1) and in air flow (v_2).

The characteristic equation of the closed loop system is

$$s^2 + \underbrace{s(\alpha_1+\alpha_2+\beta\alpha_1+\beta\ell_2+\ell_4)}_{a_1} + \underbrace{\alpha_1\alpha_2+\alpha_1\ell_4+\alpha_2\ell_1+\ell_1\ell_4-\alpha_1\ell_3-\ell_2\ell_3}_{a_2} = 0$$

The transfer function relating the state variables to the disturbances is given by

$$X(s) = \begin{bmatrix} s+\alpha_1+\ell_1 & \alpha_1+\ell_2 \\ (\alpha_1+\ell_1)+\ell_3 & s+\alpha_2+\beta\alpha_1+\beta\ell_2+\ell_4 \end{bmatrix}^{-1} \begin{bmatrix} 1 & 0 \\ \beta & 1 \end{bmatrix} V(s)$$

$$= \frac{1}{A(s)} \begin{bmatrix} s+\alpha_2+\beta\alpha_1+\beta\ell_2+\ell_4 & -(\alpha_1+\ell_2) \\ -(\beta(\alpha_1+\ell_1)+\ell_3) & s+\alpha_1+\ell_1 \end{bmatrix} \begin{bmatrix} 1 & 0 \\ \beta & 1 \end{bmatrix} V(s)$$

$$= \frac{1}{A(s)} \begin{bmatrix} s+\alpha_2+\ell_4 & -(\alpha_1+\ell_2) \\ \beta s-\ell_3 & s+\alpha_1+\ell_1 \end{bmatrix} V(s)$$

The transfer function relating the output to the disturbance is

$$X_1(s) + X_2(s) = \frac{1}{A(s)} \left[(1+\beta)s + \alpha_2 + \ell_4 - \ell_3,\ s+\ell_1 - \ell_2\right] V(s)$$

The expressions given above can be exploited to analyse conventional proportional control schemes and to design suitable regulators.

Design Using Linear Quadratic Control Theory

The head box control system can also be designed using linear quadratic control theory. To illustrate this the system introduced in the numerical example of section 5 will be used. The properties of the control strategies will be illustrated by analysing the response of

the system when the level initially is 0.05 m above its derived value and the pressure is 0.1 ρg N/m^2 above its desired value. The response of the system without control is shown in Fig. 6.2.

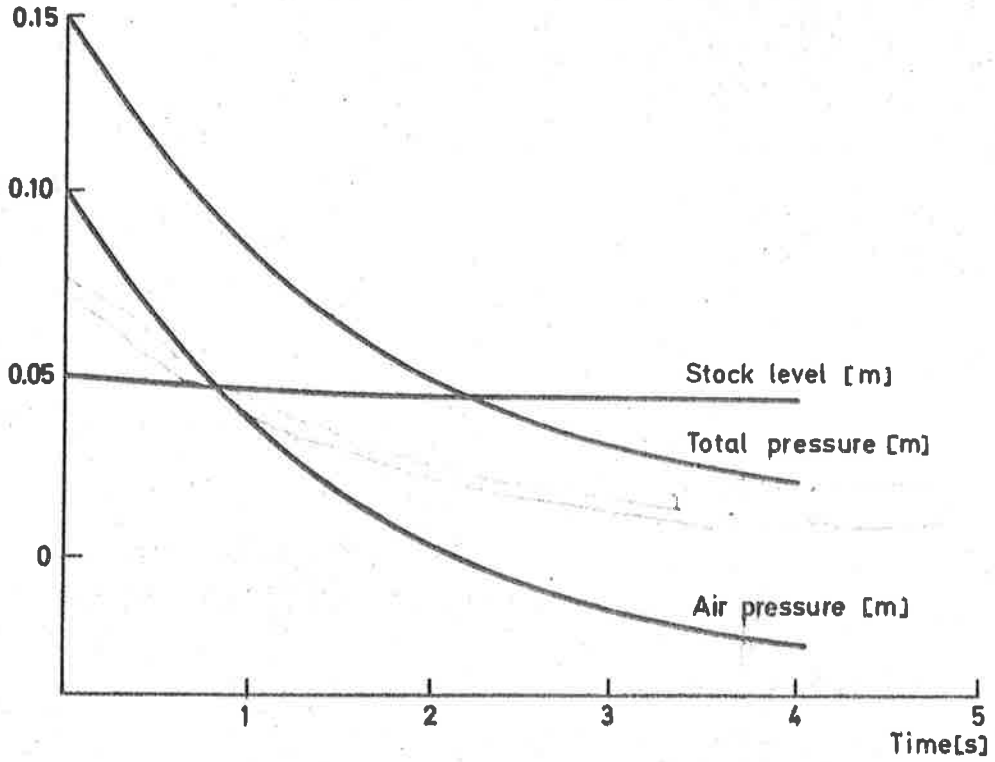

Fig. 6.2.

Simulation of the head box of Example 5.1 without control.

To design the control strategies the system was sampled with the sampling interval 0,5 s. The control strategies were then designed using straight forward linear quadratic theory.

Example 6.1

In the first case deviations in jet velocity and control actions were penalized through the loss function

$$Q_1 = \begin{pmatrix} 1 & 1 \\ 1 & 1 \end{pmatrix}$$

$$\tilde{Q}_2 = \begin{pmatrix} 100 & 0 \\ 0 & 1 \end{pmatrix}$$

The choice of relative magnitudes of the elements of the $\tilde{Q}_2$ matrix were guided by the fact that u_2 in the steady state is about 3 times larger than u_1 and that it was judged desirable to let the air flow take the major burden of control since rapid fluctuations in stock flow may generate rapid variations in head box consistency. The loss function given above gives the following steady state solution to the discrete Riccati equation

$$S = \begin{pmatrix} 1.410 & 1.396 \\ 1.396 & 1.384 \end{pmatrix}$$

and the optimal feedback is given by

$$L = \begin{pmatrix} 0.0465 & 0.0451 \\ 0.211 & 0.205 \end{pmatrix}$$

The result of a simulation of the system with the optimal feedback is shown in Fig. 6.3. The Figure shows a significant improvement in the response of the jet velocity in comparison with the uncontrolled system in Fig. 6.2. Notice, however, that the stock level still decays very slowly. This can of course be expected since the stock level was not penalized in the loss function. Also notice the relative magnitudes of the control signal. The major burden of the control is on the air flow as was stated.

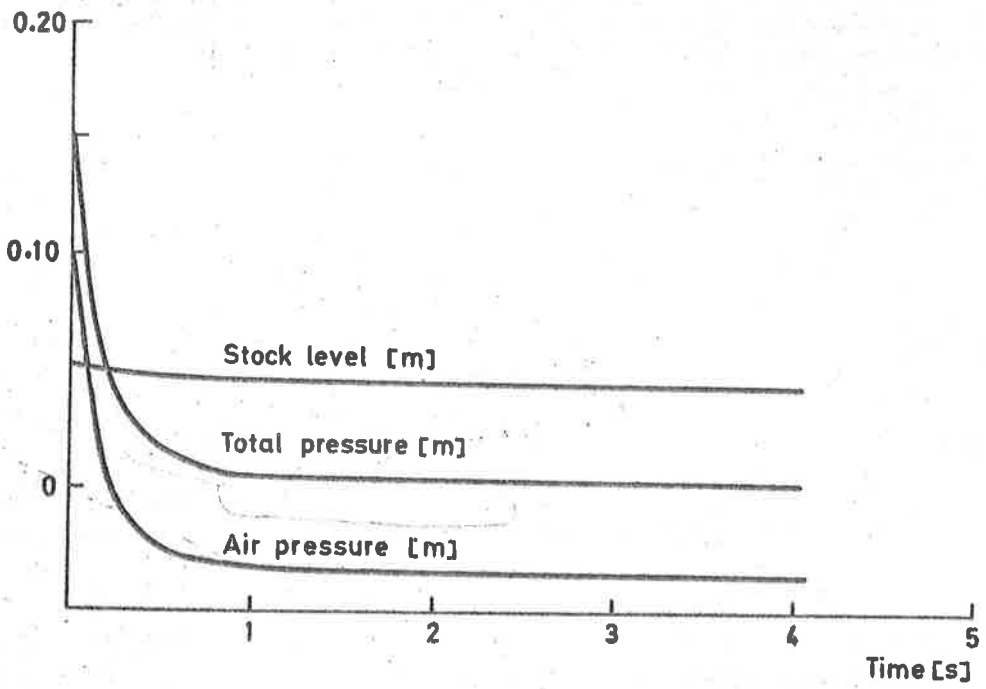

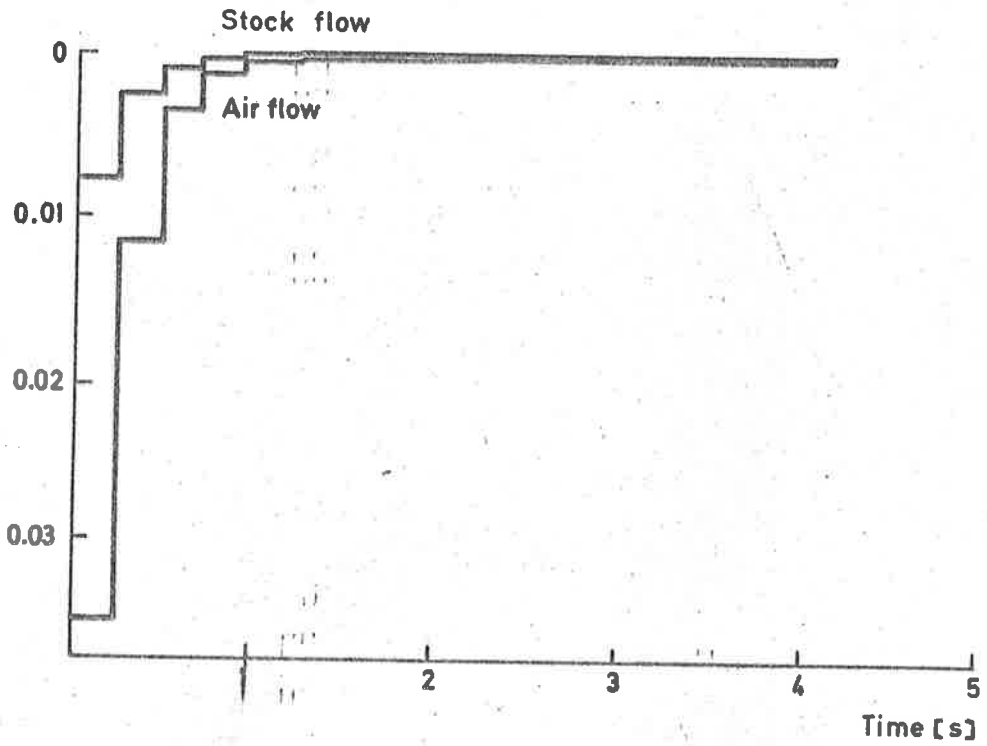

Fig. 6.3

Simulation of the closed head box with the optimal regulator corresponding to the criterion $Q_1 = \begin{pmatrix} 1 & 1 \\ 1 & 1 \end{pmatrix}$, $Q_2 = \begin{pmatrix} 100 & 0 \\ 0 & 1 \end{pmatrix}$.

Notice that both control variables will initially assume negative values. This means that both stock flow and air flow are reduced which will result in a decrease of jet velocity. The effect of the control actions on the level will more or less cancel each other which means that the level will not change very much. The regulator obtained will thus ressmeble the conventional total pressure/stock flow system. The optimal feedback can be written as

$$u_1 = - 0.0451(x_1 + x_2) - 0.0014\, x_1$$

$$u_2 = - 0.205(x_1 + x_2) - 0.006\, x_1$$

which implies that the feedbacks from total pressure $(x_1 + x_2)$ to stock flow and air flow are dominating.

Example 6.2

Suppose that we are not satisfied with the control system of Example 6.1 and that it is desired to have a control system where the stock level decays more rapidly after a disturbance. It could then be attempted to penalize deviations in the stock level as well as deviations in jet velocity. As an initial attempt we will go to the extreme and introduce a significant penalty on level errors through the loss function defined by

$$\underline{Q}_1 = \begin{pmatrix} 10 & 1 \\ 1 & 1 \end{pmatrix}$$

$$\underline{Q}_2 = \begin{pmatrix} 100 & 0 \\ 0 & 1 \end{pmatrix}$$

The selection of $\underline{Q}_1$ implies that deviations in stock level are weighted by $\sqrt{10}$ in comparison with deviations in total pressure. Using a sampling interval of 0,5 s the steady state solution to the discrete Riccati equation becomes

$$\underline{S} = \begin{pmatrix} 138.45 & -3.49 \\ -3.49 & 1.57 \end{pmatrix}$$

and the gain of the optimal sampled regulator becomes

$$L = \begin{pmatrix} 0.176 & 0.040 \\ -2.224 & 0.299 \end{pmatrix}$$

A simulation of the system with the optimal feedback is shown in Fig. 6.4.

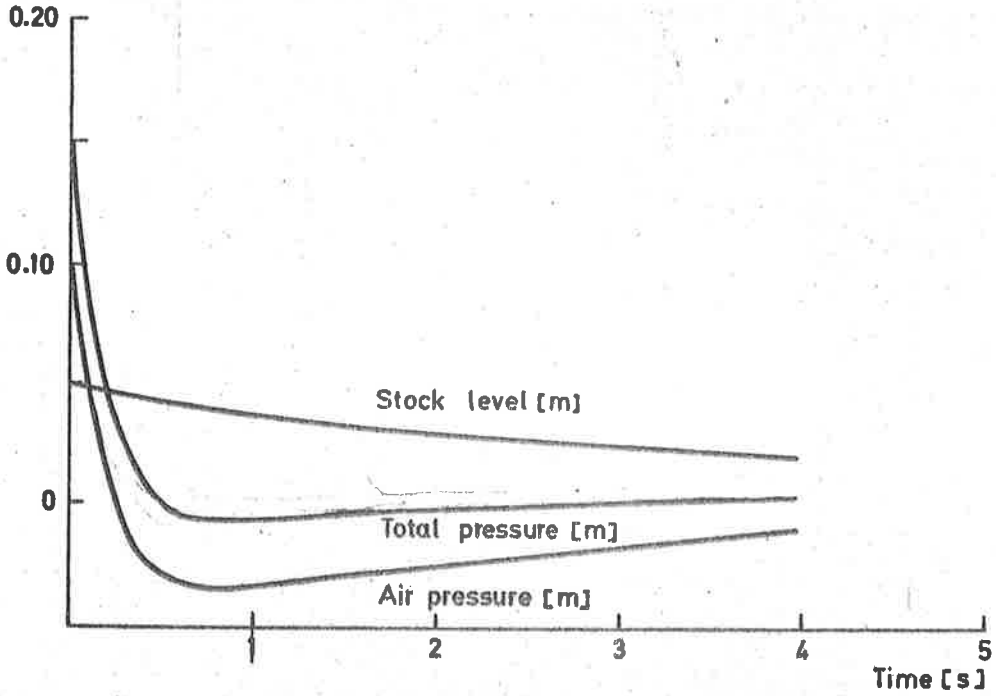

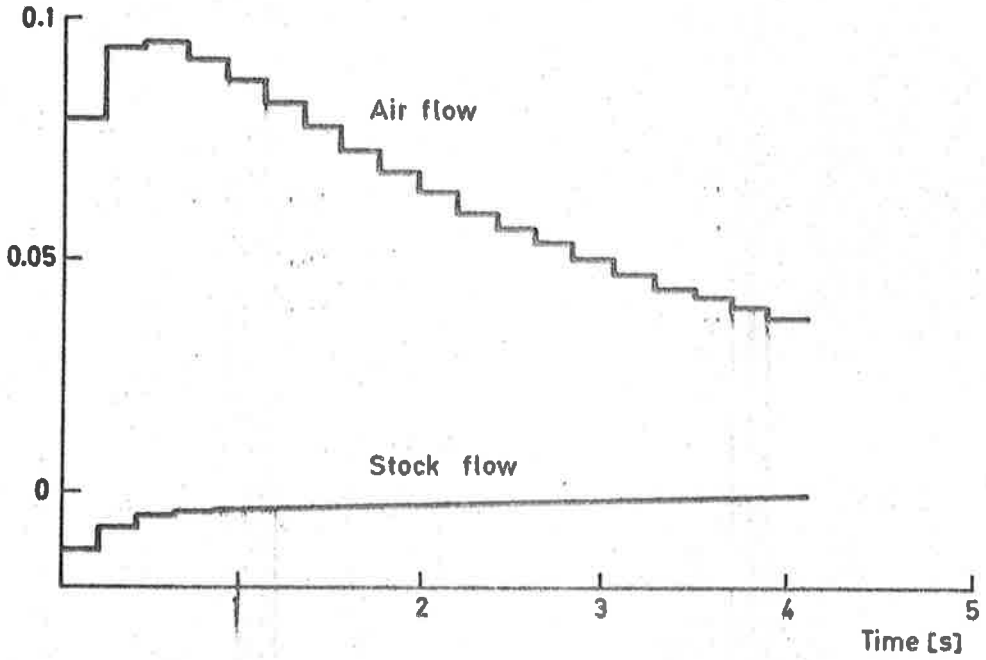

Fig. 6.4

Simulation of the closed head box with the optimal regulator corresponding to $Q_1 = \begin{pmatrix} 2 & 1 \\ 1 & 1 \end{pmatrix}$, $Q_2 = \begin{pmatrix} 100 & 0 \\ 0 & 1 \end{pmatrix}$

A comparison of Fig. 6.4 and Fig. 6.3 shows that the stock level decays more rapidly in Fig. 6.4 as could be expected. A comparison of the control signals in Fig. 6.3 and Fig. 6.4 shows that there is a significant difference between the corresponding control strategies. In Fig. 6.4 the stock flow (u_1) will initially be negative as in Fig. 6.4.The air flow (u_2) in Fig. 6.4 is, however, positive while it was negative in Fig. 6.3. The system in Fig. 6.4 will thus exert more control actions to bring down the level. In order not to change the jet velocity both control variables must be carefully matched when they are of opposite sign. Intuitively we might therefore expect the system in example 6.3 to be more sensitive to parameter variations.

The system in example 6.4 ressembles the conventional total pressure/ air flow system.

Notice the significant differences in the gains of the systems of example 6.3 and 6.4. The elements k_{11} differs by a factor of 4. The element k_{21} is of opposite sign and differs by an order of magnitude.

Sensor and Actuator Dynamics

In the analysis just carried out it was shown that the head box could be controlled with a digital regulator having a sampling interval of 0.5 s. The sensor and actuator dynamics were completely neglected in the analysis, Typical orders of magnitude are given below

- A conventional DP-cell has a time constant of about 0.5 s
- If the stock flow is controlled by a thyristor controlled motor pump the dynamics of the motor can be neglected. The dynamics associated with the acceleration of the stock depends strongly upon the details of the flow system. Time constants of about 0.3 - 0,6 s are sometimes quoted.
- If the stock flow is controlled by a by pass valve there may be time constants of about 1 s associated with the valve
- There is also a pure time delay from the stock valve to the head box

which again depends strongly on the design but can be of the order of magnitude of seconds.

To obtain a good head box control system it is apparently necessary to take sensor and actuator dynamics into account.

Exercises

1. Use the simplified head box model to explain why the closed head box can not be used without control (Hint. Analyse the effect of a step in stock flow on the level).

2. Consider the conventional schemes for head box control. Assume proportional regualtors and analyse the pole configurations that can be obtained.

3. Consider the pole placement problem. Assume that the control variables are permitted to saturate for a level error of 0.5 m and a jet velocity error of 2 m/s. Determine the admissible region of the poles of the closed loop system. Use the numerical values of the simple example.

4. Analyse the effect of sensor dynamics on the control strategies of example 6.3 and 6.4.

5. Consider the simple head box model with a general feedback according to ( ). Analyse if it is possible to choose the feedback gain in such a way that the transfer function relating fluctuations in jet velocity to disturbances in stock flow has desired properties.

7. NOTES AND REFERENCES

The closed head box was patented by B.A. Malkin USP 2, 186761. The simple level control system using a hole was patented by L Hornbostel USP 2, 509 822.

There are many papers written on design and operation of head boxes. The following papers are representative

Marden, J, Monahan, R.E. and Howe, B.I.
"On the Operation of Paper Machine Head Boxes"
Pulp and Paper Magazine of Canada
70 (1969) 57 - 80

Marden, J., Hauptmann, E.G., Monahan, R.E. and Brown, E.S.
"The Extant State of the Manifold Problem"
Pulp and Paper Magazine of Canada
72 (1971) 76 - 81

G. Stenberg
"Inloppslådor"
Stencilerat manuskript KMW 1970 - 10 - 13

Analyses of different head boxes and their control systems are found in

Mardon, R., Monahan, R.E., Mehaffey, W.H, and Dahlin, E.B.
"A Theoretical and Experimental Investigation into the Stability and Control of Paper Machine Head boxes" Part I, II and III. Papper och trä 5 (1966) 3-11, 5 (1966) 301-310 and 4a (1967) 189 - 197.

Talvio, P.A.A.
"A Study of Paper Machine Head box Control System with Linear Transfer Functions" Paper 22A
Preprints 3rd IFAC Congress London 1966

Lindström, R.
"A Study of Head Box Pressure and Level Control Systems" Paper Trade Journal 1970

Aaslid, R.
"Lineär dynamisk modell av inløpskassen i en papirmaskin. Simulering av konvensjonell og model regulering" Rapport 70-41-E
Institutt för Reguleringsteknikk
NTH

Fjeld, M, Flatabø, J and Stai, E
"Regulering av innløpskasse" Rapport 72-2-T SINTEF
Januar 1972

Lindström, R
"Reglerförsök med inloppslådemodell"
Svensk Papperstidning 72 (1969) 459 - 465

LECTURE NOTES ON PAPER MACHINE CONTROL

DYNAMICS OF THE WET END OF A PAPER MACHINE

K.J. Åström

1 INTRODUCTION

2 PROCESS DESCRIPTION

Control Variables

Outputs

Disturbances

3. PROPERTIES OF WATER FIBRE MIXTURES

4 MIXING

Mixing in Laminar Tube Flow

Input Output Relations

Applications to Tube Flow in the Paper Machine

Mixing in Pumps and Head Box

5. DRAINAGE ON THE WIRE

Simple Drainage Theory

Drainage of Water Fibre Mixtures

Dynamic Effects

Consistency of Filtrate

More Complicated Drainage Models

6 A CONSTANT RETENSION MODEL

Notation

Water Balance

Fibre Balance for Fan Pump Head Box System

Fibre Balance for the Wire

Fibre Balance for the Wire Pit

A Constant Retention Model

The Characteristic Equation

Steady State Gain

A Numerical Example

Summary

7. VARIABLE RETENTION MODELS

A Numerical Example

8 MULTICOMPONENT MODELS

9 MORE ELABORATE MODELS

10 COMPARISON OF MODEL AND MEASUREMENTS

11 NOTES AND REFERENCES

DYNAMICS OF THE WET END OF A PAPER MACHINE

1. INTRODUCTION

In this chapter we will discuss the dynamics of the wet end of the paper machine i.e. the part of the paper machine from the thick stock valve to the couch. The wet end thus includes the the head box whose flow dynamics was discussed in the previous chapter. The main purpose of the model of the wet end is to describe how variations in the thick stock flow and concentration will affect the basis weight at the couch. The basis weight at the couch is thus considered as the output of the model. There are also other important control variables, the flow through the fan pump, the slice opening, the air flow to the head box and the wire speed. The essence of the model will thus be to describe the fibre balance in the wet end of the paper machine. The physical fenomena involved include mixing and separation of the fibres. These fenomena are very complex and in contrast with the flow dynamics of the head box discussed in the previous chapter it will no longer be possible to derive an accurate model from physical principles alone.

The chapter is organized as follows. A description of the process is given in section 2. Properties of water fibre mixtures are briefly reviewed in section 3. Section 4 deals with mixing phenomena. The drainage on the wire is discussed in section 5. A crude model based on several simplifying assumptions on the mixing of the fibres and a simplified description of the drainage on the wire is discussed in section 6. A refinement of the model which considers the variation of the retention with the basis weight is discussed in section 7. The models in sections 6 and 7 assume that the stock can be considered as composed of water and fibres alone. In section 8 it is taken into account that there might be other components and also that different fibers may behave differently. More elaborate models are briefly reviewed in section 9. These models include more detailed descriptions of the drainage on the wire which permit modelling of the wet line. In section 10 the models obtained are compared with measurements of dynamics on the real machines that have been reported in the literature. Since the measurements reported in the literature are rather meager this section is very brief. Notes and references are given in section 11.

2. PROCESS DESCRIPTION

A schematic diagram of the of the process is shown in Fig. 2.1. It should be emphasized that there are many variations in process design. The following description should therefore be considered as an example only. Thick stock (tjock massa) from the machine chest enters in the left of Fig. 2.1. The concentration of the thick stock is regulated through dilution with white water as indicated in the Figure. The regulation is based on a measurement of shearing force (skärkraft). The shearing force is a function of the fibre concentration but it also depends on many other variables like velocity, viscosity, concentration of additives etc. Following the concentration regulator is the thick stock valve which controls the flow of thick stock to the wet end of the paper machine. The thick stock is diluted with white water from the wire pit and pumped by the fan pump through the screens and cleaners into the head box. The diluted stock (tunnmassa) flows out of the head box and onto the wire where the water is drained and part of the fibers remain on the wire. To obtain efficient drainage the wire is usually provided with various devices shown in Fig. 2.2.

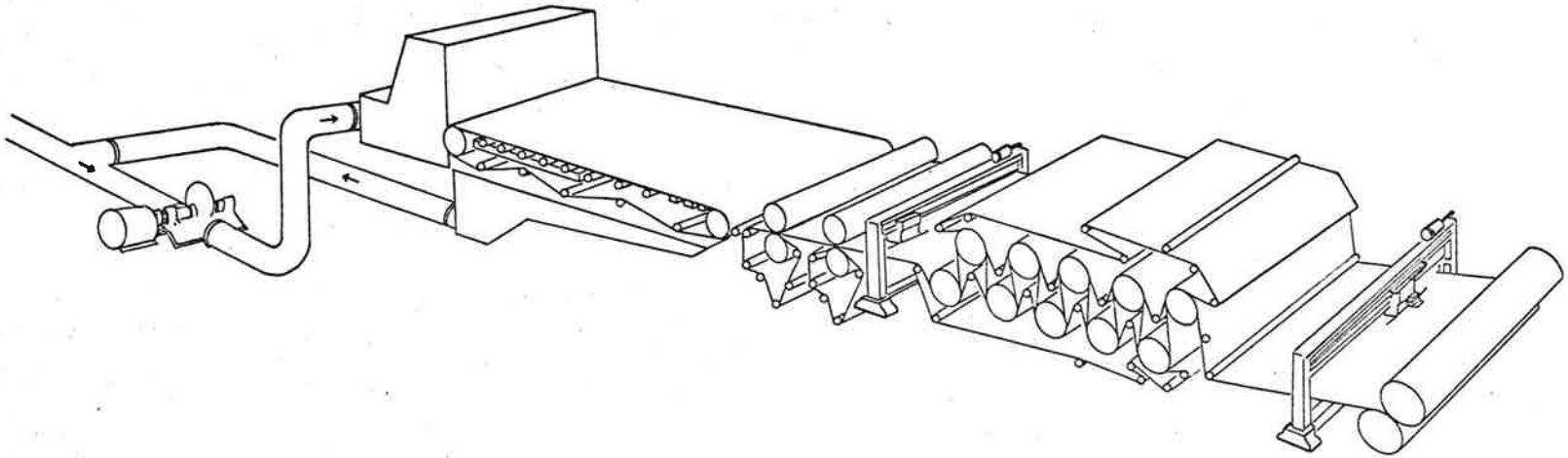

Fig. 2.2. Schematic diagram of wire part of a Fourdrinier machine

In Fig. 2.2 the slurry from the head box first passes over the wet suction boxes which simply are boxes provided with low pressure where the water is sucked out (many paper machines do not have wet suction boxes). After the wet suction boxes follows the table roll section.

The table rolls are simply rolls which are supporting the wire. Through hydrodynamic effects there will be a suction pressure at the nip of the table rolls. After the table rolls follow the dry suction boxes. These are again boxes with vertical walls provided with low pressure where water is sucked out. The paper machine is usually operated in such a way that the slurry covers the mat at the beginning of the dry suction boxes. Somewhere in the middle of the dry suction boxes the slurry is drained in such a way that there is no free water surface above the fiber mat. The position where this occurs can easily be observed visually on the paper machine. This position is called the wet line. After the dry suction boxes follows the couch roll which is usually provided with low pressure. A significant amount of water and fines are drained through the couch roll. The mat is removed from the wire after the couch roll and passed on to the press section. The water and the fibres that are drained on the wire are sometimes collected in trays and fed to a separate tank. In other cases there is a big tank underneath the wire where all the drained water and fibers are collected. This big tank is called the wire pit. The water required to dilute the thick stock is taken from the wire pit or the storage tank. There is also an overflow of white water from the wire pit which is fed to the stock preparation system.

Control Variables

The major control variables are

- thick stock flow
- thick stock concentration
- flow through fan pump
- slice opening
- air flow to head box
- head box valve
- wire speed
- pressure in wet suction boxes
- pressure in dry suction boxes
- couch vacuum

Outputs

The major output variables are

basis weight at couch
jet to wire velocity ratio

Disturbances

The major disturbances are variations in thick stock concentration and in fiber properties which affect the rentention on the wire.

3. PROPERTIES OF WATER FIBRE MIXTURES

Since the processes in the wet end of the paper machine are flow, mixing and separation of water fibre mixtures it is important to understand the properties of such solutions. Fibres are typically 2 to 5 millimeters long. They have the width 20 - 40 µ and a thickness of 10-15µ. A fibre water mixture is thus a typical 2-phase-system. A simple order of magnitude calculation where the fibres are approximated by spheres with a diameter equal to the fibre length indicate that fibres will interact at very low concentrations. (0,01 - 0.1 gramme/100 ml). It has in fact been demonstated that the fibres form an elastic network. Fibre water mixtures thus have a very complicated flow pattern. This is illustrated by the graph of Fig. 3.1 which shows the pressure loss curve for water fibre mixtures. Notice in particular that water fibre mixtures have less resistance to flow than pure water at high speeds and high concentrations. Studies of water fibre mixtures have shown that their flow pattern can be described as follows. At low velocities the fibres form a rigid network which flows like a plug in the centre of the tube. The whole velocity gradient is concentrated to a narrow region closed to the wall. At higher velocities the network is broken up into several small pieces and at very high velocities the network is completely broken down and the flow pattern is close to the turbulent flow of a Newtonian fluid.

DIAGRAM 1.

Tab. 7a *Friktionsförluster för sulfitmassa i 6" gjutjärnsrör*

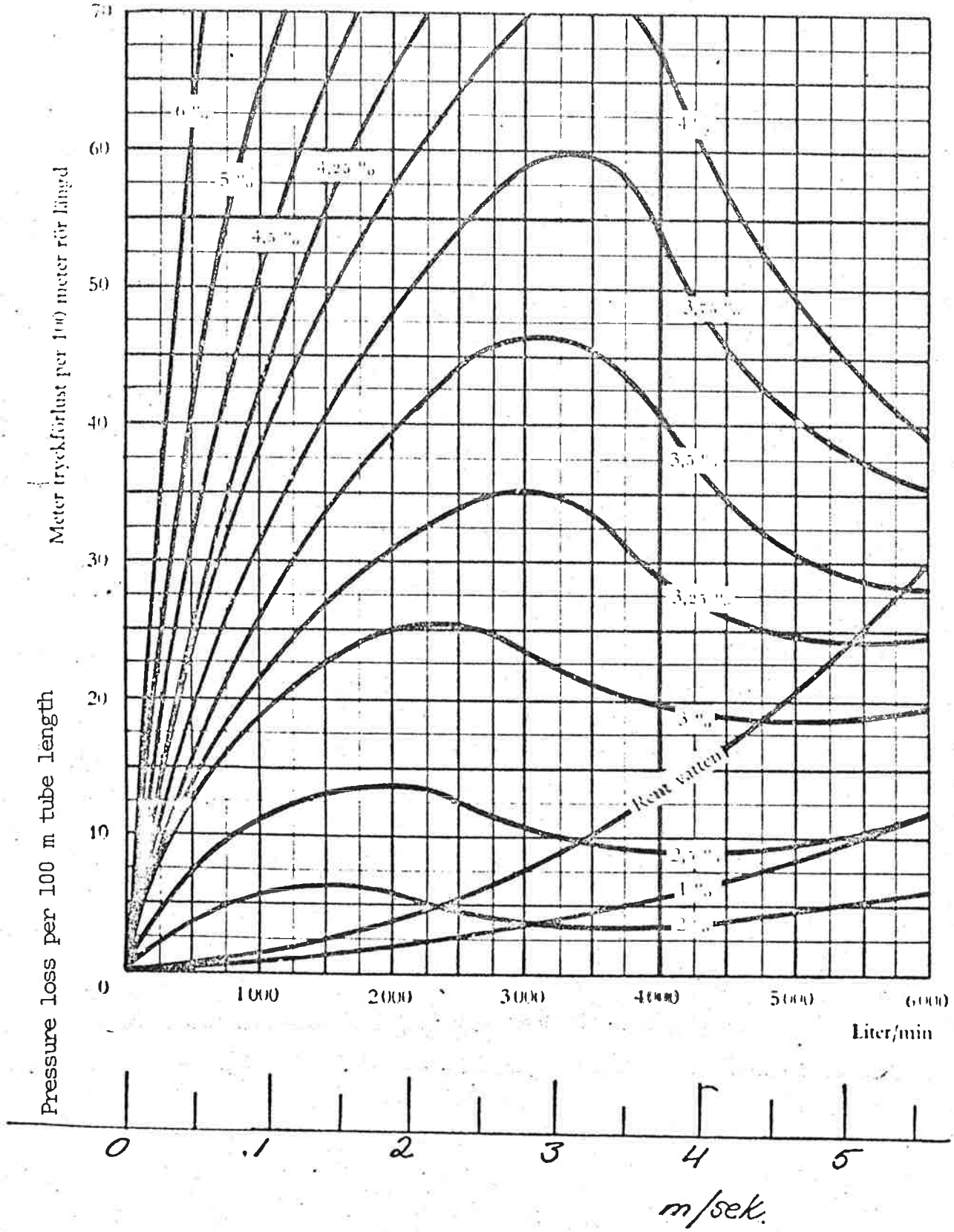

Fig. 3.1. Pressure loss versus flow rate for sulphite stock flow in 6" cast iron tubes. Notice that the pressure loss for stock is lower than for pure water at reasonable flow rates.

4. MIXING

An important part of the concentration dynamics of the wet end of a paper machine is composed of mixing phenomena. There is mixing in the wire pit, in the head box, in the fan pump, in the screens and cleaners and in the connecting tubes. From the discussion of the properties of water fibre mixtures in the previous section it is clear that the mixing phenomena are very complex. It is certainly not true that there is perfect mixing in the head box and in the wire pit and that the connecting tubes only serve at the pure transportation. According to some sources the major part of the mixing takes place not in the tanks but in the tubes themselves. These different mixing phenomena will be discussed in the following.

Mixing in Laminar Tube Flow

The dynamics of concentration variations in a tube with a stationary laminar flow will first be investigated. It is assumed that the concentration across the inlet is constant. This concentration is taken as the input to the system. The average concentration over the cross section of the tube at a distance a downstream from the inlet is taken as the output. Let the tube be circular tube with radius r_0. Let r denote the distance from the center of the tube and x the distance downstream from the tube inlet.

Let c(r,x,t) be the concentration at a point (r,x) at time t. If the flow is laminar we have

$$c(r,x,t+h) = c(r,x-hv(r),t) \tag{4.1}$$

where v(r) is the velocity at a distance r from the center of the tube. The concentration thus satisfies the following partial differential equation

$$\frac{\partial c}{\partial t} = -v(r)\frac{\partial c}{\partial x} \tag{4.2}$$

Since the concentration at x=0 is assumed independent of r we get

$$c(r,0,t) = u(t) \tag{4.3}$$

where u is the input. The output is the average concentration at x = a i.e.

$$y(t) = 2r_0^{-2} \int_0^{r_0} rc(r,a,t)dt \qquad (4.4)$$

The dynamics of the system can thus be represented by the equations (2), (3) and (4). The state is the concentration in $0 \leq r \leq r_0$, $0 \leq x \leq a$.

Input Output Relations

Introducing (1) into (3) we find that the system can be characterized by the input output relation

$$y(t) = 2r_0^{-2} \int_0^{r_0} r\, c(r, 0, t - \frac{a}{v(r)})dr = \qquad (4.5)$$

$$= 2r_0^{-2} \int_0^{r_0} r\, u(t - \frac{a}{v(r)})dr$$

Taking Laplacetransforms we find

$$Y(s) = 2r_0^{-2} \int_0^{r_0} r\, e^{-s\frac{a}{v(r)}} dr\, U(s)$$

The transfer function is thus given by

$$G(s) = 2r_0^{-2} \int_0^{r_0} re^{-s\frac{a}{v(r)}} dr = \qquad (4.6)$$

$$\int_{a/N_0}^{\infty} e^{-st}\, d(r_0^{-1}v^{-1}(a/t))^2$$

where the last equality is obtained by changing the variables $\frac{a}{v(s)} \rightarrow t$ and v^{-1} denotes the inverse function.

Now use the definition of the Laplace transform

$$G(s) = \int_0^\infty e^{-st} h(t)dt$$

and we find that the step response of the system is given by

$$H(t) = \begin{cases} 0 & t < a/v_0 \\ [r_0^{-1} v^{-1}(a/t)]^2 & t \geq a/v_0 \end{cases} \qquad (4.7)$$

Notice that the equation (6) can also be obtained by taking Laplace transform of (2), (3) and (4).

The equation (7) can be derived directly by assuming that the system is initially of rest and making a unit step change. The concentration after the step is shown in Fig. 1.

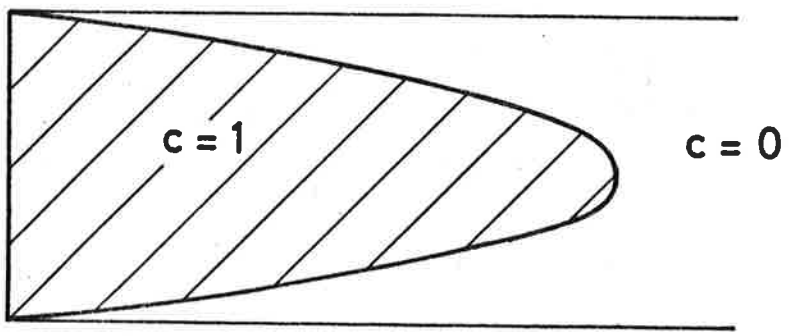

Fig. 1 Concentration after a unit step.

For x=a the concentration equals 1 for
$r \leq r_1$ where

$$tv(r_1) = a$$

i.e. $$r_1 = v^{-1}\left(\frac{a}{t}\right)$$

The average concentration of x = a is thus

$$y(t) = \begin{cases} 0 & t < a/v_0 \\ [r_o^{-1} v^{-1}(a/t)]^2 & t \geq a/v_0 \end{cases}$$

which is identical to (7)

Example 4.1

As an example the following velocity profile will be considered

$$v(r) = v_o\,[1 - (r/r_0)^n] \qquad (4.8)$$

Then

$$r = r_0\,[1 - \frac{v(r)}{v_0}]^{1/n}$$

Hence

$$(9) \quad H(t) = \begin{cases} 0 & t < a/v_0 \\ (1 - \frac{a}{v_0 t})^{2/n} & t \geq a/v_0 \end{cases}$$

Fig. 4.2 shows the step responses for different values of n.

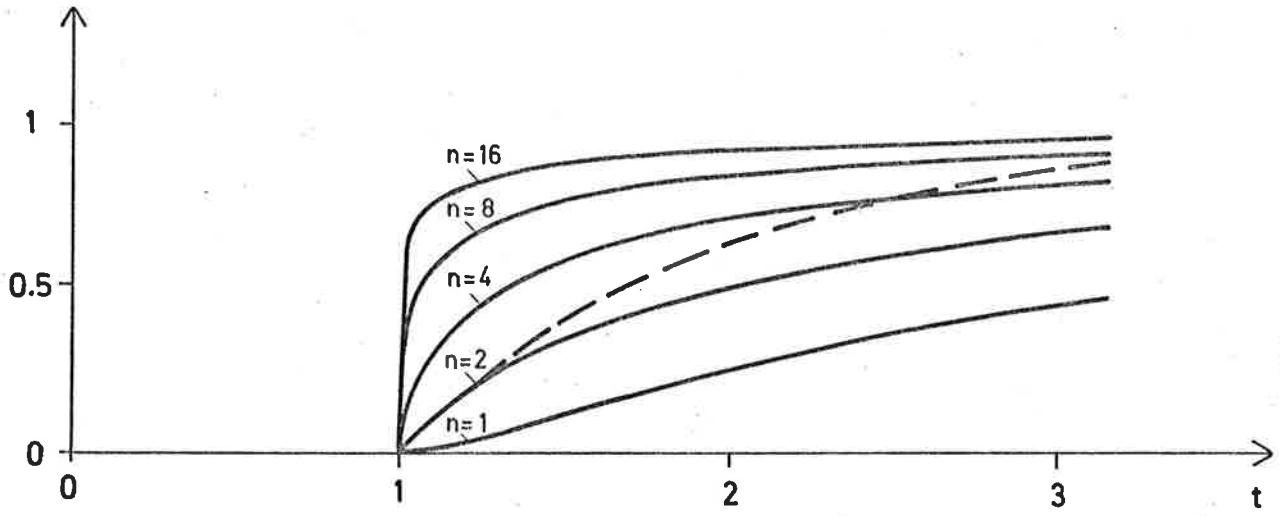

Fig. 4.2. Step responses for mixing due to the velocity profile (4.8) for n = 1,2,4,8 and 16. The dashed curve shows an exponential curve for comparsion

For n = 2 we get in particular

$$H(t) = \begin{cases} 0 & t < a/v_0 \\ 1 - \frac{a}{v_0 t} & t \geq a/v_0 \end{cases}$$

The analysis thus indicates that due to the velocity profile the concentrations of laminar tube flow will have a dynamics which can be approximated by time delay and a time constant which is of the same order of magnitude as the time delay. Notice, however, that the convergence of the step response to the steady state value is significantly slower than exponential at least for the profiles chosen in Example 4.1.

Applications to Tube Flow in the Paper Machine

The analysis just given assumed laminar flow. In turbulent flow there will be a mixing across the tube. Since the flow pattern of water fibre mixtures is complicated there might be an effect similar to the one for laminar flow for water fibre mixtures. In particular in the region where the flow is not completely turbulent. A similar mechanism will of course also occur in tube bends. A particular case is the inlet to the head box where the tube enters one end of the head box and the flow is distributed along the whole width of the paper machine.

Mixing in Pumps and Head Box

There is undoubtedly a considerable mixing in the fan pump and there can also be mixing in through the action of the perforated rolls in the head box.

5. DRAINAGE ON A WIRE

The separation of water from the fibres on the wire is a very important sub-process of the wet end of a paper machine. It is also a complicated process which is very difficult to describe.

When the slurry leaves the head box it enters the wire and water is drained from the slurry as it moves along with the wire. Underneath the wire are suction boxes, table rolls etc. In this section we will briefly review the models and measurements that are available to describe the drainage mechanism.

Simple Drainage Theory

A simplified case will first be analysed. Consider a fibre water mixture above a stationary metal net or plastic net as indicated in fig. 5.1.

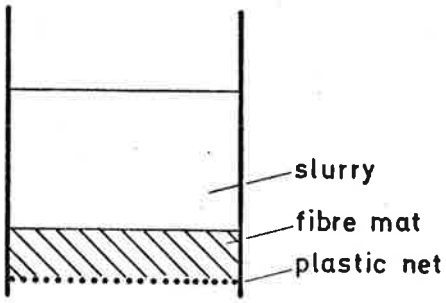

Fig. 5.1. Simple drainage element

The gravity or a suction pressure will force the slurry through the net. If the fibres are large in comparison with the net some fibres will be caught. In doing so they will form a mat which will cause more fibres to be caught. If it is also taken into account that the fibres are not of uniform size, they will not be caught on the uppermost part of the fibremat but they can also be caught inside the mat, causing the holes in the mat to be smaller.

To model this phenomena mathematically, we can use a mass balance as follows

$$\frac{d}{dt}(m) = q_o(c_s - c_f) \qquad (5.1)$$

In this equation m means the mass of the fibres in the mat, q_o is the flow through the mat which is assumed uniform, c is the fibre concentration in the slurry and cc_u is the fibre concentration in the filtrate.

The equation (5.1) simply tells that the mass accumualted in the mat equals the incoming fibres minus the outgoing fibres. Introduce the basis weight w through m = Aw and observe that the flow q_o is given by

$$q_o = A\frac{dh}{dt} = A\dot{h}$$

Furthermore let the pressure difference across the mat be Δp and assume that laminar flow we get

$$q_o = k_1\frac{\Delta p}{h} = \frac{k\Delta p \cdot c_m}{w}$$

where c_m is the average fibre concentration in the mat. Furthermore assume that the concentration of the filtrate is zero. The equation 5.1 can then be written as

$$w\frac{dw}{dt} = k_1\Delta p c_m c_o$$

Integrating this equation, we find the following relation between the basis weight of the mat above the wire and the time.

$$t = \frac{k_2}{c_o c_m \Delta p} \cdot w^2 \qquad (5.2)$$

According to this simple theory the drainage time is proportional to the square of the basis weight and its inversional proporitional to the pressure difference to the fibre concentration in the slurry and in the mat.

Drainage of Water Fibre Mixtures

Experiments of drainage of pulps paper making and consistencies have been performed by Wahlström and O'Blenes. A copy of Wahlströms paper is included in Appendix A of this section. Their experiments do not agree with equation (5.2). It has instead been found that the drainage time is given by the following equation

$$t = \frac{k_3}{c_o} \Delta p^{-n} w^{\alpha} \qquad (5.3)$$

where the number n experimently has been found to vary from 0.35 to 0.53 and the parameter α between 1.7 to 3.5. The coefficients vary with pulp type and degree of beating. The reason behind the discrepancy of (5.2) and (5.3) is that too many simplifying assumptions were made in deriving (5.2). In particular it was not taken into account that the fibre mat is compressible, neither that the filtred consistency is nonzero and that the concentration varies across the fibre mat.

Dynamic Effects

In their experiment, Wahlström and O'Blenes also found dynamic effects. If the pressure is suddenly applied across the system the flow does not response immediately. The flow q can be determined through the equation of motion (Navier Stokes equation) which gives the velocity as follows

$$\frac{dv}{dt} = \frac{\partial v}{\partial t} + \frac{\partial v}{\partial x_1} \frac{\partial x_i}{dt} = F - \frac{1}{\rho} \text{grad } p + \frac{\mu}{\rho} \nabla^2 v + \frac{\mu}{3} \nabla (\text{div } v)$$

This equation is impossible to solve in a complicated situation like fibre drainage. Order of magnitude estimates can, however, be made as well as experiments. Fig. 10 of Wahlström's paper shows a typical re-

sult. In this graph an attempt is also made to resolve the flow transient into two terms. It follows from the results that the flow has a settling time of 0.02 to 0.05 seconds. Applied to the drainage on the wire of a paper machine this implies that the flow does not sense the detail of the pressure distribution underneath the wire but rather that it takes averages of a distance corresponding to about half a meter.

Consistency of Filtrate

One reason that the formula (5.2) does not agree with the experiments is that it was derived under the assumption of zero concentration in the filtrate. A theoretical analysis which has been verified by experiments gives the following formula for the concentration of the filtrate.

$$c_f = 1 - (1 - \alpha)e^{-\gamma w} \; c_o$$

where the parameter α is called initial retention and w is the basis weight. A typical value of γ is .50 m^2/kg.

More Complicated Drainage Models

Since the simple model does not describe the drainage several more complicated models have been proposed by Meyer and Ingmansson. These models take into account that the fibre mat is compressible and that the fibre concentration varies across the mat. The models are given in terms of partial differential equations for the fibre concentration or for the drainage rate.

The Drainage of Pulps at Paper-Making Rates and Consistencies Using a New Drainage Tester

BÖRJE WAHLSTRÖM[1] and GEORGE O'BLENES[2]
Karlstads Mekaniska Werkstad, Karlstad, Sweden

A new drainage apparatus to study water removal from slurries of paper making consistencies and at drainage rates equivalent to those on a paper machine is presented. Certain aspects on the characterization of the apparatus are discussed.

The present discussion has been limited to describing the drainage after "retention equilibrium" has been obtained; that is, in the mat weight range above 30 to 70 gm./m². The drainage of paper making slurries may be expressed as the time of formation of increasing mat weight by the emperical equation

$$t = \frac{G}{s} (\Delta p_m)^{-n} W^{\alpha}$$

where

G = drainage constant, c.g.s. units
s = consistency of slurry, gram fibre/gram water
Δp_m = pressure drop across mat, dynes/cm.²
W = mat weight deposited, gm./m.²

and where

n describes the effect of pressure and compression, dependent only upon type of pulp and varying from 0.35 to 0.53.

α describes the rate of mat formation, dependent mainly upon pulp type and degree of beating and varying from 1.7 to 3.5; influence of flocculation, pressure, and consistency is secondary.

For $\alpha = 2$, the resistance to flow may be stipulated by the average specific resistance factor. As α varies, each unit weight of fibre deposited does not increase the resistance by a unit amount as given by the average specific resistance. The variation in α is postulated as being due to two factors: For values above 2, the increase is the result of the migration of fines into the previously formed mat from the layer deposited on the surface. The effect of the velocity difference through the mat results in the values below 2.

The variables of consistency, slowness and pulp types on the formation time are discussed for a cross section of pulps and at different degrees of beating.

The practical implication of this work is that neither a slowness determination nor the average specific drainage resistance is adequate in describing the drainage behaviour of pulps. Drainage analysis on the apparatus presented herein has shown the necessary criteria required to characterize the drainage behaviour of pulps of papermaking consistency.

IN THE ATTEMPT to put papermaking on a more scientific basis, a large amount of work has been carried out to find quantitative relationships regarding drainage on pulp and papermaking equipment. Any such attempt must be based on the proper knowledge of the drainage characteristics of pulps at consistencies and drainage rates used in operation. This is the necessary step before the complicated drainage behaviour at table rolls, foils etc. can be properly analysed.

Much work has been done to determine the drainage characteristics of dilute fibre suspensions of the order of 0.01 per cent consistency where fibre interaction is negligible. Due mainly to the excellent work done by Ingmanson and his co-workers [1, 2], it has been possible to put this drainage process on a purely mathematical basis. Combining Ingmanson's work with the work done on fibre retention and compression of the mat it has been demonstrated by Meyer [5] that the drainage characteristics of the pulps can be deduced and shown to agree very well with experimental results. However, it has been shown by Ingmanson that drainage at higher consistencies brings in new factors, for which no account could be made in their present mathematical and physical model. Therefore it is not justifiable to use the results obtained at these low consistencies at the higher consistencies and drainage rates used in practice without supporting experimental evidence.

The object of this work was to establish drainage data on a large number of different pulps at consistencies and drainage rates of the same order as used on paper machines. Therefore a drainage apparatus was designed on which these results could be obtained.

Previously Mardon *et al.* [3] designed a laboratory drainage apparatus for this kind of determination. Based on the experience from this apparatus, a new design was contemplated in which the inertia of the apparatus could be reduced. Drainage at constant pressure drop was considered the best method. This drainage process resembles more closely the conditions on sheet formers, at suction boxes, and on pulp equipment such as thickeners and filters. It is also impossible to simulate the high drainage rates at the initial stages of sheet formation with a constant flow drainage process. The two main difficulties in designing such a

Paper presented at the Annual Meeting of the Technical Section, Canadian Pulp and Paper Association, Montreal, Canada, January 23—26, 1962; not to be reproduced without permission of this organization.

[1] Research director.
[2] Research engineer.

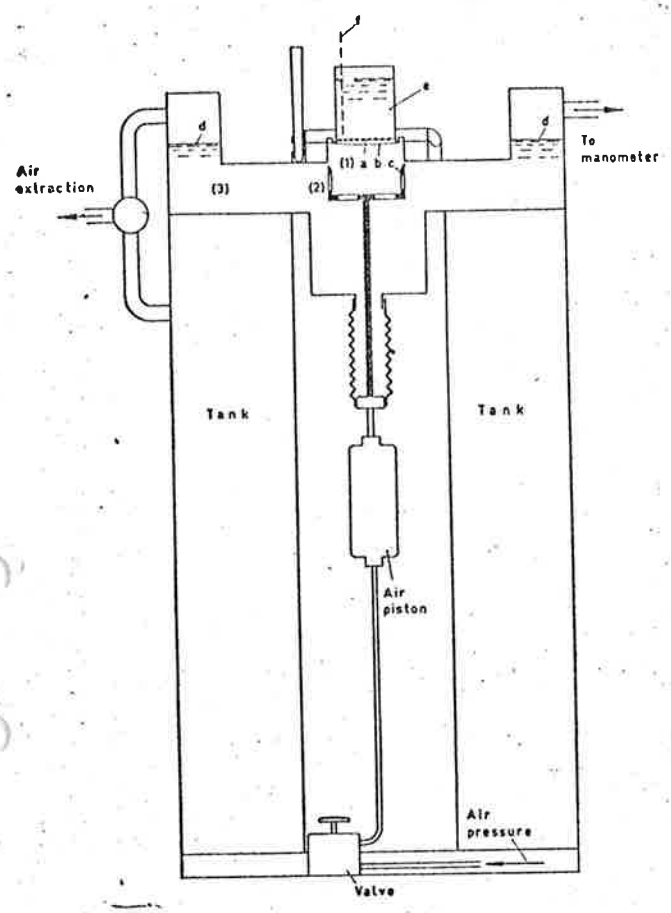

Fig. 1. Drainage apparatus.

constant pressure drainage equipment are to obtain an instantaneous pressure application and to limit the inertia of the system to the smallest possible. Both these demands have been met in the apparatus described in this paper. To the present authors' knowledge, the only other apparatus designed to meet these requirements and for the use of studying drainage is that of Mardon *et al.* [3].

After extensive testing this apparatus has been used to investigate the influence on drainage of type of pulp, beating, pressure drop, basis weight, flocculation, consistency and temperature of slurry. It has not been possible to avoid the influence of flocculation in a static drainage tester of this kind as flocculation is unavoidable without intensive turbulence and this is impossible to maintain under these drainage conditions without disrupting the sheet.

The results are presented as the time needed to form a certain basis weight taking into account consistency and pressure drop. Significant information regarding the drainage mechanism has been obtained.

DESCRIPTION OF METHOD

Drainage Tester; Demands and Design

The demands in the design of the drainage tester were:

1. application of pressure should be instantaneous,
2. the applied pressure should remain constant throughout a drainage cycle,
3. water removal may be achieved with either water or air beneath the wire.

To meet these needs the apparatus shown in Fig. 1 was constructed. This design embodies a cylinder holding the wire mesh at one extreme end, a circular saw-toothed knife, an air cylinder to drive the knife, a sealed circular chamber beneath the wire extending outwards and a tank of large volume.

A foil, secured between cylinder and circular chamber, allows for a suction pressure to be introduced and maintained in the tank and chamber at the required level. The construction was designed to enable the use of water as the transport medium: i.e., the medium below foil and wire through which pressure is applied to the under side of the wire. With water as the medium, the level in the chambers lies at the same level as the wire. Air suction is applied in the volume above this level. The areas noted as 1, 2 and 3 in Fig. 1 were designed to give the lowest possible acceleration required to move the mass of water.

As suction is applied, the foil deflects to a limited degree. When the required suction, at which the drainage test is to be performed, is reached, water is introduced from above onto the foil. Thus the volume between deflected foil and wire is filled to the wire level. The slurry is suspended in the cylinder above the wire. The pressure is applied below the wire by shearing the foil with the circular saw-toothed knife which is driven by the air piston. The volume of suction chamber and tank is of such a size, as compared with that of the slurry, that a constant suction is maintained throughout a drainage cycle. The drainage may be performed with either air or water as the transport medium. A platinum wire, immersed in the slurry, records the drainage cycle on a high-speed recorder by measuring the change in electrical resistance due to the change in level in the sheet former. This means of recording the drainage has previously been used by Mardon [3]. The main features of the apparatus are further illustrated by the photos shown in Fig. 2. (Patent applied for.)

Evaluation of Drainage Curve

The curve for water removal from a fibre slurry under a constant pressure drop is illustrated by the recorder tracing shown in Fig. 3. From this curve the time for increment drop, x, in height of slurry is determined, $t = f(x)$, where x = drop in level measured from slurry level before onset of drainage, cm.

We have chosen to express the results as time of formation as a function of mat weight retained, $t = f(W)$, where W = mat weight retained by wire, gm./m.^{2}. To relate drop in level, x, with its corresponding mat weight retained, W, it is necessary to determine the fibre retention, and the water-fibre ratio of the mat formed m, gram water/gram fibre. The mat weight retained, $W = f(x, \text{retention}, \bar{m})$.

On completion of each drainage cycle the mat deposited was recovered and its o.d. weight, w, was determined. The weight of fibres approaching the wire per increment drop, x, of total height of slurry, h, is given by

$$W_x = \frac{x}{h} \cdot \frac{w}{A} \cdot R_h^{-1} 10^4$$

where w = o.d. weight of total mat deposited, gm.
h = total height of slurry, cm.
A = area of wire medium, cm.^{2}

$$R_h = \left(\frac{W_r}{W_t}\right)_h = \text{retention ratio for total height, } h$$

Determination of Retention

Retention on the wire has only recently received much attention due to the work of Estridge [4] who treated

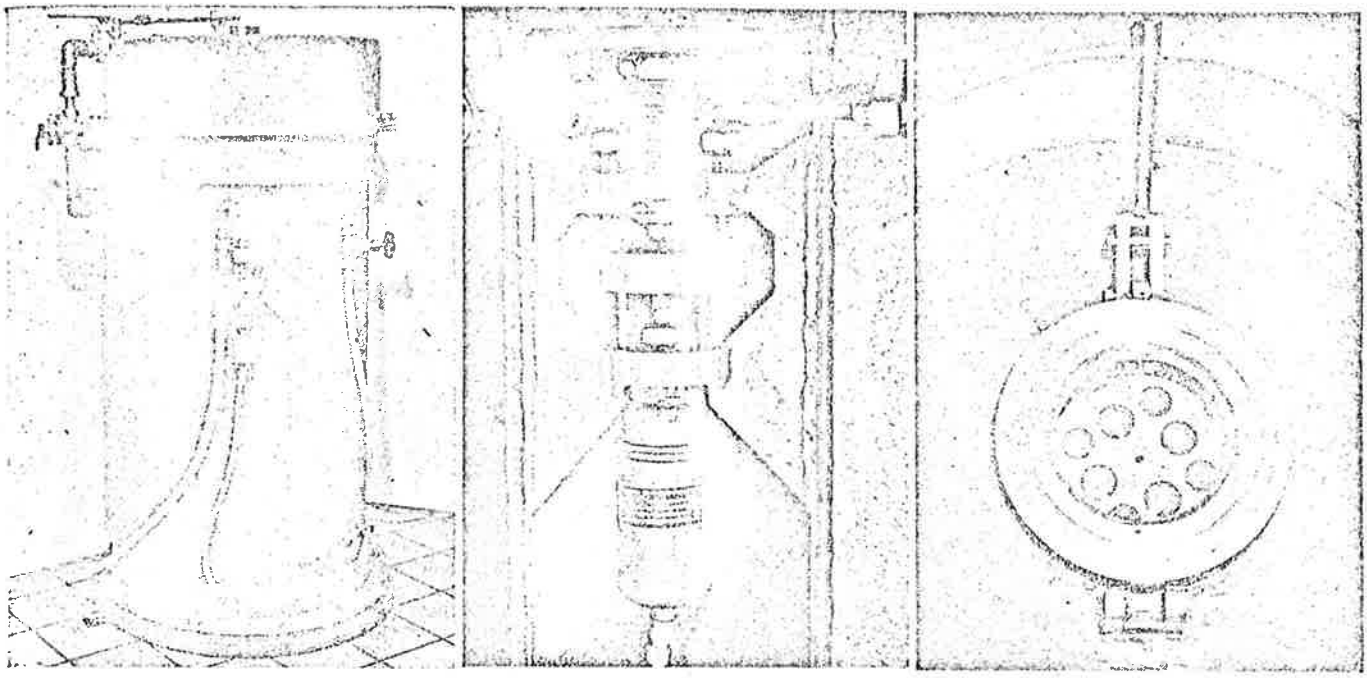

A B C

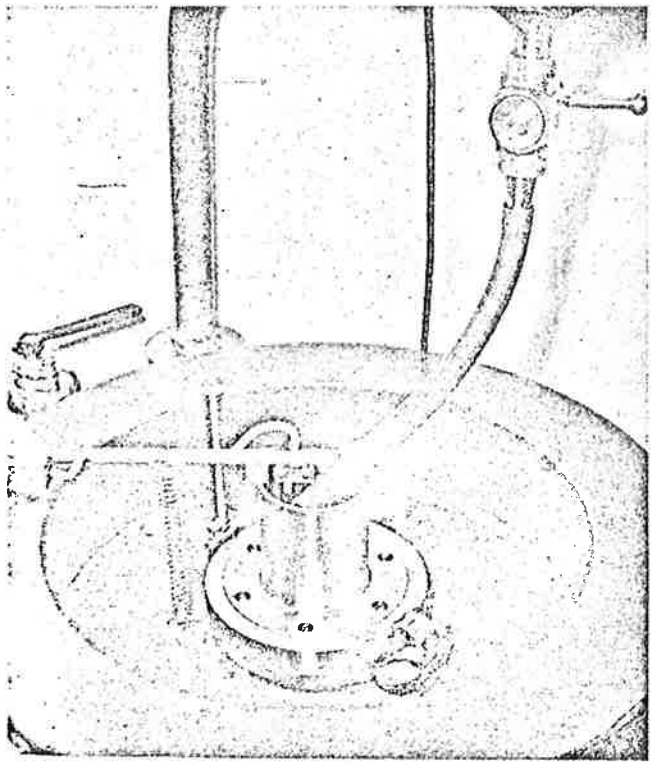

D

Fig. 2. Features of drainage apparatus. a. Overall view; b. Control for knife travel and, air piston; c. From top, cylinder removed. Knife in raised position; d. Probe and line from deflocculating device in position.

the problem by the theory of probability. The development of this theory towards application to less rigorous models has as yet to be determined. Experimental determination of the retention curve (for the conditions required) is therefore necessary. It was considered that drainage of slurries, where the height of slurry was varied before the onset of drainage, would suffice for the present purpose. Drainage of each predetermined height of slurry was carried to completion and the weights of through-fraction and of mat retained were found for each predetermined depth of slurry. Relationships, such as illustrated in Fig. 4 for a groundwood pulp at 0.2 per cent have been developed.

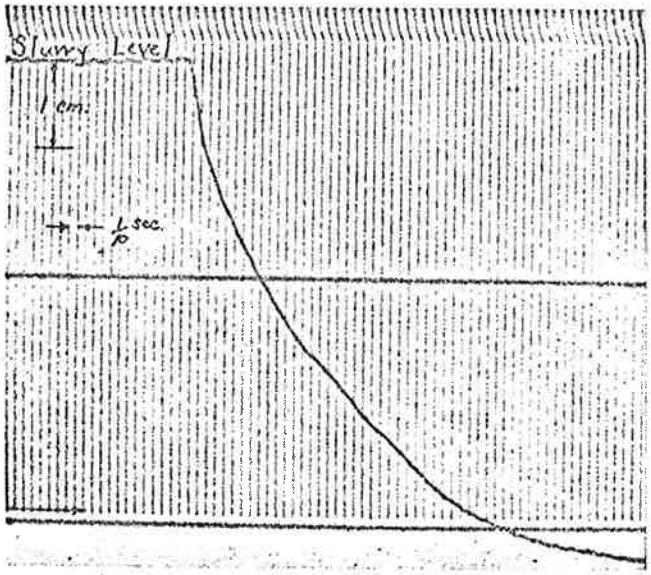

Fig. 3. Sample drainage curve.

The weight retained per increment drop in slurry can be given as

$$W_{rx} = W_x \cdot R_x$$

where

W_{rx} = weight retained for a drop, x, in slurry level, gm./m.^{2}

$R_x = (W_r/W_t)_x$ = retention ratio for drop x

Determination of Average Water/Fibre Ratio of Mat

In determining the weight formed per increment drop in slurry, the weight is being underestimated as the fibre deposited is also replacing a depth over the wire occupied by the slurry. Thus consideration must be given to the depth of mat at each stage in the drain-

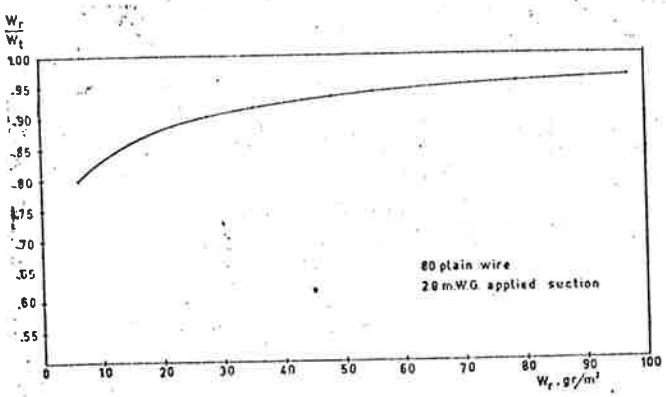

Fig. 4. Retention curve for groundwood.*

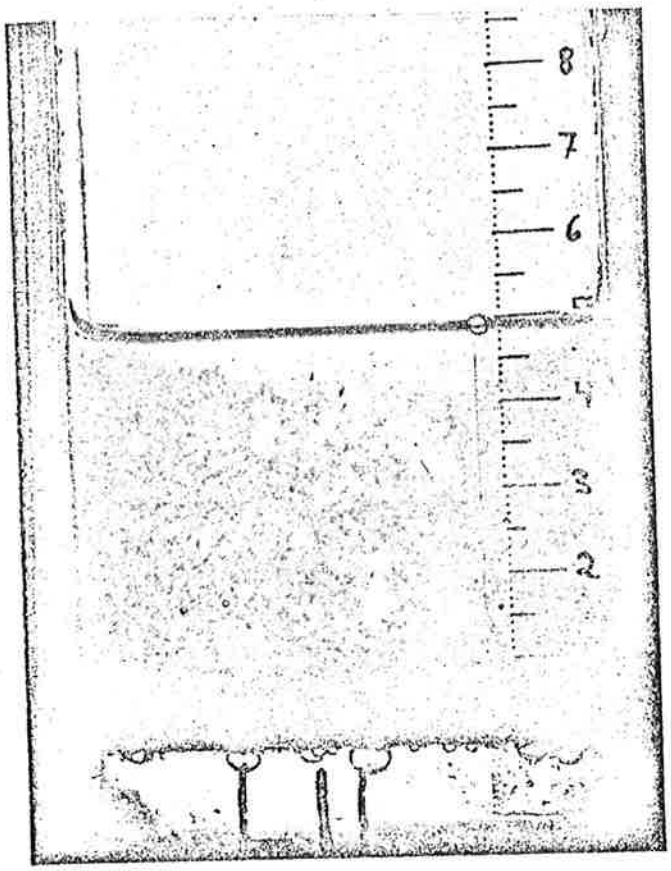

Fig. 5. Mat formation, wet beaten unbleached sulphate, 20 × 10^3 dynes/cm.² pressure drop, 0.3 per cent consistency, 160 gm./m.² deposited.

age cycle; and the mat deposited for a drop, x, in slurry level, corrected for the mat depth, will be given by:

$$W = \frac{W_{rx}}{1 - \bar{m}s}$$

where

s = consistency of the slurry, gram fibre/gram water
$\bar{m}$ = water fibre ratio of mat. gram water/gram fibre

A photographic technique was developed for the determination of $\bar{m}$. Under exact operating conditions, the formation of mat was recorded by cine or still photos through the use of a perspex section. This rectangular section was adaptable to replace the wire-holding cylinder on the drainage apparatus. Illustrative of the results of this technique is the photo shown in Fig. 5 of mat formation during the drainage of a wet beaten unbleached sulphate pulp.

The depth of the mat, formed at any instant, could be estimated by means of the scale mounted to the right in the photo. The accuracy in this determination depends largely upon the type and quality of pulp. With such pulps as groundwood, the top surface of the mat can be estimated with reasonable accuracy. For other pulps, such as the highly beaten sulphate as shown in Fig. 5, the definition of the top surface of mat is not clear. The density varies through the mat approaching the slurry consistency at the top, making exact determinations difficult. Despite the shortcomings of the method it was felt necessary to have a dynamic method, which made the previously used static methods unsuitable.

The water fibre ratio is given by:

$$\bar{m} = \frac{a \cdot d \cdot \rho}{w}$$

where

a = formation area, cm.²
d = depth of mat, cm.
ρ = density of filtrate, g./cm.³

*In the figures, pressure drop is denoted by "m.W.G.". 1 m.W.G. ~ 10^3 dynes/cm².

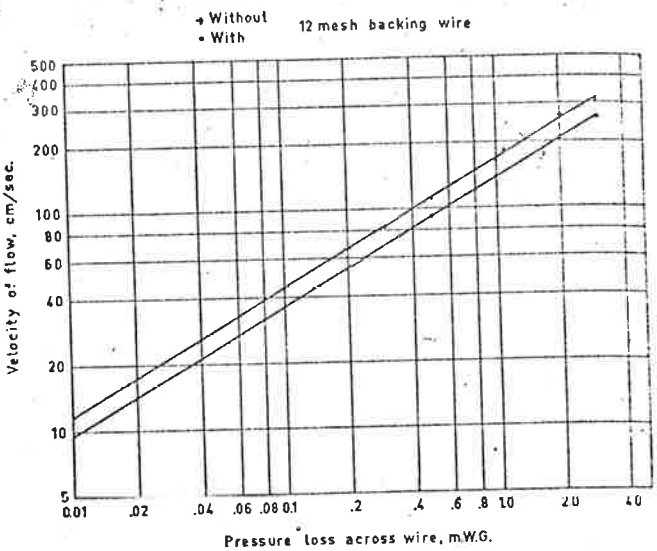

Fig. 6. Characterization of wire medium.

CHARACTERIZATION OF DRAINAGE TESTER

Preliminary investigations have shown that the use of water—opposed to air—as the medium of transport below the foil results in a decrease in time of formation of approximately 5 per cent (Appendix I). All subsequent determinations of drainage have been carried out with water as medium. Reproduceability of the apparatus is such that the standard deviation of the mean on three repeats is approximately 2 per cent. (Appendix II).

Further investigations showing the development of the pressure drop across mat and the effects of temperature and flocculation on drainage have been conducted.

Wire Medium and Development of Pressure Drop across Mat

In all determinations to be presented, an 80-mesh plain bronze wire, with and without a 12-mesh backing wire was used as the filter medium. To characterize the wire, water at 20 deg. C. was drained under pressure

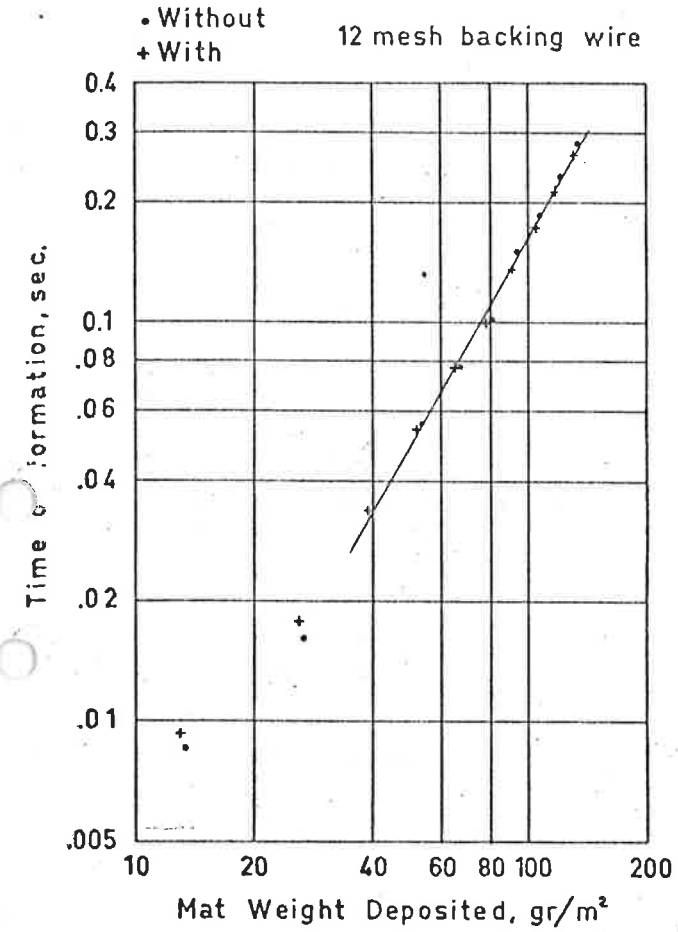

Fig. 7. Influence of backing wire.

drops in the range, 0.5×10^5 to 4×10^5 dynes/cm.². The velocity of flow, constant after acceleration, was determined as a function of the applied pressure drop; i.e., the pressure drop across the wire. (Fig. 6).

As shown in Fig. 6 the 12-mesh, backing wire presents a measurable resistance to flow. However, in the drainage of fibre slurries, the resistance to flow is apparent only in the very initial period of drainage. The influence of the backing wire is shown in Fig. 7 for the drainage of a free beaten unbleached sulphate slurry of 0.27 per cent under 10^5 dynes/cm.² applied pressure drop. In the drainage cycle shown in Fig. 7, the difference arising from the use of the backing wire extends to the point where a mat of 35 to 40 gm./m.² has formed.

The drainage process is initiated through rupture of the foil. The pressure difference causing flow is that of the constant applied pressure, p, and the static head of the slurry, $\rho h(t)$. This total pressure may be equated to that required to accelerate the mass of slurry and to overcome the resistance of wire and mat

$$p + \rho h(t) = p_a + \Delta p_r + \Delta p_m$$

where

p = constant applied pressure, dynes/cm.²
p_a = pressure corresponding to acceleration force, dynes/cm².
Δp_r = pressure loss across wire, dynes/cm.²
Δp_m = pressure drop across mat, dynes/cm.²

In the first instant upon rupture of the foil the total pressure difference is utilized in accelerating the slurry suspended above the wire. Since the slurry moves as a body, the pressure corresponding to the

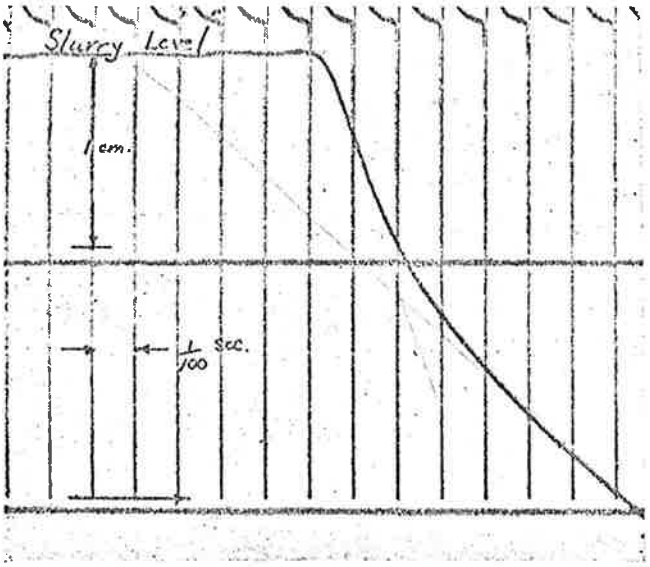

Fig. 8. Drainage curve, free beaten unbleached sulphate, 10^5 dynes/cm.² pressure drop, 0.29 per cent consistency, 20 deg. C.

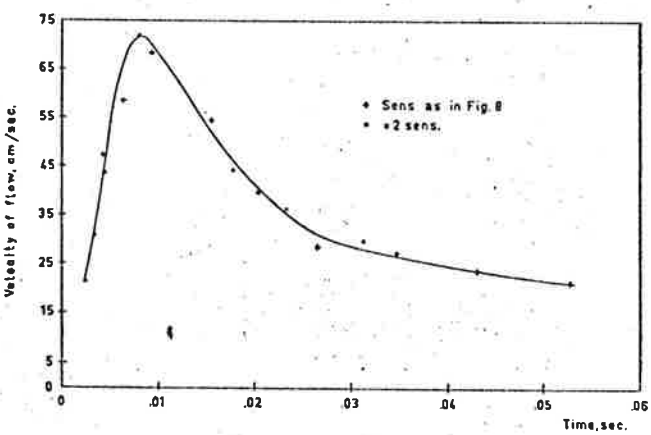

Fig. 9. Flow velocity, a function of time.

accelerative force may be written as:

$$p_a = \frac{\rho \cdot a \cdot h(t)}{g}$$

where

a = acceleration at time, t, cm.sec.$^{-2}$

To determine the extent of each of these as formation proceeds, a study has been made of the initial stage. A free beaten unbleached sulphate slurry at 0.29 per cent consistency and 20 deg. C. was chosen for analysis. A photo of the drainage curve found under a constant applied pressure of 10^5 dynes/cm.² is shown in Fig. 8. From this curve and others at twice the sensitivity, the development of the pressure drop across the mat has been determined.

Figure 9 shows the drainage velocity as a function of drainage time. The accelerative forces were calculated from this curve. The pressure loss across the wire was determined at various points on the curve—shown in Fig. 9—by finding the pressure drop across the wire for each velocity from Fig. 6.

In Fig. 10 is shown the development of the pressure drop across mat during a drainage cycle. It is seen that application of the pressure can be considered as being instantaneous in setting up a pressure gradient to accelerate the flow. The interest lies in the point from which time onwards in the drainage cycle the

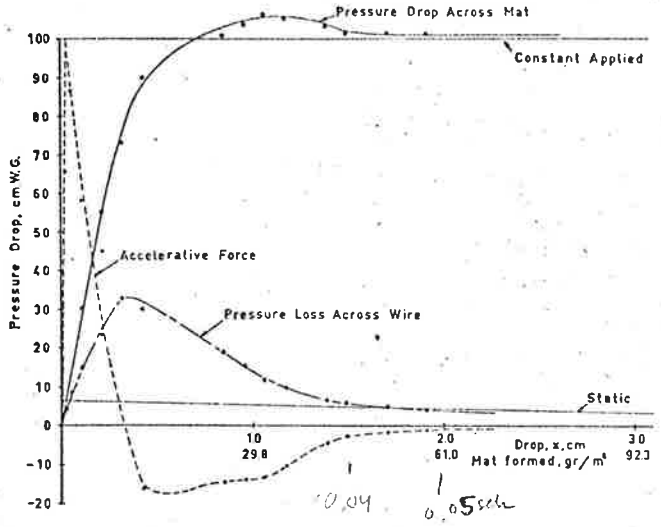

Fig. 10. Development of pressure drop across mat.

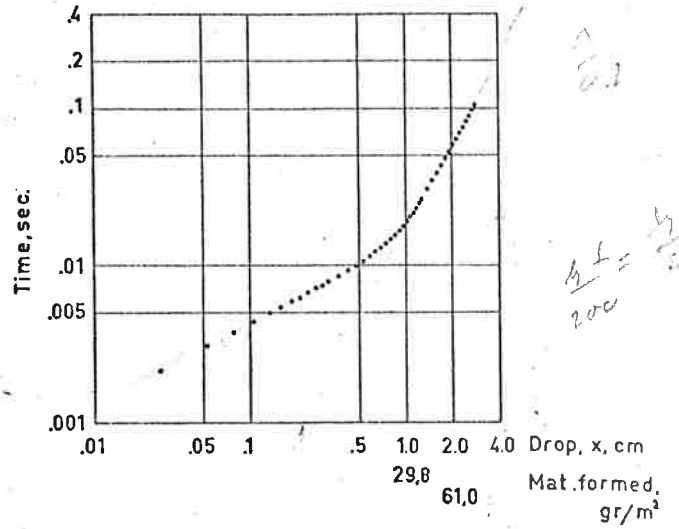

Fig. 11. Time vs. drop, x.

pressure drop across the mat may be considered as constant. In this instance that point is found when the level has dropped approximately 0.5 cm. (deviation in pressure drop less than 5 per cent); i.e., when a mat weight of approximately 15 gm./m.² has formed. However, as seen in Fig. 11, a straight-line relationship between t and W is not obtained until "retention equilibrium" is reached. This occurs only after a drop of approximately 1.0 cm.

"Retention equilibrium" in mat formation is reached when, from each layer depositing, the same quantity of each fibre size is retained within the mat's structure. "Retention equilibrium" is dependent upon fibre distribution and, as regards the point where equilibrium is obtained in a drainage cycle, upon drainage rate and consistency. "Retention equilibrium" can thus mean total retention or constant through fraction, if there is such a large difference in fibre sizes that one size will fully pass through the sheet. In both cases the retained sheet is being built up by identical increments.

In these investigations, the drainage results to be shown are based on tests with an initial height of slurry of 6.5 cm. above the wire. Such was the case in the previous example showing the development of the pressure drop across the mat. To determine the effect of varying heights, drainage cycles were made with initial heights of slurry of 6.5, 5.2, 3.9 and 2.6 cm. The results of these tests are shown in Fig. 12 as the time for drop in level. As expected the effect of using varying depths of slurry is small. The scatter is somewhat greater than the accuracy of the determinations, but the difference is not significant. The drainage process can thus be considered independent of depth of slurry after retention equilibrium is obtained, i.e., in the region investigated.

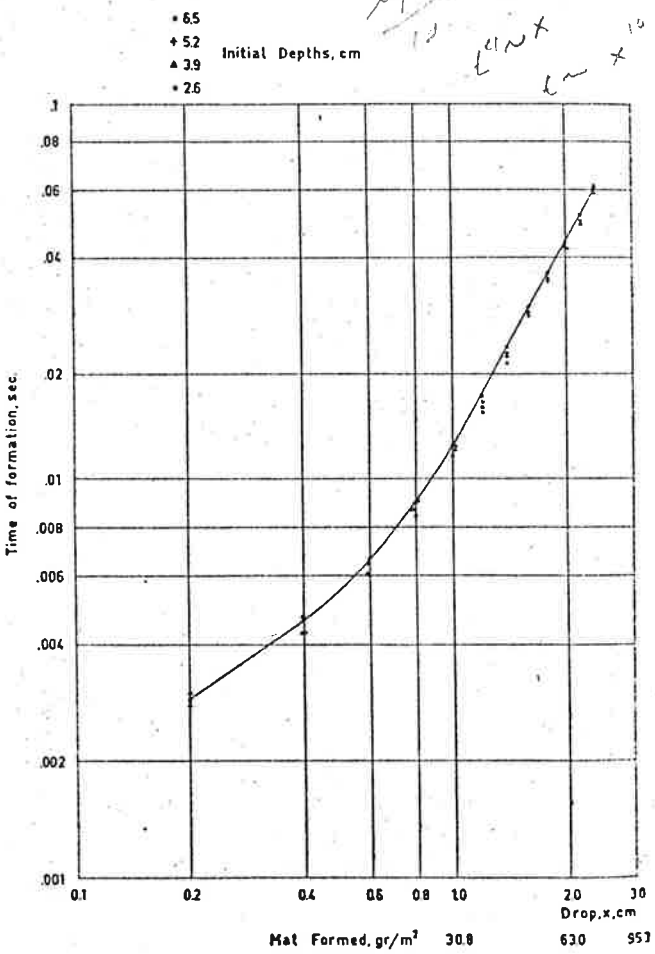

Fig. 12. Effect of slurry depth on drainage.

Flocculation

When working with fibre slurries above 0.01 per cent it has been aptly illustrated by previous authors that interaction between individual fibres is unavoidable. Such interaction leads to floc forming by mechanical entanglement. At paper-making consistencies the scale of flocculation is a balance between the strength of flocs and the stresses exerted upon them through turbulence and shear. The simple test of noting the floc formation after stopping slurry mixing shows that the time of formation is of a very low order. The conclusion would seem to be that drainage at flocculating consistencies can not be performed under deflocculating conditions without draining under turbulent conditions. This would undoubtedly lead to disruption of sheet formation. Flocs form during drainage and as such are unavoidable.

We can only hope to achieve reproduceable conditions of floc size in the slurry to be submitted for drainage. To achieve this, the "deflocculating" device shown in Fig. 13 was selected after experimentation of its effects on drainage. The slurry, after 0.5 min. dispersal time in this device, is run into the sheet

former of the drainage apparatus and the drainage cycle is initiated at the moment the required height of slurry has been suspended above the wire.

Trials on free beaten unbleached sulphate at consistencies of 0.3, 0.5 and 0.75 per cent showed that the drainage time of the "deflocculated" slurry was of the order of 10 per cent less than that of the flocculated slurry. By using the device, a constant scale of flocculation is achieved since the effect on the three consistencies is relatively the same. That flocculation does not change the drainage mechanism is shown by the fact that the slope of the relationship between drainage time and mat weight is independent of flocculation status.

Temperature of Slurry

In this work, the temperature of slurry generally covered the range of 20 deg. to 23 deg. C. The effect of varying viscosity on drainage is shown by the determinations on a wet beaten unbleached sulphate at temperatures of 22 deg. C., 32 deg. C. and 43 deg. C. (Figure 14).

The percentage decrease in the time of formation with increasing temperature of slurry is approximately 75 per cent of that given by the viscosity change from 22 deg. C. to 32 deg. C. and 40 per cent of that given by the viscosity change from 32 deg. C. to 43 deg. C.

Thus variations in drainage time of the order of 5 per cent may be expected over the temperature range of 20 deg. to 23 deg. C.; i.e. over the working range involved.

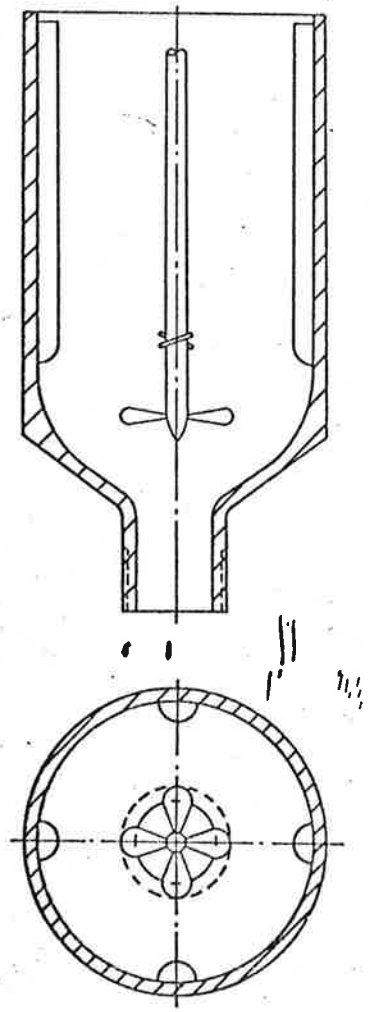

Fig. 13. Deflocculating device.

RESULTS

Presentation

The present discussion and presentation of results will be limited to that part of the drainage cycle where retention equilibrium exists. The first part of the drainage cycle occurs under a considerably lower pressure drop across the mat due to inertial forces and the appreciable pressure drop through the wire. Therefore the initial drainage phase does not occur under constant pressure drop across the mat. However, this initial phase is of such short duration, compared with the rest of the drainage cycle, that it does not significantly influence the results. This is also borne out by the fact that the same results are obtained in the constant-pressure-drop phase independent of the depth of the slurry above the wire. Omitting the initial phase these results can therefore be considered representative of drainage under constant pressure drop over the whole drainage cycle. It is understood that constant drainage conditions are obtained above mat weights of the order of 30 gm./m.^{2} to 70 gm./m.^{2}; i.e. after retention equilibrium. Constant pressure drop is obtained much before that.

From the original drainage curve the relationship between time and mat weight deposited is obtained. Plotting these two variables in a log-log diagram gives a straight-line relationship for all tests made. Drainage under constant pressure can thus be characterized by the exponential relationship.

$$t_p = kW^{\alpha}$$

where

k = a resistance factor in c.g.s. units and

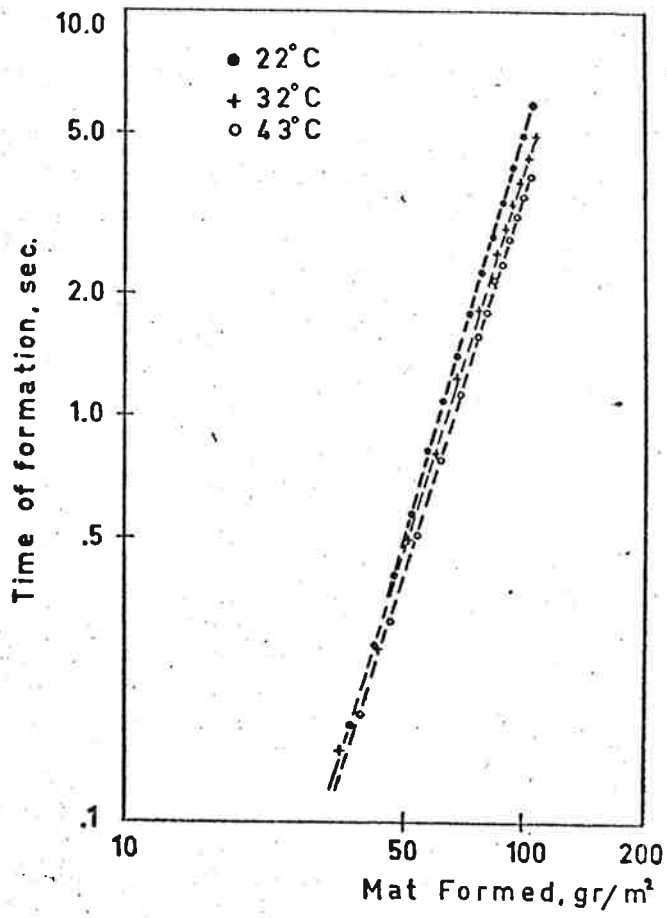

Fig. 14. Temperature effect on mat formation.

α = exponent describing rate of mat formation; the greater the value, the slower the formation.

Typical results are shown in Fig. 15 for drainage of unbleached free beaten, Jordan-refined sulphate stock under various pressure drops across mat.

Out of these plots of t_p and W, the time to form a specified mat weight may be expressed as a function of the pressure drop across the mat. Plotting t_w against $\triangle p_m$ on a log-log plot gives parallel straight-line relationships for different constant basis weights. Therefore the effect of pressure drop can be expressed as

$$t_w = d(\Delta p_m)^{-n}$$

where

d = time of formation for basis weight, W, at unit pressure drop

n = describes the combined effect of compression and pressure drop on drainage time.

Typical relationships are drawn in Fig. 16 for the influence of pressure drop across mat on time of formation of a mat weight of 100 gm./m.². For bleached bisulphite pulp at 0.3 per cent consistency the range of slowness from 13.5 deg. S.R. to 50 deg. S.R. illustrates that the same relationship holds for a given pulp at any slowness level. Not illustrated on this figure is the effect of consistency and/or basis-weight change. The relationship shown is however independent of both.

For constant-pressure filtration the drainage of a given pulp at a certain slowness and consistency can be expressed by the factors k, α, d, and n. What remains is to determine these factors and to show how they are influenced by pulp type, freeness and consistency.

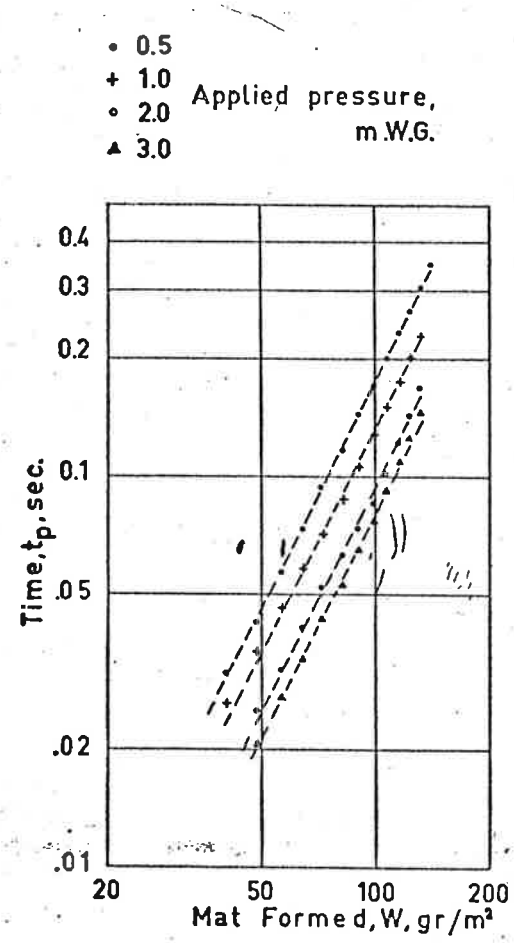

Fig. 15. t_p vs. W.

Effect of Variables

The variables studied have been pulp type, slowness and consistency. The influence of each on α, and n will be demonstrated.

Variables affecting α. The rate of mat formation, α, is slightly dependent upon pressure differential, and consistency. The very limited effect of these variables will be discussed later. The dominating variable, affecting the rate of mat formation, α, is degree of beating, expressed either as beating time or slowness. However, the type of pulp also influences α though to a smaller extent than the level of beating. α is thus a drainage criterion, characteristic of a given pulp at a given degree of beating. The variation in α is shown in Table I, where average values for a number of pulps at different degrees of beating are presented. In this table the lower slowness figures correspond to the lower α figures and vice versa. This table indicates that with increased beating, α increases; i.e., the time to form a certain additional basis weight increases. The increase is clearly demonstrated by Fig. 17, where the drainage of a bleached sulphite slurry of 0.3 per cent consistency at five different degrees of beating is shown for a pressure drop across mat of 0.5×10^3 dynes/cm.². This increase in α has the practical significance that drainage time for a 50 gm./m.² sheet at 56 deg. S.R. is approximately four times larger than at 15 deg. S.R. but ten times for a 110 gm./m.² sheet.

The effect of beating on α is further exemplified by Fig. 18 and 19. Figure 18 is based on drainage of a 0.3 per cent slurry of unbleached sulphate under four pressure drops. For 100 min. of beating, the average value of α increases from approximately 1.8 to 3.3. In Fig. 19, α values, averaged over all pressure drops and for a 0.3 per cent slurry, are plotted against the slowness for various bleached pulps. General relationships between α and slowness exist, with larger values be-

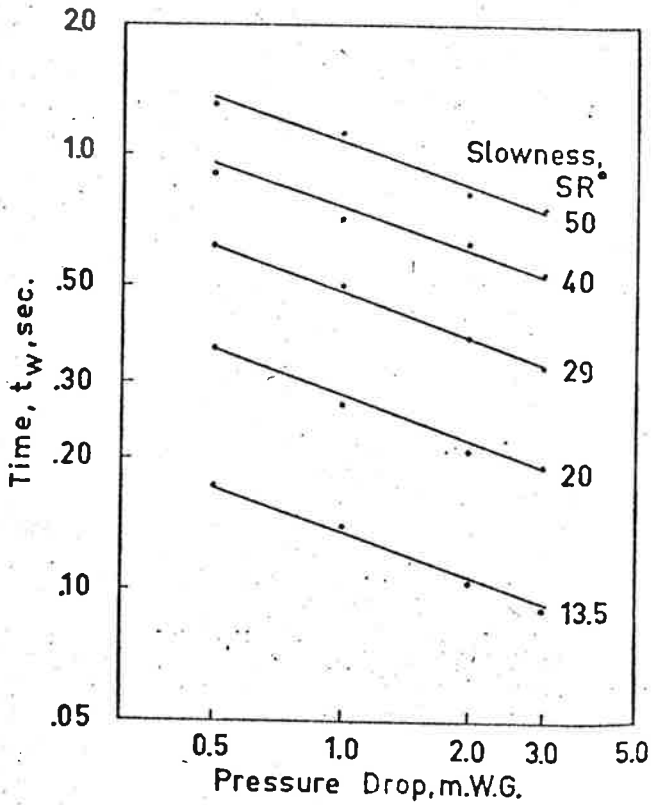

Fig. 16. t_w vs. $\triangle p_m$.

ing obtained with increasing slowness. However, pulp type enters into the picture. Especially do sulphate and neutral sulphite-bisulphite pulps deviate quite markedly from the other pulps shown.

TABLE I *Average Values of* α.

Pulp	*Slowness, °S. R. at 20°C.*	*Temp. of slurry in drainage exp., °C.*	α
Hardwood, semi-chemical	36	22	2.35
Groundwood	46	22	2.40
Rayon pulp	22	25	1.95
[illegible]-bleached sulphate	12—69	21	1.83—3.22
[illegible]ached sulphate	15—56	20	2.14—2.86
Bleached sulphite	14—48	20	2.06—2.76
Bleached bisulphite	13.5—50	21	2.07—2.83
Bleached bisulphite, soda cooked	14—50	22	2.08—2.70
[illegible]ached neutral [illegible]sulphite, bisulphite	13.5—53	24	1.92—2.75

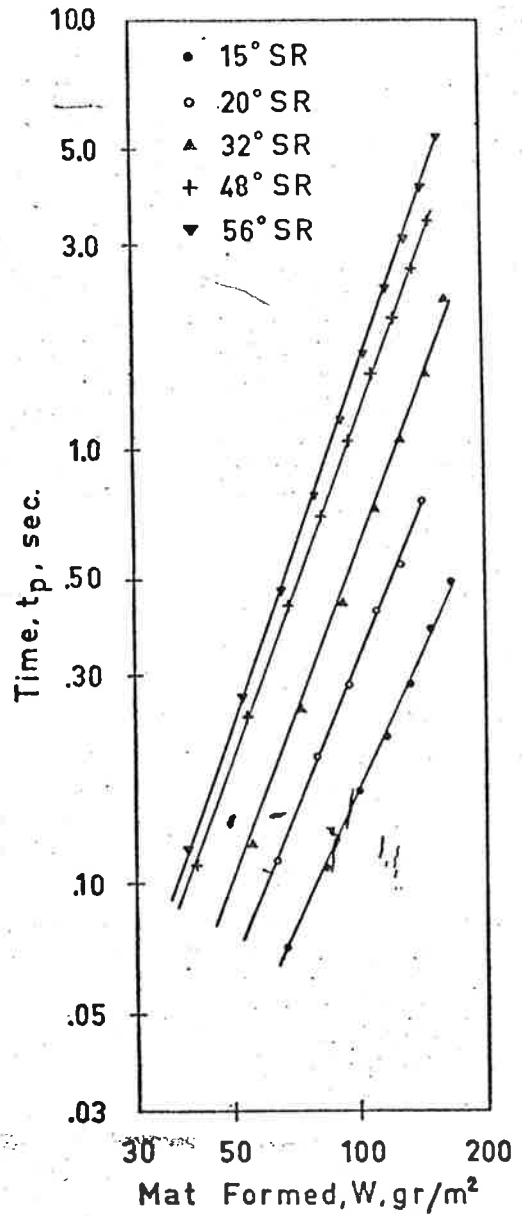

Fig. 17. Effect of freeness on rate of mat formation.

It was previously mentioned that pressure drop across mat and consistency have a limited influence on α. However, certain trends are apparent with changing pressure drops and consistencies, and will now be considered.

Table II illustrates the effect of pressure drop on α. For each pulp, the value of α, for five different levels of slowness, has been averaged for each pressure drop. For all pulps a total average has been formed showing the total effect of pressure drop for all variables. The same general tendency has been found for all pulps at all levels of slowness but this

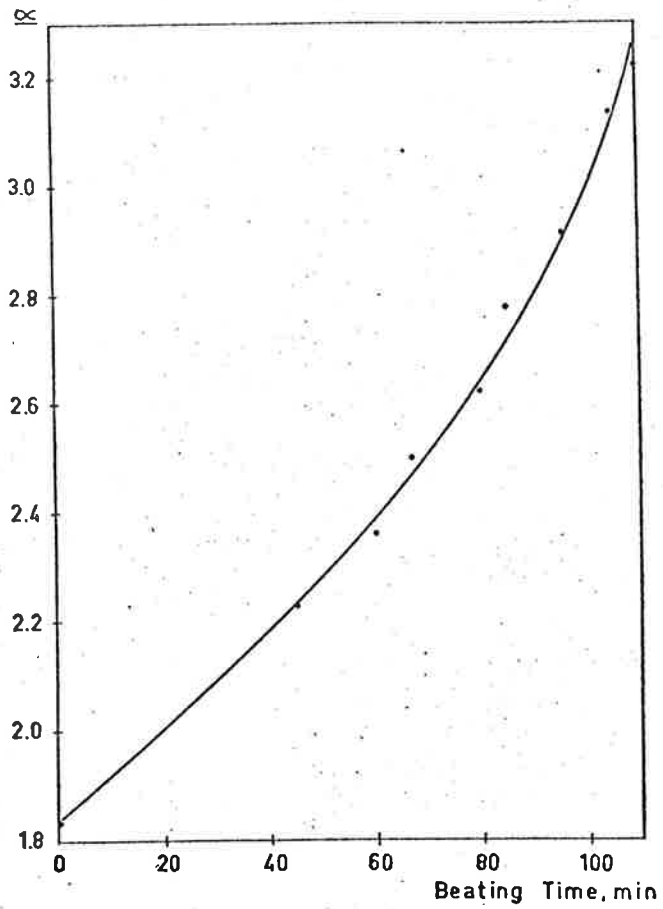

Fig. 18. Effect of beating on α.

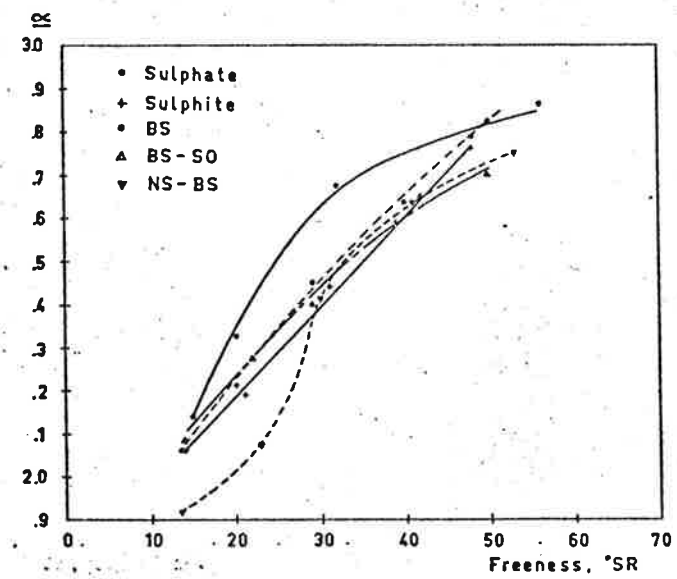

Fig. 19. α vs. slowness.

method was used to obtain a clearer picture of the influence of pressure drop on α. From this table, the total variation in α due to pressure drop is of the order of 8 per cent for an increase of pressure from 0.5×10^5 to 3.0×10^5 dynes/cm.^{2}. With increasing pressure drop, α increases though there is a general levelling off. Due to the small effect of varying pressure drop as compared with the large effect of pulp type and slowness, an average value of α has been used for characterizing a given pulp at a given degree of beating.

Figure 20 illustrates the effect of consistency on α. The results are drawn from tests on unbleached sulphate, beaten to five levels of slowness, and tested at different consistencies under a pressure drop of 10^5 dynes/cm.^{2}. As shown the effect of consistency varies to a large extent with the freeness of the pulp. At lower levels of slowness, α increases with consistency; at higher, α decreases; and in the region between, it remains constant. Tests with other pulps show the same general trend, but it can be expected that this effect will vary with pulp type.

The effect of pressure drop and consistency can not be neglected though α can be said to be mainly a function of type of pulp and degree of beating. For comparison of pulps, tests should be performed at the same pressure and consistency.

Variables affecting n. The exponent n has been found to be independent of consistency and slowness, being dependent only upon pulp type. Values of n are given in Table III for a cross section of pulps.

Requisite for the equation $t_w = d\ (\triangle p_m)^{-n}$ to hold is that α is independent of pressure drop for a given pulp at a given consistency. It has been shown previously that α is practically independent of pressure drop above 10^5 dynes/cm.^{2} and this is further substantiated by the fact that t_w against $\triangle p_m$ in a log-log plot follows a straight line relationship. With α independent of pressure drop, it follows that k can be written as $k = D\ (\triangle p_m)^{-n}$, where n is characteristic of pulp type and independent of consistency and slowness. The drainage equation can thus be written in the more general form $t = D\ (\triangle p_m)^{-n} W^{\alpha}$. To take into account the direct effect of consistency, this equation may be expressed as: $t = \frac{G}{s}\ (\triangle p_m)^{-n} W^{\alpha}$; where

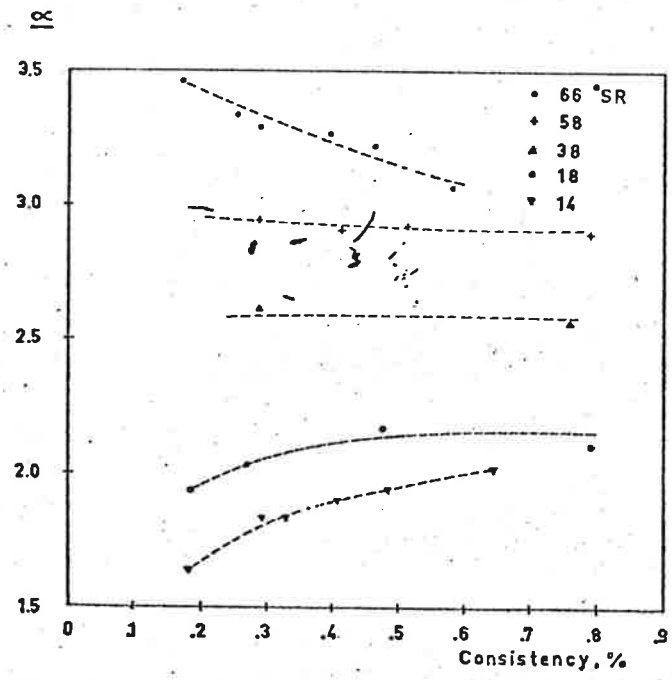

Fig. 20. α vs. consistency.

G is the drainage constant characteristic of a mat formed and thus dependent on the effect of pulp type, slowness and consistency on mat structure. We do not intend to enlarge on the quantitative relationship between G and these other variables. This presentation is mainly directed towards showing the difference in drainage behaviour between pulps at higher consistencies and high drainage rates compared to those at low consistencies, as described by the two factors α and n. The task in this work has been to provide a method by which means the time needed to form a certain mat weight can be determined for any variables chosen. The relationship shown relating drainage time, pulp type, slowness, consistency and pressure drop is very complicated and therefore does not lend itself readily to a theoretical approach. Though the general relationships developed are of great value, it is necessary to determine the actual quantitative values in each instance. Therefore, the direct determination of the appropriate relationships from the drainage curves themselves is the more practical and direct approach. The analysis of the drainage results has been carried out in order to throw some light on the drainage mechanism and has not been pursued to the point where the drainage can be calculated from the given general equation.

TABLE II *Effect of Pressure on α.*

Bleached pulps at 0.3 per cent consistency. For each pulp, α averaged over 5 freenesses at each pressure drop.

	Pressure drop, 10^5 dynes/cm.^{2}			
Pulp	*0.5*	*1.0*	*2.0*	*3.0*
Sulphate	2.40	2.54	2.68	2.65
Sulphite	2.26	2.40	2.48	2.46
Bisulphite	2.33	2.40	2.46	2.56
Bisulphite, soda cooked	2.43	2.36	2.42	2.47
Neutral sulphite, bisulphite	2.33	2.30	2.37	2.43
Mean	2.35	2.39	2.50	2.52

TABLE III *n—Relating Time of Formation as a Function of Pressure Drop across Mat.*

Pulp	*n*	*Slowness Range, °S.R.*
Softwood	0.38	38
Hardwood	0.53	45
Hardwood, semi-chemical	0.52	36
Groundwood	0.52	46
Rayon pulp	0.48	22
Unbleached sulphate	0.40—0.45	12—70
Bleached sulphate	0.35—0.38	14—56
Bleached bisulphite		
Bleached bisulphite, soda cooked		
Bleached neutral sulphite, bisulphite		

Discussion

The drainage of slurries under constant pressure drop may be expressed by the following equation.

$$t = \frac{G}{s} (\Delta p_m)^{-n} \cdot W^{\alpha}$$

The experimental determination of these different factors shows that α can vary from 1.7 to at least 3.5 and that n for the pulps tested varies between 0.36 and 0.53. The determinations have covered the pressure drop range of 0.5×10^5 to 6.0×10^5 dynes/cm.^{2}, consistencies from 0.2 to 0.8 per cent and a large number of different pulps in the slowness range of 14 deg. S.R. to 70 deg. S.R. It has been found that α is mainly a function of pulp quality and slowness and that n is a function of pulp type.

Ingmanson has shown that D'Arcy's law applies for ıe drainage of cellulose fibre suspensions of the order of 0.01 per cent consistency. The drainage characteristics of dilute fibre suspensions may then be expressed from a knowledge of free fibre surface, fibre volume, compressibility and retention characteristics of the pulp using the Kozeny-Carmen equation. The ame model of drainage has been used by Meyer [5] who obtained very good agreement between the experimental results and his theoretical deductions. In his work the pressure, density, and velocity distributions through the mat have been taken into account.

According to this theory and D'Arcy's law, the time to form a mat should be proportional to the square of the basis weight deposited; that is, α should be equal to 2. This law applies for systems where each increment of mat deposited has the same drainage resistance as that previously deposited. In such a system the drainage characteristics may be defined by the average specific drainage resistance of the material. For very dilute fibre suspensions this is obviously the case. The flow behaviour can thus be characterized by determining the average specific drainage resistance of the pulp which, in turn, may be related to the specific surface and the specific volume of the pulp.

Our work has shown that for paper making consistıcies and drainage rates, α is not equal to 2 and thus ıe drainage behaviour of pulps under practical papermaking conditions cannot be defined by the average specific drainage resistance of the pulp. α can be below 2 for very free pulps and up to 3.5 for highly beaten pulps. Therefore we have the difficult task of :plaining this very real behaviour. This can only mean that for α below 2 each increment of pulp gives an increase in drainage resistance that is below the average of the previously formed mat; and when α is above 2, the drainage resistance of each increment adds more than the average.

The explanation for this can be found in the underlying assumptions supporting D'Arcy's law. The D'Arcy law is based on two assumptions that are not met in drainage of pulps of paper making consistencies and drainage rates.

The concept of average specific drainage resistance means that each part of the fibre mat is identical in fibre composition. This holds for systems where the variation in fibre length is very small and where there is no relative movement between fibres of different sizes. As we all know this does not hold in the mat formation of pulps. In pulps we have a very large variation in fibre sizes and this size distribution varies to a large degree between pulps and with beating. Many authors have studied the distribution of fillers through a fibre mat and recently Forgacs and Atack [6] studied the distribution of fines through a hand formed sheet from a newsprint furnish. They found that the groundwood content, determined on a unit weight basis, decreased continuously from wire to top side. These determinations were made by sectioning the sheet in five equal parts and therefore the rapid decrease in groundwood fibre content in the layer adjacent the wire is masked. This can only be expressed by the movement of fines through the mat. Therefore the first criterion of the D'Arcy law does not hold, each layer of the mat is not identical. Due to the movement of the fines there exists a zone inside the mat with a much higher drainage resistance than the rest of the mat. This higher drainage resistance also, in itself, means a higher pressure drop across this part of the mat and therefore a higher compression and density of the mat at that point. Obviously the reason for these high α values is that fines from the newly deposited fibres are moving into the already formed mat and are filtered out in this dense layer giving a much faster increase in drainage resistance than would correspond to the deposit layer itself. The existence of a dense layer close to the wire side has been aptly shown by Majewsky [7]. On hand sheets, Majewsky showed that the change in air porosity, with successive stripping of layers from wire and top side respectively, was much larger on the wire than top side. This difference was dependent upon fines content and increased with fines content, the difference being nil for fines free pulp. We feel that this mechanism, of redistribution of fibres in a fibre mat, is of immense importance in the understanding of the drainage behaviour of pulps. It cannot be excluded in an analysis of drainage of pulps under papermaking conditions. The results showing α, for all practical purposes, independent of consistency and flocculation shows that this effect is not a flocculation effect, but due to the migration of fines.

The importance of the migration of fines further complicates the difficulties in applying drainage results to machine drainage elements. Since these elements will affect the migration in different ways, the drainage characteristics of the pulp will also vary.

It still remains to explain why values of α below 2 are possible. This is explained by another of the underlaying assumptions of the D'Arcy law. D'Arcy's law applies where the flow rate through the mat is equal for each part of the mat. In the case of forming a mat from paper-making consistencies, this is not the case. We have a flow rate distribution through the mat such that the flow rate at the top of the mat is lower than that at the bottom. The difference in flow rate is dependent on the difference between mat consistency and the original consistency of the slurry.

For dilute suspensions of 0.01 per cent, that is 10,000 parts of water per part of fibre, compared to 30 parts of water per part of fibre in the formed mat, the flow rate difference is negligible and thus does not affect the results. Under paper-making consistencies say of 0.5 per cent, we have 200 parts of water per part of fibre compared to 30 parts of water per part of fibre in the formed mat. Here the flow rate difference through the mat is of an appreciable magnitude. The effect of this flow rate difference through the mat is such that each additional fibre layer adds less to the total resistance than the rest of the mat which means that α is less than 2. The total resistance of the mat is the sum of the product of flow rate times the specific resistance of each unit section and as the flow rate increases through the mat this addition, for the additional increment, is less than for the rest.

Drainage under consistencies of paper-making interest and drainage rates cannot be explained without taking into account the effect of fines migration in the mat and the difference in flow rate through the mat. This means that it is impossible to predict the drainage behaviour of more concentrated fibre suspensions from results obtained from very dilute suspensions and that the average specific drainage resistance factor cannot be used to describe the drainage behaviour of pulps. The fundamental knowledge obtained from the work on dilute suspensions are still of immense importance, but this work has to be extended to be of practical value. It is very unlikely that we, in the near future, can obtain enough basic information to be able to calculate the drainage behaviour of pulps. Therefore the only reasonable approach is to use experimental measurements of the drainage behaviour of pulps under consistencies and drainage rates that are more like those as used in paper manufacture.

The question of turbulent and laminar flow has often been raised. In this connection we can only state that over the very wide range of velocities covered in this work we have never come upon a transition point. As the velocities of the drainage cycles extend to very low values, indications are that the practical drainage occurs in a laminar flow region.

The drainage apparatus has been shown to provide a meaning in respect to changes in formation time with beating which is not borne out by a slowness reading. To exemplify this point, the time to form a mat weight of 100 gm./m.^{2}, t_w, is shown as a function of the slowness for certain bleached pulps in Fig. 21. These results are strictly comparable. It can be seen that differences in t_w of the order of 40 per cent are noted between pulps at one and the same slowness value in the higher range.

The influence of consistency on formation time of a specified mat weight, t_w, is illustrated for groundwood pulp in Fig. 22. At the lower consistencies and for pressure drops across mat exceeding 0.37×10^4 dynes/cm.^{2}, t_w varies approximately with the inverse of the consistencies. The relationship between formation time and consistency does not, however, lend itself to the formulating of definite trends.

It is realized that fibre orientation affects the drainage resistance through fibre structures. This aspect has not been dealt with here. Neither has it been possible to take into account formation under turbulent conditions.

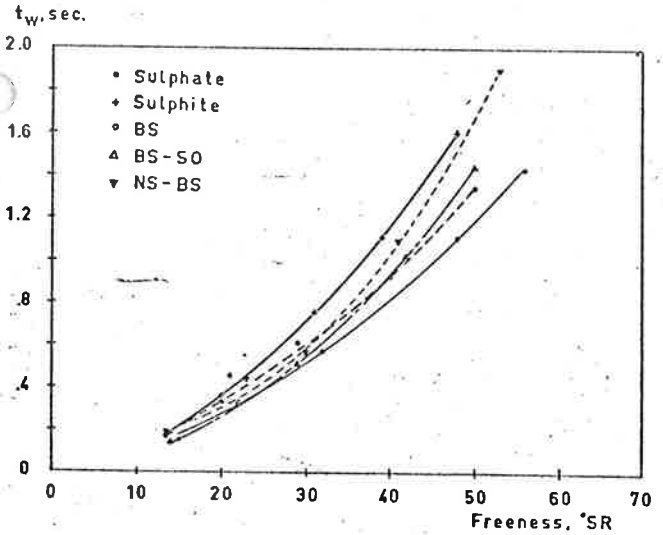

Fig. 21. t_w vs. slowness.

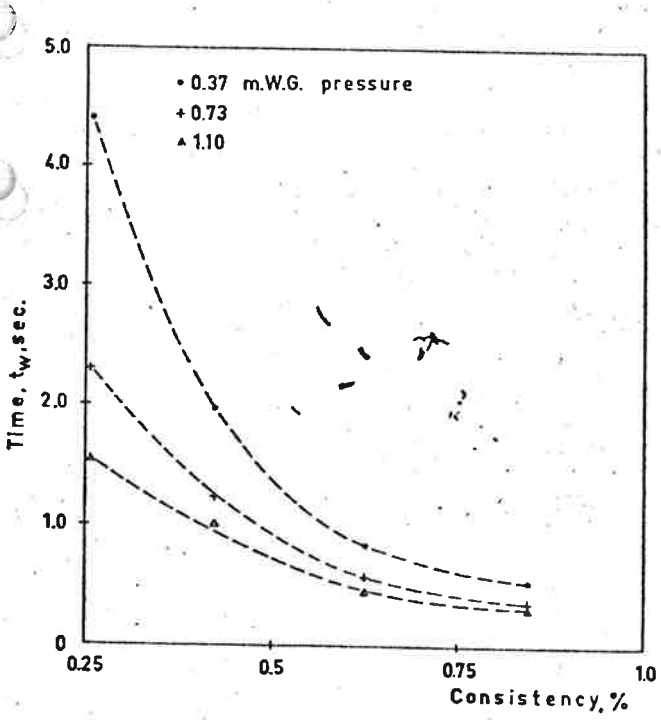

Fig. 22. Consistency and mat formation.

SUMMARY

An apparatus has been described for studying the water removal from papermaking slurries at constant pressure drop.

The present treatment has been limited to the retention equilibrium filtration period and therefore does not start until a basis weight between 30—70 gm./m.^{2} has been reached. To analyse the initial drainage stage necessitates more work, because the pressure differential across the mat is not constant. The drainage behaviour of pulps can, however, be obtained for lower basis weights from this initial drainage phase. Further work is being done along those lines.

For a constant pressure drop across mat, the time of formation may be expressed by the empirical equation

$$t = \frac{G}{s} (\Delta p_m)^{-n} \cdot W^{\alpha}$$

Values of α have shown that the resistance to drainage of slurries at paper-making consistencies cannot be expressed by the average specific drainage resistance factor excepting in the rare case where $\alpha = 2$. The value of α has been shown to be practically independent of consistency and pressure drop across mat but a function of pulp type and beating alone. The variation in α at paper-making consistencies has been shown to result from two factors, migration of fines and flow rate difference through the mat.

The practical implication of this work is that it is impossible to characterize pulps using one single figure as obtained in a freeness test or in a determination of the average specific drainage resistance. It is, however, necessary to have a good knowledge of the drainage characteristics of pulps to be able to predict the influence of changes in pulp type, pulp consistency, basis weight, speed etc. on the operation of sheet-making machines. It is also necessary to have this information to be able to size wires, filter drums, suctions needed at a certain drainage length, etc. The basis for this has to be obtained through experimental deter-

minations of the pulp characteristics using a machine of the type presented in this paper. Taking up drainage curves for the pulps of interest under a limited number of consistencies, pressure drops and degrees of beating will enable us to establish the necessary foundation.

It is, however, realized that the knowledge of the drainage behaviour of stocks under constant pressure and under undisturbed and flocculated conditions might not in all respects compare with all practical applications of drainage on sheet forming machines. We hope that on drainage elements such as wet suction boxes, sheet formers, filters, etc. where the drainage occurs without disrupting the sheet, further work will show good correlation between this drainage tester and drainage on these machines. To apply these results to drainage where disruption of the sheet occurs and where migration of fines is affected in different ways presents a much more difficult problem. However, to be able to solve this complicated problem the knowledge of the drainage characteristics under constant pressure drop will be of considerable help.

ACKNOWLEDGEMENT

The authors wish to thank Aktiebolaget Karlstads Mekaniska Werkstad for permission to publish this paper. Thanks are expressed to J. R. Andersson, J. O. Skeppstedt and C. Dodson for carrying out much of the experimental work.

REFERENCES

1. INGMANSON. W. L., "An Investigation of the Mechanism of Water Removal from Pulp Slurries", *Tappi*, 35, no. 10, 439 (Oct. 1952).
2. INGMANSON, W. G., and WHITNEY, R. P., "The Filtration Resistance of Pulp Slurries", *Pulp Paper Mag. Can.* 121 (Dec. 1954).
3. MARDON, J., GREGORY, I. R., HOWE, B. I., O'BLENES, G., and TRUMAN, A. B., "The Drainage Problem on a Newsprint Machine", *The Engineering J. of Canada* 70 (Dec. 1960).
4. ESTRIDGE, R. "The Initial Retention of Fibres by Wire Grids", Sixteenth TAPPI Eng. Conf., Oct., 1961.
5. MEYER, H., "A Filtration Theory for Compressible Fibrous Beds Formed from Dilute Suspensions", Sixteenth TAPPI Eng. Conf., Oct., 1961.
6. FORGACS, O., ATACK, D., "The Distribution of Chemical Pulp and Groundwood through the Thickness of Newsprint", PAPRIC Report No. 248.
7. MAJEWSKY, L. J., "Effect of Forming Processes on Sheet Structure" Oxford Symposium Sept. 1961.

Appendix I

A detailed experiment was conducted using both air and water as the transport medium. The results of drainage of 0.32 per cent groundwood slurry, under a constant applied suction of 10^5 dynes/cm.^{2}, are shown in Table IV.

The results are expressed as the time of formation of increasing mat weights. The effect of operating with the air medium is to increase drainage time by approximately 5 per cent. Surface tensional effects are thus of minor importance.

TABLE IV *Drainage Using Both Air and Water as the Transport Medium.*

Groundwood, 0.32 per cent, 22 deg. C. 10^5 dynes/cm.^{2} pressure drop.

		Water Transport			*Air Transport*		
Drop in Level, cm	*Basis Wt. Formed, gm./m.^{2}*	*Time Req'd (Average), sec.*	*Std. Dev.*	*No. of Readings*	*Time Req'd (Average), Sec.*	*Std. Dev.*	*No. of Readings*
0.513	15.2	0.0140	.0012	9	0.0141	0.021	8
1.026	30.4	0.0601	.0031	9	0.0639	.0034	8
1.539	45.6	0.1969	.0055	9	0.213	0.157	8
2.052	60.8	0.452	.015	9	0.479	0.378	8
2.565	76.0	0.854	.0198	9	0.903	.0619	8
3.078	91.2	1.385	.0241	9	1.466	.0844	8
3.591	106.4	2.068	.077	9	2.176	.126	8
4.104	121.6	2.877	.094	8	3.024	.161	8
4.617	136.8	3.817	.139	8	4.002	.193	8
5.130	152.0	4.891	.163	7	5.086	.256	8
5.643	167.2	6.026	.186	7	6.395	.297	6

Appendix II

On a 0.32 per cent groundwood slurry a number of repeats to the drainage cycle were conducted using both air and water as the transport medium. The standard deviations of the individual tests were determined at each level of mat formation and are given in Table IV. The standard deviation of the individual tests is, on the average, 4 per cent in the case of water and 6 per cent in the case of the air medium.* The results are normally based on three repeats which corresponds to a standard deviation of the mean of approximately 2 per cent.

*These results were determined on the first model construction. The present construction offers higher stability and thus better reproducibility.

6. A CONSTANT RETENTION MODEL

In this section a simple dynamical model of the wet end of the paper machine wil be derived. The purpose is to describe crudely the effect of the major control variables, thick stock flow and consistency, flow through the mixing pump, wire speed and slice opening. The output is taken as the basis weight at the couch. Several simplications are made in order to obtain the model. The model is obtained by taking fibre balances in the wire pit and in the fan pump head box system. Several simplifying assumptions are made when modelling the complicated flow and mixing phenomena described in the previous sections. It is assumed that the mixing phenomena can be described as perfect mixing in two volumes. It is assumed that the flow consists of two components, water and fibres. The phenomena on the wire are described by assuming that a constant traction r of the fibres flowing out of the head box will be retained on the wire which explains the name constant retention model. A model of this type was first published by Beecher

Notation

To describe the process it is necessary to introduce the flow and fibre concentrations at various points in the process, at the thick stock valve, the outlets of the head box and the wire pit and at the wire pit overflows. The flows are denoted by q; and the fibre concentrations by c_i where the index i denotes the position in the process. See Fig. 6.1

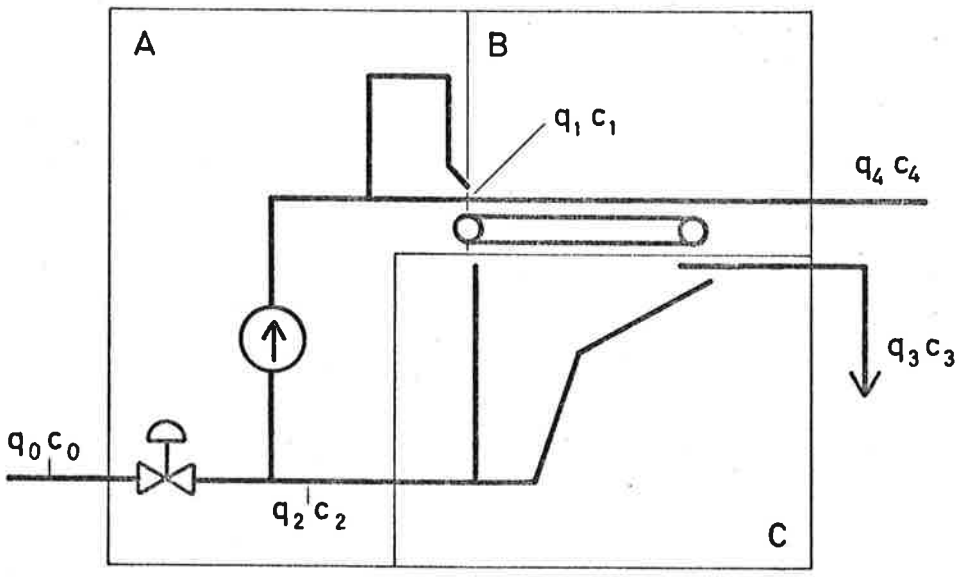

Fig. 6.1. Schematic diagram of the wet end of a paper machine

Flow diagrams of some real paper machines are shown in Appendix A. These are somewhat more complicated than the schematic diagram in Fig. 6.1. The complications vary from machine to machine and are easily handled in each separate case.

The model can in principle be obtained from material balances for fibres and water. Since the mixing, separation and flow phenomena are very complex it will be necessary to make several simplifying assumptions.

Water Balance

The water balance will first be considered. The fibre concentration is very low throughout the system with the exception of the flow leaving the couch. Recall that the concentration is about 3 % in the thick stock flow, 0.5 % in the head box, 0.05 % in the wire pit and 20 % at the couch. It is thus possible to approximate the water flow by the total flow. Several other approximations are also made. It is assumed that the head box flow dynamics is neglected. A water balance then implies that

$$q_o + q_2 = q_1$$

The overflow at the wire pit is furthermore assumed equal to the inflow q_o. This implies that the water leaving the system at the couch is neglected when making the water balance.

Fibre Balance for Fan Pump Head Box System

It is difficult to obtain the fibre balance for two reasons. The mixing phenomena in the tubes and tanks are not well understood neither are the separation phenomena on the wire. When considering the fibre balance the system will be divided into three parts as indicated in Fig. 6.1. For the part marked A in the figure there are two inflows corresponding to the fibres contained in the thick stock flow $q_o c_o$ and the fibres in the flow from the wire pit $q_2 c_2$ and one outflow $q_1 c_1$ corresponding to the fibres contained in the flow out of the head box. As was pointed out in section 4 the mixing phenomena in the fan pump, screen, cleaners, head box and their connecting tubes are very complex. As a crude approximation it will be assumed that

the mixing can be represented by an ideal mixing in a volume V_1. Notice, however, that due to the complexity of the mixing phenomena it is not obvious how this volume V_1 should be estimated from the physical parameters of the system. Under this assumption the fibre balance for the part A of the system can thus be written as

$$V_1 \frac{dc_1}{dt} = q_o c_o + q_2 c_2 - q_1 c_1 \qquad (6.1)$$

Fibre Balance for the Wire

The phenomena governing the separation of fibres from the water on the wire are very complex as was discussed in section 5. Here it is simply that a traction of the fibres out of the head box are retained on the wire. The number is called the retention. Its numerical value depends on many factors, basis weight, machine speed, pulp properties. Typical orders of magnitude are given in the table below.

Table 6.1. Numerical Values of the Retention Factor for different Paper Grades

Paper grades	Retention r
Craft paper and liner	0.8 - 0.95
Fluting	0.7 - 0.8
Newsprint	0.5
Journal paper	0.4

The fibre flow leaving the couch is thus rq_1c_1 and the basis weight at the couch is thus

$$W = \frac{rq_1c_1}{b\ v} \qquad (6.2)$$

where b is the machine width and v the wire speed.

Fibre Balance for the Wire Pit

The simple wire model implies that the fibre flow into the head box is $(1-r)q_1c_1$. The fibre flow out of the wire pit to the fan pump is q_2c_2. There are also some fibres contained in the overflow of the wire pit. The fibre content in this flow depends very much on the

design of the system. In some systems the overflow comes mostly from flow from the suction boxes and the couch. The fibre contents is then lower than the average fibre contents in the wire pit. In other systems the fibre contents may be close to the fibre contents in the wire pit. There are many different designs of white water systems and wire pits. The mixing phenomena are also complex. Some people claim that there is a reasonably good mixing in their wire pits while others claim that there is a plug flow. In the crude model it will simply be assumed that the mixing in the wire can be represented as a perfect mixing in a volume V_2. The fibre balance for the wire pit can then be written as

$$V_2 \frac{dc_2}{dt} = (1-r)q_1c_1 - q_2c_2 - q_3c_3 \tag{6.3}$$

It is clearly not trivial how V_2 should be determined.

A Constant Retention Model

Summarizing we find that the wet end of the paper machine can be characterized by the equations (6.1), (6.2) and (6.3). To get the major features it will be assumed that $c_3 = c_2$. The equations then become

$$\frac{dc_1}{dt} = -\frac{q_1}{V_1} c_1 + \frac{q_2}{V_1} c_2 + \frac{q_o c_o}{V_1}$$

$$\frac{dc_2}{dt} = \frac{(1-r)q_1}{V_2} c_1 - \frac{q_1}{V_2} c_2$$

$$w = \frac{rq_1c_1}{bv} \tag{6.4}$$

The assumptions made thus implies that the dynamics of the wet end can be characterized by a second order dynamical system. Assuming that the flows q_1, q_2, the volumes V_1, V_2 the retention r and the wire speed are constant the equations (6.4) are linear and can be represented as

$$\frac{d}{dt}\begin{bmatrix} c_1 - c_1^s \\ c_2 - c_2^s \end{bmatrix} = \begin{bmatrix} -\alpha_1 & (1-\beta_1)\alpha_1 \\ (1-r)\alpha_2 & -\alpha_2 \end{bmatrix}\begin{bmatrix} c_1 - c_1^s \\ c_2 - c_2^s \end{bmatrix} + \begin{bmatrix} \beta_2 \\ 0 \end{bmatrix}(q_o - q_o^s)$$

$$y = \gamma\left[c_1 - c_1^s\right] \tag{6.5}$$

where the parameters are given by

$$\alpha_1 = q_1/V_1$$
$$\alpha_2 = q_2/V_2$$
$$\beta_1 = q_o/q_1$$
$$\beta_2 = c_o/V_1$$
$$\gamma = \frac{rq_1}{bv}$$

The model is thus characterized by five parameters which can be determined from the efficient mixing volumes V_1 and V_2, the steady state values of the flows q_o, q_1 and q_2, the retention r, the wire b and the wire speed w. Assuming steady state conditions we find from (6.4) that

$$r = 1 - c_2/c_1 \tag{6.6}$$

The rentention can thus be determined from measurements of the fibre concentration in the head box and in the wire pit.

In the model (6.4) the thick stock flow was regarded as the input and the basis weight as the output.

The Characteristic Equation

The characteristic equation for the system is

$$d(s) = s^2 + s(\alpha_1 + \alpha_2) + \alpha_1\alpha_2(\beta + r - \beta r) = 0$$

when r = 1 the roots are $-\alpha_1$ and $-\alpha_2$ corresponding to the mixing time constants of the fan pump head box system and the wire pit respectively.

When $r < 1$ the roots are given by

$$s_{1,2} = -\frac{\alpha_1 + \alpha_2}{2}\left[1 \pm \sqrt{1 - \frac{4\alpha_1\alpha_2(r+\beta-\beta r)}{(\alpha_1+\alpha_2)^2}}\right]$$

The root locus of the characteristic equation is shown in Fig. X.2

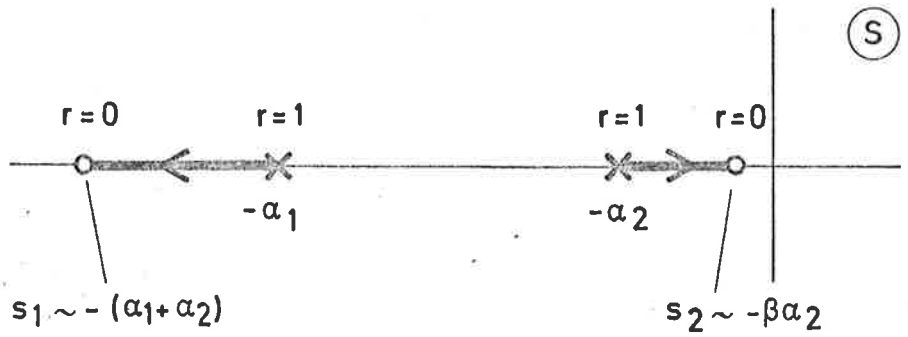

Fig. 6.2. Root locus of the characteristic equation of the constant retention model with respect to the retention factor r.

Steady State Gain

It follows from the model (6.5) that the steady state values of head box and wire pit consistencies are given by

$$c_1 = \frac{q_o c_o}{q_1(r+\beta-r\beta)}$$

$$c_2 = \frac{q_o c_o(1-r)}{q_1(r+\beta-r\beta)}$$

$$w = \frac{rq_o c_o}{bv(r+\beta-r\beta)}$$

Notice that an increase of $q_o c_o$ will result in an increase of both c_1 and c_2. Also notice that since β is small and r often close to 1 the basis weight increase due to a unit increase of $q_o c_o$ will be practically independent of the retention.

A Numerical Example

In order to get a feeling for the orders of magnitude involved a specific example will be considered. A flow diagram of a craft paper machine is shown in Fig. 6.3.

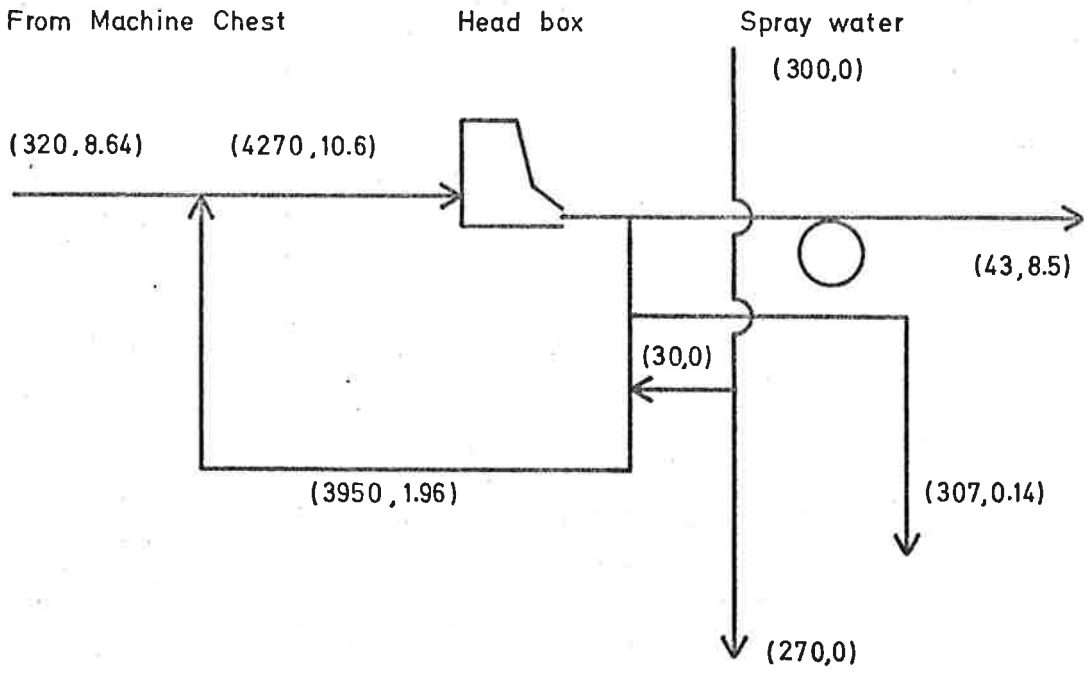

Fig. 6.3. Flow diagram of a typical craft paper machine. The total flow q_t and the fibre flow q_f of various points of the process are denoted as (q_t, q_f) where the units are kg/s.

The diagram in Fig. 6.3 is more involved than the simplified. The volume of the wire pit is 110 m^3 and the head box volume is 10 m^3. The mixing volumes are arbitrarily estimated as

$V_1 = 10\ m^3$
$V_2 = 100\ m^3$

Assuming a stock density of 1000 kg/m^3 the following flows are obtained.

q_o = 320 ton/h = 0.089 m^3/s

q_1 = 4270 ton/h = 1.19 m^3/s

q_2 = 3950 ton/h = 1.10 m^3/s

q_3 = 277 ton/h = 0.077 m^3/s

q_4 = 43 ton/h = 0.012 m^3/s

From Fig. 6.3 the following values of the fibre concentrations are obtained

c_o = 27 kg/m^3

c_1 = 2.5 kg/m^3

c_2 = 0.5 kg/m^3

c_3 = 0.5 kg/m^3

The wire speed and the effective wire width are

v = 6 m/s (10)
b = 6 m

We thus find that it is reasonable to neglect the flow q_4 in comparison with the other flows in the water balance. In this particular case the concentration of the overflow in the wire pit also equals the concentration in the wire pit i.e. $c_3 = c_2$. To obtain the model it is also necessary to know the retention factor. The retention is determined from (6.6) which gives r = 0.75.

The constant retention model now becomes

$$\frac{d}{dt}\begin{bmatrix} c_1 \\ c_2 \end{bmatrix} = \begin{bmatrix} -0.12 & 0.11 \\ 0.003 & -0.012 \end{bmatrix}\begin{bmatrix} c_1 \\ c_2 \end{bmatrix} + \begin{bmatrix} 2.7 \\ 0 \end{bmatrix} q_o$$

$$y = 0.025\ c_1$$

The transfer function relating basis weight to thick stock flow is thus given by

$$G(s) = \frac{0.067(s+0.012)}{s^2 + 0.132s + 0.00111} = \frac{0.067(s + 0.012)}{(s+0.009)(s+0.123)} =$$

$$= \frac{0.12(1 + 83s)}{(1+111s)(1+8s)} = \frac{0.52}{1+8s} + \frac{0.20}{1+119s}$$

A step response of the constant retention model is shown in Fig. 6.4.

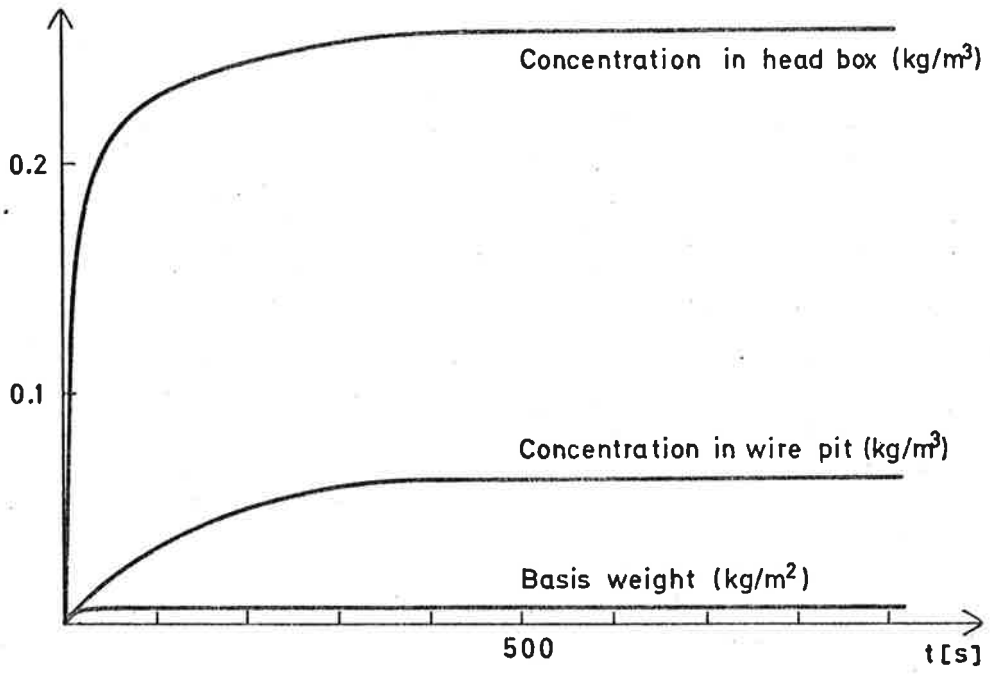

Fig. 6.4. Response in head box concentration c_1, wire pit concentration and basis weight to a step change of 1 % in thick stock flow.

Summary

The constant retention model gives a second order dynamics for the wet end of the paper machine. The characteristic equation for the linearized model has real roots for all values of the retention. For retentions close to one the models correspond to the head box and wire pit mixing time constants. When the retention decreases the small eigenvalue will decrease and the large eigenvalue will increase. In response to a step change in thick stock flow the fibre concentrations in the head box and in the wire pit will both increase.

7. VARIABLE RETENTION MODELS

The model in the previous section was obtained using many simplifying assumptions.In this section it will be discussed what happens when it is assumed that the retention is a function of the basis weight This will have a significant effect on the system dynamics as will be seen in the following.

In the simple drainage theory discussed in section 5 the experimental and theoretical results indicate that the retention strongly depends on the basis weight. The following semiempirical formula was proposed by Han

$$r = r(w) = 1 - (1-\alpha)\, e^{-\gamma w} \tag{7.1}$$

where α is called the initial retention,w is the basis weight and γ is a constant. A typical value is $\gamma = 50\ m^2/kg$.

The equation (7.1) was obtained for the drainage of a simple element as was discussed in section 4. In the wire model of section 4 the retention r was the average retention for the whole wet end. Since (7.1) holds for each section it is clear that the average retention factor must also depend on the basis weight. Assuming that (7.1) also holds for the average retention and introducing (7.1) into (6.4) the following nonlinear model is obtained

$$\frac{dc_1}{dt} = -\frac{q_1}{V_1} c_1 + \frac{q_2}{V_1} c_2 + \frac{q_o c_o}{V_1}$$

$$\frac{dc_2}{dt} = (1-r(w))\frac{q_1}{V_2} c_1 - \frac{q_1}{V_2} c_2 \tag{7.2}$$

where the function r(w) is implicitely defined through

$$w = \frac{r(w) q_1 c_1}{bv}$$

$$r(w) = 1 - (1-\alpha)e^{-\gamma w} \tag{7.3}$$

Notice that it is not trivial to eliminate w analytically!
To linearize (7.2) the following derivatives are needed

$$\frac{dr}{d\omega} = \gamma(1-\alpha)e^{-\gamma w} = \gamma(1-r)$$

$$\frac{dw}{dc} = \frac{r^2}{r+\gamma w(r-1)} \frac{q_1}{V} \qquad (7.4)$$

Assuming small perturbations around a steady state col $\begin{bmatrix} c_1^s & c_2^s \end{bmatrix}$ the following linearized model is obtained

$$\frac{d}{dt}\begin{bmatrix} c_1 - c_1^s \\ c_2 - c_2^s \end{bmatrix} = \begin{bmatrix} -\alpha_1 & (1-\beta_1)\alpha_1 \\ \beta_3(1-r)\alpha_2 & -\alpha_2 \end{bmatrix}\begin{bmatrix} c_1 - c_1^s \\ c_2 - c_2^s \end{bmatrix} + \begin{bmatrix} \beta_2 \\ 0 \end{bmatrix}(q_o - q_o^s)$$

$$y = \gamma \begin{bmatrix} c_1 & -c_1^s \end{bmatrix} \qquad (7.5)$$

where

$$\alpha_1 = \frac{q_1}{V_1}$$

$$\alpha_2 = \frac{q_1}{V_2}$$

$$\beta_1 = \frac{q_o}{q_1}$$

$$\beta_2 = \frac{c_o}{V_1}$$

$$\beta_3 = -\frac{r-\gamma w}{r-(1-r)\gamma w} \qquad (7.6)$$

Notice that this model is identical to the constant retention model (6.5) when the coefficient β_3 equals one. Assuming $\alpha = 0.5$ β_3 is a function of r. A few values of this function are given in the table below

Table 7.1. The parameter β_3 as a function of r for $\alpha = 0.5$

r	β_3
0.5	1
0.6	0.73
0.7	0.35
0.75	0.01
0.8	-0.15
0.9	-0.95
0.95	-1.67

The parameter β_3 is always less than one. This means that the variable retention model is equivalent to the constant retention model with a higher value of the apparent retention. Notice, however, that it is also possible to obtain negative values of β_3.

In such a case the dynamics of the model will change. The steady state responses in c_1 and c_2 to a step change in thick stock flow are given by

$$c_1 - c_1^s = \frac{c_o}{q_1 [1 - \beta_3 + \beta_3(r+\beta_1-\beta_1 r)]}(q_o - q_o^s)$$

$$c_2 - c_2^s = \frac{c_o \beta_3 (1-r)}{q_1 [1 - \beta_3 + \beta_3(r+\beta_1-\beta_1 r)]}(q_o - q_o^s)$$

Notice that if β_3 is negative an increase of q_o will result in a decrease of c_2!

A Numerical Example

Consider the craft paper machine discussed in section 6. For this machine we get $\beta_3 = 0.01$ from table 7.1. In this particular case the variable retention model thus implies that there is virtually no coupling between the equations in the model. The fibre concentration in the wire pit will thus not be influenced by changes in the thick stock flow and the dynamics can be approximated by a first order system.

8. MULTICOMPONENT MODELS

So far it has been assumed that the stock is composed of fibres and water only. This is certainly a gross oversimplification. The fibres are not uniform, their sizes and properties may vary. The stock can also contain other material for example clay and fillers. Fibres of different size will certainly behave differently in the drainage process. In order to illustrate the effect a diagram of a journal paper machine is shown in Fig. 8.1.

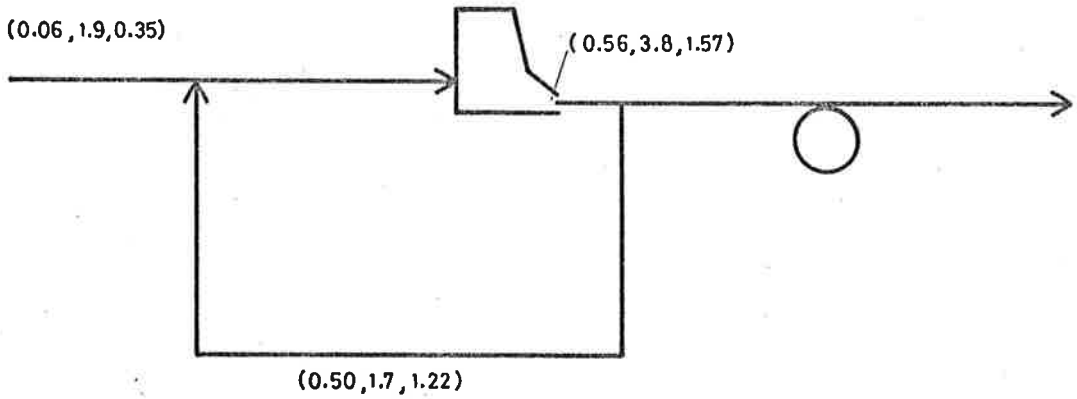

Fig. 8.1. Flow diagram of a typical journal paper machine. The total flow q_t m^3/s, the fibre flow w_f kg/s and the clay flow w_c kg/s at different positions of the process are denoted as (q_t, w_f, w_c)

Assuming constant retention we find that the fibre retention is

$$r_f = 1 - \frac{1.7}{3.8} = 0.55$$

and that the clay retention is

$$r_c = 1 - \frac{1.22}{1.57} = \frac{0.35}{1.57} = 0.22$$

It is thus clear that fibres and clay are drained quite differently and it thus seems reasonable to take care of this in the modelling by considering multicomponent flow.

9. MORE ELABORATE MODELS

The models discussed in section 6 and 7 describe the complicated drainage phenomena on the wire very crudely through a simple retention factor only. As a result it is not possible to get any information about the position of.the wet line on the wire. It would thus seem reasonable to describe the wire by a nonlinear static model.An example of such a model is given in the following preprint.

AN ON-LINE MATHEMATICAL MODEL OF A FINE PAPER MACHINE

O. Alsholm
J. D. Schoeffler
P. R. Sullivan

IBM Systems Development Division
Development Laboratory
San Jose, California

Prepared for Presentation at the
20th Annual ISA Conference and Exhibit
Los Angeles, California
October 4 - 7, 1965

AN ON-LINE MATHEMATICAL MODEL OF A FINE PAPER MACHINE

O. Alsholm**
J. D. Schoeffler*
P. R. Sullivan
IBM Systems Development Division
Development Laboratory
San Jose, California

ABSTRACT

The objective of this paper is to describe a mathematical model of the Fourdrinier paper-making process which is suitable for on-line computer control. Control of the paper-making process requires knowledge of variables such as wet line position, concentrations of individual fibers throughout the system, and the like, which can not be easily measured on-line. Consequently it is necessary to use a mathematical model to compute such variables as they are needed. The approach to model building described in this paper is to first separate the system into a number of simpler subsystems, for each of which a mathematical model is built. The separate subsystems are then incorporated into an overall mathematical model by introducing interconnection constraints (flow and material balances).

The major emphasis in this paper is on the most complex subsystem, the paper machine itself. A relatively complete mathematical model of the machine predicated on basic principles was constructed. This model involves a set of partial differential equations relating flows, concentrations, and pressure throughout the mat. Such a model is too complex to be run on-line, but is very useful for generating simpler models. The structure of a simplified model derived from the larger model is presented. Parameters in the simplified model are determined from actual operating data and a curve-fitting procedure. The overall system model is a set of nonlinear difference equations. Techniques for efficient simulation of the system together with results for a typical fine paper machine are presented. In addition, the use of the models for control purposes is briefly discussed.

I. INTRODUCTION

The objective of this paper is to present a mathematical model of the Fourdrinier paper-making machine and associated white water system which is suitable for on-line computer control during grade changes.

Consider the simplified schematic of the papermaking process shown in Fig. 1. Paper is a mixture of various wood fibers and fillers, the fillers being added to control opacity, color, and other quality characteristics.[1] Basically, the slurry (a mixture of fibers, fillers, and water) is placed on a moving wire screen (the Fourdrinier), permitting the water to drain through in such a manner that the fiber and filler is uniformly deposited in the form of a mat on the wire. This

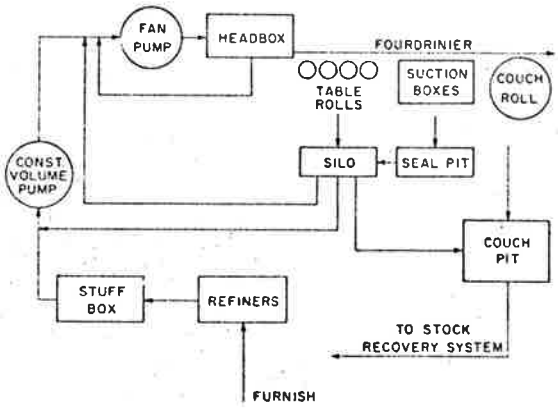

Fig. 1 Simplified schematic of paper making process

* Systems Research Center, Case Institute of Technology, Cleveland, Ohio and Consultant to IBM Corporation, San Jose, California.

** Presently with Billeruds Aktiebolog, Sweden.

1. Superior numbers refer to similarly-numbered references at the end of this paper.

mat is then dried in order to form the paper sheet. This process is run continuously with the slurry being deposited on the wire from the head box, a small-volume tank with interior baffles. The wire moves with a velocity of approximately 1000 feet per minute from the head box to the couch roll. At this point enough water has been drained out of the mat to insure adequate sheet strength for removal from the wire. The sheet is then sent to the dryer section of the process and finally rolled up.

The drainage process is quite critical for two reasons. If too little water is removed from the mat, the sheet at the couch roll may break as it is removed from the supporting wire, causing significant lost production. On the other hand, if the water drains too quickly, the resulting sheet formation may be poor, yielding unacceptable paper. The purpose of the table rolls and suction boxes on the Fourdrinier machine is to control the drainage profile within acceptable limits. Most of the water drainage occurs over the table roll section because of the weight of the slurry and a pressure produced by the "nip" in the wire as it passes over each roll. The equivalent pressure applied to the slurry is a function of the number of table rolls and the speed at which the wire is driven. By the end of the table roll section, the mat is well formed with little slurry left above it, but with much water trapped inside it. The suction box section consists of a number of flat boxes to which a controlled suction is applied. This has the effect of draining the remainder of the slurry above the partially formed mat and removing the interior water by compressing the mat. The point at which all of the slurry above the mat has drained through is clearly visible and is called the wet line.

Some suction is also maintained on the couch roll to provide a final amount of drainage before the sheet is removed from the wire. The process operator must control the speed of the wire, the amount of applied suction, and the amount of slurry flow onto the wire in such a way that the drainage profile is satisfactory. A good indication of adequate drainage is the position of the wet line which is usually maintained at a fixed point on the machine.

The dynamics of the paper-making process are interesting in that much fiber and filler drains through the wire along with the water, and economics dictates the recovery and reuse of these solids. Most of the flow through the wire enters the silo, a large level-controlled tank, in which the concentration of solids is approximately 20% of that in the head box. To make efficient use of these solids, the concentration of solids in the main source of stock is made higher than needed on the wire. This stock is then diluted with the output of the silo to the proper concentration. In Fig. 1, two recycles from the silo are shown. The first is to the inlet of the fan pump (which supplies the head box) where the recycle flow and the main source of stock flow are mixed and pumped to the head box. The second recycle is back to the vicinity of the stuff box, the tank containing the high-concentration stock.

In addition to the flow into the silo, some water and fiber drains into the couch pit, a tank in the vicinity of the couch roll. If the sheet should break coming off the couch roll, all of the production is diverted to the couch pit until the sheet can be rethreaded. Hence the flow into the couch pit is somewhat intermittent, sometimes being low in solids concentration and sometimes very high. Solids in the couch pit are recovered by a device called a saveall, the output of which is stored in white water tanks and later used to make up the input to the stuff box.

Typically, a paper machine makes many grades of paper, a grade being a sheet with a given weight per unit area and with a given relative concentration of various fibers and fillers. To change from one grade to another is an interesting control problem because of the large time lags introduced by the volumes of the various tanks (mainly the sile) and the long transport times. This is especially true if the grade change involves a significant change in the relative concentrations of the components since the concentrations in the recycle streams must then be carefully considered.

In order to control such a process during a grade change, a mathematical model is necessary because the critical variables are either not measurable or else subject to long measurement time lags. The main objective of a successful grade change is to reach the new grade quickly without breaking the sheet (which causes significant lost production) and in such a way that the system is left in the steady state. That is, because of the large recirculation in the system, it is common to find the system on grade at one time but drifting far off grade again some time later. Drainage on the Fourdrinier is significantly affected by the relative concentration of each component (fiber and filler) and consequently it is necessary not only to follow the flows in the process but also the concentration of each component in the flow.

Fig. 2 is a schematic diagram of the most difficult portion of the system, the Fourdrinier, together with the variables of interest.[1] To provide a suitable basis for control, the mathematical model must be capable of predicting these variables on-line. In particular, the wet line position is the chief indicator of sheet strength and its calculation is fundamental to any control policy and therefore must be possible from the mathematical model.

The approach to mathematical model building described in this paper is to first separate the system into a number of unconnected subsystems (not necessarily corresponding to the actual system units themselves). Each such subsystem is

then modeled by a combination of scientific and empirical model-building techniques. The mathematical model is then completed by specifying the constraints between variables in the subsystems which correspond to interconnecting the subsystems again. The resulting equations are in the form of nonlinear difference equations which are particularly well suited to on-line use by a digital computer.

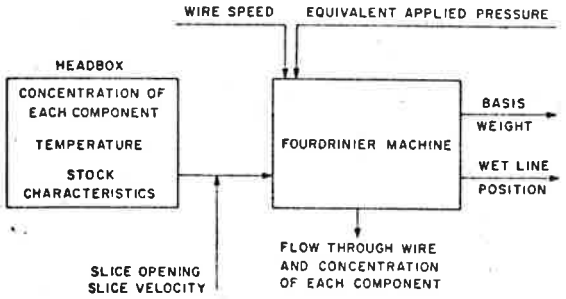

Fig. 2 Schematic diagram of the Fourdrinier

The most difficult portion of the system to model is the Fourdrinier itself and the emphasis in this paper is on that portion of the system. The model is verified by comparing available experimental and predicted data. In addition, good operating points predicted by the mathematical model for various grades of paper are compared to those actually used at present by operators and found to be in close agreement.

II. MODELING OF THE FOURDRINIER

Consider first the Fourdrinier and its pertinent variables separate from the remainder of the process (Fig. 2). Definition of variables is shown in Table I. Input to the Fourdrinier consists of the slurry in the headbox which may be characterized by the concentrations of each of the components (three are most significant in fine papermaking: kraft fiber, sulfite fiber, and clay filler), the temperature of the slurry, and some measure of the pulp characteristics. The pulp characteristics affect drainage rate significantly and depend upon the amount of refining previously done on the stock.

The amount of slurry in the headbox flowing onto the moving wire depends upon the slice opening (height of opening in the headbox) and the velocity of the stream (which in turn depends upon headbox pressure). The wire speed usually differs slightly from the slice velocity (the difference is called drag) in order to control

Table I Definition of variables

Concentrations (lbs. of solids/gal)

$i = 1$	concentration of sulfite fiber
$i = 2$	concentration of kraft fiber
$i = 3$	concentration of clay filler
x_{1i}	silo
x_{2i}	midway between stuff box and fan pump
x_{3i}	inlet to fan pump
x_{4i}	inlet to headbox
x_{5i}	headbox
x_{6i}	flow through table roll section
x_{7i}	flow through wet suction box section
x_{8i}	stuff box

Flows (gal/min)

g_0	constant flow from stuff box to fan pump
g_1	headbox flow
g_2	flow through table roll section
g_3	flow out of table roll section
g_4	constant fresh water flow (shower)
g_5	flow through wet suction box section
g_6	flow past wet line
g_7	flow through dry suction box section
g_8	flow off couch roll
g_9	fresh water flow into seal tank pump

Manipulated Variables

u_1	stuff box flow (gpm)
h	slice opening (inches)
v	slice velocity (feet/min)
p_s	suction box pressure (inches Hg)
p_c	couch pressure (inches Hg)

Constants

Δ	time increment (0.1 minute)
V_1	volume of silo
V_2	volume of headbox
N	number of suction boxes
w	machine width (feet)
α_i	initial retention
K_i	gain coefficients
γ_i, γ_i'	constants

Miscellaneous

B	basis weight (lbs/ft^2)
d	length of wet suction box section
R_{1i}	solids retentions
RP	refiner power (KWH/ton)
T	headbox temperature (degrees F)

formation of the paper on the wire. The remaining variable affecting performance on the wire may be considered to be an equivalent applied pressure along the wire. Over the table rolls, this is due to the weight of the slurry and the "nip" in the wire over the rolls; over the suction box section, it is due to actual applied pressure.

Of course it must be noted that there are a multitude of other variables actually affecting the process, but these cannot be considered without making the mathematical model excessively complex. For example, the wire type and age is a significant variable, as are the effect of nonuniform mixing in the headbox, nonuniform deposition on the wire, nonvertical flow on the wire, and others.[1] Nonetheless, the effects of these and other variables which do not change radically over a relatively short time period may be accounted for by an updating of some well-chosen empirical constants in the models--a necessity for on-line work. See Table II for a list of assumptions.

Table II Major assumptions used in model

1. The drainage on the wire is nondynamic in the sense that slurry deposited on the wire reaches the end of the table roll section in less than 10% of one sample interval and hence wire drainage for each sample interval depends only upon conditions existing during that interval rather than on previous intervals.
2. All tanks are perfectly mixed.
3. Flow through all pipes is plug flow.
4. All fiber in the system of a given type (Kraft or Sulfite) has the same characteristics.
5. Slurry deposited on the wire is uniformly mixed and doesn't selectively drain. That is, slurry above the mat on the wire has the same concentration at every point on the wire.
6. Drainage on the wire is uniform in the cross-machine direction.
7. Drainage is affected by an equivalent pressure over a given section. Thus, the actual non-uniform pulsating pressure needn't be considered as far as control is concerned.
8. Concentration of the input stock is known. This may be difficult in practice if a significant amount of broke is added, since the concentration of the broke may not be known.
9. Filler components other than clay need not be explicitly considered in the mathematical model. Their effects (such as TiO_2) may be absorbed in the empirical parameters.

The mathematical model should calculate the flows through the wire and off the couch roll, and the concentration of each component in the flows as a function of the manipulated and uncontrolled variables. In addition, the output variables, basis weight and wet line position, must be calculated.

The drainage process has been the subject of many investigations reported in detail in the literature. Of particular interest is the recent work of Meyer,[2] Nelson,[3] Ingmanson,[4] Han,[5] and Abrams[6] who considered the drainage process from a fundamental point of view. In particular, they formulate a partial differential equation description of the flow, pressure, and concentration distribution throughout the mat as a function of physical parameters of the stock. In order to describe the drainage process this way, many idealizing assumptions must be made. Their formulation is essentially limited to drainage with a single fiber component; but, nonetheless, their results are in good agreement with observed data.

As a basis for testing and evaluating simplified model structures, this work was extended to the multiple component case and simulated on a digital computer. Numerical solution of the partial differential equations involves satisfaction of many boundary values, leading to a long solution time. Although this prohibits the use of such a model in any on-line application, the model still serves as a valuable guide in the formation of a simpler on-line model whose structure is deliberately chosen to facilitate the control problem discussed earlier. Details of this model are too lengthy to be included here and will be reported elsewhere.

From the simulation, it was concluded that the paper machine may be separated into three lumped sections. The first section extends from the headbox to the end of the table rolls, the second from the suction boxes to the wet line (consequently it is of variable length), and the third to the end of the machine. Each lumped section can be considered to be a separate process whose output variables are the inputs to the next section. The sections and the variables considered are shown in Fig. 3.

Slice opening and velocity are considered manipulated variables. The concentrations of the slurry above the mat are assumed constant and equal to the headbox concentrations. Inputs to the table roll section are the headbox concentrations, headbox flow, wire speed (since this determines the equivalent applied pressure for this section) and refining and temperature. Outputs are the flows through the wire and into the next section as well as the concentrations of the flows. The difference between wire speed and slice velocity is less than 3% and need not be considered in the model.

The wet suction box section has similar inputs and outputs except that the wet line position (length of this section) is an additional output and

the actual suction box pressure is the input. The dry suction box section has no slurry above it and its outputs are the flow through the wire (virtually all water and no fiber), the basis weight, and production.

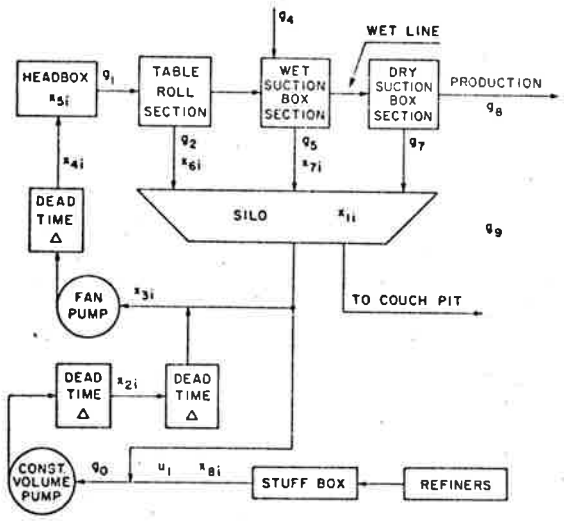

Fig. 3 Lumped model of the Fourdrinier

Most of the equations describing each section of the wire are simply material balance equations and are easily derived. However, several key relations must be derived from a combination of theoretical and experimental work together with verification via simulation of the more complete model. The first of these is the equation for flow through the wire.

The flow onto the wire from the opening in the headbox is proportional to the product of slice opening and slice velocity:

$$g_1 = K_o h v \qquad (2.1)$$

The flow through the table roll section, g_2, is the difference between the input flow, g_1, and the flow to the wet suction-box section, g_3. The fraction of g_1 which flows through the table roll section depends upon the resistance of the mat over that section, and the applied pressure. The resistance of the mat is essentially proportional to the basis weight but also depends upon headbox temperature and refining. The equivalent applied pressure is a function of wire speed. Consequently, an approximate relation may be deduced:

$$\frac{g_2}{g_1} = K f_1(v)/f_2(B, RP, T) \qquad (2.2)$$

where f_1 and f_2 are some functions to be determined, RP is the refiner power (in KWHR/Ton), and T is the headbox temperature. Experimental work reported in the literature[7,8] and the simulation of the partial-differential equation model indicate that reasonable approximations for both unknown functions are simply the chief arguments raised to some power. Since g_1 is proportional to slice opening and velocity, the resulting expression for g_2 is simply

$$g_2 = K_1 h^{e_1} v^{e_2} B^{e_3} \qquad (2.3)$$

where e_1, e_2, and e_3 are empirically determined exponents and K_1 is a gain term which is updated often on-line. The effect of temperature and refining is absorbed into exponent e_3 of the basis weight in the form of a linear relation

$$e_3 = c_1 + c_2 T + c_3 RP \qquad (2.4)$$

The basis weight used in Eq. 2.3 is the final basis weight of the sheet rather than the average sheet weight over the table roll section. This is convenient from a measurement point of view and is possible because, for normal operation, most of the sheet is formed over this section and consequently the average weight of solids above the table roll section is proportional to the final basis weight. The many approximations which enter into the determination of this expression are absorbed into the empirical exponents and gain terms which may (as for example when a grade change is to be made), the fit is quite satisfactory.

be adapted or updated when the model is used on-line. That this expression can fit experimental data well is indicated in Fig. 4 which shows the fit of this equation to a large number (60) of different grades of fine paper made at a particular mill. When used over a small region

In a similar fashion, an empirical expression for the wet-suction box section flow (g_5) may be deduced. In this case, the flow depends upon the applied suction box pressure and directly on the length of the section (d)

$$g_5 = K_2 p_s^{e_4} v^{e_5} B^{e_6} d \qquad (2.5)$$

Here again the e_i are empirically determined exponents and the effect of temperature and refining is absorbed into the exponent of basis weight in the same form as Eq. 2.4. If the wet line position is defined as the distance from the wet line to the end of the machine, it is simply the distance from the end of the table roll section to the end of the machine minus the length (d) of the wet-suction box section.

A second set of non-material balance relations are the relations between the concentrations in the flows through the sections and the variables of the sections. Here extensive experimental and

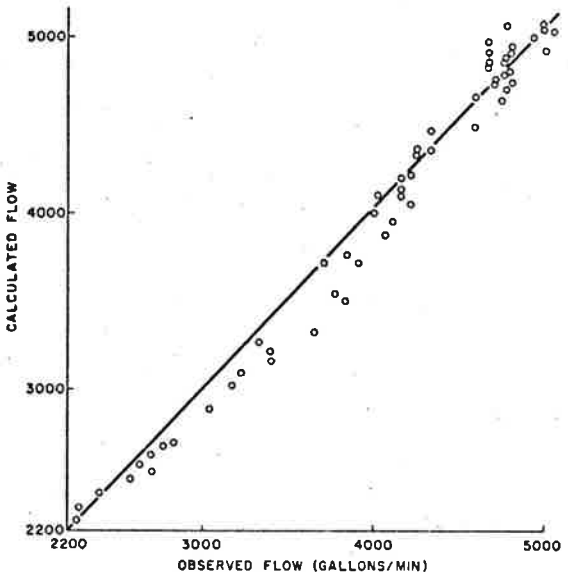

Fig. 4 Experimental results for flow equation

theoretical work is available to indicate that a perfect filtration model is sufficiently accurate for modeling purposes.[2,9] In particular, the concentration of any component depends on the concentration of that component in the slurry and the resistance of the mat (as measured by basis weight). The perfect filtration equation is

$$\frac{dx_i}{dB} = -\gamma_i x_i \qquad (2.6)$$

where γ_i is a proportionality constant which is different for each component. This equation has the solution

$$x_i = K_i e^{-\gamma_i B} \qquad (2.7)$$

The proportionality constant may be evaluated at $B = 0$ by noting that the concentration of the flow differs from the concentration of the slurry (x_{5i}) only because the wire itself without any mat formed on it retains a portion of the fiber. This fraction retained by the wire is termed the initial retention by Estridge[9] and is denoted by α_i. The resulting equation is

$$x_i = x_{5i}(1 - \alpha_i)e^{-\gamma_i B} \qquad (2.8)$$

This expression, with empirically determined initial retention and parameters γ_i for each component fits experimental data quite well and agrees closely with simulation results. Fig. 5 shows the fit for approximately 25 different paper grades for which concentration data was available. The fit is plus or minus 10% and is well within the limits of accuracy of the data itself. Moreover, the concentration of the flow through the wire is about 20% of headbox concentration and hence 10% accuracy in its calculation suffices.

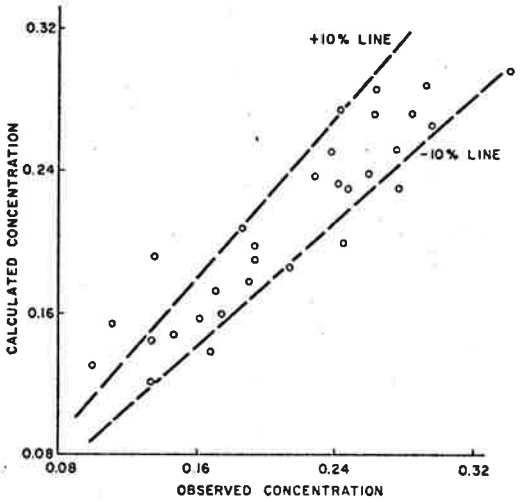

Fig. 5 Experimental results for concentration equation

The remaining relation which is important to the wire model is the mechanism for determining the wet line position. The simulation of the partial differential equation model gives the wet line position since the height of slurry above the partially formed mat is calculated at each increment and the point at which it equals mat height may be observed. At this point, all that remains above the wire is the partially formed mat together with water trapped inside. Beyond this point, the mat is compressed by squeezing some of the trapped water through the wire. At the wet line position, the compression has not yet begun significantly, and the amount of trapped water is essentially dependent only upon the basis weight of the sheet provided the basic stock does not change radically (as for example from bleached to unbleached stock). Hence the concentration may be assumed constant with little error. This is borne out by results of the simulation and by experimental data.

An additional consideration here is that 80 to 90% of the flow onto the wire flows through the table roll section and hence an appreciable error in the wet line concentration does not greatly affect the accuracy of the model. Nonetheless,

this assumption of constant wet line concentration is important because the wet line position in the lumped model may not be determined without it.

The remaining equations are simply material balance equations and are summarized in Table III. Observe that the resulting set of wire model equations are implicit in that basis weight and wet line position appear both as output variables and as variables in each of the flow and concentration equations. This implies an iterative solution is necessary if they must be calculated. In practice, the operation of the system is calculated step by step in time; from one step to the next, these variables change by such a small amount that only one or two iterations are ever required. Thus the equations are capable of being used in an on-line fashion.

Table III Wire model equations

Flow (gal/min)

$$g_1 = K_o whv$$

$$g_2 = K_1 h^{e_1} v^{e_2} B^{e_3}$$

$$g_3 = g_1 - g_2$$

$$g_4 = \text{constant}$$

$$g_5 = K_2 p_s^{e_4} v^{e_5} B^{e_6} d$$

$$g_6 = g_3 + g_4 - g_5$$

Concentrations (lbs/gal)

$$x_{6i} = x_{5i}(1 - \alpha_i) e^{-\gamma_i B}$$

$$x_{7i} = x_{5i}(1 - \alpha_i) e^{-\gamma_i' B}$$

Retentions (no units)

$$R_{1i} = 1 - g_2 x_{6i} / g_1 x_{5i}$$

$$R_{2i} = 1 - g_6 x_{7i} / g_1 x_{5i} R_{1i}$$

Basis Weight (Lbs/ft^2)

$$B = \left(\sum_{i=1}^{n} x_{5i} R_{1i} R_{2i} \right) \left(7.481 g_1 \right) / wv$$

Wet Line Concentration (lbs/gal)

$$c_{w1} = Bwv/g_6 = \text{constant}$$

III. THE SYSTEM EQUATIONS

Of the components in the system shown in Fig. 1, only two (aside from the Fourdrinier) need explicit modeling, the pipes and tanks. The pumps merely serve to provide the proper flows and the junctions are equivalent to interconnection constraints. The tanks are particularly simple because they are not only maintained with constant volume, but also are designed to be as perfectly mixed as possible. The assumption of perfect mixing is then well borne out by experimental evidence and allows the following formulation.[10]

If g is the flow through the tank (that is, both input and output flow since the tank is constant volume) and if x_i and x_i' are the concentrations of the ith component in the input stream and tank respectively, the differential relation between tank concentration and input is the usual first order equation

$$\frac{dx_i'}{dt} = \frac{g}{V}(x_i - x_i') \qquad (3.1)$$

This may be transformed to a difference equation by assuming the flow and input concentration remain constant over one sample period:

$$x_i'(t+\Delta) = e^{-g\Delta/V} x_i'(t) + (1 - e^{-g\Delta/V}) x_i(t) \qquad (3.2)$$

With little error, each exponential may be replaced by its linear expansion. This difference equation then serves for the headbox and the silo tanks. Notice that the coefficients in the equation change with time as flow changes, but that this does not complicate the numerical solution of the equations. This equation may be applied to the silo and headbox tanks by using the appropriate variables in Table I.

The pipes, the other component, are treated as pure deadtime devices.[10] That is, plug flow is assumed, with the output of a pipe becoming the input, a time increment later which depends upon the flow rate and pipe volume. Hence if x_i and x_i' are the input and output concentrations, they are related by

$$x_i'(t) = x_i(t - \tau) \qquad (3.3)$$

where τ is the dead time and is given by

$$\tau = V/g \qquad (3.4)$$

where V is the volume of the pipe and g is the flow rate through the pipe. The two pipes with sufficient length to have appreciable dead time are the pipes connecting the stuff box to the fan pump and the pipe from the fan pump to the headbox. In the former case, the flow rate is constant and hence the dead time is constant. Not shown in Fig. 1 is a recirculation from the head-

box to the fan pump which absorbs much of the variation in headbox flow. As a result, the flow rate in the pipe varies by less than 10% for most grades of paper, permitting the dead time to be assumed constant. For the particular paper mill considered in the simulation and control system design, the ratio of dead times in the two pipes was almost exactly 2:1. The sample time was conveniently chosen to be the smaller dead time (6 seconds), thereby simplifying the difference equations. Fig. 3 is a schematic of the system showing the dead time.

State variables were chosen as shown in Fig. 3 and the component mathematical models were interconnected by specifying constraints. For example, the sum of the flows from the stuff box must equal the (constant) flow through the long pipe since material must balance and there is a constant volume pump in the line. Similar constraints hold for concentrations where pipes and tanks are interconnected. The resulting equations of the system are shown in Table IV. Observe that when coupled with the equations of the wire itself, they form a set of first-order nonlinear difference equations. As mentioned, their solution is quite straightforward despite their implicit nature.

Table IV System equations

$$x_{1i}(t+\Delta t) = x_{1i} + \frac{\Delta t}{V_1}\left\{g_2 x_{6i} + g_5 x_{7i} - (g_2 + g_5 + g_7 + g_9)\, x_{1i}\right\}$$

$$x_{2i}(t+\Delta t) = \left\{x_{8i}\, u_1 + (g_0 - u_1)\, x_{1i}\right\}/g_0$$

$$x_{3i}(t+\Delta t) = \frac{x_{2i} g_0}{g_1} + \frac{(g_1 - g_0)}{g_1}\left\{x_{1i} + \frac{\Delta t}{V_1}(g_2 x_{6i} + g_5 x_{7i} - (g_2 + g_5 + g_7 + g_9)\, x_{1i})\right\}$$

$$x_{4i}(t+\Delta t) = x_{3i}$$

$$x_{5i}(t+\Delta t) = x_{5i} + \frac{\Delta t}{V_2}(x_{4i} - x_{5i})\, g_1$$

$$\ldots i = 1, 2, 3$$

It should be pointed out that the small flow from the silo to the fan pump inlet may actually reverse direction, depending upon the headbox flow. In this case, the dynamics of the process change significantly, but the only changes in the equations are the flow and concentration constraints at the inlet to the fan pump. This set of equations is similar in form although different in detail and is not shown here. In the simulation of the system, these equations were included.

IV. RESULTS AND CONCLUSIONS

The objective of this paper was to present a mathematical model of a paper-making process suitable for on-line use in a grade change control scheme. From basic principles, simulations, and experimental data, a simplified model was generated. The form of the model is a set of nonlinear difference equations with parameters to be empirically determined. The type of data that is available and the form of the model equations requires a fitting procedure which is essentially a sequential search scheme. In general, there are multiple solutions to the parameter fitting problem and much care and judgement must be used in selecting reasonable starting points and investigating alternate starting points for additional (and more reasonable) solutions. These problems are common to any nonlinear curve fitting or parameter estimation problem and need not be elaborated on here.

In order to verify the mathematical model created, the parameters were determined for a given paper mill, using data available from past records for approximately 60 grades of paper. Using the same operating conditions (stuff box concentrations and flow, slice opening, wire speed, etc.), the model predicts the actual basis weight almost without error and is capable of predicting the actual wet line position close enough for control purposes. These are verifications of the steady state portion of the model only, but it is this part which is most complex since the dynamics of the system are very well approximated by dead time and perfectly mixed tanks. For the various grades for which data was available, the fit of the flow and concentration equations is shown in Figs. 4 and 5.

The real objective of the model is not merely to be able to predict system performance at given operating conditions, but to calculate new and better conditions. As part of the development of a control system, it is necessary to specify conditions given desired output variables. Consider the problem of specifying machine speed and slice opening when a given basis weight sheet is to be made. Since wet line concentration is fixed, the flow g_6 may be calculated from

$$g_6 = Bwv/c_{w1} \qquad (4.1)$$

where w is machine width and c_{w1} is wet line concentration. Good operating practice fixes the wet line position, and the suction box pressure is not available for control. Consequently in the expression for g_5, all variables except velocity are specified. If some arbitrary machine speed is selected (it is desirable to run as fast as possible in order to maximize production), g_5 is determined and since g_4 is a fixed shower, g_3 is specified. In the expressions for g_1 and g_2, only slice opening is unspecified and g_1 is constrained to be the sum of g_2 and g_3. Hence a

constraint on slice opening results which is of the form

$$k_1 h - k_2 h^{e_1} - k_3 = 0 \qquad (4.2)$$

where the k are constants. The form of this equation is sketched in Fig. 6. Observe there that there are two solutions for slice opening for which that grade of paper may be made. If machine speed is allowed to vary, its effect is to move the curve vertically, either up or down. As a consequence, there are an infinite different number of operating points at which a given grade of paper can be made. Of more interest is the fact that for a given speed, there are either one or two slice openings, or none--that is, the curve in Fig. 6 may not intersect the axis, indicating no solution at any slice opening. This condition arises when there is too much drainage on the table roll section to satisfy the drainage requirements previously determined for the suction box section. The result is that the mat develops too rapidly resulting in poor formation. Increasing machine speed, however, shifts the curve in Fig. 6 upward to a point where a solution is possible. This required change in operating speed at low basis weight sheets agrees closely with actual mill operating experience and conditions.

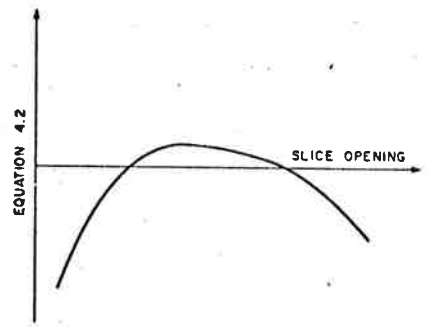

Fig. 6 Determination of allowable slice openings

Based on these evaluations, it was concluded that the resulting mathematical model is sufficiently simple for on-line computation and sufficiently accurate for on-line grade change control.

REFERENCES

1. Stephenson, J. N., (Editor), Pulp and Paper Mfg., Vol. 3, "Manufacture and Testing of Paper and Board," McGraw-Hill Book Co., Inc., New York, 1953, Ch. 1 and 2.

2. Meyer, H., "A Filtration Theory for Compressible Fibrous Beds Formed from Dilute Suspensions," TAPPI, Vol. 45, No. 4, April, 1962, pp. 296-310.

3. Nelson, R. W., "Approximate Theories of Filtration and Retention," TAPPI, Vol. 47, No. 12, December, 1965, pp. 752-764.

4. Igmanson, W. L., "Filtration of High-Consistency Fiber Suspensions," TAPPI, Vol. 47, No. 12, December, 1964, pp. 742-749.

5. Han, S. T., "Retention of Small Particles in Fiber Mats," TAPPI, Vol. 47, No. 12, December, 1964, pp. 782-787.

6. Abrams, R. W., "Retention of Fibers in Filtration of Dilute Suspensions," TAPPI, Vol. 47, No. 12, December, 1964, pp. 773-778.

7. Wahlstrom, B. and O'Blenes, G., "The Drainage of Pulps at Paper-Making Rates and Consistencies Using a New Grainage Tester," Pulp & Paper Mag. of Canada, Vol. 63, No. 8, T-405--T-417, August, 1962.

8. Beecher, A. E., "Dynamic Modeling Techniques in the Paper Industry," Proc. 17th TAPPI Conf., October, 1962.

9. Estridge, R., "Initial Retention of Fibers by Wire Grids," TAPPI, Vol. 45, No. 4, April, 1962, pp. 285-291.

10. Sullivan, P. R. and Schoeffler, J. D., "A General Approach to the Simulation of Stock Preparation and Fourdrinier Dynamics," 50th TAPPI Conf., NYC, February, 1965. To appear in TAPPI, August, 1965.

10. COMPARISON OF MODEL AND MEASUREMENTS

There are measurements available which relate inputs like thick stock flow and pressure in drying cylinders to basis weight and moisture content. These measurements indicate that the dynamics can be described by fairly low order models. It is, however, very difficult to measure concentrations and there are to the best of my knowledge no dynamic models available which relate the input to head box concentration or concentration at the outlet of the wire pit. Such measurements are of course highly desirable in order to evaluate what complexity is needed for a model. Experiments of this type are currently being made by B.Häggman on an experimental paper machine at Svenska Träforsknings Institutet.

One crucial problem is if the simple model where the wire is characterized by a retention factor only as in section 7 is appropriate. To judge this it is obviously necessary to know the retention r as a function of basis weight. It follows from (6.2) that the retention is given by

$$r(w) = \frac{bv}{q_1 c_1} = \frac{v}{h \cdot v_u \cdot c_1} \qquad (10.1)$$

where

b = effective machine width
v wire speed
v_u jet velocity
q_1 flow through slice
h slice opening
c_1 concentration in head box

All factors above are easily measured except head box concentration. If this could be measured e.g. by sampling or by an online optical gauge the retention function r(w) can obviously be determined statically.

If the simple model is valid it also follows from (6.4) that

$$r = 1 - \frac{c_2}{c_1} \qquad (10.2)$$

where c_2 is the fibre concentration at the outlet of the wire pit. Measuring c_2 it is thus possible to get a cross check and an indication

of the validity of the model. Experiments of this type are currently being evaluated by B. Häggman.

The more elaborate wire models have also been tested experimentally. One typical example is found in the paper by Alstrom et al which is included in section 9. Similar results have also been obtained by Ohlin.

11. NOTES AND REFERENCES

There are extensive references in the papermaking litterature on most of the phenomena that are briefly described in this chapter.
A general source is

Gavelin, G "Fourdrinier Papermaking" Lockwood Trade Journal Co, NYC 1963

The properties of water fibre mixtures and their flow are discussed in the following papers

Symposium Ind. Eng. Chem. 51, 839 (1959)

A. Bergholm, Massasuspensioners Reologi. Föredrag vid SCA 27.3.63

A. Bergholm, Cellulosa- och pappersindustrins vätskor. Föredrag vid STF-kurs Rörledningar inom industrin 23 - 26 oktober 1962

R.A. Diehm. Paper Ind. 42, 723, 776, 867 (1961)
43, 22, 87, 225, 305, 368 (1961)

D.W. Dodge, AB Metzner, J. AICHE 5, 189 (1959)

T.B. Drew, J.W. Hoopes, Adv. in Chem. Eng. Vol. 1, 77, Acad. Press, New York 1956

R.E. Durst, A.J. Chase, L.C. Jenness, Tappi 35 No 12, 529 (1952)

R.E. Durst, L.C. Jenness, Tappi 37 No 10, 417 (1954)

R.E. Durst, L.C. Jenness, Tappi 38 " 4, 193 (1955)

R.E. Durst, L.C. Jenness, Tappi 39 " 5, 277 (1957)

B. Hedström, Ind. Eng. Chem. 44, 651 (1952)

W.L. Ingmanson, Chem. Eng. Progr. 49, 577 (1953)

S.G. Mason, Pulp & Paper Mag. Canada 51, No 4, 93 (1950)

S.G. Mason, Tappi 33, 440 (1950)

S.G. Mason, Pulp Paper Mag. Can. 49 No 13, 99 (1948)

A.B. Metzner, J. Reed, A.I.Ch.E. 1, No 4, 434 (1955)

A.B. Metzner, Tappi 43, 300 (1960)

L.A. Moss, E.O. Bryant, Paper Trade J. 106, No 15, 46 (1938)

M. Reiner, Deformation, Strain and Flow, H.K. Lewis & Co Ltd, London 1960

A.A. Robertson, S.G. Mason, Pulp Paper Mag. Can., 55, No 3, 263 (1954)

A.A. Robertson, S.G. Mason, Tappi 40, 326 (1957)

B. Steenberg, B. Johansson, Svensk Paperstidning 61, 696 (1958)

B.J. Trevelyan, S.G. Mason, J. Coll. Sci. 6, 354 (1951)

D. Wahren, Doktorsavhandling 1964

There is an extensive litterature on filtration theory. The paper by Wahlström and O'Blenes that has been mentioned before and was in fact included as an appendix of section 5. Among other references on drainage with particular emphasis on theory we can mention the following

Meyer, H, "A Filtration Theory for Compressible Fibrous Beds Formed from Dilute Suspensions", Tappi, Vol 45, No 4, April 1962, pp 296 - 310

Nelson, R.W., "Approximate Theories of Filtration and Retention", Tappi, Vol. 47, No 12, Dec. 1964, pp 752 - 764

Han, S.T, "Retention of Small Paricles in Fiber Mats", Tappi, Vol 47, No. 12, Dec. 1964, pp 782-787

Ingmanson, W.L., "Filtration of High-Consistency Fiber Suspensions", Tappi, Vol. 47, No. 12, Dec. 1964, pp 742 - 749

Estridge, R, "Initial Retention of Fibers by Wire Grids", Tappi, Vol. 45, No 4, April 1962, pp 285 - 291

Abrams, R.W., "Retention of Fibers in Filtration of Dilute Suspensions", Tappi, Vol 47, No 12, Dec. 1964, pp 773 - 778

Ingmanson, W.L. and Adrews, B.D., "High Velocity Water Flow Through Fiber Mats", Tappi, Vol. 46, No 3, March 1963, p 150

Alsholm, O. and Schoeffler, J.D. and Sullivan, P.R., "An On-Line Mathematical Model of a Fine Paper Machine", ISA Conf., Los Angeles, California, October, 1965

The model given in the above references are in general fairly detailed and not suitable for on-line control. For such a purpose it is necessary to make rather drastic simplifications of the models. Such models are presented in

Alsholm, O., Schoeffler, J.D., Sullivan, P.R.: "On-Line Mathematical Model of a Fine Paper Machine", ISA Conference, Los Angeles, California, October 1965.

This paper presents a wire model in terms of a non-linear static model. The model has also been compared with experiments on a fine paper machine. Another similar model is presented in

Ohlin, C.: "A Mathematical Model of the Wire Part of a Fourdrinier Paper Machine", Report IBM Nordic Laboratory.

Ohlins model is also given in terms of a non-linear static model with a lumped parameter model of a wire. Ohlins model has been tested carefully against experiments made on an experimental paper machine at KMW. A third model which is quite similar to the two given above is presented in

Rosenberg, B.: "Matematisk modell av Pappersmäskin samt Modellstudium av kombinerad reglering av arkvikt och kvarvarande mäld i Registervalsarna", Rapport nr 1, December 1965, Institutionen för Reglerteknik, Chalmers Tekniska Högskola, Göteborg S

The constant retention model is given in

Beecher, A.E.: "Dynamic Modeling Techniques in the Paper Industry", Tappi 46 (1963) 117 - 120

LECTURES ON PAPER MACHINE CONTROL

A SIMPLE PAPER MACHINE MODEL

K.J. Åström

1. INTRODUCTION

2. NOTATION

3

3. NONLINEAR EQUATIONS

4. LINEARIZATION

5. PARAMETERS

6. STEP RESPONSES

1. INTRODUCTION

The results obtained in the previous sections will now be combined in order to obtain a model of the whole paper machine. Only very simple models of the subprocess will be used. The head box is modeled by two differential equations. A simple retention factor model is used for the wire. The concentration dynamics of the wet end is described using two differential equations. The presses are modeled simply by assuming that the fibre concentration after the presses are constant and the water removed in the dryers is described by a first order system only. There is not yet available any experimental verifications of the complete model. The gross features are, however, believed to be correct. The model obtained will be of fifth order with seven inputs and seven outputs.

2. NOTATION

A schematic diagram of the paper machine is shown in Fig. 2.1

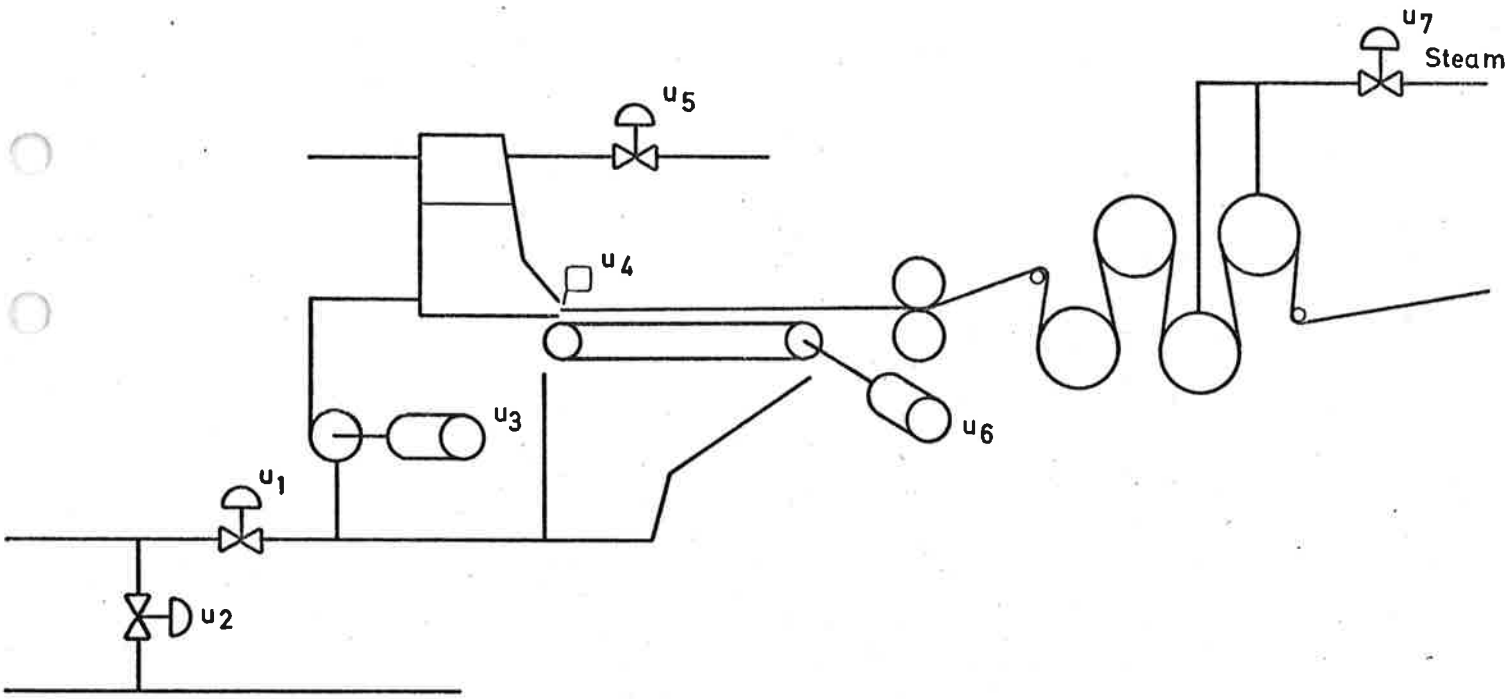

Fig. 2.1. Schematic diagram of paper machine

The control variables are chosen as follows

u_1	thick stock flow	$[m^3/s]$
u_2	fibre concentration in thick stock	$[kg/m^3]$
u_3	flow through fan pump	$[m^3/s]$
u_4	slice opening	$[m]$
u_5	air flow to head box	$[kg/s]$
u_6	wire speed	$[m/s]$
u_7	pressure in last drying section	$[N/m^2]$

The state variables are chosen as follows

x_1 head box level [m]

$x_2 = \frac{p-p_o}{\rho_2 g}$ where p is pressure in head box [m]

x_3 fibre concentration in head box $[kg/m^3]$

x_4 fibre concentration in flow out of wire pit $[kg/m^3]$

x_5 water removal rate in drying section [kg/s]

The outputs are arbitrarily chosen as follows

$y_i = x_i$ $\quad i = 1, 2, 3, 4$

y_5 jet velocity

y_6 fibre weight

y_7 water to fibre ratio at dry end

Many other outputs are often of interest e.g.

$y_8 = y_5/u_6$ velocity ratio

$y_9 = y_6(1+y_7)$ wet basis weight

y_{10} retention factor

The model is easily modified to take additional outputs into account.

3. NONLINEAR EQUATIONS

The models for the flow dynamics in the head box and the concentration dynamics have previously been derived. These models wil now be combined with models of the presses and the drying section and a model for the fan pump hydraulics in order to arrive at a complete nonlinear model.

Head Box Flow Dynamics

Using the notation introduced in section 2 of this chapter the head box model can be written as

$$\frac{dx_1}{dt} = -\frac{bu_4}{A}\sqrt{2g(x_1+x_2)} + \frac{u_3}{A}$$

$$\frac{dx_2}{dt} = -\frac{\kappa p_o A_1}{\rho_o \rho_2 g V}\cdot\left[\frac{\rho_2 g x_2}{p_o}+1\right]^{\frac{\kappa-1}{\kappa}}\sqrt{\frac{2\kappa}{\kappa-1}p_o\rho_o\left[\left(\frac{\rho_2 g x_2}{p_o}+1\right)^{\frac{\kappa-1}{\kappa}}-1\right]}$$

$$-\frac{\kappa b p_o u_4}{\rho_2 g V}\left[\frac{\rho_2 g x_2}{p_o}+1\right]\sqrt{2g(x_1+x_2)}$$

$$+\frac{\kappa p_o}{\rho_o\rho_2 g V}\left[\frac{\rho_2 g x_2}{p_o}+1\right]^{\frac{\kappa-1}{\kappa}}\cdot u_5 + \frac{\kappa p_o}{\rho_2 g V}\left[1+\frac{\rho_2 g x_2}{p_o}\right]u_3 \qquad (3.1)$$

where it is assumed that the velocity out of the head box is subsonic.

Concentration Dynamics of the Wet End

To describe the concentration dynamics of the wet end only water and fibres are considered. It is assumed that the wire can be modeled simply by assuming a retention factor and that the mixing is described through ideal mixing in two equivalent mixing volumes. Assuming that the fibre concentration at the wire overflow equals the fibre concentration in the wire pit the model becomes

$$V_1\frac{dx_3}{dt} = -q_1x_3 + (u_3-u_1)x_4 - u_1u_2$$

$$V_2\frac{dx_4}{dt} = (1-r(w))q_1x_3 - u_3x_4 \qquad (3.2)$$

where q_1 denotes the flow out of the head box and w the basis weight which are given by

$$q_1 = A\sqrt{2g(x_1 + x_2)} \tag{3.3}$$

$$w = \frac{r(w)q_1x_3}{bu_6} \tag{3.4}$$

where A is the area of the slice outlet and b the effective slice width.

Notice that (3.2) differs somewhat from the equation in chapter X because in chapter X it was assumed that head box inflow and outflow were always the same.

Model for the Presses

To describe the presses it is simply assumed that the water to fibre ratio f_p in sheet leaving the presses is constant. According to Häggman and Wahren [ ] a reasonable value is $f_p = 2$.

The dryers

The drying section is again a complicated process which is difficult to describe in detail. Here it is assumed that the water removal rate w_d kg/s in the drying section is related to the steam pressure through a first order dynamical system i.e.

$$\dot{w}_d + \alpha w_d = \beta u_7 \tag{3.5}$$

Using the simple model for the presses it follows that the water is entering the drying section at the rate

$$r \cdot q_1 c_1 \cdot f_p$$

Since the water removal rate is w_d it follows that the water to fibre ration at the dry end becomes

$$f_d = \frac{rq_1c_1f_p - w_d}{rq_1c_1} = f_p - \frac{w_d}{rq_1c_1} \qquad (3.6)$$

It is wellknown that it is much more difficult to remove water from a sheet with a low water to fibre ratio. To describe this we use an ad hoc model which does not have a direct physical interpretation by replacing the equation for f_d with

$$f_d = k(f_p - \frac{w_d}{rq_1c_1}) \qquad (3.7)$$

where k is the function

$$k(x) = a(x + \frac{1}{x+1}) \qquad (3.8)$$

A graph of k is given in Fig 2.2.

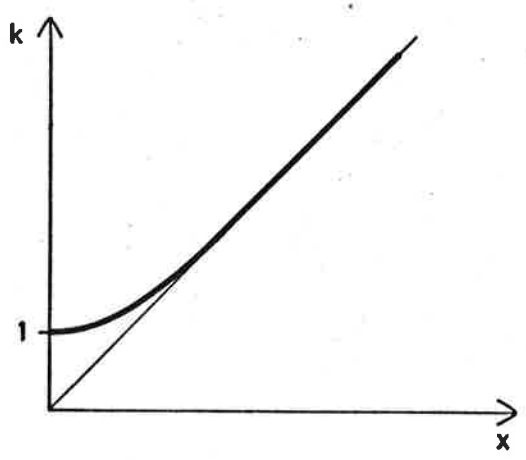

Fig. 2.2. Graph of the function $k = (x + \frac{1}{x+1})$

Summary

Summing up we find that the paper machine can be described by the following set of equations.

$$\frac{dx_1}{dt} = -\frac{bu_4}{A}\sqrt{2g(x_1 + x_2)} + \frac{u_3}{A}$$

$$\frac{dx_2}{dt} = -\frac{\kappa p_o A_1}{\rho_o \rho_2 g V}\left[\frac{\rho_2 g x_2}{p_o} + 1\right]^{\frac{\kappa-1}{\kappa}}\sqrt{\frac{2\kappa}{\kappa-1}p_o\rho_o\left[\left(\frac{\rho_2 g x_2}{p_o} + 1\right)^{\frac{\kappa-1}{\kappa}} - 1\right]}$$

$$-\frac{\kappa p_o bu_4}{\rho_2 g V}\left[1 + \frac{\rho_2 g x_2}{p_o}\right]\sqrt{2g(x_1 + x_2)} + \frac{\kappa p_o}{\rho_o \rho_2 g V}\left[1 + \frac{\rho_2 g x_2}{p_o}\right]^{\frac{\kappa-1}{\kappa}} u_5 +$$

$$+\frac{\kappa p_o}{\rho_2 g V}\left[1 + \frac{\rho_2 g x_2}{p_o}\right]u_3$$

$$\frac{dx_3}{dt} = -\frac{q_1 x_3}{V_1} + \frac{(u_3 - u_1)x_4}{V_1} - \frac{u_1 u_2}{V_1}$$

$$\frac{dx_4}{dt} = \frac{[1 - r(w)]q_1 x_3}{V_2} - \frac{u_3 x_4}{V_2}$$

$$\frac{dx_5}{dt} = -\alpha_5 x_5 + \beta_5 u_7 \qquad (3.9)$$

where the functions V_1, q_1 and r are given by

$$V_1 = A(h_o - x_1)$$

$$q_1 = A\sqrt{2g(x_1+x_2)} = bu_4\sqrt{2g(x_1+x_2)}$$

$$r = r(w) \qquad (3.10)$$

The outputs are given by

$$y_i = x_i \qquad i = 1, 2, 3, 4$$

$$y_5 = \sqrt{2g(x_1+x_2)} = v_u$$

$$y_6 = w = \frac{r(w)q_1x_3}{bu_6} = \frac{r(y_6)q_1x_3}{bu_6} = \frac{r(w)u_4x_3\sqrt{2g(x_1+x_2)}}{u_6}$$

$$y_7 = k(f_p - \frac{x_5}{r(w)x_3q_1(x_1,x_2,u_4)})$$

where the function k is given by

$$k = a(x + \frac{1}{x+1})$$

The model is thus charaterized by 5 physical constants

g	acceleration of gravity
ρ_o	air density at reference pressure
p_o	reference pressure
ρ_2	stock density
κ	

by 8 physical parameters

b	effective machine width
A	area of wet surface in head box
A_1	area of air outlet
V	air volume in head box
V_1	mixing volume in fan pump, screens, cleaners and head box system
V_2	mixing volume in wire pit
α_5	inverse time constant of dryers
β_5	dryer gain

and by three empirical functions

V	air volume in head box as a function of x_1
r	retention function
k	function which characterizes the dryer

The operating conditions are uniquely given by the values of the 7 control variables

u_1 thick stock flow
u_2 thick stock concentration
u_3 fan pump flow
u_4 slice opening
u_5 air flow to head box
u_6 wire speed
u_7 pressure in drying cylinders

and by the moisture to fibre ratio f_p at the presses.

4. LINEARIZATION

The derivatives of the state variables of (3.9) are not given explicitly in terms of the state variables due to the implicit equation (3.10) for the retention factor r. When deriving the linearized equations it is thus necessary to evaluate the partial derivatives of r with respect to x_1, x_2, x_3, u_4 and u_6. To do so it is necessary to take into account that w depends on x_1, x_2, x_3, u_4 and u_6. Taking partial derivatives of w with respect to q_1 we get

$$\frac{\partial w}{\partial q_1} = \frac{r x_3}{b u_6} + \frac{r' q_1 x_3}{b u_6} \frac{\partial w}{\partial q_1} = \frac{w}{q_1} + \frac{r'}{r} w \frac{\partial w}{\partial q_1}$$

Hence

$$\frac{\partial w}{\partial q_1} = \frac{1}{1-r'w/r} \frac{w}{q_1}$$

where r' denotes $\frac{dr}{dw}$. This implies

$$\frac{\partial r}{\partial q_1} = r' \frac{\partial w}{\partial q_1} = \frac{r'w/r}{1-r'w/r} \frac{r}{q_1}$$

The element a_{41} of the A-matrix of the linearized equation now becomes

$$a_{41} = \frac{\partial}{\partial x_1} \frac{[1-r(w)] q_1 x_3}{V_2} = \left\{ \frac{[1-r(w)] x_3}{V_2} - \frac{q_1 x_3}{V_2} \frac{\partial r'}{\partial q_1} \right\} \frac{\partial q_1}{\partial x_1}$$

$$= \left\{ \frac{(1-r)x_3}{V_2} - \frac{q_1 x_3}{V_2} \frac{r'w/r}{1-r'w/r} \frac{r}{q_1} \right\} \cdot \frac{q_1}{2(x_1+x_2)}$$

$$= \frac{q_1 x_3}{2V_2(x_1+x_2)} \frac{1-r-r'w/r}{1-r'w/r} = \frac{q_1 x_3}{2V_2(x_1+x_2)} \left(1 - \frac{r}{1-r'w/r}\right)$$

The other elements of the linearized system are obtained analogously. Skipping the details we find that a linearized model of the paper machine can be written in standard form with the following parameters.

$$a_{11} = -\frac{q_1}{2A(x_1+x_2)} = -\alpha_1$$

$$a_{12} = -\alpha_1$$

$$a_{21} = -\beta\alpha_1$$

$$a_{22} = -\alpha_2 - \beta\alpha_1$$

$$a_{31} = -\alpha_3 \cdot \frac{c_1}{2(x_1+x_2)} \qquad \alpha_3 = q_1/V_1$$

$$a_{32} = -\alpha_3 \cdot \frac{c_1}{2(x_1+x_2)}$$

$$a_{33} = -\alpha_3$$

$$a_{34} = \frac{q_2}{V_1}$$

$$a_{41} = \frac{q_1 x_3}{2V_2(x_1+x_2)} \left(1 - \frac{r}{1-r'w/r}\right)$$

$$a_{42} = \frac{q_1 x_3}{2V_2(x_1+x_2)} \left(1 - \frac{r}{1-r'w/r}\right)$$

$$a_{43} = \frac{q_1}{V_2} \left(1 - \frac{r}{1-r'w/r}\right)$$

$$a_{44} = -\frac{u_3}{V_2}$$

$$a_{55} = -\alpha_5$$

where

$$\beta = \frac{\kappa A \ell}{V}$$

$$\ell = p_o(\rho_o/\rho_o)^{\kappa}/(\rho_2 g)$$

$$\alpha_2 = \begin{cases} \dfrac{w_s}{2\rho_s V} \cdot \dfrac{(\kappa-1)(\rho_s/\rho_o)^{\kappa-1}}{(\rho_s/\rho_o)^{\kappa-1}-1} & \dfrac{\rho_s}{\rho_o} < \left(\dfrac{\kappa+1}{2}\right)^{\frac{1}{\kappa-1}} \\ \dfrac{w_s}{2\rho_s V}(\kappa+1) & \dfrac{\rho_s}{\rho} \geq \left(\dfrac{\kappa+1}{2}\right)^{\frac{1}{\kappa-1}} \end{cases}$$

$$b_{13} = \frac{1}{A}$$

$$b_{14} = -\frac{b}{A}\sqrt{2g(x_1+x_2)} = -\frac{u_3}{Au_4} = -\frac{q_1}{Ad}$$

$$b_{23} = \frac{\kappa p_o}{\rho_2 g V}\left[1 + \frac{\rho_2 g x_2}{p_o}\right] = \beta/A = \frac{\kappa \ell}{V}.$$

$$b_{24} = -\frac{\kappa p_o b}{\rho_2 V g}\left[1 + \frac{\rho_2 g x_2}{p_o}\right]\sqrt{2g(x_1+x_2)} = \beta b_{14}$$

$$b_{25} = \frac{\kappa p_o}{\rho_o \rho_2 g V}\left[1 + \frac{\rho_2 g x_2}{p_o}\right]^{\frac{\kappa-1}{\kappa}} = \frac{\kappa \ell}{\rho V} = \frac{\beta}{\rho A}$$

$$b_{31} = \frac{u_2 - x_4}{V_1} = \frac{c_o - c_2}{V_1}$$

$$b_{32} = \frac{u_1}{V_1} = \frac{q_o}{V_1}$$

$$b_{33} = \frac{x_4}{V_1} = \frac{c_2}{V_1}$$

$$b_{34} = -\frac{q_1 x_3}{u_4 V_1} = -\frac{q_1 c_1}{V_1 d}$$

$$b_{43} = -\frac{x_4}{V_2} = -\frac{c_2}{V_2}$$

$$b_{44} = \frac{q_1 c_1}{V_2 d}\left[1 - \frac{r}{1-r'w/r}\right]$$

$$b_{46} = \frac{q_1 c_1}{V_2 u_b} \quad \frac{r'w}{1-r'w/r}$$

$$b_{57} = \beta_5$$

$$c_{ij} = \delta_{ij} \qquad i = 1,2,3,4,\ j = 1,2,3,4,5$$

$$c_{51} = \frac{v_u}{2(x_1+x_2)}$$

$$c_{52} = \frac{v_u}{2(x_1+x_2)}$$

$$c_{61} = \frac{w}{2(x_1+x_2)} \quad \frac{1}{1-r'w/r}$$

$$c_{62} = \frac{w}{2(x_1+x_2)} \quad \frac{1}{1-r'w/r}$$

$$c_{63} = \frac{w}{x_3} \quad \frac{1}{1-r'w/r}$$

$$c_{71} = \frac{x_5}{2rq_1 x_3 (x_1+x_2)} \quad \frac{1}{1-r'w/r} \cdot k'(k^{-1}(m))$$

$$c_{72} = \frac{x_5}{2rq_1 x_3 (x_1+x_2)} \quad \frac{1}{1-r'w/r} \cdot k'(k^{-1}(m))$$

$$c_{73} = \frac{x_5}{rq_1x_3^2} \quad \frac{1}{1-r'w/r} \cdot k'(k^{-1}(m))$$

$$c_{75} = -\frac{1}{rq_1x_3} \cdot k'(k^{-1}(m))$$

$$d_{64} = \frac{w}{u_4} \quad \frac{1}{1-r'w/r}$$

$$d_{66} = -\frac{w}{u_6} \quad \frac{1}{1-r'w/r}$$

$$d_{74} = \frac{x_5}{rq_1u_4x_3} \quad \frac{1}{1-r'w/r} \cdot k'(k^{-1}(m))$$

The linearized equations have the structure illustrated below where • denotes a nonzero element.

$$\frac{dx}{dt} = \left[\begin{array}{cc:cc:c} \bullet & \bullet & 0 & 0 & 0 \\ \bullet & \bullet & 0 & 0 & 0 \\ \hdashline \bullet & \bullet & \bullet & \bullet & 0 \\ \bullet & \bullet & \bullet & \bullet & 0 \\ \hdashline 0 & 0 & 0 & 0 & \bullet \end{array}\right] x + \left[\begin{array}{cc:cc:c:c} 0 & 0 & \bullet & \bullet & 0 & 0 & 0 \\ 0 & 0 & \bullet & \bullet & \bullet & 0 & 0 \\ \hdashline \bullet & \bullet & \bullet & \bullet & 0 & 0 & 0 \\ 0 & 0 & \bullet & \bullet & 0 & \bullet & 0 \\ \hdashline 0 & 0 & 0 & 0 & 0 & 0 & \bullet \end{array}\right] u$$

$$y = \left[\begin{array}{cc:cc:c} \bullet & 0 & 0 & 0 & 0 \\ 0 & \bullet & 0 & 0 & 0 \\ 0 & 0 & \bullet & 0 & 0 \\ 0 & 0 & 0 & \bullet & 0 \\ \bullet & \bullet & 0 & 0 & 0 \\ \bullet & \bullet & \bullet & 0 & 0 \\ \bullet & \bullet & \bullet & 0 & \bullet \end{array}\right] x + \left[\begin{array}{ccccccc} 0 & 0 & 0 & 0 & 0 & 0 & 0 \\ 0 & 0 & 0 & 0 & 0 & 0 & 0 \\ 0 & 0 & 0 & 0 & 0 & 0 & 0 \\ 0 & 0 & 0 & 0 & 0 & 0 & 0 \\ 0 & 0 & 0 & 0 & 0 & 0 & 0 \\ 0 & 0 & 0 & \bullet & 0 & \bullet & 0 \\ 0 & 0 & 0 & \bullet & 0 & 0 & 0 \end{array}\right] u$$

Notice that the system matrix A is block triangular where the blocks correspond to flow dynamics of the head box, wet end dynamics and

dryer dynamics.

We can thus immediately conclude that the eigenvalues of the total system are equal to those of the subsystems. Notice, however, that the inputs u_3 (flow through fan pump) and u_4 (slice opening) will directly influence the state variables x_1, x_2, x_3 and x_4.

5. PARAMETERS

The linearized model obtained in the previous section can be characterized by five physical constants g, ρ_o, p_o, ρ_2, κ by eight physical parameters b, A, A_1, V, V_1, V_2, α_5, β_5, by three functions V, r and k and by seven variables which characterizes the steady state operating point. There are obviously no problems associated with the physical constants. The determination of the other parameters will be discussed in the following.

The Physical Parameters

The parameters b, (width of the paper sheet), A (wet surface in head box) and V (air volume in head box) are easy to determine. The parameter A_1 (area of outlet surface) can conventiently be determined from the total air flow and the outflow velocity which is determined by the head box air pressure. The parameters V_1 and V_2 which represent mixing volumes are difficult to determine. Dynamical experiments are essential to obtain good estimates. The same is true for the parameters α_5 and β_5 which characterizes the drying section.

The Function $V = V(x_1)$

The function V gives the air volume of the head box as a function of head box level x_1. This function can easily be determined from the head box geometry. We assume that the function is simply

$$V = A(h_o - x_1)$$

The only quantity which enters the linearized model is the steady state value V. This is very reasonable because most modern headboxes are operated in such a way that the level does not change much.

The Retention Function

It is not easy to determine the retention function r which tells how the average retention depends on the basis weight. As was discussed in the chapter on wet end models the function can of course be determined from the partial differential equation models for the wet end. These models are, however, not very tractable and they also contain many unknown parameters.

The linearized model does, however, only contain the value of r and its derivative r' at the reference value of the basis weight. The appropriate values of r and r' can be determined experimentally e.g. by measuring the fibre concentrations in the head box (c_1) and in the outlet of the wire pint (c_2) at different basis weights. The value of the retention function is then given by

$$r(w) = 1 - \frac{c_2}{c_1}$$

If c_1 and c_2 are determined for different values of w the value of r' can then be determined through numerical differentiation.

Example

In tests on an experimental paper machine producing sack paper. Häggman obtained the following values

Fibre weight	c_1	c_2	r
61.47	0.312	0.0479	0.846
58.04	0.299	0.0487	0.837
55.46	0.280	0.0477	0.830
58.71	0.303	0.0469	0.845
63.47	0.327	0.0442	0.865
67.89	0.348	0.0435	0.875
70.37	0.353	0.0413	0.882

A graph of the function r is shown in Fig. 5.1.

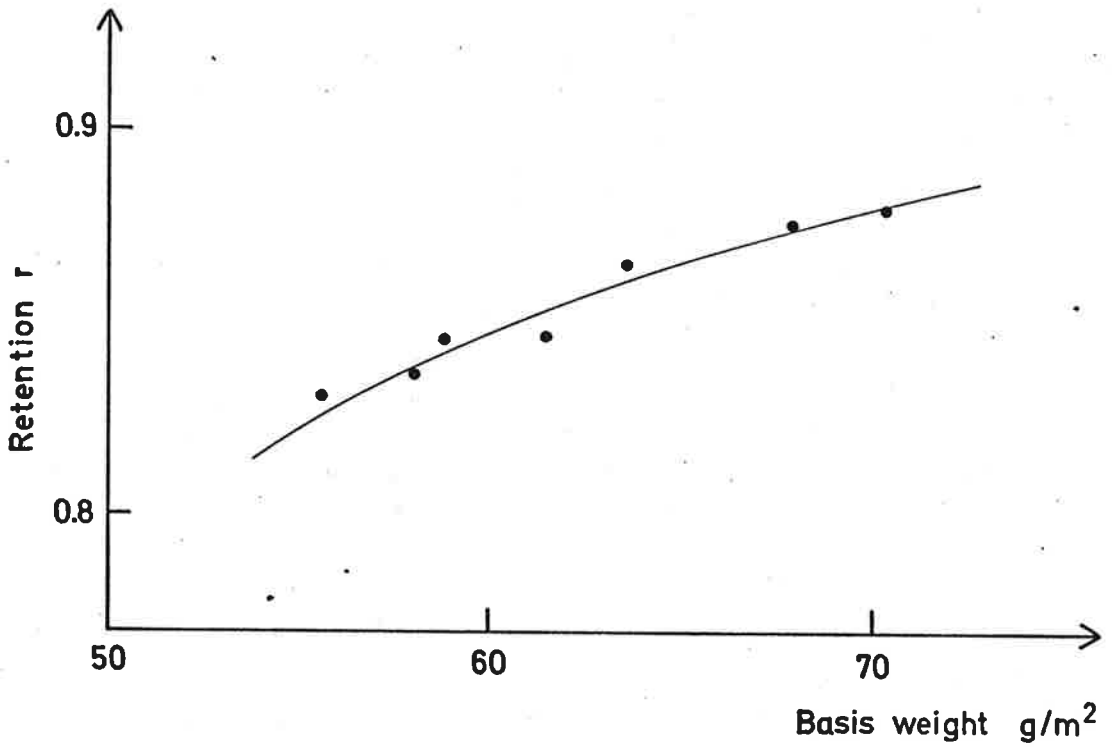

Fig. 5.1. Retention r as a function of basis weight obtained experimentally by Häggman for a kraft paper pulp.

Han's Drainage Formula

An analytical form of the retention function for a small drainage element was proposed by Han. See Chapter on Wet End Models. Han gave the following formula

$$r(w) = 1 - (1 - \alpha)e^{-\gamma w}$$

Assuming that this formula holds also for the average retention we get

$$r'(w) = (1-\alpha)e^{-\gamma w} = \gamma(1-r)$$

The functions entering the coefficients of the linearized model then becomes

$$\frac{r}{1-r'w/r} = \frac{r^2}{r-\gamma w(1-r)}$$

$$\frac{r'w}{1-r'w/r} = \frac{\gamma r(1-r)}{r-\gamma w(1-r)}$$

$$\frac{1}{1-r'w/r} = \frac{r}{\gamma-\gamma w(1-r)}$$

Some Numerical values of these functions are given below for $\alpha = 0.5$.

Table 5.1

γw	r	$r-\gamma w(1-r)$	$\frac{r}{1-r'/r}$	$\frac{r'w}{1-r'w/r}$
0	0.5	0.5	1.00	0
0.233	0.6	0.507	1.18	0.184
0.510	0.7	0.547	1.28	0.281
0.692	0.75	0.576	1.31	0.304
0.919	0.8	0.617	1.29	0.296
1.61	0.9	0.739	1.24	0.217
2.30	0.95	0.835	1.14	0.138
3.90	0.99	0.961	1.03	0.041

Since Han's results were derived for a small drainage element it is questionable if they are valid for the average retention for the whole wire section. If the formula should have any success it is obvious that w has to be interpreted as the average basis weight. It would then be more natural to represent the average retention for the whole wire section with the formula

$$r_1(w) = \frac{1}{w}\int_0^w \left[1 - (1-\alpha)e^{-\gamma u}\right] du$$

$$= 1 - \frac{(1-\alpha)(1-e^{-\gamma w})}{\gamma w}$$

Hence

$$r_1'(w) = \frac{(1-\alpha)\left[1-(1+\gamma w)e^{-\gamma w}\right]}{(\gamma w)^2} \cdot \gamma$$

A few values of the function r, are given in the table below for $\alpha = 0.5$

Table 5.2

γw	r_1
0	0.5
0.5	0.606
1	0.685
2	0.785
3	0.842
4	0.878
5	0.90
10	0.95

The function r_1 seems much more reasonable than r because the value of γ is about 0.05 m^2/g. For a 60 g/m^2 sack paper we get $\gamma w = 3$. Table 5.1 gives r = 0.97 while Table 5.2 gives $r_1 = 0.84$. The latter value is much more reasonable compare e.g Fig. 5.1.

Sammanfattning av matematisk modell

för pappersmaskiner.

I appendix finns en översiktsskiss över en pappersmaskin. Följande styrvariabler finns:

u_1 tjockmassaflöde
u_2 tjockmassakoncentration
u_3 blandningspump
u_4 läppöppning
u_5 flöde in i eller ut ur inloppslådan
u_6 virahastighet
u_7 tryck i torkcylindrarna

Vi har tidigare tagit fram följande modeller för de olika delarna.

Inloppslådemodell.

$$\frac{d}{dt}\begin{bmatrix} h-h_s \\ p-p_s \end{bmatrix} = \begin{bmatrix} -\alpha_1 & -\alpha_1 \\ -\beta\alpha_1 & -(\alpha_2+\beta\alpha_1) \end{bmatrix} \begin{bmatrix} h-h_s \\ p-p_s \end{bmatrix}$$

$$+ \begin{bmatrix} 1 & 0 \\ \beta & 1 \end{bmatrix} \begin{bmatrix} u_1^* \\ u_2^* \end{bmatrix}$$

$$y = v_u = \frac{v_s}{2h_{eff}}((h-h_s)+(p-p_s))$$

h=mäldhöjd
p=tryck i luftkudden
$u_1^*=u_3$ eller u_4
$u_2^*=u_5$
v_u=hastighet ut ur inloppslådan

Index s anger att det är variabelns värde i stationärt tillstånd som åsyftas.

Korta cirkulationen.

Följande ekvationer fås ur vätske- och fiberbalans.

$$\frac{dc_1}{dt} = -\frac{q_1}{V_1} c_1 + \frac{q_2}{V_1} c_2 + \frac{q_o c_o}{V_1}$$

$$\frac{dc_2}{dt} = q_1 \frac{(1-r(w))}{V_2} c_1 - \frac{q_1}{V_2} c_2$$

$$w = \frac{r(w) q_1 c_1}{bv}$$

$$r(w) = 1-(1-\alpha)e^{-\gamma w}$$

där q_i betecknar flöden och c_i koncentrationer på de ställen som anges i figur i appendix.

v= virahastighet, b=virabredd

r(w)=retentionen

w=ytvikt

V_1, V_2=effektiva blandningsvolymer (var och hur blandning egentligen sker är osäkert)

Insignalerna är

tjockmassaflöde q_o, u_1

tjockmassakoncentration c_o, u_2

flöde genom blandningspump u_3

läppöppning u_4

virahastighet v, u_6

utloppshastighet (fås ur inloppslådsekvationerna)

Pressar

Vi antar att det är konstant fukthalt efter pressarna.

Torkpartiet.

Insignaler är ingående totalflöden och tryck i torkpartiet. Utsignal är fukthalt. Följande samband används

$$m = f\left(\left(\frac{\rho}{c_4} - 1\right) - \frac{\rho q_u}{r q_1 c_1}\right)$$

m=fuktkvot
q_u=mängd vatten som avlägsnas per tidsenhet
c_4=fiberkoncentration efter pressarna
q_1=flöde ut ur inloppslådan
c_1=fiberkoncentration i inloppslådan
ρ=vattnets täthet
r=retentionen

Empiriskt får f utseendet

$$f(x) = a\left(x + \frac{1}{x+1}\right)$$

Dynamiken i torkcylindrarna approximeras med

$$T\frac{dq_u}{dt} + q_u = k\, u_7$$

Diskussion av de olika modellerna

Modellen för inloppslådan har vi fått direkt ur välkända fysikaliska grundekvationer och enligt litteraturen stämmer en sådan här linjäriserad modell bra med verkligheten. Observera dock att det finns inloppslådor av något annorlunda typ som kan kräva modifikation av ekvationerna. För den korta cirkulationen används en väldigt grov modell. Hur blandningen egentligen sker vet man inte. Retentionsfaktorn får ensam representera hela det komplicerade förloppet på viran. Retentionsfaktorns beroende på ytvikten är väsentligt eftersom det leder till att första termen i uttrycket för dc_2/dt skiftar tecken jämfört med fallet konstant retention. Modellen för presspartiet är bara ett tillyxat antagande om konstant fukthalt. Torkpartiet slutligen bygger på vätskebalans och en enkel dynamik "tagen ur hatten".

En stor brist hos denna modell av pappersmaskinen är att en viktig utsignalinte finns med, nämligen läget hos våta linjen. För detta skulle krävas en betydligt mer avancerad viramodell.

Sammanställning av modell för pappersmaskin.

Tillståndsvariabler

x_1 nivå, inloppslåda

x_2 tryck, inloppslåda

x_3 fiberkonc. inloppslåda

x_4 fiberkonc. viragrop

x_5 tillståndsvariabel för att representera torkpart-dynamiken

Utsignaler

$y_i = x_i \quad i=1,2,3,4$

$y_5 = v_{ut}$

$y_6 = ytvikt$

$y_7 = fukthalt$

Ur de tidigare uppställda modellerna erhålls följande ekvationer.

$$\dot{x}_1 = a_{11}x_1 + a_{12}x_2 + b_{13}u_3 + b_{14}u_4$$

$$\dot{x}_2 = a_{21}x_1 + a_{22}x_2 + b_{23}u_3 + b_{24}u_4 + b_{25}u_5$$

$$\dot{x}_3 = a_{31}x_1 + a_{32}x_2 + a_{33}x_3 + a_{34}x_4 + b_{31}u_1 + b_{32}u_2 + b_{33}u_3 + b_{34}u_4$$

$$\dot{x}_4 = a_{41}x_1 + a_{42}x_2 + a_{43}x_3 + a_{44}x_4 + b_{44}u_4 + b_{46}u_6$$

$$\dot{x}_5 = a_{55}x_5 + b_{57}u_7$$

$$y_5 = c_{51}x_1 + c_{52}x_2$$

$$y_6 = c_{61}x_1 + c_{62}x_2 + c_{63}x_3 + d_{64}u_4 + d_{66}u_6$$

$$y_7 = \underline{\qquad} + \underbrace{c_{71}x_1 + c_{72}x_2 + c_{73}x_3 + d_{74}u_4 + d_{76}u_6}$$

De termer som står inom klammer bör egentligen komma in med en tidsfördröjning.

Matriserna för systemet får alltså det utseende som anges i appendix där även de numeriska värdena är insatta.

A-matrisen är som synes block-triangulär. Egenvärdena för det totala systemet blir då de som man får fram ur de olika diagonala blocken. De ungefärliga numeriska värdena är

x_1, x_2: $1/\lambda = 45, 600\,s$

x_3, x_4: $1/\lambda = 85, 120\,s$

x_5: $1/\lambda = 60\,s$

Konventionell reglering.

Det finns pappersmaskiner som går praktiskt taget helt utan reglering. Om man har en sluten inloppslåda måste man dock ha någon forma av reglering på denna, t.ex. en loop som mäter lufttrycket och styr luftflödet och en annan som mäter nivån och styr blandningspumpen. Det kan också finnas lokala reglersystem för koncentration, för virahastighet och hastighet i torkpartiet. Mer sällan finns reglering av spänningen i pappersbanan i torkpartiet. Många maskiner går utan vare sig ytvikts- eller fukthaltsreglering. Man tar prover från färdiga pappersrullar, låter laboratoriet analysera dem och meddelar resultatet till maskinföraren som gör en manuell ändring.

För att föra ytviktsreglering krävs lämpliga givare. Bland de första metoderna var β-mätare. Man har en β-strålningskälla och på andra sidan papperet en detektor som mäter hur mycket som har absorberats. Eftersom β-strålarna absorberas lika mycket i fibrer som i vatten måste man, om man vill mäta ytvikten fibrer, också göra en fukthaltsmätning. Ofta görs β-mätarna traverserande så att de kan mäta variationer tvärs papperet. En β-mätare kostar 100 000-400 000 kr. Fukthaltsmätare kan vara av kapacitiv typ; papperet fungerar som ett dielektrikum mellan två kondensatorplattor och man mäter kapacitansen. Det finns också mikrovågsmätare som antingen mäter absorptionen eller dielektricitetskonstanten. Mikrovågsmätarna kan mäta betydligt högre fuktbalter än de kapacitiva mätarna.

En annan metod är att använda infrarödmätare. De bygger på att både absorptionen i fibrer och i vatten är starkt frekvensberoende. Genom att mäta vid frekvenser där fibrerna respektive vattnet har dominerande absorption kan man få en mätning av både fiber- och vattenmängd. Infrarödmätaren har också fördelen att man kan mäta vid våta ändan vilket β-mätaren inte klarar eftersom det är svårt att mäta de höga fukthalter man har där.

En annan svårighet med β-mätare är att man måste räkna ett tillräckligt stort antal partiklar för att få god noggrannhet. Detta betyder att man vid en traverserande mätare inte kan utföra rörelsen i sidled alltför fort.

Det finns två trender i ytviktsregleringen. Den ena är att försöka göra en koncentrationreglering som elimi-nerar de störningar som kommer in via feeden. Den andra är att man försöker minska tidsfördröjningen genom att flytta fram ytviktsmätningen till våta ändan.

Fukthalten regleras i allmänhet genom en återkopplimg från fukthaltsmätare i slutet på maskinen till torkpar-tiet. Ofta kombineras detta med en signal från framän-dan på maskinen som anger fiberflödet in i maskinen, eftersom detta påverkar hur stor torkkapacitet som behövs.

Det finns olika åsikter om huruvida ytvikts- och fukt-haltsmätareskall vara fixa eller traverserande. En nackdel med traversering är att den tar lång tid, upp till 1.5 min., vilket introducerar en extra tidsfördröjning. Före-språkarna för fixa mätare menar att tvärsprofilen i all-mänhet är så fix att man kan mäta i en enda punkt, medan anhängarna av traversering säger att man kan få stora fel om man ligger och mäter på kanten av en topp i tvärspro-filen när denna förskjuts i sidled. Man bör notera att en traverserande mätare i praktiken mäter diagonalt över papperet eftersom detta rör sig med stor hastighet (10m/s).

Kriteriet för regleringen är ofta att man skall ligga nära någon produktionsgräns, vilket betyder att man skall minimera variansen och sedan lägga börvärdet så nära som möjligt. I en del processer används s.k. börvärdesopti-mering, där börvärdet ändras beroende på intensiteten hos de inkommande störningarna.

På många maskiner är torkkapaciteten den begränsande fak-torn. Maskinen körs då oftast så att torkpartiet konstant kör med full kapacitet medan man varierar hastigheten på maskinen.

Appendix

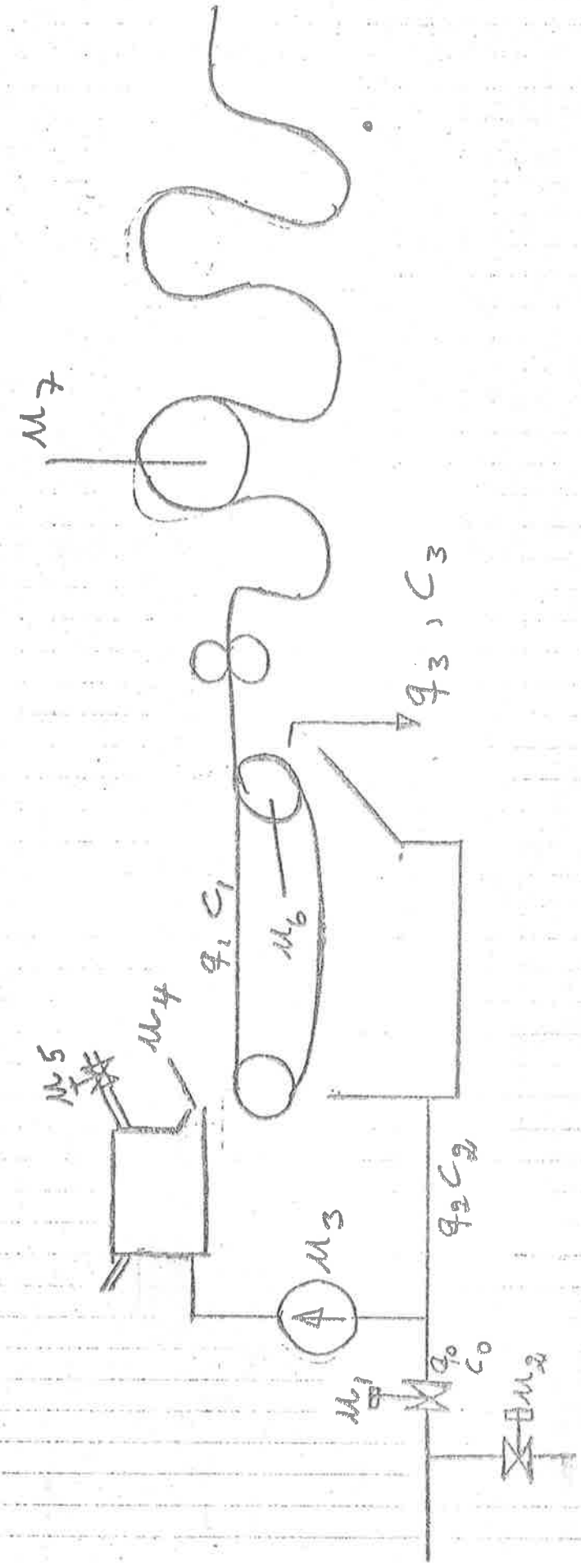

PAPPERSMASKN 72-04-23

A

-0.10000G-01	-0.10000G-01	0.00000	0.00000	0.00000		
-0.21000	-0.25000	0.00000	0.00000	0.00000		
-0.30000G-01	-0.30000G-01	-0.12000	0.11000	0.00000		
-0.10900G-02	-0.10900G-02	-0.24000G-03	-0.12000G-01	0.00000		
0.00000	0.00000	0.00000	0.00000	-0.10000G-01		

B

0.00000	0.00000	0.10000	-6.0000	0.00000	0.00000	0.00000
0.00000	0.00000	2.1000	-125.00	1.2900	0.00000	0.00000
2.7000	0.89000G-02	0.50000G-01	-14.900	0.00000	0.00000	0.00000
0.00000	0.00000	0.00000	-0.27000	0.00000	0.54000G-03	0.00000
0.00000	0.00000	0.00000	0.00000	0.00000	0.00000	1.0000

C

1.0000	0.00000	0.00000	0.00000	0.00000
0.00000	1.0000	0.00000	0.00000	0.00000
0.00000	0.00000	1.0000	0.00000	0.00000
0.00000	0.00000	0.00000	1.0000	0.00000
1.0000	1.0000	0.00000	0.00000	0.00000
0.70000G-02	0.70000G-02	0.36600G-01	0.00000	0.00000
0.26000	0.26000	1.0500	0.00000	0.00000

D

0.00000	0.00000	0.00000	0.00000	0.00000	0.00000	0.00000
0.00000	0.00000	0.00000	0.00000	0.00000	0.00000	0.00000
0.00000	0.00000	0.00000	0.00000	0.00000	0.00000	0.00000
0.00000	0.00000	0.00000	0.00000	0.00000	0.00000	0.00000
0.00000	0.00000	0.00000	0.00000	0.00000	0.00000	0.00000
0.00000	0.00000	0.00000	0.45500	0.00000	-0.92000G-02	0.00000
0.00000	0.00000	0.00000	2.2000	0.00000	-0.61000G-01	0.00000

Chapter 1

APPLICATIONS TO PAPERMAKING

TABLE OF CONTENTS

Chapter 1 - APPLICATIONS TO PAPERMAKING

1.1 Introduction

1.2 Description of a Paper Mill

Brief Description of the Process

The Art of Paper Making

Paper Mills as Control Objects

1.3 The Systems Approach

Introduction

An Example of a Feasibility Study

An Example of an Integrated System

1.4 Paper Machine and Stock Preparation Control

Introduction

Objectives of the Control

Measurements and Control Variables

Basis weight

Moisture content

Other quality variables

Mathematical Models

1.5 Steady State Control

Introduction

Review of Linear Stochastic Control Theory

Model Structures

Single Output Systems

Minimum Variance Control Strategies

Sensitivity of the Minimal Variance Strategies

1.6 Process Identification

Introduction

The Maximum Likelihood Method

Single Output Systems

Properties of the Maximum Likelihood Estimates

1.7 Basis Weight Control

Introduction

Preliminary Investigations

The Measurement Errors of the Basis Weight Gauge

The Identification Experiments

Choice of input signal

Practical aspects of the experiments

Computation of the Maximum Likelihood Estimates

Experiences with Online Control

1.8 Quality Control

Introduction

Statistical Properties of Fluctuations in Typical Quality Variables

Application of Estimation Theory

The Prediction Problem

The Interpolation Problem

Summary of Results

1.9 References

Section 1 — Introduction

This chapter deals with the application of computers to the control of paper making processes. Paper making which is an old industrial practice, poses interesting problems to the control engineer.

In most existing plants there are a number of regulators for simple tasks like level and flow regulation while the control of the major quality variables is done manually.

The fundamental properties of the paper making process are not understood to the extent that the mathematical models required for control can be obtained from first principles. Techniques for determination of mathematical models from plant experiments are thus important.

Many of the important quality variables can not be measured on-line. Instead, they have to be measured in test laboratories on samples taken from the production. The use of such data in control is another important area of application.

This chapter is based largely on experiences obtained in a joint venture between Billerud AB in Sweden and IBM, aimed at integrated control of a paper mill. A brief description of a paper mill is given in section 2. This section also outlines some of the characteristic features of paper making processes as control objects. Section 3 emphasizes the fact that the economic incentive in solving a particular control problem can be evaluated only by its influence on the overall plant economy. An example of a feasibility study aimed at obtaining a gross picture of the total plant economy is also given in this section. Section 4 deals with the control of one important part of the paper making process namely the

paper machine and the stock preparation system. This section gives an overview of the control problems. It covers objectives, models, and measurements.

In section 5 we discuss a technique for the steady state control of process variables based on linear stochastic control theory. The determination of mathematical models of the system dynamics and the disturbances from plant experiment is the theme of section 6. This section describes a method which is designed to develop the models needed in order to apply linear stochastic control theory.

In section 7 we give a practical example of the techniques described in sections 5 and 6 to a typical regulation problem, namely, basis weight control. This section also illustrates several of the practical problems which have to be overcome when applying theory to a practical problem. Practical experiences with actual use of optimal control strategies are also given.

The problem of quality control based on off-line measurements is discussed in section 8. It is shown that considerable improvements can be obtained through the use of filtering theory and data processing. This section is also based on plant data.

Section 9 finally contains a list of references.

Section 2 — Description of a Paper Mill

Brief Description of The Process

In this section we will give a very brief description of an integrated mill. A schematic diagram is shown in Figure 1. The process can be divided into the following stages:

- Pulping
- Stock preparation
- Paper machine

In the pulping stage the wood is chopped into small pieces and fed into the digester. After the digester, washing, bleaching, and chemical recovery take place. The result of the pulping stage is a mixture of wood fibers and water with a consistency (fiber concentration) of 3% to 6%, called the stock. The stock may be unbleached, bleached or semi-bleached, it is frequently mixed with repulped broke.

The stock preparation stage is a complex system of tanks and pipes. It contains the pulp storage chest, the machine chest, the refiners, screens and centrifugal cleaners. In the refiners the pulp is subject to mechanical treatment which changes the length and the structure of the fibers and influences the strength properties of the paper.

After the refining process chemicals like rosin, alum and sulphuric acid are added and the stock is further diluted so that the consistency in the headbox is 0.2 to 1.0%. If the consistency is higher, the fibers will cluster. Filler may also be added to the stock.

The paper machine consists of a wire supported by table rolls with suction boxes, couch and wire pit, presses, dryers, calender, and pope. A paper mill usually has several paper machines. The purpose of the paper

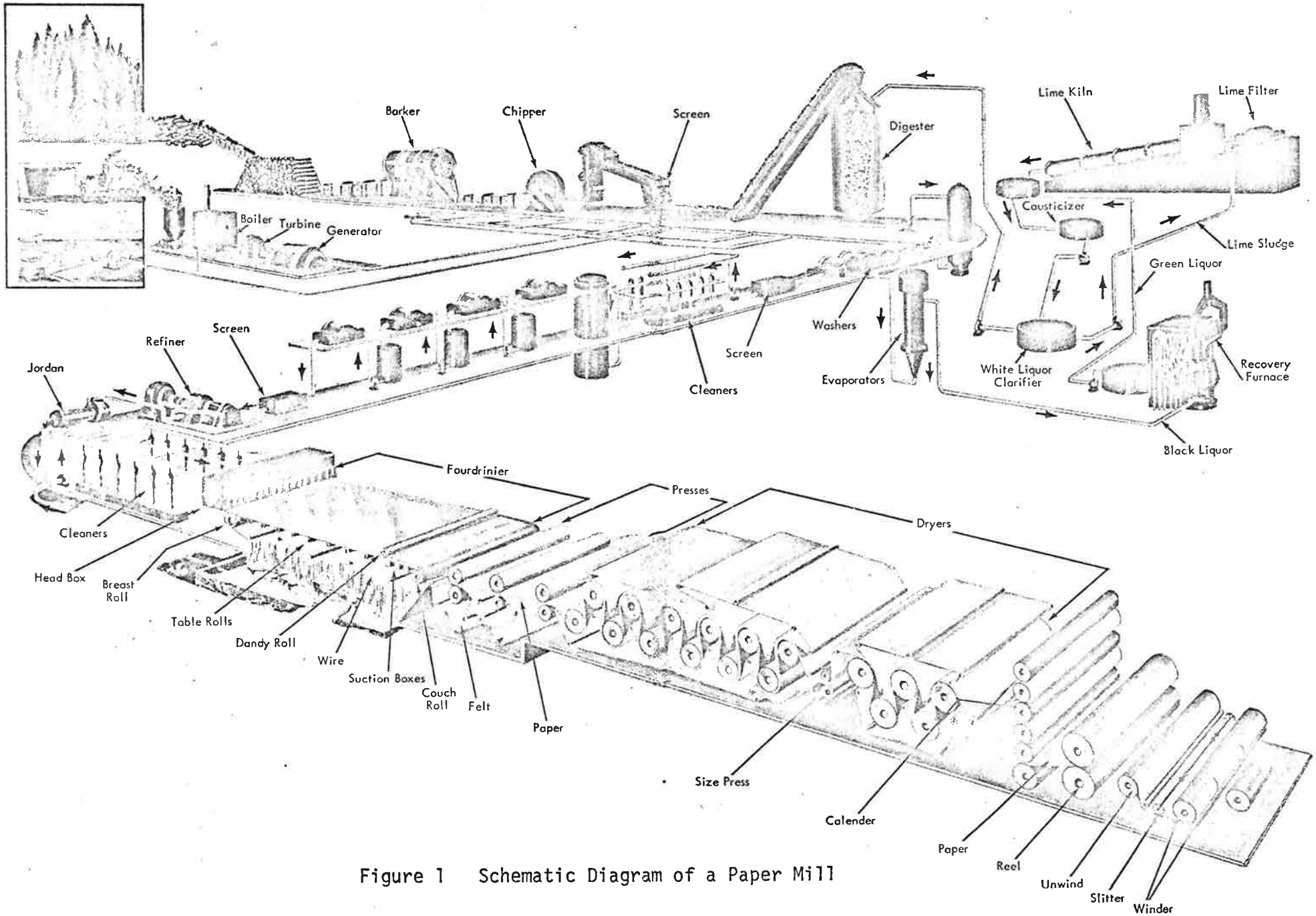

Figure 1 Schematic Diagram of a Paper Mill

machine is to separate the fibers from the water and to form a sheet of paper from the fibers. The pulp flows out of the headbox through a thin slice on to the wire in a jet. The velocity of the jet is determined by the headbox level and is normally chosen so as to match the wire speed. The paper sheet is formed on the wire. The amount of water removed on the wire is determined by the properties of the pulp (fiber length, distribution and fiber structure, temperature), the number of table rolls, and their dimensions, the pressures on the suction boxes under the wire, etc. The water passing through the wire is called white water. When the paper leaves the wire the consistency is about 20 to 25%. Water removal in the presses depends on the forces that keep the press rolls together, felt conditions, and temperature of the paper sheet. The consistency after the presses is 40 to 60%.

The dryers consist of a sequence of steamheated cylinders, and the water removal is given by the steam pressure, which is set separately for different groups of drying cylinders, and the ventilation of the dryer section. Fiber content after the drying section is about 5 to 10%. After passing through the dryers, the paper is smoothed in the calender and rolled up in a reel on the pope.

The reel is lifted to a winder which winds and slits the paper lengthwise and cuts it crosswise into rolls of proper lengths and widths. The rolls are sorted on the basis of samples taken from them. Rolls which meet the customers specifications are shipped and those which do not are rejected. The rolls may also be cut to sheets before delivery.

There are many different types of paper machines which essentially differ in the type of paper they produce, e.g., kraft paper for sacks and

paper bags, newsprint, high quality printing paper, etc. The different machines have the same basic configuration; the details may, however, be very different. There are, e.g., paper machines with multiple headboxes for multilayer paper.

A certain paper process is usually designed for manufacture of many different paper grades. The orders may differ with respect to dimension, basis weight, strength properties, color, chemical additives, etc. The length of an order may run from hours to days. Profitable operation poses interesting scheduling and control problems aimed at minimizing the cost of making transitions from one grade to another. A change from unbleached to bleached pulp requires cleaning of the whole stock preparation system. However, a change in basis weight can be obtained through flow or machine-speed change only. The quality of the produced paper is determined by basis weight, moisture content, and strength properties, as well as special properties like printability, opacity, and thickness. The first-mentioned properties are reasonably well defined. There are a large number of strength properties of interest. Properties like printability, etc., are only defined as the results of particular off-line measurements and cannot be measured on-line.

The Art of Papermaking

Papermaking has by tradition been more of an art than a science. The tools of applied physics, chemistry, and mechanics have only recently been applied to the papermaking process. Many fundamental physical problems are not yet well understood. For example, the strength properties of a paper sheet must certainly be related to the strength properties of the individual fibres. The nature of this relation is not known. The lack of knowledge of the basic processes involved has important implications on the solution of control problems. One consequence is that it is

extremely difficult to obtain reliable mathematical models from prior knowledge. Another is that very few gauges for on-line measurement of physical variables are available. Many important properties of pulp and paper are defined only through specific off-line measuring procedures and not related to physical properties. The on-line instruments that are available do not have very high accuracy unless elaborate calibration procedures are used. Typical accuracies are consistency ±.5 units of a maximum reading of 3 units, moisture content ±0.3 units of a reading of 10 units. The measurement of basis weight, i.e., the weight of fibres per unit area of the finished paper is an exception. With accurate calibration basis weight can be measured with an accuracy which is better than 0.2%. One consequence of the lack of on-line instrumentation is the potential for inventions which might change our present outlook on the control problems considerably.

Paper Mills as Control Objects

In paper mills there are examples of a large variety of control problems. Paper mills are traditionally designed to be operated with little control equipment. Most of the important variables are controlled manually on the basis of information from laboratory measurements of samples from the process. The traditional way to eliminate disturbances has been to use large mixing tanks which makes the process dynamics very slow. Analysis of many existing plants has also shown that the mixing tanks are often not as effective as was originally anticipated.

Section 3 - The Systems Approach

Introduction

In order to evaluate the possible gains that can be achieved by introducing specific control systems, it is necessary to know the effect on the overall plant economics. This usually involves some type of operations research analysis. Often such studies are performed continuously in connextion with modifications and expansions of a mill.

In connection with installations of process control computers, a separate feasibility study of the overall system is often performed. The purpose of such a study is to find economic benefits, bottlenecks, and possible improvements. A feasibility study is also very helpful when evaluating the performance of a control system after installation.

It is not easy to make a good feasibility study. It usually has to be done in a short time. The results will have a major influence since they tell if it is economically feasible to increase the degree of automation in a process, and if so, which applications should be given priority. It is often very difficult to obtain reliable estimates of different production losses. It is even more difficult to estimate what improvements could possibly be realized by introducing more sophisticated control schemes and more efficient production planning.

The feasibility study requires a large amount of engineering judgment which occasionally can be enhanced by the application of scientific methods. In the example given below, the only sophistication used was an application of time series analysis to analyze statistical properties of fluctuations in process variables.

An Example of a Feasibility Study

We will now give an example of a feasibility study. The example is taken from the Billerud project. In that case, the study took about five months with two persons working full time and various support facilities. The study included:

- Preparation of process flow diagrams
- Listing of costs for material and energy throughout the process
- Investigation of possible process variables during normal operation and during grade changes
- Study of disturbances and variations of important process variables
- Analysis of variations of quality variables in machine and cross-machine directions
- Investigation of production and quality control
- Investigation of possible improvements in uniformity of quality and increasing production rate
- Investigation of possibility of reducing time for grade changes
- Investigation of need for data acquisition and information flow
- Investigation of pulp variations and their effect on the paper quality

A complete study of the integrated pulp and paper mill was conducted in parallel with the feasibility study. In particular, the production planning problem was analyzed in some detail. One of the essential problems can be formulated as follows: Allocate the orders on the different paper machines in such a way that the sum of the costs for trim losses, grade change losses, and machine time is minimal, subject to restrictions of fixed delivery dates for the different orders, available pulp capacity,

and available storage capacity for the finished orders. There are a number of disturbances that influence planning, e.g., incoming orders which have to be run on short notice, changes in delivery dates, failure of finished rolls to meet specifications, equipment malfunction, etc.

The possible use of a control computer was evaluated on the basis of the results of the feasibility study and the overall mill study. It was found that a computer installation, including the costs of instrumentation, could be economically justified on the basis of improvements in:

- More uniform quality
- Reduced down time
- Reduced raw material consumption
- Higher production

More uniform quality is obtained through reduction of variations in basis weight, moisture content, and cross-machine stretch. Variations in basis weight are reduced by more efficient control of the stock feed, the wire, and the dryers. Variations in cross-machine stretch are reduced by better control of the drag and the velocity differences in the drying section. A higher production rate is achieved essentially through an increase in machine speed. Improvements in grade change time, reduction of trim losses, and less rejection due to better control of the machine parameters will also increase the net production.

The profit gains discussed above are obtained partly through the solution of isolated control problems and partly through improved production planning and improved quality control.

An Example of an Integrated System

The feasibility study also resulted in a gross picture of the overall system that should be implemented. A block diagram of this system is shown in Figure 1. The integrated system consists of six subsystems:

- Production Planning
- Production Supervising
- Production Evaluation and Reporting
- Process Control
- Process Data Collection
- Quality Control

These subsystems are illustrated by blocks in Figure 1. In this Figure we also show a schematic of the process, the manual operators, and the test laboratory. In the particular application production planning was done for all paper machines of the mill, while the other functions were done for one paper machine only.

The production planning subsystem has the following functions. The customers orders are entered into the system and grouped with respect to delivery dates and grade specifications. The orders are allocated to the different paper machines. The optimal sequencing with respect to minimal grade change costs is determined subject to constraints given by the delivery dates. It is also determined how to cut a reel into rolls of a given size with minimal losses.

The purpose of the production supervising is to supervise the production according to the schedule given by the production planning, and to administrate process and quality data. Since the process is not

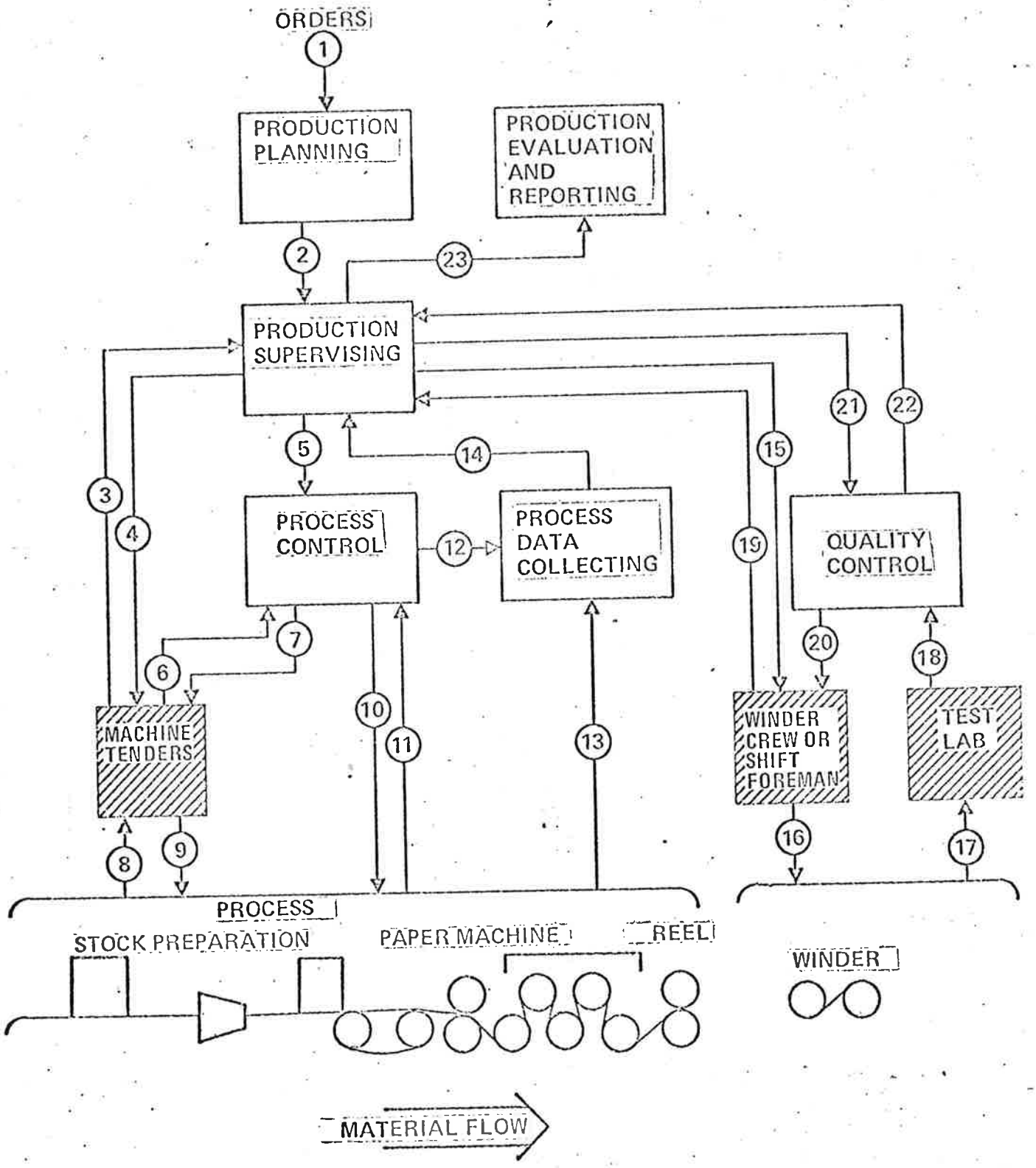

Figure 1 An Example of an Integrated System

perfect, the actual production does not necessarily follow the schedule given by the production planning. The production supervisory system thus acts like a regulator for the production. It also provides data for the human operators of the system and it interacts with the quality and process control functions.

The process control subsystem contains the proper control functions. It handles the actual control of the system according to the directions given by the production supervising. The control functions have been divided into three categories:

- Steady state control
- Grade change control
- Emergency control

Steady state control aims at keeping the process variables as close as possible to given reference values, in spite of disturbances.

Grade change control aims at changing the process from production of one grade of paper to another in the shortest possible time.

The purpose of the emergency control is to control the process during emergency conditions, for example, during a paper break.

The process data collection subsystem gathers data for various reports and for statistical purposes.

The quality control subsystem has two functions: a) to provide the machine tender with information about quality data which can not be measured on line, and b) to determine whether or not the produced paper meets the customer's specifications. Paper failing to meet specifications is rejected.

In this particular application the system is not fully automatic. It contains humans which have important system functions.

The machine tender supervises all manual process operations. He receives information about the process both from the control computer and from his own operations. He sends commands to the control computer.

The winder crew sets the winder slitters and rejects faulty rolls based on data from the quality control subsystem. They also inspect the rolls visually checking for wet spots, curled paper, etc.

The test laboratory analyses quality variables on samples taken from the finished paper. The data are fed to the quality control subsystem. The data are also used, e.g., in the control of the refiners.

Section 4 — Paper Machine and Stock Preparation Control

Introduction

In this section we will give an overview of the problems of controlling the paper machine with its associated stock preparation system. The discussion refers specifically to a kraft paper machine. Figure 1 shows a simplified diagram of the main parts of the process including pulp storage chest, refiners, machine chest centrifugal cleaners, screens, headbox, wire, press section, drying section, reel, and the travelling crane.

Objectives of The Control

The feasibility study indicated that major savings could be obtained from improved control during steady state and grade changes. Moreover, the control system must be able to handle emergency situations.

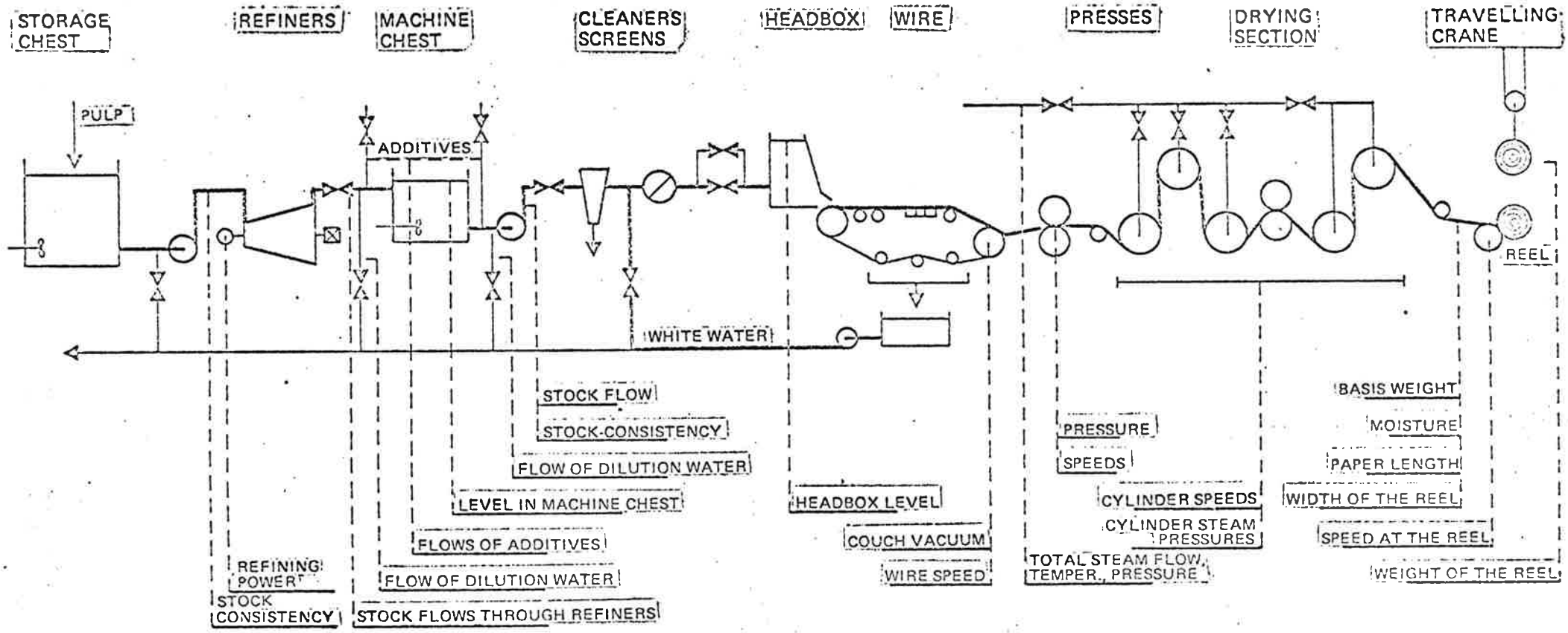

Figure 1
Simplified Diagram of Process With Measured Variables and Control Variables

The economic incentive for improved steady state control can be evaluated by an argument of the following type. The quality variables will fluctuate during normal operations due to disturbances. The customers are guaranteed specific upper or lower limits through general trade rules. When manufacturing a specific grade, the set points for the controls are then chosen with due regard to the fluctions so that a given percentage of the production will remain within the customer's specifications* (see Figure 2).

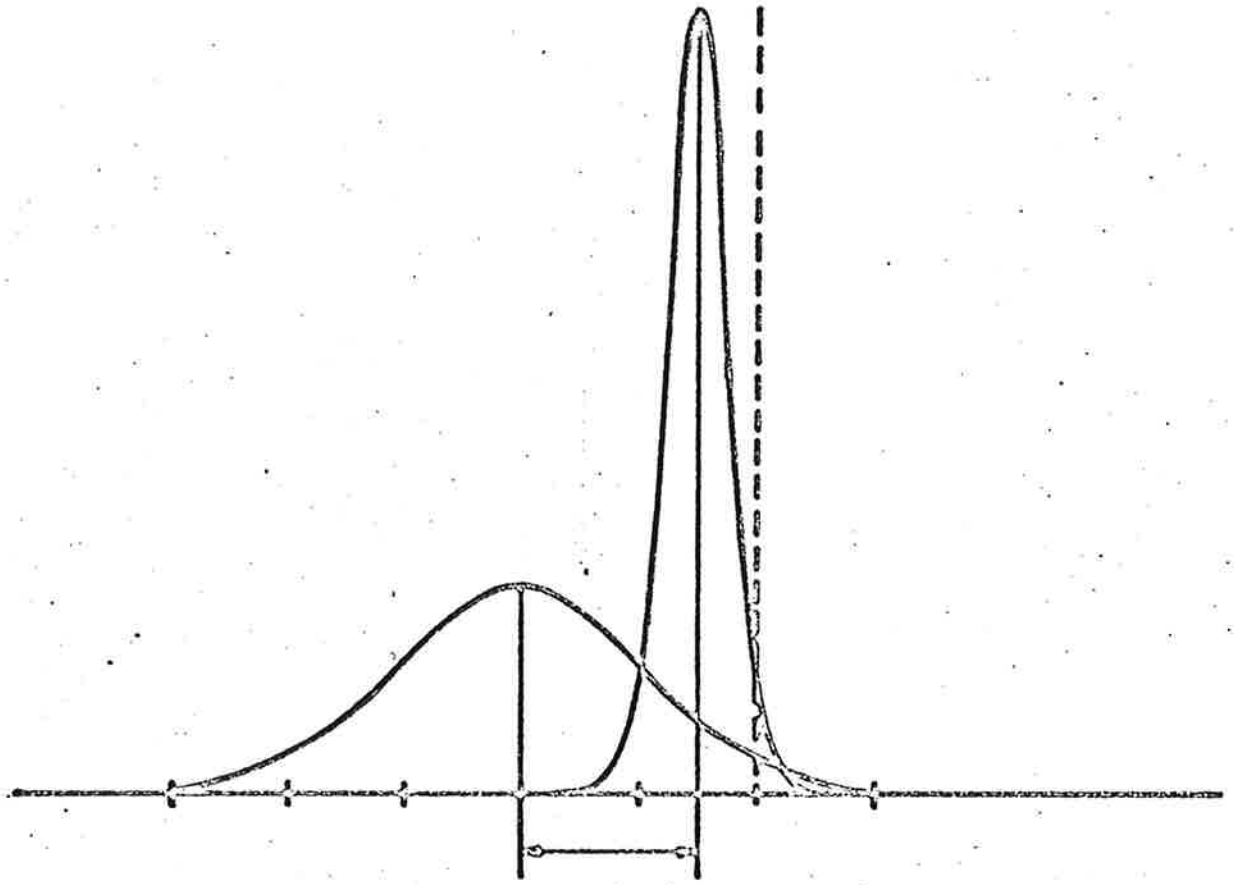

Figure 2 Illustration of the incentive for decreasing the variances of fluctuations in process variables.

*The particular choise of the set point is easily determined through a simple optimality argument.

An improved control will diminish the magnitude of the fluctuations, thus making it possible to move the set points closer to the tolerance limits with the same probability for the product to be accepted. By moving the set point closer to the tolerance limit, several benefits such as reduced raw material consumption or increased production can be obtained. Apart from these tangible benefits from a better control of quality variables during normal operation, there are often several intangible benefits. For example, it might be easier for the customer to process paper with a more uniform quality.

For kraft paper the important quality variables are:

- Basis weight
- Moisture content
- Strength properties

Reduced fluctuations in basis weight makes it possible to use less raw material and less steam in the drying section, and to increase production in those cases where the production is limited by the capacity of the dryers. (It requires less steam to dry a paper which is thinner!)

It is often desirable to have high moisture content in the paper. Too high moisture content will, however, give rise to wet spots. An improved control of moisture content will thus make it possible to increase the average moisture content. Since paper is often sold by weight this will influence the profit directly.

Better control of strength properties will reduce the risk of paper being sorted out in the quality control. An increase of the strength properties will also be of immediate benefit to the customer since he can either make a stronger product or use thinner (cheaper) paper with the same strength.

The nature of the benefits obtained from better control of steady state operation, is different for different types of paper machines. For printing paper the strength properties may be of secondary importance, while other quality variables such as opacity and printability are much more important. For most types of paper machines there is, however, a considerable economic incentive for improved basis weight and moisture control.

The economic incentive for improved control of grade changes comes from a direct reduction of the time required for shifting from one grade to another. The problem can thus be formulated simply as to minimize the time for changing from one grade to another subject to constraints. One of the most important constraints is that the paper does not break during the change, since this will give rise to considerable loss in production time.

The relative importance of steady state control and grade change control will be different for different applications and different operating conditions. For the specific kraft paper machine discussed in this chapter, the benefits from steady state control are greater than those obtainable from the grade change control.

Apart from the control of the major variables discussed above there are also many simple control tasks which must be performed in order to keep the process running. Typical examples are level and flow control. Many of these secondary control problems are not critical and it is not possible to assign a monitary value to the performances. In the Billerud project there were about 40 secondary variables of this nature.

Measurements and Control Variables

The difficulty of obtaining reliable on-line measurements was mentioned previously in section 2. In Figure 1 the most important control variables

and measured signals are indicated. We will now discuss the different control problems.

Basis Weight

Basis weight can be influenced both by machine speed and by fiber flow. There are however several constraints on the choice of these control variables. When production is machine-speed limited the fiber flow is the natural control variable, while the machine speed is the logical choice when production is limited by the capacity of the dryers. For the small changes required during normal operation, one usually keeps the machine speed constant and manipulates the fiber flow either by changing the consistency or by changing the thick stock flow. In the following we will assume that the thick stock flow is constant and that the consistency is chosen as control variable.

The on-line determination of consistency is traditionally made by measuring apparent viscosity or shearing force of the thick stock flow. In our particular case the shearing force on a pin submerged in the pulp flow is measured. The output of such a gauge will depend not only on concentration but also on flow, rheological properties of the pulp, temperature, viscosity of additives, etc. It is very difficult to calibrate the consistency meter, taking all these factors into account. It is in particular very difficult to take the rheological properties of the pulp into account, since they will depend on the degree of refining and on the properties of the additives. It should also be mentioned that it is not possible to measure consistencies lower than 1 to 2% by this technique, while the headbox consistency is 0.2 to 1.0%. This explains the arrangement shown in Figure 1, with the dilution after the consistency regulator.

New methods for measuring very low consistencies, e.g. by using transmission photometry have recently been proposed.

The basis weight at the end of the dryers is determined by a Beta Gauge. Since the coefficient of absorption of beta rays in water and fibers is approximately the same, the Beta Gauge reading has to be compensated for the moisture content of the paper sheet in order to give oven-dry basis weight. The errors of the Beta Gauge basis weight meter are due to electronic drift, changes in temperature and moisture of the air, dust contamination, static electricity when paper is overdry, etc. Due to cross-machine fluctuations a Beta Gauge set at a fixed position might also give a biased estimate of the cross-machine average of basis weight.

The calibration of the Beta Gauge is not trivial. Gauges which traverse across the paper can be calibrated by moving the gauge outside the paper web to a foil of known thickness. Another way to calibrate the gauge is to determine the weight and the dimensions of each produced reel. This can be done quite accurately.

When accurate measurement of basis weight and a mathematical model is available it is also possible to calibrate the consistency gauges.

The lack of primary sensors, can thus to some extent, be compensated by a scheme of indirect measurements where the information from different primary sensors are combined through the use of mathematical models.

Moisture Content

The moisture content is influenced mainly by changing the steam pressure in the drying cylinders. The cylinders are usually divided into groups which can be controlled individually. Moisture is also influenced by the fiber flow through the paper machine. An increase of stock flow

will thus increase the moisture content. To obtain an efficient scheme for moisture control, it is thus necessary to provide the moisture control system with information concerning the changes in stock flow, which for example, may be introduced by the basis weight control system.

The moisture content at the dry end can be measured by a moisture gauge of capacity type. There are also techniques for measuring the moisture content which are based on infrared or microwave technology. It is also possible to measure the basis weight in front of the drying section using a Beta Gauge. Measurement of moisture content in the front end of the drying section can only be done by a Microwave Gauge.

Other Quality Variables

Quality variables like strength properties and porosity are influenced by many factors, by the refining, the speed difference between the wire and the jet coming out of the slice, and by the heat profile in the drying section. The underlying physical phenomena are not well understood.

Most strength properties cannot be measured on-line. They are instead measured in the test laboratory based on samples taken at the reel and at the winding machine. A detailed discussion of the measurement of quality variables is given in Section 8 which deals with quality control.

Occasionally it is possible to measure some variable on-line which is related to quality variables which are otherwise available only as off-line measurements.

In such a case it is possible to devise indirect schemes where the high-frequency part is supplied by the on-line gauge. It is then updated from the laboratory data analogous to the updating of the Beta Gauge based on measurements of reel weight and dimensions.

In connection with the Billerud project, such a scheme was tested experimentally for refiner control based on on-line measurements of couch vacuum and laboratory measurements of porosity.

At the time the Billerud system was implemented it was decided that control of basis weight and moisture control should be done automatically, while control of the other quality variables should be done manually.

Mathematical Models

To complete the characterization of the control problem it is also necessary to have mathematical models which describe the process dynamics and the disturbances.

The parts of the process which are involved in the basis weight control are pipes, tanks, pumps, screens and cleaners and the wire. The model required for the basis weight control is in essence a mass balance for the fibers. It is fairly straightforward to model the pipes and the tanks. To a large extent it can be done from construction data. The only difficulty is to estimate the time constants of some of the storage tanks which usually are not perfectly stirred. It is, however, very difficult to obtain a mathematical model for the transport of fibers through the wire since the physical processes governing this mass transport are very complicated. In simple models it is usually assumed that the fiber flow through the wire is proportional to the total fiber flow out of the headbox. A slightly more refined model is obtained by having the coefficient

of proportionality depend on the average basis weight on the wire. This might seem to be a minor point, but the effect has a decided influence on the dynamic properties of the system. Let α be the proportion of the fibers that passes through the wire. The simple models will give as a result that the apparent time constant of the white water tank is multiplied by the factor $1/(1-\alpha)$. The constant α will depend on the properties of the fibers: small fibers will have large α-values, and vice versa. The total effect is that there might be long transients for the fiber distribution.

The average value of α in the simplified model is very difficult to estimate. Crude calculations indicate a value of about 0.1 in our particular case. For paper machines using mechanical pulp and large amounts of fillers, the average α for all the fibers may be as high as 0.8.

Similarly the screens and cleaners may sometimes be difficult to model.

The disturbances occuring during normal operation are frequently so small that the models required for steady state control can be linear. It is sometimes necessary to have different models for different operating conditions.

In connection with the Billerud project, several attempts were made to model the basis weight dynamics from construction data. The models obtained were of high order and it was also necessary to adjust several parameters in order to fit the models to observed data. Due to these difficulties it was instead attempted to determine linearized model directly from exerpeimental data using suitable identification techniques.

This approach was found to be very expedient. It can be done quickly and experience has shown that it leads to models of low order.

Modeling of the dynamics relating steam pressure to the moisture of the paper is even more difficult than to model the basis weight dynamics.

The disturbances entering in the different control loops were analyzed in great detail in various phases of the Billerud project. The analysis was done by setting control variables to constant values and observing the fluctuations in the output. It was frequently found that the fluctuations in the process variables could be described as stationary stochastic processes or sometimes integrals of such processes (drift). The amplitude distributions were often found to be close to Gaussian. Notable exceptions were also noticed. It was occasionally found that larger steplike or ramp-like "upsets" were superimposed on the stationary processes. These "upsets" could often be traced back to changes between different tanks, increased mixing of broke, etc. .

Section 5 - Control of Steady State Operation

Introduction

In this section we will describe an approach to the steady state control of industrial processes which has been successfully applied in practice. In the Billerud project the approach was used for control of basis weight and moisture content. It was also used in experimental schemes for refiner control.

The characteristic features of the steady state control problems discussed in the previous section are the following:

- The process dynamics can be characterized by linear differential equations with time delay.
- Disturbances can be described as sample functions of second order random processes.
- The criterion is to minimize the variances of fluctuations in the quality variables.

These characteristics match the assumption made in the linear stochastic control theory and it thus seems natural to apply this theory to derive control strategies.

Review of Linear Stochastic Control Theory

We will now give a brief review of some relevant aspects of linear stochastic control theory. For more details we refer, e.g. to Åström (1970).

Since a digital computer will be used to implement the control law we will consider discrete time systems only.

Consider a dynamical system described by

$$x(t+1) = \Phi\, x(t) + \Gamma\, u(t) + v(t) \tag{1}$$

$$y(t) = \theta\, x(t) + e(t) \tag{2}$$

where the state x is an n-vector, the control variable u a p-vector and the output y and r-vector. $\{v(t)\}$ and $\{e(t)\}$ are sequences of independent Gaussian random vectors with zero mean values and covariances R_1 and R_2 respectively.

The initial state of (1) is Gaussian with mean value m_0 and covariance R_0. The initial state is assumed to be independent of $\{e(t)\}$ and $\{v(t)\}$. Introduce the criterion

$$3 \qquad E \sum_{t=t_0}^{t_1} \left[x^T(t)\, Q_1\, x(t) + u^T(t)\, Q_2\, u(t) \right]$$

and let the admissible control strategies be such that $u(t)$ is a function of the outputs observed up to time $t-1$, i.e. $y(t-1)$, $y(t-2)$,... and m_0. Under suitable regularity conditions (which essentially assures that the equations (8) and (9) below have solutions), we find that the optimal control strategy is given by

$$4 \qquad u(t) = -\, L(t)\, \hat{x}(t|t-1)$$

where

$$5 \qquad \hat{x}(t+1|t) = \Phi\, \hat{x}(t|t-1) + \Gamma\, u(t) + K(t) \left[y(t) - \theta\, \hat{x}(t|t-1) \right]$$

and

$$6 \qquad L(t) = \left[Q_2 + \Gamma^T S(t+1)\, \Gamma \right]^{-1} \Gamma^T S(t+1)\, \Phi$$

$$7 \qquad K(t) = \Phi\, P(t)\, \theta^T \left[R_2 + \theta\, P(t)\, \theta^T \right]^{-1}$$

$$8 \qquad S(t) = \Phi^T S(t+1)\, \Phi + Q_1 - \Phi^T S(t+1)\, \Gamma\, L(t), \quad S(t_1) = Q_1$$

$$9 \qquad P(t+1) = \Phi\, P(t)\, \Phi^T + R_1 - K(t)\, \theta\, P(t)\, \Phi^T, \quad P(t_0) = R_0$$

Notice that linear stochastic control theory covers a more general situation since it allows for the parameters describing the system and the disturbances to be time varying.

Also notice that it is possible to have a model with time delay simply by substituting $u(t)$ in (5) by $u(t-k)$. The optimal control low then changes to

10 $$u(t) = - L(t)\, \hat{x}(t|t-k-1)$$

For details as well as proofs we refer to Åström (1970).

Model Structures

Since the models of the system and its environment are seldom known a priori it is frequently necessary to determine them from experiments on the process. In such cases, the choice of model structure becomes very important. If the matrices Φ, Γ, Θ, R_1 and R_2 are constant the model contains

11 $$N = n^2 + np + nr + \frac{1}{2}n(n+1) + \frac{1}{2}r(r+1)$$

parameters. It is not possible to determine all these parameters from measurements of inputs and outputs of the system, since there is an equivalence class of systems described by (1) and (2) which have the same input output properties.

To be specific, we say that two systems are equivalent if:

12 Their input output relation for zero disturbances, i.e. ($e=0$ and $v=0$), are the same

and

13 The stochastic properties of the output for zero input are the same.

For the purpose of identification, it is highly desirable to represent a class of equivalent system by a representative having a structure such that its parameters can be uniquely determined from input output data. We will call such a structure a canonical structure. In the general case canonical structures are not known nor is it clear that they exist. For special cases, e.g. systems with only one output, it is however possible to find such structures and we will now discuss their properties.

Two equivalent systems differ in their choice of state variables.

It follows from the Kalman filtering theorem that the system described by (1) and (2) is equivalent to the system

14 $$\hat{x}(t+1|t) = \Phi\, \hat{x}(t|t-1) + \Gamma\, u(t) + K\, \varepsilon\,(t)$$

15 $$y(t) = \theta\, \hat{x}(t|t-1) + \varepsilon(t)$$

where K is given by (7) and $\{\varepsilon(t)\}$ is a sequence of independent Gaussian vectors with zero mean value and the covariance $\theta P(t)\, \theta^T + R_2$ where P is given by (9).

The state variable $x(t)$ of the representation (14) has physical interpretation as the conditional mean of the state $x(t)$ of given $\{y(s),\ t_0 \le s \le t-1\}$. The Kalman filtering problem is thus trivial for the structure described by (14) and (15). The Kalman filter is obtained simply by eliminating $\varepsilon(t)$

from (15) and substituting into (14) to yield

16 $$\hat{x}(t+1|t) = \Phi\,\hat{x}(t|t-1) + \Gamma\,u(t) + K\,[y(t) - \theta\,\hat{x}(t|t-1)]$$

The quantity $\varepsilon(t)$ of (14) and (15) thus has physical interpretation as the error in predicting the output one step ahead. The representation (14) (15) is sometimes called an innovations representation and the random variables $\varepsilon(t)$ are then the so-called innovations.

If we want to model a system for the purpose of designing Kalman filters (as we do in the applications to linear stochastic control theory) the structure (14) (15) has several advantages compared to the structure (1) (2). It contains fewer parameters and the determination of the Kalman filter requires no extra computations. It also turns out that the structure (14) (15) is easier to identify.

17 Exercise

Prove that the systems described by (1) (2) and (14) (15) are equivalent with respect to the relations (12) and (13).

18 Exercise

Show that two systems with the structure (14) (15) are equivalent if

19 $$\theta\,\Phi^k\,\Gamma = \tilde{\theta}\,\tilde{\Phi}^k\,\tilde{\Gamma}, \quad k = 0, 1, \ldots, n$$

where θ, Φ, Γ are the matrices of one system and $\tilde{\theta}$, $\tilde{\Phi}$, $\tilde{\Gamma}$ those of the other system.

Single Output Systems

In special cases it is possible to obtain a canonical structure. For example, if the system is completely observable and has only one output it can always be transformed to the observable canonical form

$$20 \quad x(t+1) = \begin{bmatrix} -a_1 & 1\ 0 \ldots 0 \\ -a_2 & 0\ 1 \ldots 0 \\ \vdots & \\ -a_{n-1} & 0\ 0 \ldots 1 \\ -a_n & 0\ 0 \ldots 0 \end{bmatrix} x(t) + \begin{bmatrix} b_{11} & b_{12} \cdots b_{1p} \\ b_{21} & b_{22} \cdots b_{2p} \\ \vdots & \\ b_{n1} & b_{n2} \cdots b_{np} \end{bmatrix} u(t) + \begin{bmatrix} k_1 \\ k_2 \\ \vdots \\ k_n \end{bmatrix} \varepsilon(t)$$

$$21 \quad y(t) = [1\ 0\ 0 \ldots 0]\, x(t) + \varepsilon(t)$$

The input output relation of this system can be represented as

$$22 \quad \begin{aligned} &y(t) + a_1 y(t-1) + \ldots + a_n y(t-n) = b_{11} u_1(t-1) + \ldots + b_{n1} u_1(t-n) \\ &+ \ldots + b_{1p} u_p(t-1) + \ldots + b_{np} u_p(t-n) + \varepsilon(t) + c_1 \varepsilon(t-1) + \ldots + c_n \varepsilon(t-n) \end{aligned}$$

where

$$23 \quad c_i = a_i + k_i, \quad i = 1, 2, \ldots, n$$

For simplicity we will in the following assume that the system only has one input. This makes it possible to simplify the writing but it does not change anything essential.

By introducing the shift operator q defined by

24 $$q\, y(t) = y(t+1)$$

the polynomials

25 $$A(z) = z^n + a_1 z^{n-1} + \ldots + a_n$$

26 $$B(z) = b_1 z^{n-1} + \ldots + b_n$$

27 $$C(z) = z^n + c_1 z^{n-1} + \ldots + c_n$$

and the corresponding reciprocial polynomials

28 $$A^*(z) = z^n \quad A(z^{-1}) = 1 + a_1 z + \ldots + a_n z^n$$

29 $$B^*(z) = z^{n-1} B(z^{-1}) = b_1 + b_1 z + \ldots + b_n z^n$$

30 $$C^*(z) = z^n \quad C(z^{-1}) = 1 + c_1 z + \ldots + c_n z^n$$

the equation 22 can be written in the compact form

31 $$A^*(q^{-1})\, y(t) = B^*(q^{-1})\, u(t-1) + C^*(q^{-1})\, \varepsilon(t)$$

32 $$A(q)\, y(t) = B(q)\, u(t) + C(q)\, \varepsilon(t)$$

If the system also has a time delay which is an integer multiple of the sampling interval we get instead

33 $$A^*(q^{-1})\, y(t) = B^*(q^{-1})\, u(t-k) + C^*(q^{-1})\, \varepsilon(t)$$

The canonical form (33) can also be derived by a different argument. A sampled time invariant linear system with one input and one output and a time delay which is an integer multiple of the sampling interval can be described by the equation

$$34 \qquad y(t) = \frac{B_1^*(q^{-1})}{A_1^*(q^{-1})} u(t-k)$$

where A_1^* and B_1^* are polynomials.

Assuming that the influence of the environment on the system can be characterized by disturbances which are stochastic processes and using the principle of superposition we get the following model of the process and its environment

$$35 \qquad y(t) = \frac{B_1^*(q^{-1})}{A_1^*(q^{-1})} u(t-k) + v(t)$$

If it is furthermore assumed that the disturbance $v(t)$ is a stationary gaussian process with rational spectral density it can be represented as

$$36 \qquad v(t) = \frac{C_1^*(q^{-1})}{A_2^*(q^{-1})} \varepsilon(t)$$

where $\{\varepsilon(t),\ t=0,\ \pm1,\ \pm2,\ldots\}$ is a sequence of equally distributed independent normal $(0,\lambda)$ random variables and C_1^* and A_2^* are polynomials.

We thus find that the system and its environment can be represented by the equation

$$37 \qquad y(t) = \frac{B_1^*(q^{-1})}{A_1^*(q^{-1})} u(t-k) + \lambda \frac{C_1^*(q^{-1})}{A_2^*(q^{-1})} e(t)$$

The equation (37) is thus a canonical form for a sampled time invariant dynamical system with one input and one output with a time delay that is an integer multiple of the sampling interval subject to disturbances which are stationary with rational spectral densities. The polynomials $A_2(z)$ and $C_1(z)$ can always be chosen to have their zeros inside or on the unit circle. Since the disturbance v was assumed to be stationary A_2 cannot have any zeros on the unit circle.†

Introducing $A = A_1A_2$, $B = B_1A_2$ and $C = C_1A_1$ we have now obtained the model (33).

Minimum Variance Control Strategies

The problem of steady state control can be solved by a straightforward application of linear quadratic control theory. The problem of steady state control has, however, some particular features which can be exploited to simplify the theory.

We will thus consider the problem of regulating the system (33) in such a way that the variance of the output is as small as possible. The admissible control strategy should be such that the control signal at

---

†It is possible to include nonstationary disturbances, e.g. by assuming an A which has zeros outside the unit circle.

time t, i.e. u(t) is a function of the outputs observed up to time t, i.e. y(t), y(t-1),... and all the previous inputs u(t-1), u(t-2)...

To solve the problem we consider the situation at time t. We have thus obtained the measurements y(t), y(t-1),... and we know all past control actions u(t-1), u(t-2),... . The problem is to determine u(t) in such a way that the variance of the output is as small as possible. It follows from the equation (33) that the control signal u(t) will influence y(t+k) but not any earlier outputs. Consider

$$38 \qquad y(t+k) = \frac{B^*(q^{-1})}{A^*(q^{-1})} u(t) + \lambda \frac{C^*(q^{-1})}{A^*(q^{-1})} e(t+k)$$

The last term is a linear function of e(t+k), e(t+k-1),..., e(t+1), e(t), e(t-1),... . It follows from (33) that e(t), e(t-1),... can be computed from the information available at time t. To do this explicitely we rewrite (38) using the identity

$$39 \qquad C^*(q^{-1}) = A^*(q^{-1})\, F^*(q^{-1}) + q^{-k}\, G^*(q^{-1})$$

where F and G are polynomials of degrees k-1 and n-1. Hence,

$$40 \qquad y(t+k) = \lambda\, F^*(q^{-1})\, e(t+k) + \frac{B^*(q^{-1})}{A^*(q^{-1})} u(t) + \lambda \frac{G^*(q^{-1})}{A^*(q^{-1})} e(t)$$

Eliminating the e's in the last term using the equation (38) we get

$$y(t+k) = \lambda F^*(q^{-1})\, e(t+k) + \left[\frac{B^*(q^{-1})}{A^*(q^{-1})} - q^{-k}\,\frac{B^*(q^{-1})\,G^*(q^{-1})}{A^*(q^{-1})\,C^*(q^{-1})}\right] u(t)$$

41

$$+ \frac{G^*(q^{-1})}{C^*(q^{-1})}\, y(t)$$

or after reduction of the terms in the square bracket using the identity (39)

42 $$y(t+k) = \lambda F^*(q^{-1})\, e(t+k) + \frac{G^*(q^{-1})}{C^*(q^{-1})}\, y(t) + \frac{B^*(q^{-1})\,F^*(q^{-1})}{C^*(q^{-1})}\, u(t)$$

Now let u(t) be an arbitrary function of y(t), y(t-1),... and u(t-1), u(t-2),... . Then

$$Ey^2(t+k) = E[\lambda F^*(q^{-1})\, e(t+k)]^2$$

43

$$+ E\left[\frac{G^*(q^{-1})}{C^*(q^{-1})}\, y(t) + \frac{B^*(q^{-1})\,F^*(q^{-1})}{C^*(q^{-1})}\, u(t)\right]^2$$

The mixed terms will vanish because e(t+1), e(t+2),...,e(t+k) are independent of y(t), y(t-1),... and u(t-1), u(t-2),... , and all e:s have zero mean. Hence

44 $$Ey^2(t+k) \geq \lambda^2 \left[1 + f_1^2 + f_2^2 + \ldots + f_{k-1}^2\right]$$

where equality holds for

45 $$B^*(q^{-1})\, F^*(q^{-1})\, u(t) + G^*(q^{-1})\, y(t) = 0$$

which gives the desired control law.

Summing up we get:

46 Theorem

Consider the process described by (33), i.e.

$$A^*(q^{-1})\, y(t) = B^*(q^{-1})\, u(t-k) + C^*(q^{-1})\, e(t)$$

where $\{e(t),\ t \in T\}$ is a sequence of independent normal (0,1) random variables. Let the polynomial $C(z)$ have all its zeros inside the unit circle. The minimum variance control law is then given by

47 $$B^*(q^{-1})\, F^*(q^{-1})\, u(t) = -\, G^*(q^{-1})\, y(t)$$

where the polynomials F and G of order $k-1$ and $n-1$ respectively are defined by the identity (39), i.e.

$$C^*(q^{-1}) = A^*(q^{-1})\, F^*(q^{-1}) + q^{-k}\, G^*(q^{-1})$$

The regulation error of the optimal system is a moving average of order k

48 $$y(t) = \lambda F^*(q^{-1})\, e(t) = \lambda[e(t) + f_1 e(t-1) + \ldots + f_{k-1}\, e(t-k+1)]$$

49 Remark 1

Notice that the result still holds if it is only assumed that $e(t)$ and $e(s)$ are uncorrelated for $t \neq s$ but a linear control law is postulated.

50 Remark 2

Notice that the control error is a moving average of order k when the minimum variance strategy is used. The covariance function of the control error will thus vanish for arguments greater than k. This observation is very convenient to use if we want to test a system in operation to find out if the control strategy in use is optimal.

51 Remark 3

Notice that poles of the closed loop system equals the zeros of the polynomial $C(z)$.

52 Example

The following model which relates changes in the dry basis weight to changes in the stock flow has been found

53 $$y(t) = \frac{26.5q^{-5}}{1-1.352q^{-1}+0.352q^{-2}}\, \nabla u(t) + 0.419\, \frac{1-0.444q^{-1}}{1-1.352q^{-1}+0.352q^{-2}}\, e(t)$$

To find the feedback from y to ∇u which minimizes the variance of the fluctuations in dry basis weight we proceed as follows.

We have

54 $$A^*(z) = 1 - 1.352z + 0.352z^2$$

55 $$B^*(z) = 26.5$$

56 $$C^*(z) = 1 - 0.444z$$

The identity (39) gives

57 $$1-0.444z = (1-1.352z+0.352z^2)\,(1+e_1z+e_2z^2+e_3z^3) + z^4(f_0+f_1z)$$

Identification of the coefficients gives

$$-0.444 = -1.352 + e_1$$

$$0 = 0.352 - 1.352\,e_1 + e_2$$

$$0 = 0.352e_1 - 1.352e_2 + e_3$$

$$0 = 0.352e_2 - 1.352e_3 + f_0$$

$$0 = 0.352e_3 + f_1$$

Hence

$$e_1 = 0.908$$

$$e_2 = 0.876$$

$$e_3 = 0.865$$

$$f_0 = 0.861$$

$$f_1 = 0.304$$

We thus find

58 $$E^*(z) = 1 + 0.908z + 0.8762^2 + 0.865z^3$$

59 $$F^*(z) = 0.861 + 0.304z$$

The minimal variance control strategy thus becomes

60 $$\Delta u(t) = -\frac{1}{26.5} \cdot \frac{0.861 - 0.304q^{-1}}{1 + 0.908q^{-1} + 0.876q^{-2} + 0.865q^{-3}}\ y(t)$$

The control error is a moving average of fourth order

61 $$y(t) = \lambda[e(t) + 0.908\ e(t-1) + 0.876\ e(t-2) + 0.865\ e(t-3)]$$

which has the variance

62 $$Ey^2(t) = \lambda^2[1 + e_1^2 + e_2^2 + e_3^2] = 0.588$$

63 Exercise

Determine the minimum variance control law for the system

$$y(t) = \frac{24.9q^{-4}}{(1 - 0.55q^{-1}) + 0.20q^{-2})(1 - q^{-1})}\ u(t)$$

64

$$+ \quad \frac{1 - 0.77q^{-1} + 0.352a^{-2}}{(1 - 0.555q^{-1} + 0.20q^{-2})(1 - q^{-1})}\ e(t)$$

Sensitivity Of The Minimal Variance Strategies

It is well-known that optimal solutions under special circumstances may be very sensitive to parameter variations. We shall therefore investigate this matter in our particular case. To do so we shall assume that the system is governed by the equation (33) which we write as

65 $$A^0(q)\ y(t) = B^0(q)\ u(t-k) + \lambda^0 C^0(q)\ e(t)$$

but that the control law is calculated under the assumption that the system model is

66 $$A(q)\ y(t) = B(q)\ u(t-k) + \lambda\ C(q)\ e(t)$$

where the coefficients of the polynomials A, B, and C differ slightly from those of A^0, B^0, and C^0.

Notice that the orders n of the models (65) and (65) are the same. The minimal variance control strategy for the model (66) is

$$67 \qquad u(t) = -\frac{G^*(q^{-1})}{B^*(q^{-1})\,F^*(q^{-1})}\,y(t) = -\frac{q^k\,G(q)}{B(q)\,F(q)}\,y(t)$$

where F and G are polynomials of degree k-1 and n-1 defined by the identity (39).

We shall now investigate what happens if the system (65) is controlled with the control law (67). Introducing (67) into (65) we get

$$68 \qquad \left[A^0(q) + \frac{B^0(q)\,G(q)}{B(q)\,F(q)}\right]\,y(t) = \lambda^0 C^0(q)\,e(t)$$

Let q^{n+k-1} operate on the identity (39) and use the definition of reciprocal polynomial. We find

$$69 \qquad q^{k-1}\,C(q) = A(q)\,F(q) + G(q)$$

The equations (68) and (69) now give

$$70 \qquad \left[q^{k-1}B^0(q)C(q) + (A^0(q)B(q) - A(q)B^0(q))\,F(q)\right]\,y(t) = \lambda^0 B(q)C^0(q)F(q)e(t)$$

The characteristic equation of the system is thus

$$71 \qquad z^{k-1}B^0(z)C(z) + [A^0(z)B(z) - A(z)B^0(z)]\,F(z) = 0$$

If $A = A^0$, $B = B^0$ and $C = C^0$ the characteristic polynomial reduces to $z^{k-1}B^0(z)C^0(z)$. For small perturbations in the parameters the modes of the system (66) are thus close to the modes associated with $z^{k-1}B^0(z)C^0(z)$, i.e. k-1 modes with poles at the origin, n modes with poles at the zeros of B^0 and n modes with poles at the zeros of C^0. Furthermore when the design parameters equal the true parameters the factor B^0C^0 cancels in (70). This implies that the modes associated with B^0C^0 are uncoupled to the input e if $A = A^0$, $B = B^0$ and $C = C^0$ or that the corresponding state variables under the same conditions are not controllable from the input e. Now if the control law is calculated from a model which deviates from the true model, the input might excite all the modes associated with the solutions of the characteristic equation (71). This is not a serious matter if the modes are stable. However, if some modes are unstable, it is possible to get infinitely large errors if the model used for designing the control law deviates from the actual model by an arbitrarily small amount. This situation will occur if the polynomial B^0C^0 has zeros outside or on the unit circle. It follows from a representation theorems for stationary random processes that C^0 can always be chosen to have zeros inside or on the unit circle. As far as C^0 is concerned the only critical case would be if C^0 had a zero on the unit circle. The polynomial B^0 will have zeros outside the unit circle if the dynamics of the sampled system is nonminimum phase. Hence, if either the

dynamical system to be controlled is nonminimum phase or if the numerator of the spectral density of the disturbances has a zero on the unit circle, the minimum variance control law will be extremely sensitive to variations in the model parameters.

In these situations it is of great practical interest to derive control laws which are insensitive to parameter variations whose variances are close to the minimal variances. There are many ways to do this. One possibility is to proceed as follows.

To fix the ideas assume that the polynomial $B(z)$ can be factored as

$$B(z) = B_1(z)\, B_2(z) \tag{72}$$

where B_1 is of degree n_1 and has all zeros inside the unit circle and B_2 is of degree n_2 and has all zeros outside the unit circle.

When resolving the identity (39) we impose the additional requirement that $G(z)$ contain $B_2(z)$ as a factor, i.e. we use the identity

$$q^{n_2+k-1}\, C(q) = A(q)\, F'(q) + B_2(q)\, G'(q) \tag{73}$$

instead of

Going through the arguments used when deriving Theorem 46 we find the control law

$$u(t) = -\frac{q^k\, G'(q)}{B_1(q)\, F'(q)}\, y(t) \tag{74}$$

which gives the control error

$$y(t) = \lambda\{e(t) + f_1\, e(t-1) + \ldots + f_{k-1}\, e(t-k+1) + f'_k\, e(t-k) + \ldots + f'_{k+n_2-1}\, e(t-k-n_2+1)\} \tag{75}$$

The control low (74) which is not optimal gives an error with the variance

$$\text{Var } y = \text{Min (Var } y) + \lambda^2\{f'^2_k + \ldots + f'^2_{k+n_2-1}\} \tag{76}$$

Section 6 - Process Identification

Introduction

It was mentioned earlier in section 4 that mathematical models can seldom be obtained from a priori physical knowledge. This has also been verified in practice. In particular it has been found very difficult to model the disturbances from a priori knowledge. The mathematical models required to determine the control strategies for steady state operation have instead been determined directly from data obtained from process experiments. In the experiments the control variables were perturbed systematically. The inputs and the outputs were recorded and the data obtained was used to determine the mathematical models required for the design of the control strategies.

The Maximum Likelihood Method

Since the result of the identification will be used to obtain control strategies for the steady state control, it is natural to fit a model given by the equations (5.14), (5.15) to the data. This can be done by using the method of maximum likelihood.

We will thus consider the situation when a sequence of inputs and outputs $\{u(t),y(t),t = 1, 2, \ldots, N\}$ have been observed and it is desired to determine a model of the structure

$$\hat{x}(t + 1) = \Phi\hat{x}(t) + \Gamma u(t) + K\varepsilon(t) \tag{1}$$

$$y(t) = \theta\hat{x}(t) + \varepsilon(t). \tag{2}$$

To determine the likelihood function we will thus have to write down the probability density function for the outputs assuming that all parameters of (1) and (2) are known. Since the random vectors Y and E defined by

$$3 \qquad Y = \begin{bmatrix} y(1) \\ y(2) \\ \vdots \\ y(N) \end{bmatrix}, \qquad E = \begin{bmatrix} \varepsilon(1) \\ \varepsilon(2) \\ \vdots \\ \varepsilon(N) \end{bmatrix}$$

are related through an equation

$$4 \qquad Y = AE + b$$

where the matrix A has all diagonal elements equal to one and only zeros above the diagonal, the Jacobian of the transformation equals one and the probability distributions of Y and E are the same. The likelihood function thus becomes

$$5 \qquad -\log L = \frac{1}{2} \sum_{t=1}^{N} \varepsilon^T(t) R^{-1} \varepsilon(t) + \frac{N}{2} \log \det R + \frac{nN}{2} \log 2\pi.$$

The function L is considered as a function of the unknown parameters of the matrices Φ, Γ, θ, K and R and of the initial condition $\hat{x}(1)$ of the equation (1). To evaluate the function L for a particular value of the parameter the quantities $\varepsilon(t)$ are thus computed from

the equations

$$\hat{x}(t+1) = \Phi\hat{x}(t) + \Gamma u(t) + K[y(t) - \theta\hat{x}(t)] \tag{6}$$

$$\varepsilon(t) = y(t) - \theta\hat{x}(t) \tag{7}$$

which are immediate consequences of (1) and (2). Since the parameters are fixed, the coefficients as well as initial conditions of the equation are thus assured to be known. When the vectors $\varepsilon(t)$ are obtained the likelihood function is then given by (5).

Notice that the optimization of the likelihood function with respect to R and the other parameters can be performed separately. Minimizing the right-hand side of (5) with respect to R we find that

$$\min_R \left\{ \frac{1}{2} \sum_{t=1}^{N} \varepsilon^T(t) R^{-1} \varepsilon(t) + \frac{N}{2} \log \det R \right\} = \frac{N}{2} \det \frac{1}{N} \sum_{t=1}^{N} \varepsilon(t)\varepsilon^T(t). \tag{8}$$

The minimum is assumed for

$$R = \hat{R} = \frac{1}{N} \sum_{t=1}^{N} \varepsilon(t)\varepsilon^T(t). \tag{9}$$

To apply the maximum likelihood method it is thus possible to first find the unknown parameters α of Φ, Γ, θ, K and $\hat{x}(1)$ such that the loss function

$$V(\alpha) = \det \frac{1}{N} \sum_{t=1}^{N} \varepsilon(t)\varepsilon^T(t) \tag{10}$$

is minimized. The maximum likelihood estimate of R is then given by (9).

11 Exercise

Prove that (9) holds. [Hint. Notice that

$$\frac{d}{dA} \log \det A = A^{-1}$$

$$\frac{d}{dA} \sum_{t=1}^{N} e^T(t)Ae(t) = \sum_{t=1}^{N} e(t)e^T(t)$$

where $\frac{df}{dA}$ where f is a scalar means a matrix whose ij^{th} element is $\frac{df}{da_{ij}}$.]

There are several numerical techniques which can be used to perform the minimization. Method based on straightforward search and function evaluation as well as techniques based on evaluation of gradients and higher derivatives like Newton Raphson, Fletcher Powell, etc. can be used.

The evaluation of the gradient of the loss function can be done very effectively using the sensitivity derivatives.

Single Output Systems

In the particular case of single output systems the function minimization required to compute the maximum likelihood estimate can be done very efficiently. Using the system representation (5.33) the likelihood function can be written as

12 $$-\log L = \frac{1}{2\lambda^2} \sum_{t=1}^{N} \varepsilon^2(t) + N \log \lambda + \frac{N}{2} \log 2\pi$$

where

13 $$C^*(q^{-1})\varepsilon(t) = A^*(q^{-1})y(t) - B^*(q^{-1})u(t - k).$$

In analogy with the multivariable case the maximization of L with respect to λ and the other parameters θ can be done separately. It is thus possible first to minimize the loss function V defined by

14 $$V(\theta) = \sum_{t=1}^{N} \varepsilon^2(t)$$

where θ is a vector whose components are the unknown parameters $a_1, \ldots, a_n, b_1, \ldots, b_n, c_1, \ldots, c_n$ and the unknown initial conditions of (13). The estimate of λ is then given by

15 $$\hat{\lambda}^2 = \frac{V(\hat{\theta})}{N} .$$

The function V is linear in the parameters a_i and b_i but strongly nonlinear in the parameters c_i. To minimize V we can use the generalized Newton-Raphson algorithm, i.e.

16 $$\theta^{k+1} = \theta^k - [V_{\theta\theta}(\theta^k)]^{-1} V_\theta(\theta^k)$$

where, V_θ is the gradient of V and $V_{\theta\theta}$ the matrix of second partial derivatives.

The algorithm (16) can be interpreted geometrically as follows. At each step of the iteration the function V is approximated locally by a quadratic function which is obtained from a Taylor series approximation. The next iterate is then obtained as the extremum of the approximating quadratic function.

The algorithm will converge very fast (quadratically) if the initial value is chosen close to the true minimum. The algorithm might, however, diverge if the initial state is chosen at a point where $V(\theta)$ is concave.

The gradient and the matrix of second partial derivatives which are needed in the calculations are obtained as follows

$$17 \qquad \frac{\partial V}{\partial \theta_i} = 2\sum_{t=1}^{N} \varepsilon(t)\frac{\partial \varepsilon(t)}{\partial \theta_i}$$

$$18 \qquad \frac{\partial^2 V}{\partial \theta_i} = 2\sum_{t=1}^{N} \frac{\partial \varepsilon(t)}{\partial \theta_i} \cdot \frac{\partial \varepsilon(t)}{\partial \theta_i} + 2\sum_{t=1}^{N} \varepsilon(t) \frac{\partial^2 \varepsilon(t)}{\partial \theta_i \partial \theta_j} .$$

If the second term of (18) is dropped, we get an approximation to the matrix of second partial derivatives which has the advantage of always being positive semi-definite. Using this approximation we get a procedure such that the step taken always has a non-negative projection as the gradient thereby bypassing the difficulty with the pure Newton-Raphson algorithm.

The derivatives of ε with respect to θ are obtained simply by differentiating (13), i.e.,

$$19 \qquad C^*(q^{-1}) \frac{\partial \varepsilon(t)}{\partial a_i} = q^{-i} y(t)$$

$$20 \qquad C^*(q^{-1}) \frac{\partial \varepsilon(t)}{\partial b_i} = -q^{-i} u(t - k)$$

$$21 \qquad C^*(q^{-1}) \frac{\partial \varepsilon(t)}{\partial c_i} = -q^{-i} \varepsilon(t).$$

The derivatives can thus be obtained simply by solving difference equations. Notice that the difference equations can be interpreted as dynamic systems with inputs as $y(t)$, $u(t)$ and $\varepsilon(t)$. Also notice that we have relations of the type

$$22 \qquad \frac{\partial \varepsilon(t)}{\partial a_i} = \frac{\partial \varepsilon(t - i + 1)}{\partial a_1} .$$

This makes it possible to reduce the computations significantly.

Properties of the Maximum Likelihood Estimate

We will now briefly state some of the properties of the maximum likelihood estimate. To obtain these we assume that the process is actually characterized by a model of the structure (13) with parameters θ_0. Under reasonable conditions it can be shown that

- The estimate $\hat{\theta}$ converges to the true parameter θ_0 as the record length N increases.
- The estimate is asymptotically normal with mean θ_0 and covariance

$$\frac{2\lambda^2}{N} \left[\lim_{N \to \infty} \frac{1}{N} V_{\theta\theta} \right]^{-1} .$$

- The estimate satisfies the lower bound in the Cramer Rao inequality asymptotically.

For specific statements as well as proofs we refer to Åstrom et al. (1965).

Section 7 - Basis Weight Control

Introduction

In this section we will give a fairly detailed account of a case study devoted to the solution of one steady state control problem, i.e., basis weight control. In particular, we will touch upon some of the practical problems which have been encountered. The particular data are taken from the Billerud project. Fluctuations in basis weight were investigated in a feasibility study done before the computer was installed. Analyses revealed that variations in basis weight were approximately normal with a standard deviation greater than $1.3 g/m^2$. In the feasibility study it was estimated that this could be decreased to $0.7 g/m^2$. We have actually been able to reduce the standard deviation of basis weight fluctuations to $0.5 g/m^2$ wet basis weight and $0.3 g/m^2$ dry basis weight.

Figure 1 shows the basis weight fluctuations obtained during a pre-installation test, and the results obtained with on-line basis weight control.

In Figure 1 curve A represents a sample of basis weight variations obtained during a pre-installation evaluation of fluctuations in basis weight. Curves B and C represent variations during a run in which basis weight was controlled on-line. The upper curve B shows the fluctuations in basis weight; the lower curve C shows the control variable. The scale for the control variable is chosen so that one unit represents $1 g/m^2$ of basis weight. Notice the similarity between the low frequency component of curve A and the control-variable variations in curve C.

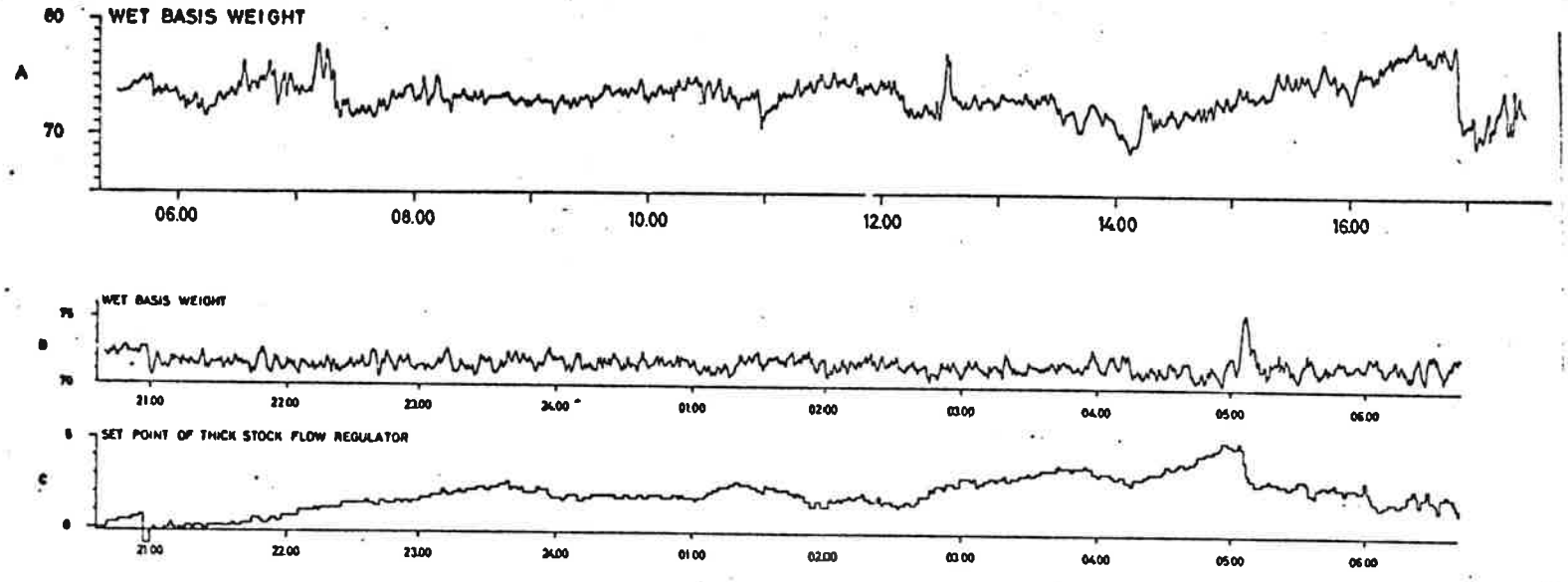

Figure 1
Basis Weight Variations -- Before A and After B

The basic difficulties of the control can be appreciated from the graphs of Figure 1. The variations of basis weight during normal operation can be characterized roughly as a slow drift with superimposed rapid fluctions. Since there is a delay of about 0.02 hours from the control variable (thick stock flow) to the basis weight measured by the Beta Gauge at the dry end, it is clear that feedback cannot eliminate the rapid variations in basis weight. The problem is to eliminate the drift without feeding the rapid fluctuations back into the system. Stochastic control theory is well suited for this type of problem.

Preliminary Investigations

A schematic diagram of the parts of the paper machine that are involved in the basis weight control is shown in Figure 1 of Section 4. Since dry basis weight is proportional to the ratio of the rate at which fibre flows out of the headbox to wire speed, it can be controlled using either of these two quantities. The rate at which fibre flows out

of the headbox can be influenced in several different ways: by adjusting the headbox level, by changing the consistency in the headbox, etc. The choice of primary control variables depends on the constructional details of the paper machine and will depend on the particular application. In the particular case the following primary control variables were available:

- machine speed
- thick stock consistency
- fibre flow at thick stock flow regulator.

The consistency and the flow-regulator determine the rate at which fibre flows into the headbox and, thus, the basis weight. The machine speed has a direct effect on the basis weight as explained above. The possibility to reduce the fluctuations in basis weight by a careful regulation of the three factors mentioned above were investigated.

Experiments were performed to determine the correlation of the fluctuations in basis weight with the fluctuations in fibre flow and machine speed. The results showed that it was not possible to keep the basis weight constant by good regulation of machine speed and fibre flow. To regulate the fibre flow it is necessary to measure fibre concentration, i.e., consistency. Traditionally, consistency is determined by measuring the apparent viscosity or shear force of the thick stock. In the particular case the shear force on a pin submerged in the flowing pulp was measured. A consistency meter of this type will indicate not only fibre concentration but also the rate of flow, the rheological properties of the pulp, the temperature, the viscosity

of additives, etc. It is very difficult to calibrate the consistency meter taking all these factors into account. The rheological properties of the pulp are particularly difficult since they depend on the degree of refining and on the properties of the additives.

It should also be mentioned that it is not possible to measure consistencies lower than one to two percent by this technique, while the headbox consistency is 0.2 - 0.3 percent. This explains why dilution takes place after the consistency regulation as shown in Figure 1 of Section 4. As a result, the fibre concentration may show considerable variation even if the consistency meter reading remains constant.

Our investigation showed that it is impossible to regulate basis weight sufficiently accurately by controlling consistency and machine speed, a conclusion that has been confirmed by others. However, it should be noted that this situation might change drastically with the development of new instruments.

It was thus decided to regulate basis weight by feeding back basis weight measurements taken at the dry end of the paper machine so as to control the rate at which fibre flows into the headbox.

Characteristics of the Fluctuations in Basis Weight

The characteristics of the basis weight fluctuations have been investigated. There are variations in the machine direction as well as in the cross direction. In the particular case, the cross direction profile was found to be stable if certain precautions are taken. We have therefore concentrated on the variations in machine direction. The

character of the fluctuations is illustrated by the covariance function in Figure 2. Roughly speaking the fluctuations can be described as a slow drift with superimposed rapid fluctions.

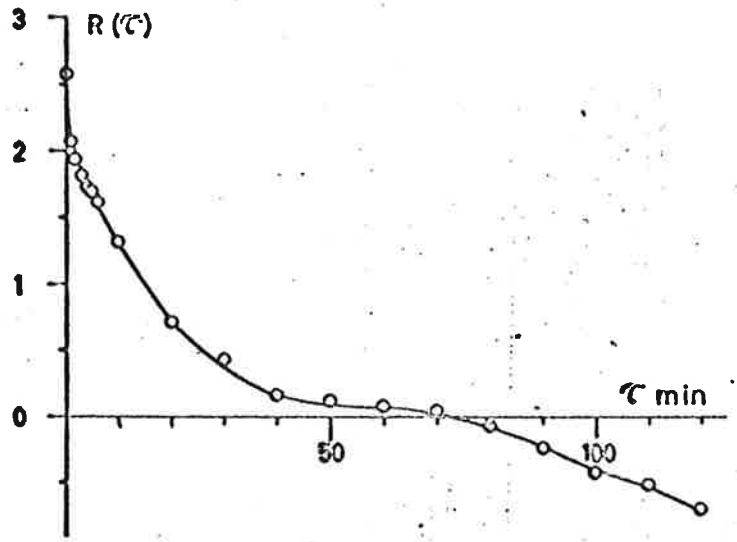

Figure 2
Covariance Function of Basis Weight Variations
During Normal Operation

The covariance function of Figure 2 is computed from a sample recorded with a sampling interval of 1 min. When computing the covariance function of Figure 2 the usual techniques for trend removal were used. Such a procedure naturally raises several questions as to the proper interpretation of the low frequency variations. The result shown in Figure 2 can, however, at least be used for a qualitative discussion.

The curve shown in Figure 2 is computed from data logged with a sampling interval of one minute. To obtain a better resolution of the high frequency components we have also logged data with a shorter sampling interval. In Figure 3 we show the covariance function computed from a sample of 20 minutes duration with a sampling interval of 0.001h (= 3.6 sec).

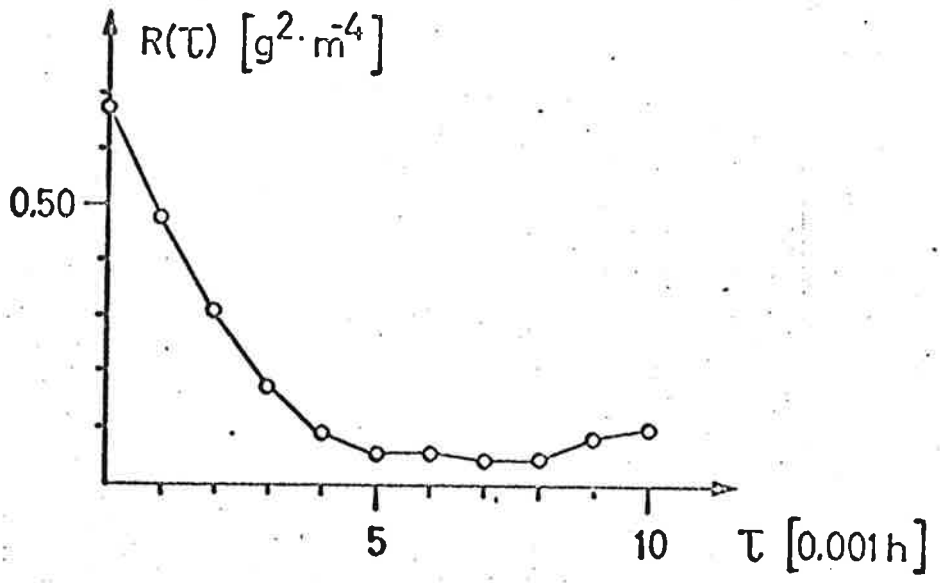

Figure 3
Covariance Function of Rapid Variations in the Basis Weight

Summarizing, we thus find that the basis weight fluctions observed can be described as random processes. Analyses of the amplitude distributions show that the processes are normal. The process is not

stationary. To describe the processes we can either use a model including drift terms or we can describe process time differences as stationary processes. In many cases it has been sufficient to assume that the first time difference of the time series describing the fluctuations is a stationary process.

Identification Experiments

In order to design the control laws it is necessary to know the process dynamics and the character of the disturbances. To arrive at this information we performed experiments on the plant. The input variable was changed and variations in the output observed. From the sequence of input-output pairs $\{u(t), y(t), t = 0,1,2,...N\}$ obtained in this way we estimated the coefficients of a mathematical model (5.33) of the process as described in Section 5. In this section we will discuss some practical aspects in connection with a description of a case study.

The experiments were performed using the control computer. The input signal used in the experiment is represented as a number sequence and stored in the core storage. The numbers in this sequence are read periodically and converted to analog signals using the D/A converter and the regular D/A conversion subroutines of the control computer. The output signals from the process are converted to digital numbers using the D/A converter. Both the input and output signals are thus represented by digital numbers in the computer storage in precisely the same way as they occur when the computer is used to control the process.

The dynamics of the signal transducers, transmission lines, A/D, and D/A converters are thus included in the model. The disturbances that occur in the signal transmission as well as round-off errors caused by a finite word length are also included in the model of the disturbances. The whole experiment is executed by a program which carries out the following tasks:

- Read control variable from table
- Call analog output subroutine
- Read measured output signal
- Store control variable (u) and output signal (y)

Typical results of an identification experiment are given in Figure 4 which shows the values of several signals measured at different points in the plant, i.e.,

- set point of thick stock flow regulator
- wet basis weight
- moisture content at dry end
- dry basis weight

When designing the control law we need only the input (set point of thick stock flow regulator) and output (dry basis weight) sequences. However, experience has shown that when logging data to determine the process dynamics it is very valuable to record many auxiliary variables. This makes it possible to evaluate the operating conditions under which the data was taken. When modeling the relation between thick stock flow and the basis weight, it is, for example, very important to know that neither the headbox level nor the consistency have changed

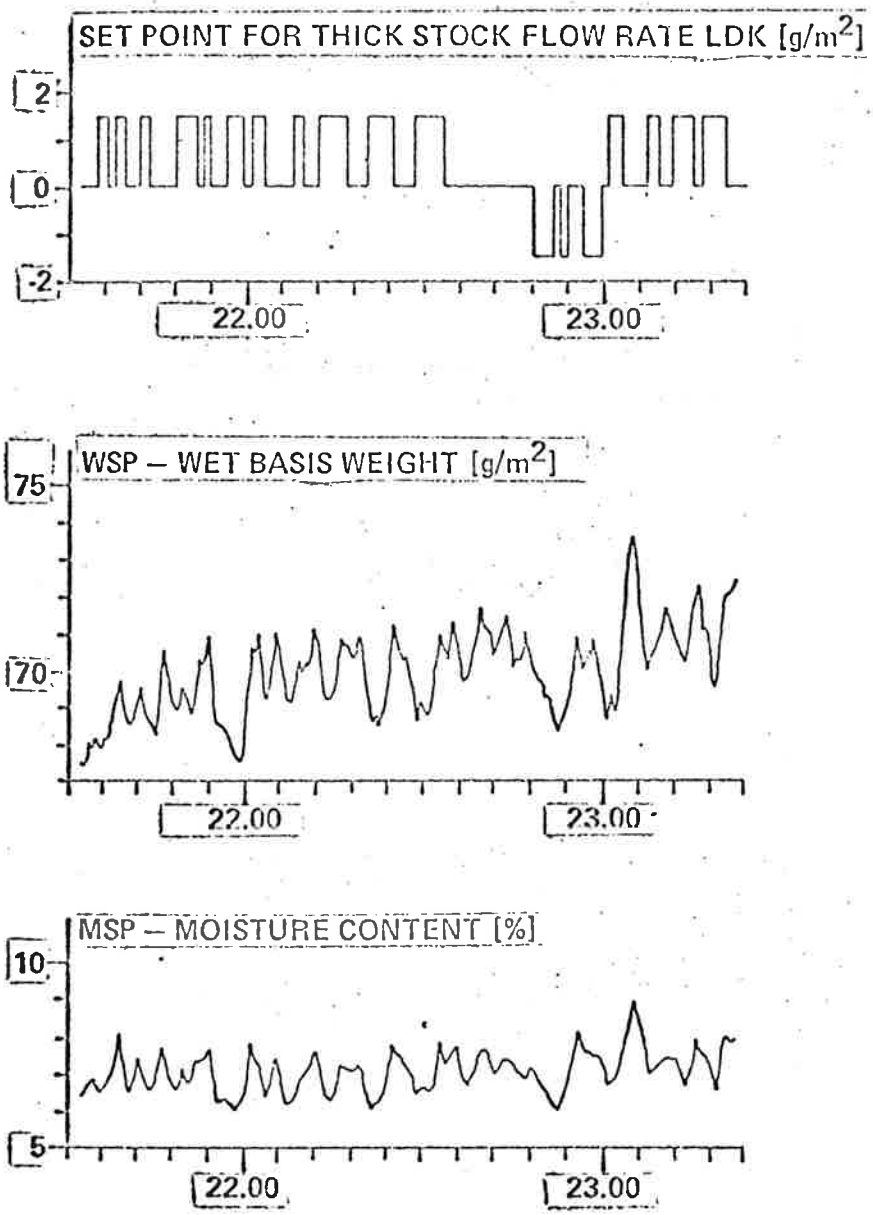

Figure 4
Results of Experiments Made to Determine Process Dynamics

significantly during the experiment.

Figure 4 shows very clearly that changes in the flow rate have a significant influence on the moisture content. The practice of logging many auxiliary variables has proven very useful in finding dynamic models for variables needed in future work. The data in Figure 4 can, for example, be used to find a model relating the set point of the thick stock flow regulator to wet basis weight, moisture content, and dry basis weight.

Choosing the Input Signal

It is desirable to have large signal amplitudes in order to get good estimates. However, excessive signal amplitudes might drive the system outside the linear region and might also provide unacceptably large output variations when experiments are performed during normal operation. A compromise between signal amplitude and sample length can be made in order to obtain a specified accuracy of the coefficients of the model. The length of the sample is limited by the maximum time interval between grade changes. When no control is maintained the output may drift; in such a case, the maximum sample length is also limited by the permissible deviations. In the identification of the models used to design basis weight control algorithms we typically used sample lengths of two to ten hours. The amplitude of the input signal shown in Figure 4 is quite representative. The peak-to-peak amplitude corresponds to $1.7 g/m^2$. This number represented a suitable compromise between the factors discussed above. Recall that the standard typical deviation

during normal operation is $1.3g/m^2$. This compromise provides the same signal level that is used during normal control.

The input signal must also be chosen so that it is persistenly exciting. This is always the case if the input signal is a sample of a stationary stochastic process with constant spectral density. In the first experiments we used pseudo-random signals, but there are other factors which should also be taken into account. A few long pulses provide a good estimate of the low frequency gain. A sequence of uncorrelated random variables of sufficiently long duration will have the desired properties. However, when short samples are used, there is no guarantee that long pulses will be obtained.

The intervals between pulses may, for example, be chosen as randomly distributed intervals with a mean value that matches the delay and the time constants of the system. It is also convenient to have a signal which remains constant over several sampling intervals so that the data may be used to fit models for different sampling intervals. If, for example, we wish to use the results to obtain models with sampling intervals of 36, 72, and 108 seconds, the input signal must be constant over intervals that are multiples at 216 seconds. We can then select every second measurement to form a 72-second sampling interval series and select every third measurement to form a 108-second sampling interval series.

For the reasons given above it is often advantageous to design the input signals based on all the available a priori knowledge about the process and its disturbances. This is not essential from the point of

view of principle but it reduces the experimentation time.

Practical Aspects of the Experiments

Experiments on complex industrial processes are difficult to perform, the main reason being that it is impossible to obtain ideal conditions on production units and that there is always the risk of production losses. The problem of choosing the input signal has been covered briefly. We have also made other observations which, although trivial, may be of value to those initiating similar experiments.

It is recommended that a multi-channel recorder be connected to the process during the experiment so that malfunctions can be detected immediately.

log all experimental data meticulously: observations, manual adjustments, malfunctions, operating conditions, etc. It is often wise to log many auxiliary variables.

It is recommended that a preliminary experiment be made to determine suitable sampling intervals, signal levels and experiments duration. This should be repeated after a few weeks to see whether conditions have changed.

We have found it useful to plot the data before making extensive analyses, thus precluding the processing of meaningless data. The data should be checked against prior knowledge of gains, time constants, and time delays wherever possible.

Instrument calibration requires special attention. We found it very helpful to include systematic calibration methods based on cross-checks by means of mass balances and other known relationships between

the measured signals. It is also very important to consider the programming aspects of process experiments when planning the computer system so that experiments can be performed without extensive reprogramming of the system.

Computation of Maximum Likelihood Estimates

The following examples will illustrate the numerical identification procedure. These examples are based on the data shown in Figure 4. We shall discuss mathematical models relating dry basis weight and wet basis weight to changes in the set point of the flow regulator. Figure 4 shows that both wet and dry basis weight are drifting. This is even more apparent in records of greater length (see, e.g., Figure 1).

We therefore identify models of the type (5.33) where the polynomials $A(z)$ and $B(z)$ are constrained to have zeros at $z=1$. The following model structure will thus be used

$$1 \qquad y(t) = \frac{b_0' + b_1'q^{+1} + \ldots + b_n'q^{-n}}{1 + a_1'q^{-1} + \ldots + a_n'q^{-n}} u(t-k) + \lambda \frac{1 + c_1q^{-1} + \ldots + c_nq^{-n}}{(1-q^{-1})(1 + a_1'q^{-1} + \ldots + a_n'q^{-n})} e(t)$$

The time interval is chosen as 0.01 hour in all cases. The minimum variance control law for the model (1) will contain an integrator which implies that the controlled system will respond to step inputs with no steady error. As stated in Section 6, the identification procedure is carried out recursively starting with a first order system, continuing with a second order system, etc. To obtain the value of the delay k for a model fixed order, the identification is repeated with the input signal shifted.

2 Example

As the first numerical example we present a model relating dry basis weight to thick stock flow. First we identify a first order model having the structure (1). Applying the maximum likelihood identification algorithm we get the results shown in Table 3.

3 Table - Successive parameter iterates for a first order model relaging dry basis weight to thick stock flow

Step	$\theta_1=a'$	$\theta_2=b'$	$\theta_3=c'$	V	$\frac{\partial V}{\partial a'}\cdot 10^5$	$\frac{\partial V}{\partial b'}\cdot 10^5$	$\frac{\partial V}{\partial c'}\cdot 10^5$
0	0	0	0	6.7350	91683	39509	-91683
1	-0.0122	13.0054	0	4.1603	0	0	193777
2	-0.3924	13.9356	-0.6320	3.3764	-78727	1190	51707
3	-0.3492	14.6689	-0.6542	3.3360	1339	-69	2575
4	-0.3502	14.6468	-0.6572	3.3360	106	-3	-165
5	-0.3500	14.6468	-0.6569				

Starting with the initial parameter estimate $\theta=0$, the first step of the identification algorithm gives the Kalman estimate of the parameters and this estimate is then successively improved until the loss function $V(\theta)$ is minimized and the maximum likelihood estimate obtained. Notice in particular the significant difference between the Kalman estimate (step 1) and the maximum likelihood estimate.

The value of the matrix of second partial derivatives at the last step of the iteration is

4 $$V_{\theta\theta} = \begin{bmatrix} 19.283 & -0.290 & -8.963 \\ -0.290 & 0.035 & 0.062 \\ -8.863 & 0.062 & 12.048 \end{bmatrix}$$

Repeating the identification for different values of the time-delay k we obtain the results given in Table 5.

5 Table - Results of identification of first-order models relating dry basis weight to thick stock flow for different time-delays.

k	a_1'	b_0'	c_1'	λ	V
3	-0.807	9.846	-0.994	0.297	4.491
4	-0.350	14.647	-0.657	0.257	3.336
5	-0.749	1.286	-0.958	0.351	6.152

We thus find that the loss function V has its smallest value for $k=4$. To find the accuracy of the model parameters we proceed as follows: An estimate of Fisher's information matrix is obtained from the matrix of second partial derivatives (Åström and Bohlin 1965, Lemma 2),

6 $$I = \lambda^{-2} V_{\theta\theta}.$$

If $V_{\theta\theta}$ is non-singular the estimate is asymptotically normal (θ_0, I^{-1}) and we thus have the following estimate of the covariance of the asymptotic distribution:

7 $$I^{-1} = \lambda^2 V_{\theta\theta}^{-1} = \begin{bmatrix} 0.006 & 0.042 & 0.004 \\ 0.042 & 2.202 & 0.020 \\ 0.004 & 0.020 & 0.008 \end{bmatrix}.$$

Summarizing, we thus find the following numerical values for the best first-order model, where the computations are based on 100 pairs of input-output data:

$k = 4$ $\quad$ $c = -0.66 \pm 0.09$

$a = -0.35 \pm 0.08$ $\quad$ $\lambda = 0.257 \pm 0.017$

$b = 14.6 \pm 1.5$ $\quad$ $V = 3.34 \pm 0.44.$

Proceeding to a second-order model the identification algorithm gives the following results, based again on 100 pairs of input-output data:

$k = 3$ $\quad$ $c_1 = -0.73 \pm 0.18$

$a_1 = -0.46 \pm 0.14$ $\quad$ $c_2 = 0.12 \pm 0.16$

$a_2 = 0.04 \pm 0.12$ $\quad$ $\lambda = 0.249 \pm 0.017$

$b_0 = 3.4 \pm 1.6$ $\quad$ $V = 3.15 \pm 0.43$

$b_1 = 12.3 \pm 2.2$

The matrix of second partial derivatives at the minimum is:

$$8 \qquad V_{\theta\theta} = \begin{bmatrix} 22.47 & 13.82 & -0.08 & 0.36 & -7.61 & -1.87 \\ 13.82 & 22.47 & -0.17 & -0.08 & -4.94 & -7.59 \\ -0.08 & -0.17 & 0.04 & 0.02 & 0.05 & -0.05 \\ 0.36 & -0.08 & 0.02 & 0.04 & 0.06 & 0.06 \\ -7.61 & -4.94 & 0.05 & 0.06 & 11.06 & 6.60 \\ -1.87 & -7.59 & -0.05 & 0.06 & 6.60 & 10.56 \end{bmatrix}.$$

It now follows from Åström and Bohlin (1965), Theorem 4, that the parameter estimates for a large number of input-output pairs is asymptotically normal $N(\theta_0, \lambda^2 V_{\theta\theta}^{-1})$. Inspecting the estimates of the coefficients of the second-order model given above, it seems reasonable to assume that the coefficients a_2 and c_2 are zero. Assuming that asymptotic theory can be applied we can now solve various statistical problems. We will, for example, test the hypothesis that the model is of first order, i.e., our null hypothesis is

$$9 \qquad H_0 : (a_2^0 = b_0^0 = c_2^0 = 0).$$

Using the asymptotic theory we find that asymptotically the statistic

$$10 \qquad \xi = \frac{V_2 - V_1}{V_2} \quad \frac{N - 6}{3}$$

has an $F(3,N-6)$ distribution under the null hypothesis. (For large N this is approximately chi squared.) The symbol V_2 denotes the

minimal value of the loss function for the second-order model; V_1, the minimal value for the first-order model and N, the number of input-output pairs. In this particular case we have $\xi = 1.9$. At a risk level of ten percent we have $F(3,96) = 2.7$ and the null hypothesis, that the system is of first order, thus has to be accepted.

The results of the identification procedure are illustrated in Figure 5 which shows

- the input u
- the output y
- the deterministic output y_d defined by

$$\text{11} \quad \bullet\, y_d(t) = \frac{b_0' + b_1'z^{-1} + \ldots + b_n'z^{-n}}{1 + a_1'a^{-1} + \ldots + a_n'z^{-n}}\, u(t)$$

- the error in the deterministic model $e_d(t) = y(t) - y_d(t)$
- the one-step-ahead predictor $\hat{y}(t|t-1)$
- the one-step-ahead prediction error $e_1(t) = y(t) - \hat{y}_1(t|t-1)$

Figure 5 illustrates the properties of the estimation procedure. We recall that the estimator is constructed in such a way that $H\Sigma e_1^2(t)$ is minimal. The deterministic output $y_d(t)$ shows how much of the output can be explained by the deterministic part of the model. The error $e_d(t)$ thus represents the part of the output that cannot be explained by the deterministic model. The signals $y_d(t)$ and $e_d(t)$ thus demonstrate how much of the output is caused by the input and by

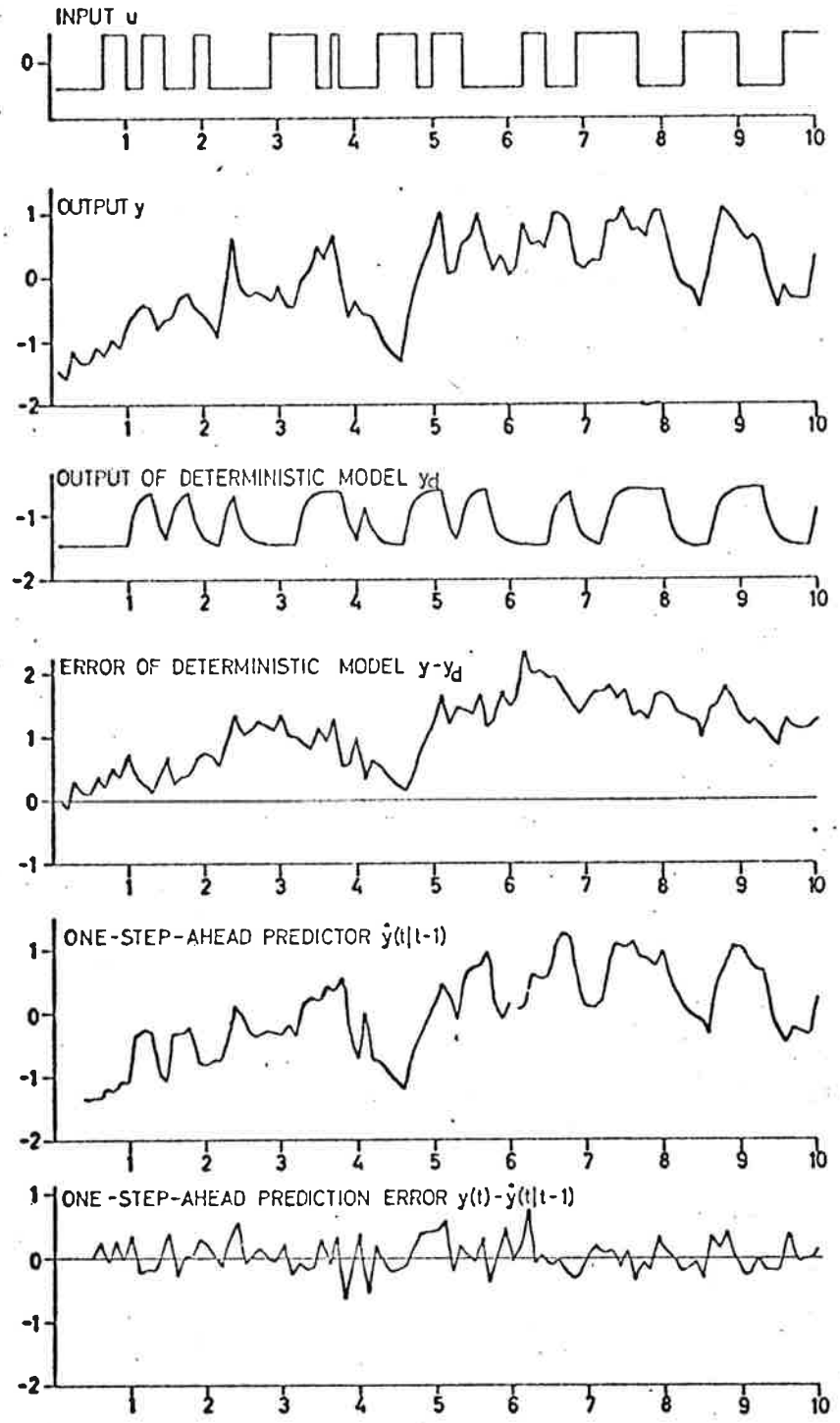

Figure 5a - 5b
Illustration of the identification of a linear model relating dry basis weight to thick stock flow. The first order model is shown in Figure 5a and a second order model in 5b.

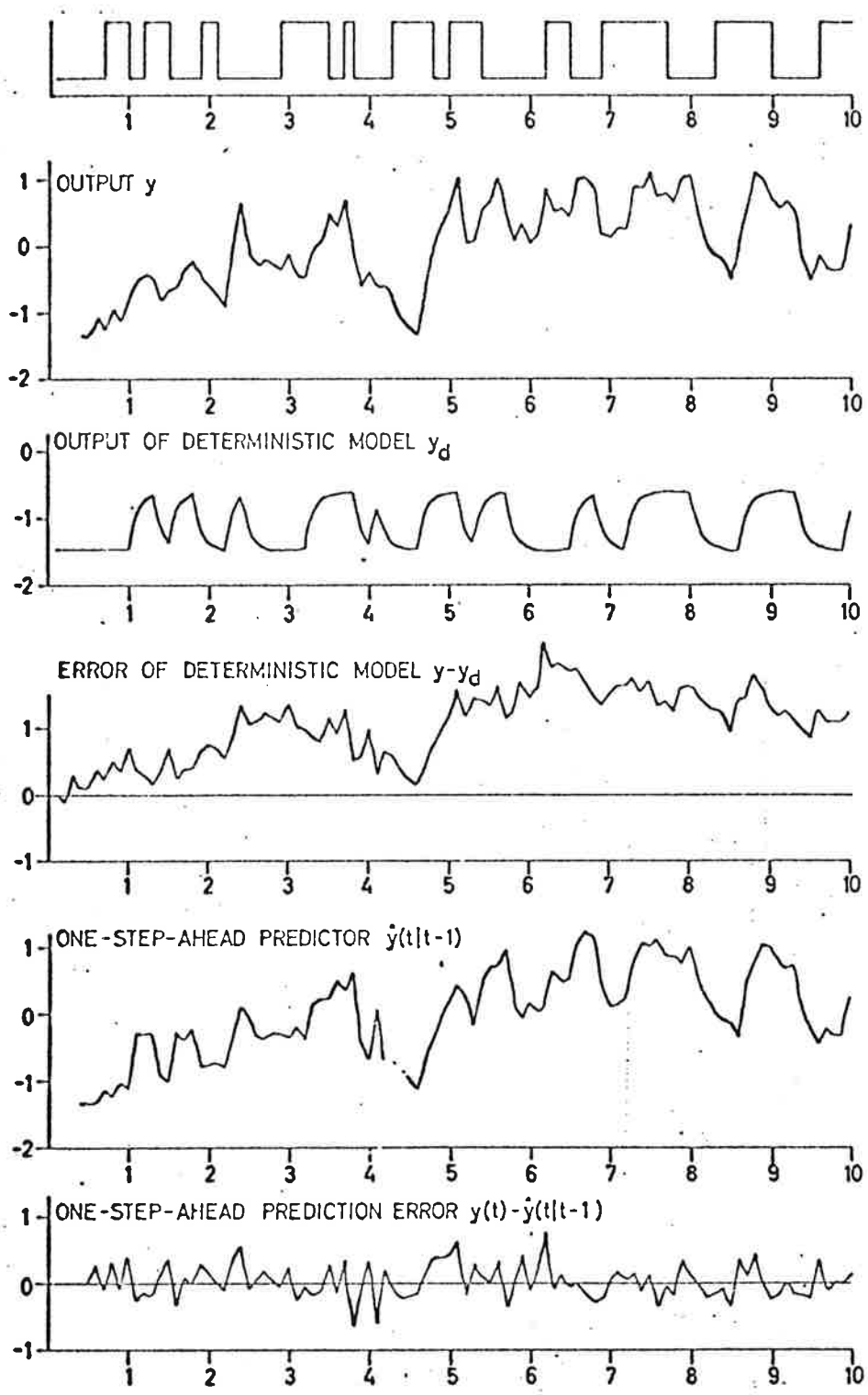
OUTPUT y
OUTPUT OF DETERMINISTIC MODEL y_d
ERROR OF DETERMINISTIC MODEL $y-y_d$
ONE-STEP-AHEAD PREDICTOR $\hat{y}(t|t-1)$
ONE-STEP-AHEAD PREDICTION ERROR $y(t)-\hat{y}(t|t-1)$

Figure 5b

the disturbances. Notice in particular the drifting character of the error $e_d(t)$. The signal $\hat{y}(t|t-1)$ illustrates how well the output can be predicted one step ahead using the input signal and previously observed outputs.

Figure 5 also illustrates the results for a second-order model. Figure 6 shows the sample covariances of the residuals of the first- and second-order models.

12 Example

As a second illustration of the numerical identification scheme we shall now present a model relating changes in the wet basis weight to changes in the set point of the thick stock flow regulator. The computations are based on the data of Figure 4. The output is drifting in this case, too, and for this reason we again used a model with $A(z)$ and $B(z)$ constrained to have a zero at $z=1$, i.e., a model of the structure (1). Using the numerical identification program we find that the minimum value of the loss function occurs at $k=4$ for the first order case, and the coefficients of the best first-order model are given in the table below.

13 Table - Coefficients of first order model relating to set basis weight to thick stock flow rate.

$k = 4$
$a_1 = -0.384 \pm 0.054$
$b_1 = 27.107 \pm 2.06$
$c_1 = -0.619 \pm 0.097$
$\lambda = 0.364 \pm 0.025$
$V = 6.597 \pm 0.935$

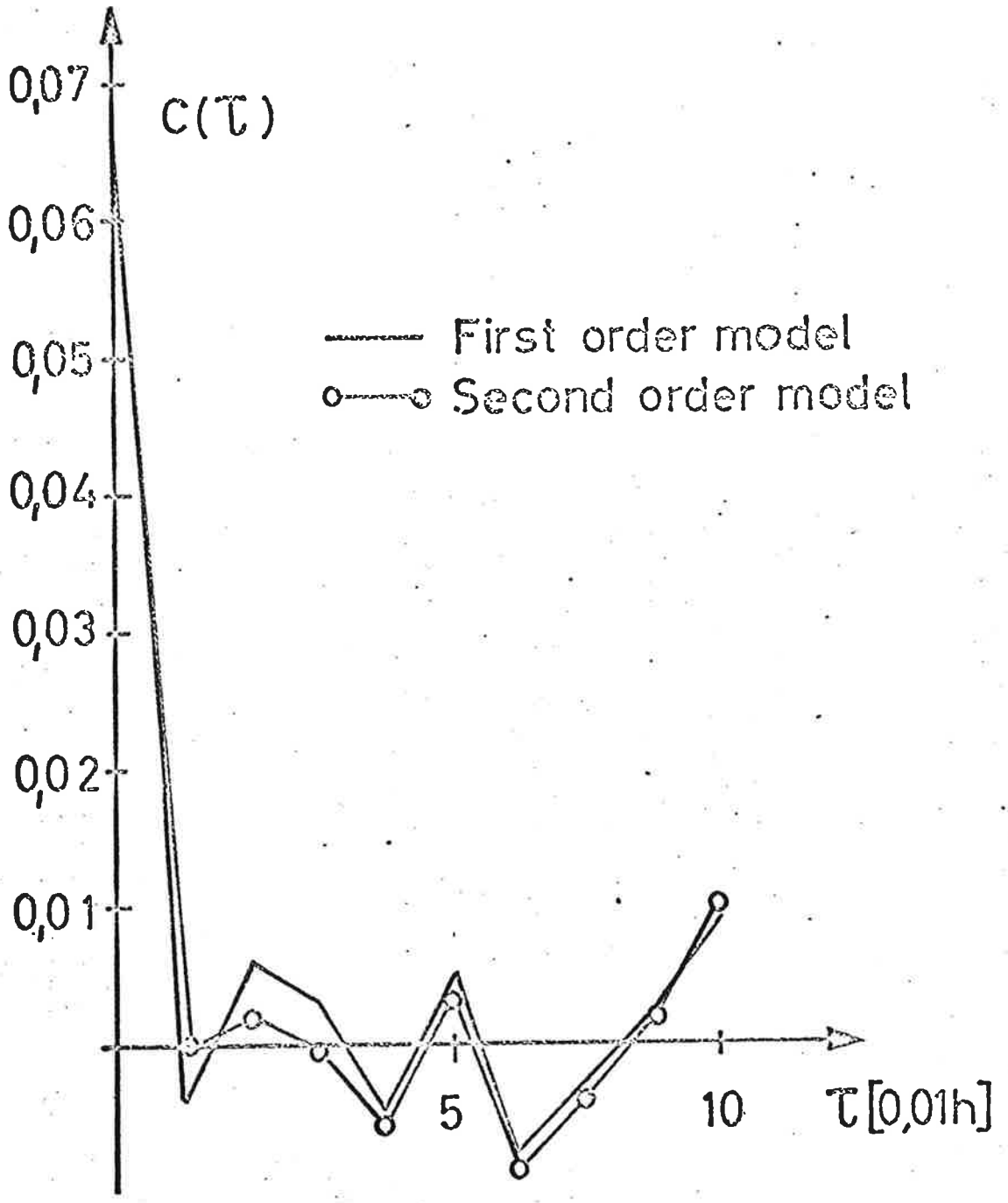

Figure 6
Covariance functions for residuals of first and second order models relating dry basis weight to thick stock flow rate: note the small difference between the two curves. An hypothesis test gives no significant difference between the two models.

The best second order models are listed below.

14 Table - Coefficients of second order models relating wet basis weight to thick stock flow rate.

k = 3	4
a_1' = -0.639 ± 0.106	-0.551 ± 0.073
a_2' = 0.224 ± 0.089	0.197 ± 0.076
b_0' = 6.393 ± 2.02	24.919 ± 2.19
b_1' = 20.151 ± 2.99	------
c_1' = -0.823 ± 0.138	-0.773 ± 0.120
c_2' = 0.212 ± 0.143	0.233 ± 0.123
λ = 0.335 ± 0.024	0.352 ± 0.025
V = 5.728 ± 0.805	6.273 ± 0.885

The matrix of second-order partial derivatives of the minimal point is

15 $$V_{\theta\theta} = \begin{bmatrix} 79.24 & 53.37 & -0.13 & 0.76 & -12.68 & -0.13 \\ 53.37 & 79.12 & -0.40 & -0.13 & -5.93 & -11.44 \\ -0.13 & -0.40 & 0.04 & 0.02 & 0.06 & -0.07 \\ 0.76 & -0.13 & 0.02 & 0.04 & 0.10 & 0.10 \\ -12.68 & -5.93 & 0.06 & 0.10 & 17.64 & 7.83 \\ -0.13 & -11.44 & -0.07 & 0.10 & 7.83 & 15.12 \end{bmatrix}.$$

We now test the null hypothesis that the system is of first order; i.e.,

16 $$H : (a_2^0 = b_0^0 = c_2^0 = 0)$$

Using the asymptotic results, we find $\xi = 4.8$ and the hypothesis thus has to be rejected. Increasing the order to three does not give any significant improvements in the loss function.

Hence if we consider dry basis weight as the output of the system, we find that the model is of first order, but if we consider wet basis weight as the output, the model is of second order. This also shows up very clearly in Figure 7 where we illustrate the results of the identification in the usual way. Notice in particular the differences in behavior of the outputs of the deterministic models of the first and second order systems. There is a physical explanation for this difference of behavior between the responses of dry and wet basis weight to changes in rate of thick stock flow. As mentioned earlier, and as can be seen from Figure 4, a change in the rate of thick stock flow will influence dry basis weight as well as moisture content. After an increase in the thick stock flow rate we find that both dry basis weight and moisture content will increase. The increase in moisture content will then be eliminated by the moisture control feedback loop, which controls the set point of the last drying section (counting from the moisture meter). These two effects will explain the overshoot in the response of the wet basis weight. It is also clear from this discussion that the response of the wet basis weight will be influenced by the settings of the moisture control loop. This fact provides another argument for using dry basis weight as the control variable.

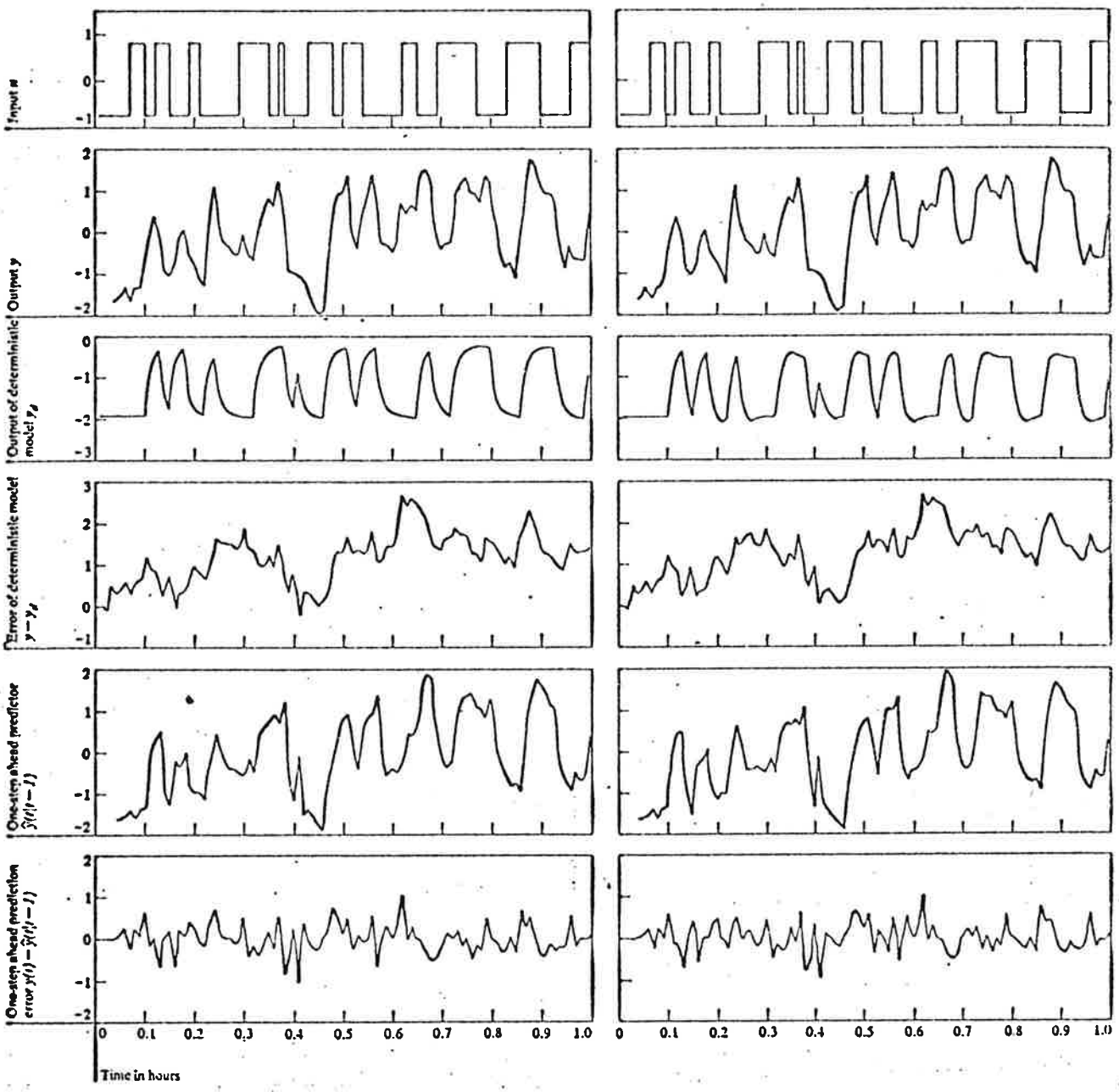

Figure 7
Illustration of the identification of a linear model relating variations in wet basis weight to variations in thick stock flow. The first order model is on the left and the second order model on the right.

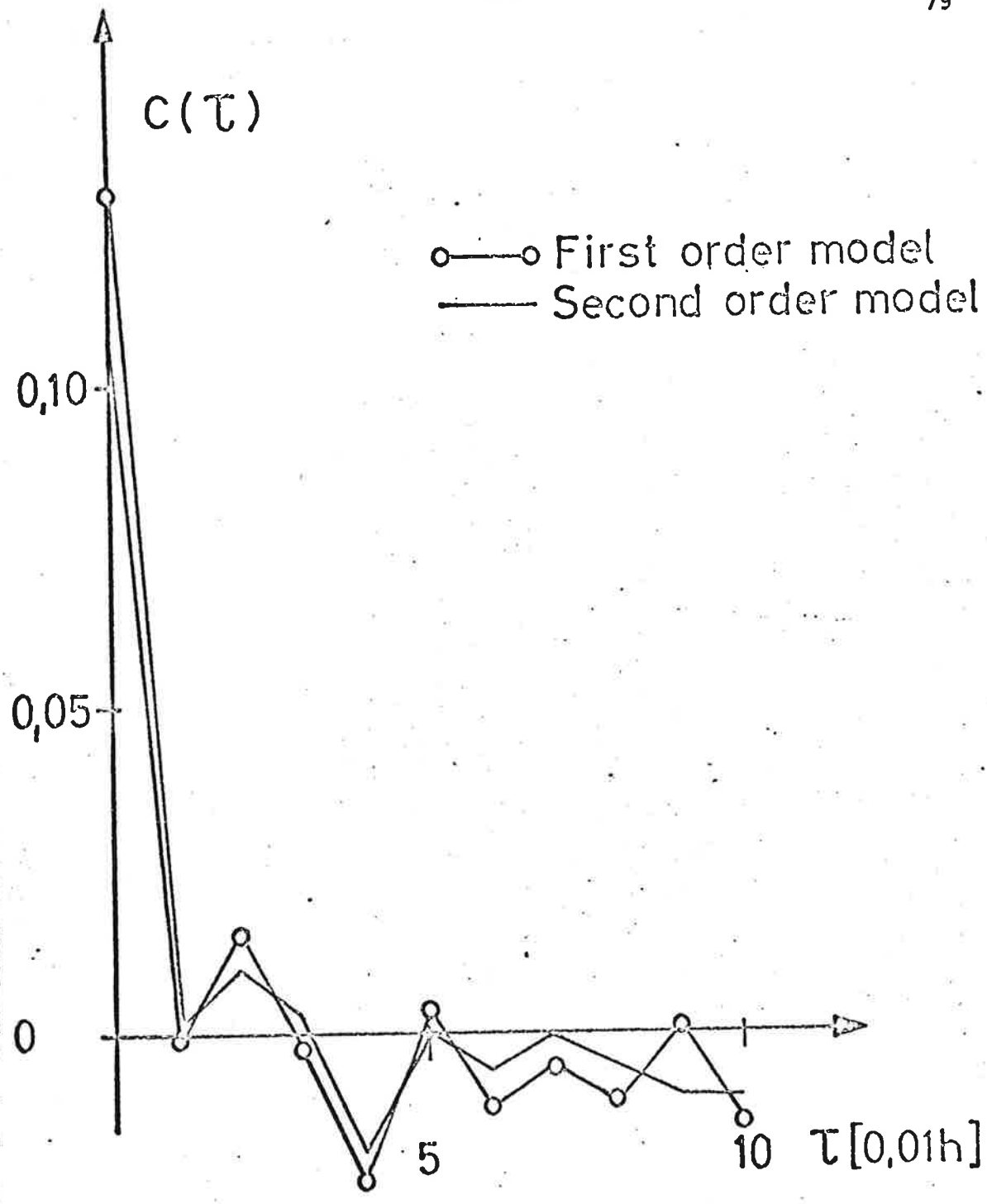

Figure 8
Covariance function for residuals of first and second order models relating wet basis weight to thick stock flow rate. Notice that an hypothesis test gives a significant difference between the models.

Experiences With On-Line Control

In this section we will summarize some of the practical experiences and some results that have been obtained with on-line basis weight control. The experimental program that has been carried out has had a dual purpose: to arrive at control strategies suitable for the particular application and to test the general procedures developed for the design of control strategies for steady state control. Consequently, we continued some experiments, even though the particular loops were working satisfactorily, to answer problems concerned with methodology. Several control schemes have been investigated. We have chosen both the set point of the thick stock flow regulator and the set point of the thick stock consistency regulator as control variables. We have also regulated dry basis weight as well as wet basis weight. In the first experiments the consistency of the thick stock was chosen as a control variable. Later we changed to the thick stock flow rate for two reasons: the basis weight responds faster to changes in the set point of the thick stock flow regulator than to changes in the set point of the consistency regulator, and the dynamics of the consistency regulator change with the operating conditions, thereby introducing variations in the system dynamics.

In general it is very difficult to evaluate the performance of the control loops, particularly with regard to comparing the different control laws, the main reason being that the disturbance level varies considerably. This implies that in order to evaluate the control loops we need test periods of considerable length. Moreover it is often

difficult to judge improvements if reference values are not available.

For basis weight control we had the results of the feasibility study as a reference. These results also indicated that there was considerable variability in the basis weight variations as shown in Figure 1. When analyzing the variations the records were first divided into samples of about five hours duration. After trend removal the samples were analyzed as time series. In all cases studied the variations had standard deviations greater than or equal to $1.3 g/m^2$, and this value was chosen as a conservative reference value. The target value for basis weight regulation was set at $0.7 g/m^2$ in the feasibility study.

The first successful on-line basis weight control operation was on April 28, 1965. It covered a test period of ten hours and since then we have conducted a large number of tests.

Two types of experiments have been performed. In one type we let the control loop operate normally for several weeks while collecting data at comparatively large sampling intervals. The results have not been extensively analyzed but the performance of the control system has been evaluated subjectively. This evaluation was based on laboratory test data and the judgment of the machine tenders.

The second type of test was a controlled experiment extended over periods ranging from 30-100 hours. Data was logged at sampling intervals of 0.01 hour and analyzed. The analysis of such tests usually includes the following steps:

- Plotting all process variables logged, particularly controlled variables and inputs to the control loops.

- Calculating covariance functions of controlled variables and testing to ascertain whether variations are moving averages [$y(t) = E_{k-1}(q^{-1})e(t)$] of appropriate order (see Section 5).

- Identifying dynamic models.

- Comparing models with those used to calculate the control laws.
- Comparing variances of the outputs with those previously obtained.

Example

In Figure 9 we give a sample covering 24 hours of operation of the basis weight control loop. In the diagram we show wet basis weight, dry basis weight (the controlled output), and thick stock flow (the control signal). The scale for the control signal, thick stock flow, is chosen as dry basis weight. The magnitude of the control signal will thus directly indicate how much of the fluctuations in dry basis weight are removed by the control law. The control signal will thus approximately show the disturbances in the output of the system. Notice the different characteristics of the disturbances at different times. The large disturbances occurring at times 14.30 and 18.00 are due to large fluctuations in thick stock consistency.

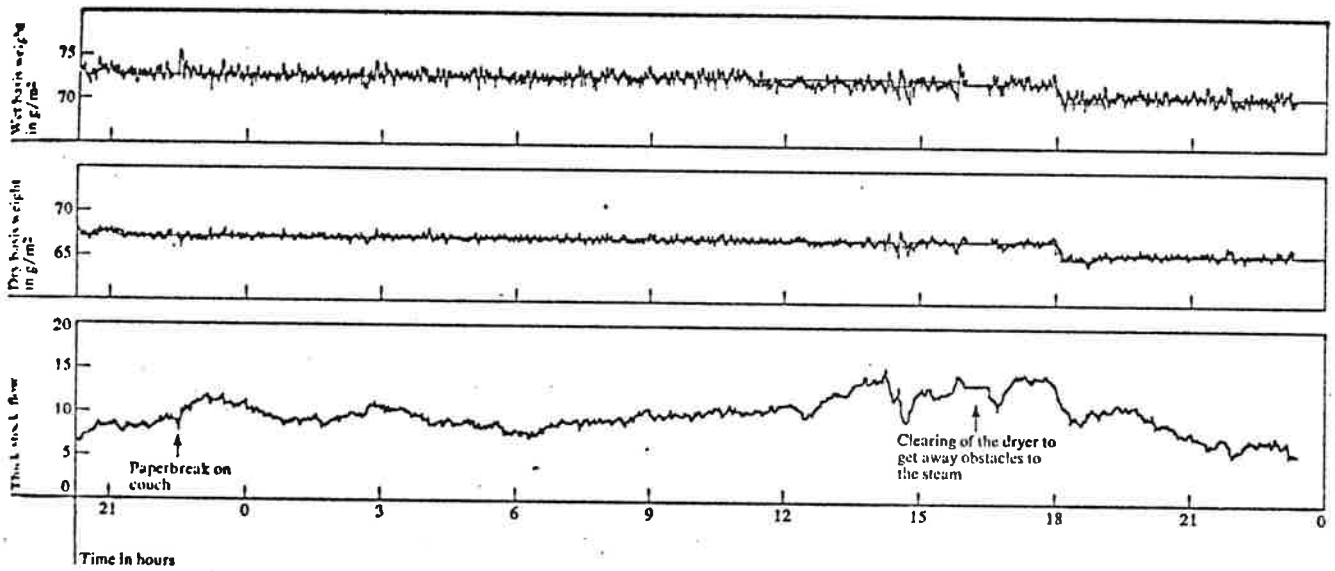

Figure 7 Results of test run with on-line control of basis weight.

Figure 9
Results of test run with on-line control of basis weight.

Also notice that there are two interrupts in the operation of the system, one paper break, and one interrupt to clear the drying section. In these instances the basis weight control loop is automatically switched off and the control signal is kept constant until the disturbances are cured when the loops are automatically switched on again. Notice that a paper break does not introduce any serious disturbances. Also notice that there are some grade changes from which we can judge the response of the controlled system to step changes in the references values.

Moisture content was controlled by feedback from the moisture meter to the set point of the pressure regulator of the fourth drying section. The standard deviation of moisture content was 0.4 percent. In Figure 10 we show the covariance function of dry basis weight. As is to be expected from Theorem 5.46 this is the covariance function of a moving average of fourth order.

We have also made experiments to verify that the high frequency fluctuations in moisture content and basis weight have the same characteristics. This was one essential assumption made in Section 5. If this was true, the variance in dry basis weight would be independent of dry or wet basis weight control. In the table below we give standard deviations recorded during a 30-hour test, where alternatively wet and dry basis weight was controlled.

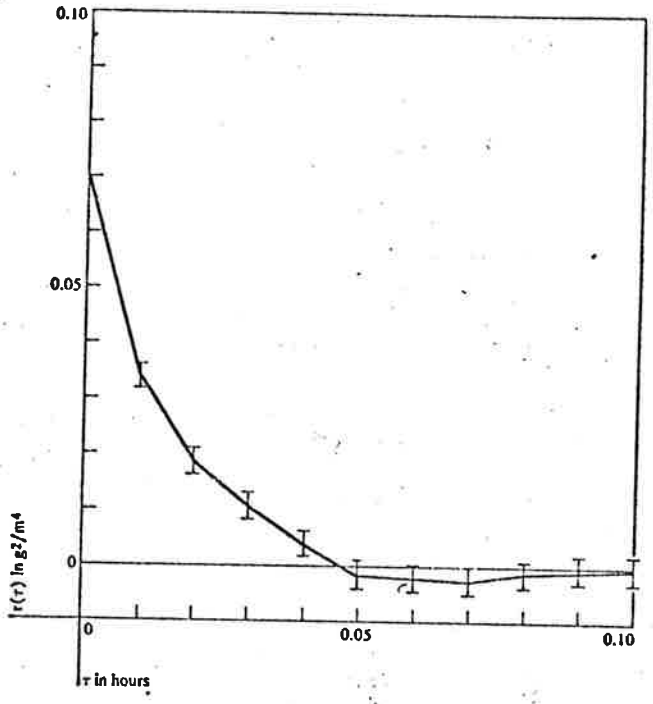

Figure 10

Covariance function for fluctuations of dry basis weight in the time interval 23.00 to 12.00 of Figure 9. Compare with Figure 8 which shows the covariance function without computer control.

	Standard Deviation	
	Wet Basis Weight	Dry Basis Weight
Wet basis weight controlled	0.50	0.32
Dry basis weight controlled	0.52	0.28

When testing the control algorithms the control actions were initially multiplied by a gain factor ($\alpha < 1$) as a safety precaution. The gain factor was then changed step-wise to approach the optimum value. The standard deviations of the fluctuations were evaluated on-line for each α and compared with precomputed data. An example is given in the table below:

Hour	α	σ
1	0	1.27
2	0.6	0.82
3	1.0	0.55
4	1.2	0.57
5	1.0	0.54

To evaluate the results of a computer controlled experiment we fitted a model to the actual input-output sequence obtained during the experiment and compared the actual result with what could possibly be achieved for the particular model. After some discrepancies in early experiments which were due to inaccurate models the data showed very good agreement. Below we give

some typical numbers obtained from an experiment sequence:

Experiment Number	Ratio of actual variance to minimum variance
1	1.25
2	1.11
3	1.09
4	1.02

Section 8 — Quality Control

Introduction

Many important quality variables in a paper mill can not be measured on-line. Typical examples are cross direction tensile strength and cross direction stretch for a kraft paper machine. These variables are measured on samples taken from running web, the end of the reel and the end of each set of rolls on the winder. Samples are tested by the machine tender or at the test laboratories.

Information about quality variables is used in two different ways: by the machine tender to adjust the paper machine settings and by the winding crew and shift foreman to determine whether the produced paper fulfills specifications and can be delivered or whether it must be rejected (sorting). At present, the machine tender's decisions are based on the measurement of samples taken from the running web and samples taken at the end of each reel. Sorting is based essentially on laboratory measurements of samples taken at the winder at the end of each set of rolls.

The uncertainty in the determination of quality variables is one of the essential difficulties with quality control. This uncertainty is due to several factors. The overall quality of a long paper sheet is estimated from a very small sample. The measurements involve considerable error. The sampling procedure introduces considerable delay between paper production and sampling. The paper sample must also be conditioned in a room at controlled temperature and humidity before testing in order to obtain reproductible results. We have investigated the variations in quality variables during normal production and found that there are strong correlations between quality variables of neighboring rolls.

By making use of this fact and basing the estimate of quality variables of one roll on measurements of neighboring rolls, considerable improvement of the existing procedure are possible.

In a particular case, it has been shown that the accuracy of the estimation of cross direction stretch can be improved by a factor of three and and that it is possible to predict cross direction stretch 30-90 minutes in advance to the same accuracy as it was previously measured.

In principle the problem of quality control does not differ from the basis weight control problem discussed in section 7. Suitable mathematical models can be derived using the maximum likelihood method and control strategies can be obtained using linear stochastic control theory. On the whole, the problem is not as well defined as the basis weight control problem. For example, there are often several choices available for the suitable control actions. For this reason it might often be sensible to present the state estimate to an experienced operator and let him choose an appropriate control action. In many cases the dynamics of the control system can be neglected and the problem is then a pure estimation problem. In such a case, the actions taken by the operator must naturally be fed into the estimator.

In this section we will give some of the experiences obtained with such an approach.

Statistical Properties of Fluctuations In Typical Quality Variables

In Figure 1 we show the covariance function of a typical quality variable, cross direction stretch. The data shown in Figure 1 is taken using the ordinary sampling procedure. Each measurement thus represents the mean value of measurements taken from 5 strips approximately 5m apart.

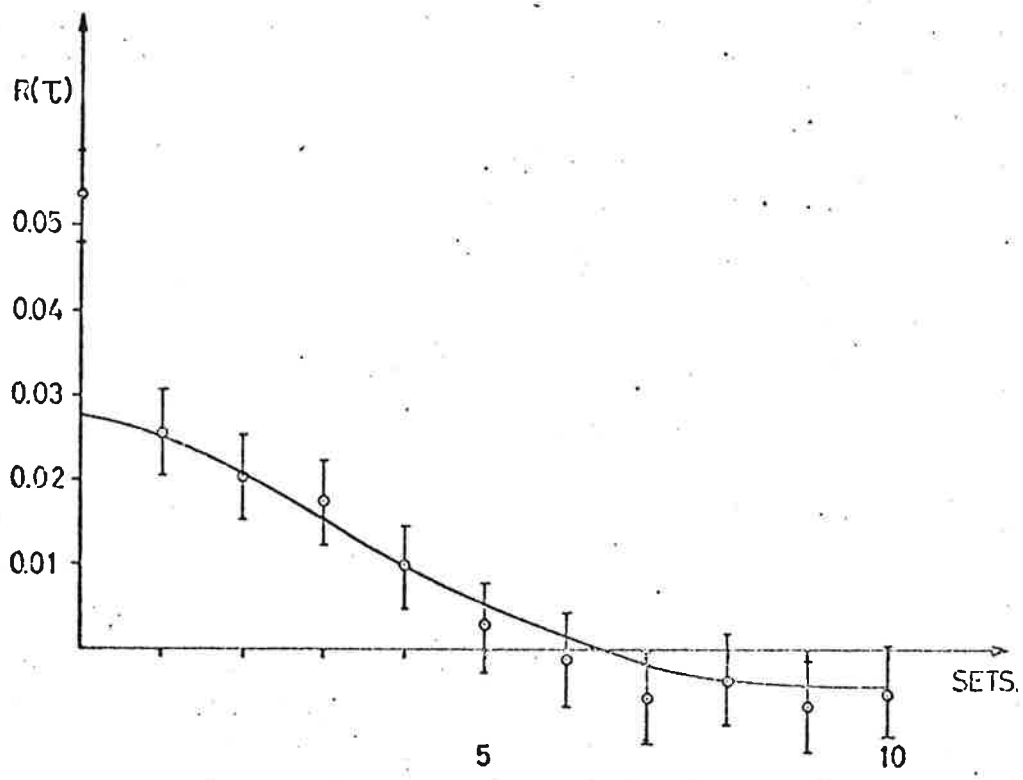

Figure 1 Sample Covariance Of Cross Direction Stretch Of Samples Taken From Consecutive Rolls Of Flat Kraft Paper. (Each Unit On The X-Axis Corresponds To One Roll 3000 m Long.)

The difference $R(0) - R^*(0)$ between $R(0)$ and the extrapolated value $R^*(0)$ can be interpreted as the sum of the measurement errors and the short scale variations. In the particular case the numerical value of $R(0) - R^*(0) = 0.026$ is in good agreement with the variance of the measurement errors which is 0.029. It follows from Figure 1 that there is a strong correlation between the values of cross-direction stretch at points 3000 m apart. This fact can be exploited by using the measurements of neighboring rolls to estimate the mean value of the stretch of a particular roll.

Using the identification techniques discussed in section 6 we find that the data illustrated in Figure 1 can be represented by a model with the structure given by (5.1) and (5.2), i.e.

1 $$x(t+1) = \Phi\, x(t)\, v(t)$$

2 $$y(t) = \theta\, x(t) + e(t)$$

with

3 $$\Phi = \begin{bmatrix} 0 & 1 \\ -0.678 & 1.556 \end{bmatrix}$$

4 $$\theta = \begin{bmatrix} 1 & 0 \end{bmatrix}$$

5 $$R_1 = \begin{bmatrix} 0 & 0 \\ 0 & 0.0021 \end{bmatrix}$$

6 $$R_2 = 0.026$$

The covariance function of the output model is shown by the full line in Figure 1.

The statistical character of the fluctuations will vary considerably with the particular quality variable as well as with the paper grade. In Figure 2 we show, e.g. the cross direction tensile strength for flat kraft paper.

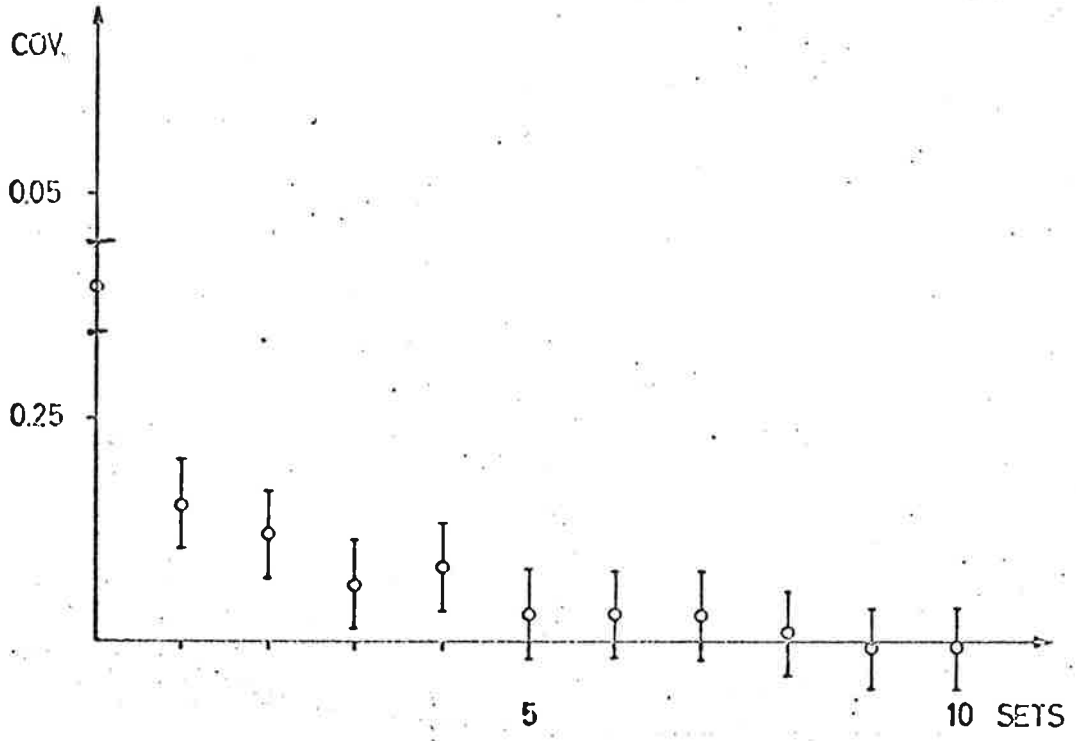

Figure 2 Sample Convariance Function Of Cross Direction Tensile Strength Samples Taken From Consecutive Rolls Of Flat Kraft Paper. (Each Unit On The X-Axis Corresponds To One Roll 3000 m Long.)

Application Of Estimation Theory

Once the mathematical models of the variations are known, the design of estimators, interpolators and predictors is a straightforward application of filtering theory. There are many types of estimation problems which occur, and the details may often be complicated by some peculiarities in production. However, we shall not discuss such peculiarities since only slight changes are required to handle them.

The Control Problem – Cross Direction Stretch Prediction

In most applications, cross-direction stretch is controlled by the machine tender. Samples for measurement of cross direction stretch are taken at the reel. Before the samples are tested, the paper has to be conditioned. Typical conditioning time is 30 minutes. There is thus considerable delay before the machine tender obtains the value of cross direction stretch. Due to this delay and measurement errors of considerable size, the machine tender gets very inaccurate information on the current value of cross direction stretch. A more satisfactory approach would be to evaluate the best estimate of the actual value of cross direction stretch on the basis of all measurements obtained. In other words, we have to solve the following prediction problem: given a set of measurements, $y(0),\ldots,y(t-k)$, find the "best" prediction of cross direction stretch at time t, where k is the measurement delay.

The Sorting Problem – Cross Direction Stretch Estimation and Interpolation

After the individual rolls comprising an order are manufactured, it must be ascertained whether they are within the customers' specifications. If not, the unacceptable rolls have to be sorted out, and new ones manufactured. On a sack kraft paper machine, the sorting is done essentially on the basis of measurements of basis weight, cross direction tensile strength and cross direction stretch. As mentioned previously, measurements of cross direction stretch are very inaccurate. There is, however, a strong correlation with the cross direction stretch of neighboring rolls. We can expect to get estimates which are considerably better than individual measurements if the estimates are based on measurements of all the rolls in

the order. To best utilize the observed measurements, we have to solve the following problem: given measurements of cross direction stretch for N successive rolls of an order, find the best estimate of average cross direction stretch of each individual roll.

The Prediction Problem

We will now discuss the prediction problem in more detail. Using a model with the structure (1), (2), the problem as stated in the beginning of this section is a typical prediction problem. As discussed previously, the solution given by Kalman is particularly well suited for our purposes because the estimate is obtained recursively as the measurements are obtained. Since the mean value of cross direction stretch is unknown, we have to include it as an extra state variable $x_{n+1}(t)$. Let x denote the augmented state vector:

7 $$x = \text{col.}\ [x_1, x_2, \ldots, x_{n+1}]$$

Applying Kalman's formulas, we get the following equations for calculating the estimate

8 $$\hat{x}(t+1|t+1) = \Phi\, \hat{x}(t|t) + K(t)\,[y(t+1) - \theta\, \Phi\, \hat{x}(t|t)]$$

9 $$\hat{x}(0|0) = m$$

10 $$\hat{x}(t+k|t) = \Phi^K\, \hat{x}(t|t) \quad k = 1, 2, \ldots$$

where $\hat{x}(t|k)$ is the minimum mean square estimate of $x(t)$ based on the observation $y(1),\ldots,y(k)$. The vectors $K(t)$ are filter gains given by the recursive equations

11 $$K(t) = S(t)\,\Phi^T\,[\theta\,S(t)\,\theta^T + R_2]^{-1}$$

12 $$S(t) = \Phi\,P(t-1)\,\Phi^T + R_1$$

13 $$P(t) = [I-K(t)\,\theta]\,S(t)$$

14 $$S(0) = R_0$$

where $S(t)$ and $P(t)$ have physical interpretations as covariance matrices of the estimation errors in $\hat{x}(t|t-1)$ and $\hat{x}(t|t)$ respectively, and R_0 is the covariance matrix of the initial state. Notice that the formula 8 is well suited for real-time computations. The filter gains $K(t)$ can be precomputed from prior knowledge. The term $\Phi\,\hat{x}(t|t)$ represents the a priori estimate of $x(t+1|t+1)$ and the term $[y(t+1) - \theta\,\Phi\,\hat{x}(t|t)]$ is thus the difference between the measurement at time $t+1$ and the a priori estimate of this measurement. The filter gains $K(t)$ express the weighing between the last measurement and the a priori estimate.

15 Example

By way of illustration we shall consider a cross direction stretch estimator based on the covariance function of Figure 1.

The model of the process is as follows

$$16 \qquad x(t+1) = \begin{bmatrix} 0 & 1 & 0 \\ -0.68 & 1.56 & 0 \\ 0 & 0 & 1 \end{bmatrix} x(t) + \begin{bmatrix} 0 \\ 1 \\ 0 \end{bmatrix} v(t)$$

$$17 \qquad y(t) = [1, 0, 1]\, x(t) + e(t)$$

where $\{e(t)\}$ and $\{v(t)\}$ are sequences of independent, equally distributed, random variables, and the state variable $x_3(t)$ represents the constant but unknown mean. Assume

$$18 \qquad R_0 = \text{diag. } [0.03, 0.03, 1.00]$$

and we get from equations (11) - (14) the filter gains given in Figure 3. The variances of the a priori and a posteriori estimates $P(t)$ and $S(t)$ are also shown in Figure 3.

Figure 4 shows examples of estimation and prediction for a flat kraft paper. Figure 5 shows the variance of prediction error for n step predictors.

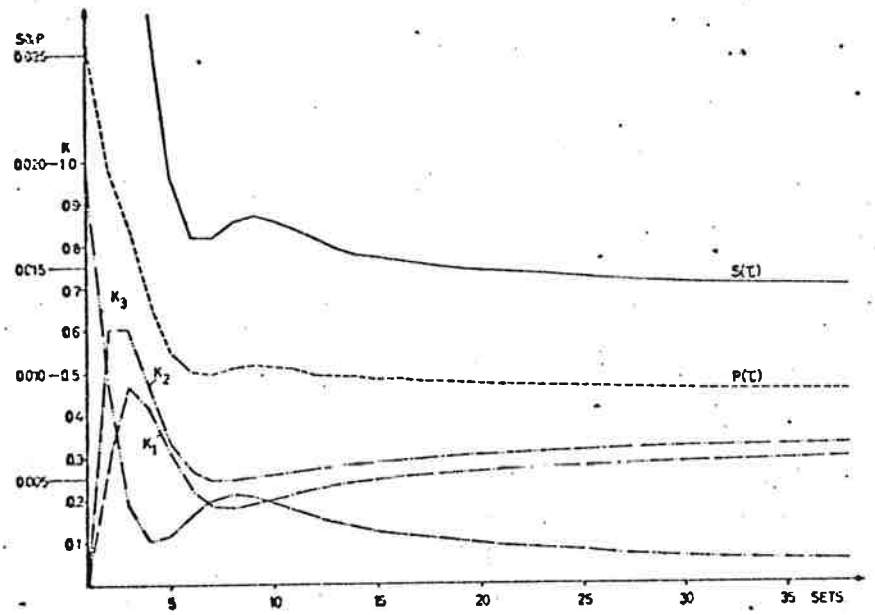

Figure 3 Typical Filter Gains For Cross Direction Stretch Of Flat Kraft Paper

The filter gains shown in Figure 3 are typical for the cross direction stretch of flat kraft paper. The filter gain $K_3(t)$ corresponds to the estimate of the mean value. The rapid initial change of the filter initial estimate (variance 0.025) is rather poor, but after 5 steps the variance is down to 0.01. This should be compared with the variance of one single measurement $\sigma_m^2 = 0.026$. The unit on the x-axis corresponds to 20 minutes.

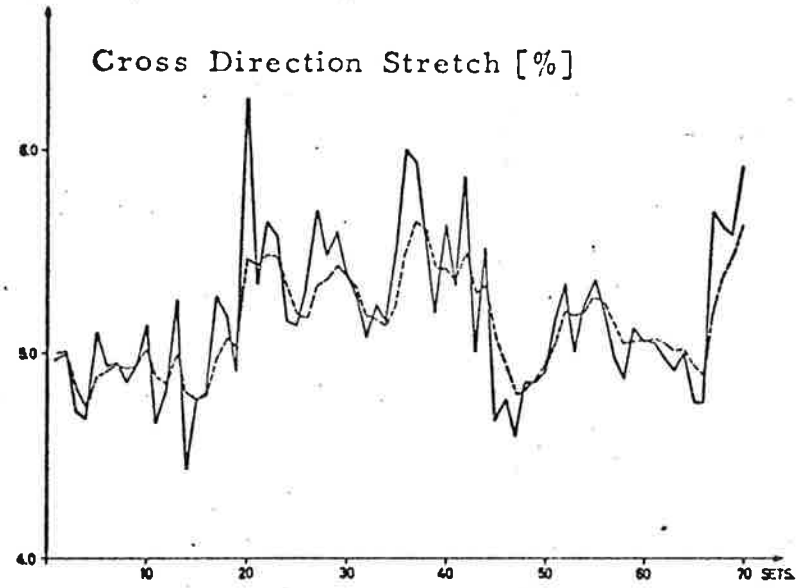

Figure 4 Actual Measured And Estimated Values Of Cross Direction Machine Stretch

Notice in Figure 4 that the estimator eliminates peaks very effectively. This graph shows the results of a test run. The continuous line shows the measured values of cross direction stretch, and the dashed line shows the estimate based on the filter calculated from average data.

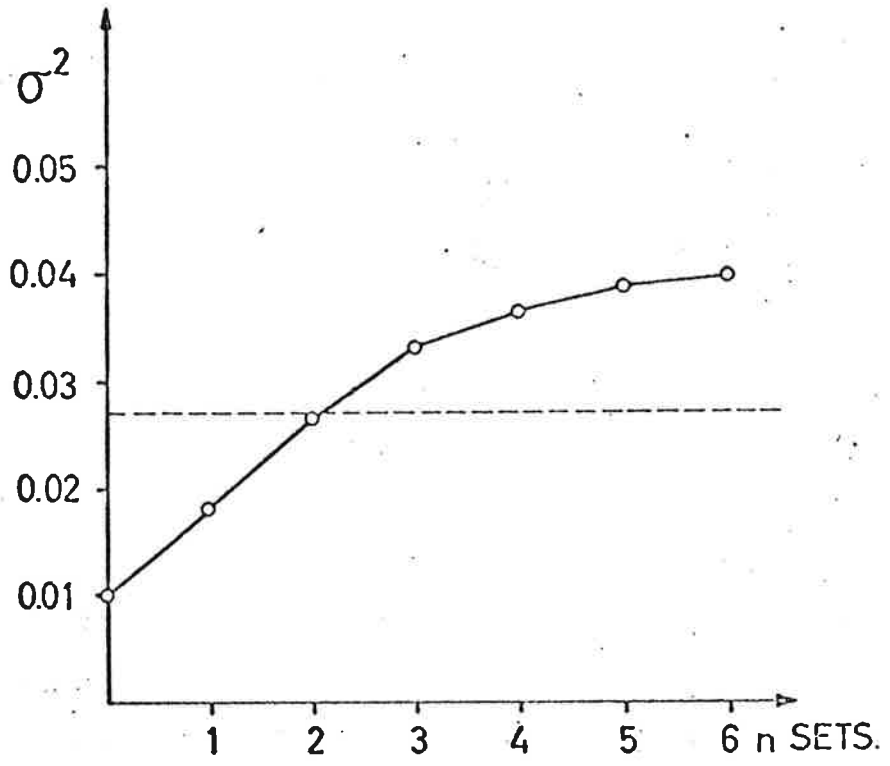

Figure 5 Variance Of The Prediction Error For n Step Predictor Of Cross Direction Stretch

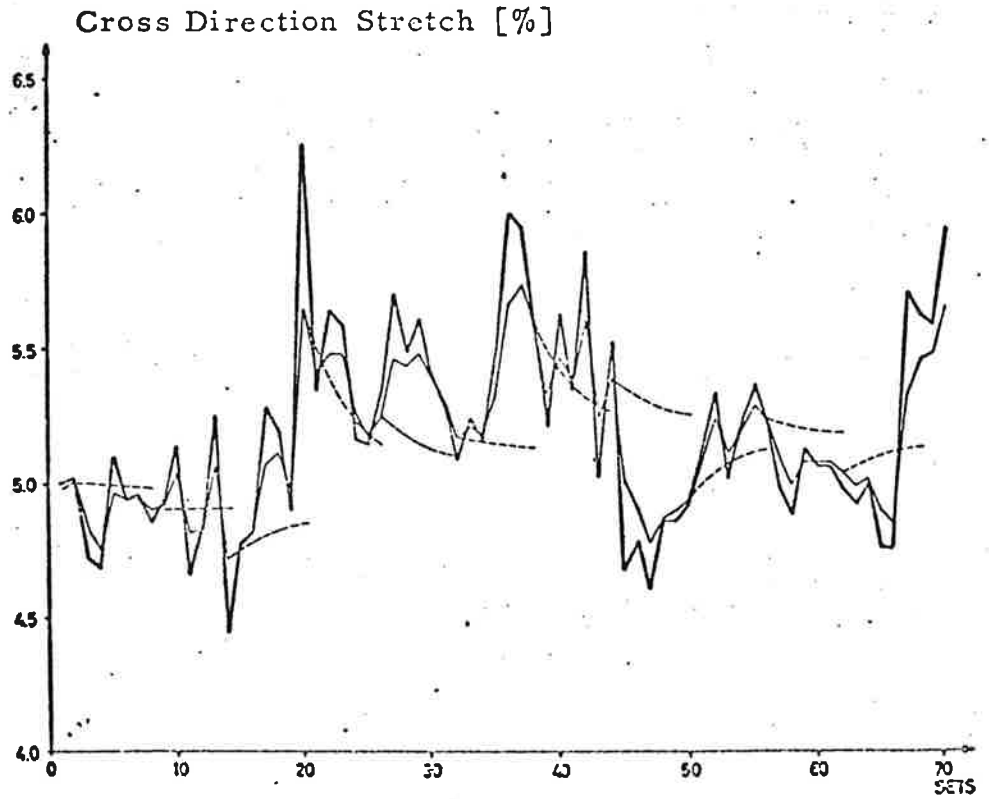

Figure 6 Simulation Of Cross Direction Stretch Predictors Using The Data Shown In Figure 4

19 Example

In the second example, we will consider an estimator for cross direction tensile strength of flat kraft paper based on the covariance function in Figure 2. The following model has been obtained:

20 $$x(t+1) = \begin{bmatrix} 0.715 & 0 \\ 0 & 1 \end{bmatrix} x(t) + \begin{bmatrix} 1 \\ 0 \end{bmatrix} e(t)$$

21 $$y(t) = [1, 1]\, x(t) + v(t)$$

By assuming

22 $$R_0 = \text{diag. } [0.03, 1.00]$$

we get the filter gains given in Figure 7 with the a priori and a posteriori estimates $P(t)$ and $S(t)$. Figure 8 illustrates estimation for a sequence of 30 sets.

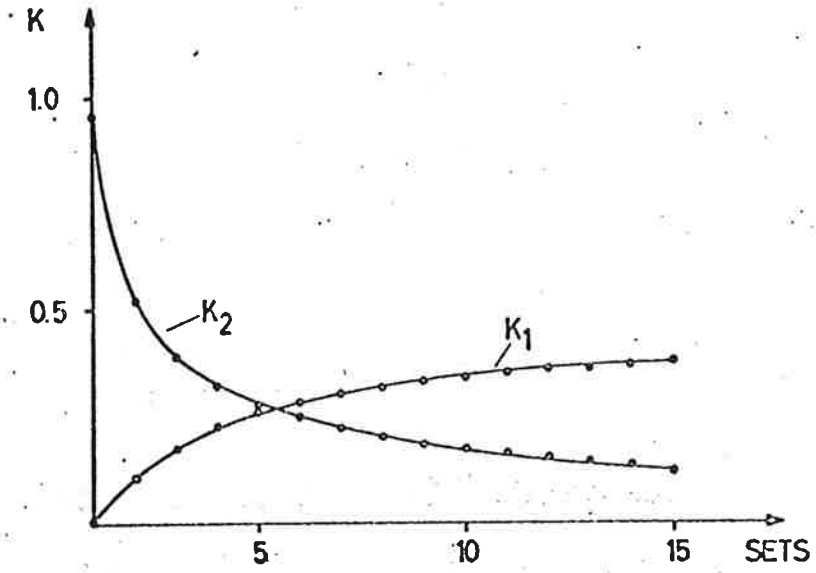

Figure 7 Typical Filter Gains For Cross Direction Tensile Strength Of Flat Kraft Paper. The Filter Gain K (t) Corresponds To The Estimate Of The Mean Value

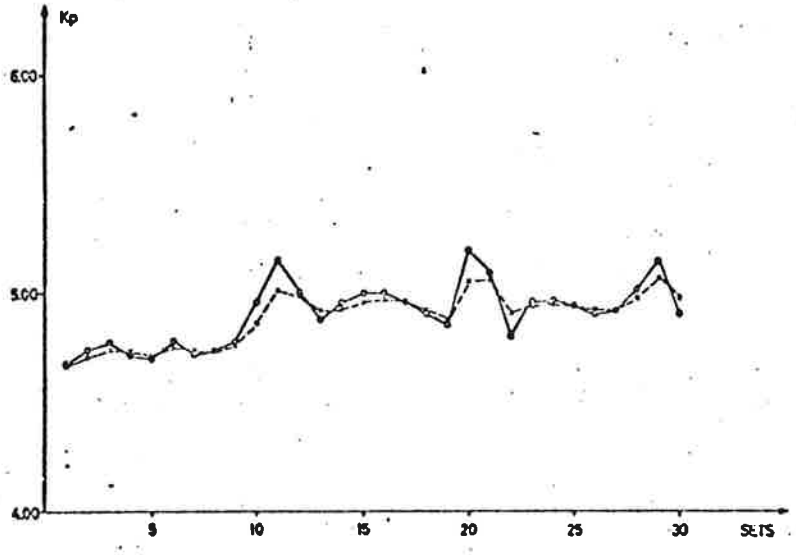

Figure 8 Measured And Estimated Values Of Cross Direction Tensile Strength

The Interpolation Problem

The sorting problem, as stated at the beginning of this chapter, is an interpolation problem of the type discussed and solved by Wiener and Kolmogorov. The analytical solution given by Wiener-Kolmogorov is not very convenient from a computational point of view, and we will therefore consider a different approach. The method used is attributed to Bryson and Kelly, and it takes advantage of the particular representation of the process given by equations (1) and (2).

We have measured values of cross direction stretch on different rolls of the order $\{y(t),\ t = 1,\ldots,N\}$, and obtained an a priori estimate, m, of the mean value of cross direction stretch for each roll. The covariance of the a priori estimate m is R_0. The problem is to find the minimum mean square estimate of $x(t),\ t = 1,\ldots,N$. Since the random variables $\{e(t)\}$ and $\{v(t)\}$ are gaussian, the minimum mean square estimate is equal to the maximum likelihood estimate. We shall therefore derive the estimator by using the method of maximum likelihood.

We introduce the likelihood function L given by

$$-2 \log L = \sum_{t=1}^{N-1} e^T(t)\, R_1^{-1}\, e(t) + \sum_{t=1}^{N} [y(t)-\theta\, x(t)]^T\, R_2^{-1}\, [y(t)-\theta\, x(t)] \qquad (23)$$

$$+ [x(1) - m]^T\, R_0^{-1}\, [x(1) - m] + \text{constant}$$

The maximum likelihood estimate of $x = \{x(t),\ t = 1,\ldots,N\}$ is obtained as the x which maximizes (1) subject to the constraints.

24 $$x(t+1) = \Phi\, x(t) + e(t) \quad t = 1, 2, \ldots, N$$

To maximize (23) subject to the constraints given by (24), we introduce the Lagrangian multipliers $\{\lambda(t),\ t = 2, 3, \ldots, N\}$ and we get, after some calculations, the following equations for the maximum likelihood estimate $\hat{x}(t|N)$ of $x(t)$.

25 $$\hat{x}(t+1|N) = \Phi\, \hat{x}(t|N) + R_1\, \lambda(t+1) \quad t = 1, 2, \ldots, N-1$$

26 $$\lambda(t) = \Phi^T\, \lambda(t+1) + \theta^T R_2^{-1} [y(t) - \theta\, \hat{x}(t|N)] \quad t = 2, 3, \ldots, N-1$$

These difference equations have the boundary conditions

27 $$\Phi^T \lambda(2) = R_0^{-1} [\hat{x}(1|N) - m] - \theta^T R_2^{-1} [y(1) - \theta\, \hat{x}(1|N)]$$

28 $$\lambda(N) = \theta^T R_2^{-1} [y(N) - \theta\, \hat{x}(N|N)]$$

To determine the maximum likelihood estimate, we will have to solve a boundary value problem for the difference equations (25) and (26) which are the discrete analogues of the Euler equations of a continuous variational problem. Since the equations are linear, the problem can be solved in a straightforward way by matching the initial conditions.

We note that if the filtering problem is solved, we know $\hat{x}(N|N)$, and $\lambda(N)$ is then expressed by the boundary condition (28). If the filtering problem is solved, the interpolation problem will thus be reduced to an initial value problem for the above equations (25), (26).

This procedure has one disadvantage. The homogeneous part of the equations (25) and (26) is unstable, and we will have numerical difficulties if the solution has to be calculated for large number of steps. For a few steps, the method works very well.

In order to obtain estimates for large values of N, the boundary value problem has to be solved by a different technique. This problem has lately been the subject of much analysis, and there are several techniques available. One example is the method of steepest descent introduced by Bryson and Kelley. In most cases, simple backward integration is sufficient. See Figure 9.

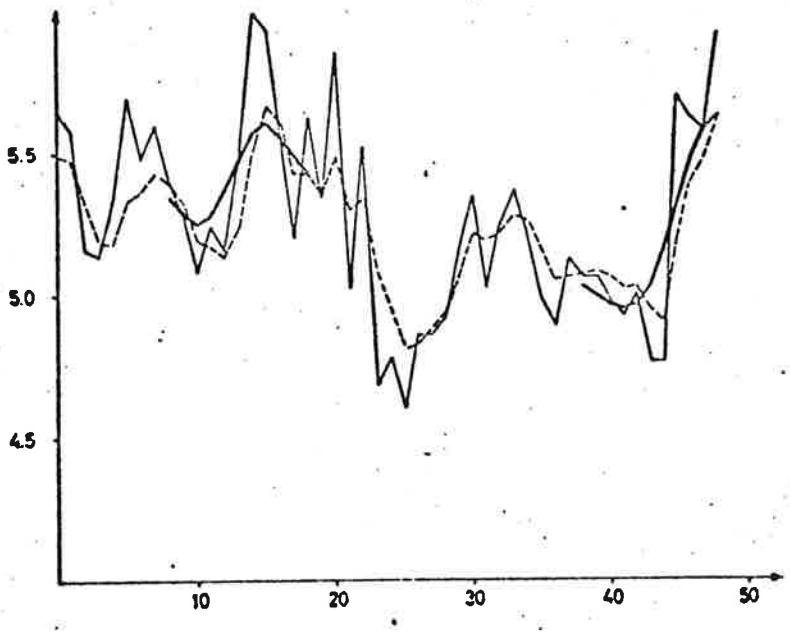

Figure 9 Interpolation By Backward Integration Of The Cross Direction Stretch Data Shown In Figure 4

Summary Of Results Obtained

Some results obtained in practice are summarized in the tables below.

Table 1

Variances Of Measurements Estimates And Predictions Of Cross Direction Stretch

PAPER	MEASUREMENT	ESTIMATE	ONE STEP PREDICTION
Flat Kraft	0.026	0.008	0.015
Wet Strength Extensible	0.210	0.007	0.100
Extensible	0.065	0.020	0.031

Table 2

Variances Of Measurements Estimates And Predictions Of Tensile Strength

PAPER	MEASUREMENT	ESTIMATE	PREDICTION
Flat Kraft	0.018	0.007	0.015
Wet Strength	0.046	0.017	0.035
Extensible	0.030	0.014	0.021

Thus, by processing the data obtained using filtering theory, it was possible to obtain current estimates which were about twice as accurate as a single measurement, and to predict the quality variable over a period of 30-90 minutes as accurately as a single measurement made after the paper had been manufactured.

1.9 References

There are several survey articles which cover computer control in the pulp and paper industry, e.g.,

Bakke, R. M., "Case Study in the Paper-Making Industry" 1968 Case Studies in System Control, University of Michigan, June 24-25, 1968, sponsored by IEEE Group on Automatic Control, and

Brewster, D. B. and Bjerring, A. K., "Computer Control in Pulp and Paper 1961 - 1969", Proc. IEEE 58:1 (1970) 49-69.

These papers also contain many references. Apart from the control journals, there is also much useful information in the journals specifically devoted to the paper industry, e.g., TAPPI (Journal of the Technical Association of the Pulp and Paper Industry), Pulp and Paper, Paper Trade Journal, The Paper Maker and Svensk Papperstidning.

The papers

Åström, K. J., "Control Problems in Papermaking", Proceedings of the IBM Scientific Computing Symposium on Central Theory and Applications, Yorktown Heights, October 1964, and

Åström, K. J., "Application of Linear Stochastic Control Theory to Paper Machine Control", IEEE Case Studies in Control, June 1970

deal specifically with the application of control theory to some problems in the paper industry.

There are several sources for linear stochastic control theory, e.g.,

"Curriculum and Methods in Control and Systems Engineering", Systems Department, IBM Research, San Jose, California, 1969,
and
Åström, K. J., "Introduction to Stochastic Control Theory", Academic Press, 1970.

In these works there are additional references.

There are at present no good books available on process identification. The state of the art can, however, be assessed from the survey papers:

Eykhoff, P., P. M. van der Grinten, H. Kwakernaak, B. P. Veltman. Systems modelling and identification, Third Congress IFAC, London 1966, (83 references);

Cuenod, M., A. P. Sage. Comparison of some methods used for process identification, IFAC Symposium on "Identification in Automatic Control Systems", Prague, 1967; also in: Automatica, 4, (1968), 235-269, (79 references);

Eykhoff, P., Process parameter and state estimation, IFAC Symposium on "Identification in Automatic Control Systems", Prague, 1967; also in: Automatica, 4, (1968), 205-233, (11 references);

Balakrishnan, A. V., V. Peterka. Identification in automatic control systems, Fourth Congress IFAC, Warsaw, 1969, (125 references);

Åström, K. J. and P. Eykhoff, "System Identification - A Survey", 2nd IFAC Symposium on Identification and Process Parameter Estimation, Prague, June 1970, (213 references).

The particular techniques discussed in section 6 are based on

Åström, K. J., T. Bohlin and S. Wensmark "Automatic Construction of Linear Stochastic Dynamic Models for Stationary Industrial Processes with Random Disturbances Using Operating Records", Technical Paper TP18.150, IBM Nordic Laboratory, and

Åström, K. J. and T. Bohlin, "Numerical Identification of Linear Dynamic Systems from Normal Operating Records", Proc. IFAC Symposium on Self-Adaptive Control Systems, Teddington (1965) also in Hammond, P. H. editor "Theory of Self-Adaptive Control Systems", Plenum Press, New York, 1966.

An overview of the Billerud System can be obtained from the reports

Ekström, Å., "Integrated Computer Control of a Paper Machine - System Summary", Technical Paper TP18.169, IBM Nordic Laboratory, Lidingö, Sweden, 1966;

Mårtensson, E., "Integrated Computer Control of a Paper Machine - Production Planning", Technical Paper TP18.168 IBM Nordic Laboratory, Lidingö, Sweden, 1966;

Alsholm, O. and G. Sangregorio, "Integrated Computer Control of a Paper Machine - Process Control", Technical Paper TP18.170, IBM Nordic Laboratory, Lidingö, Sweden, 1966;

Åström, K. J. and O. Tveit, "Integrated Computer Control of a Paper Machine - Quality Control", Technical Paper TP18.171, IBM Nordic Laboratory, Lidingö, Sweden, 1966;

Astrom, K. J. and T. Bohlin, "Integrated Computer Control of a Paper Machine - Control Strategy Design - New Methods in Operation", Technical Paper TP18.172, IBM Nordic Laboratory, Lidingö, Sweden, 1966;

Meurman, O., G. Sangregorio and B. Strid, "Integrated Computer Control of a Paper Machine - Instrumentation and Computer Connections", Technical Paper TP18.173, IBM Nordic Laboratory, Lidingö, Sweden, 1966;

Ekström, Å., and A. Hempel, "Integrated Computer Control of a Paper Machine - Production Supervising System", Technical Paper TP18.174 , IBM Nordic Laboratory, Lidingö, Sweden, 1966.

These papers, which were all presented in a symposium organized jointly by Billerud and IBM in June 1966, also give references to more detailed reports on the project.

The particular technique used to derive the minimal variance control strategies appeared first in

Åström, K. J., "Notes on a Regulation Problem", Technical Report, IBM Nordic Laboratory, Sweden, 1965.

Section 7 is based on

Åström, K. J., "Computer Control of a Paper Machine - An Application of Linear Stochastic Control Theory", IBM Journal of Research and Development, 11 (1967), 389-405,

and section 8 is based upon

Åström, K. J. and O. Tveit, "Integrated Computer Control of A Paper Machine - Quality Control - Designing and Implementing Estimators, Interpolators and Predictors for Quality Variables", Technical Paper TP18.166 IBM Systems Development Division, Nordic Laboratory, Sweden, 1968.